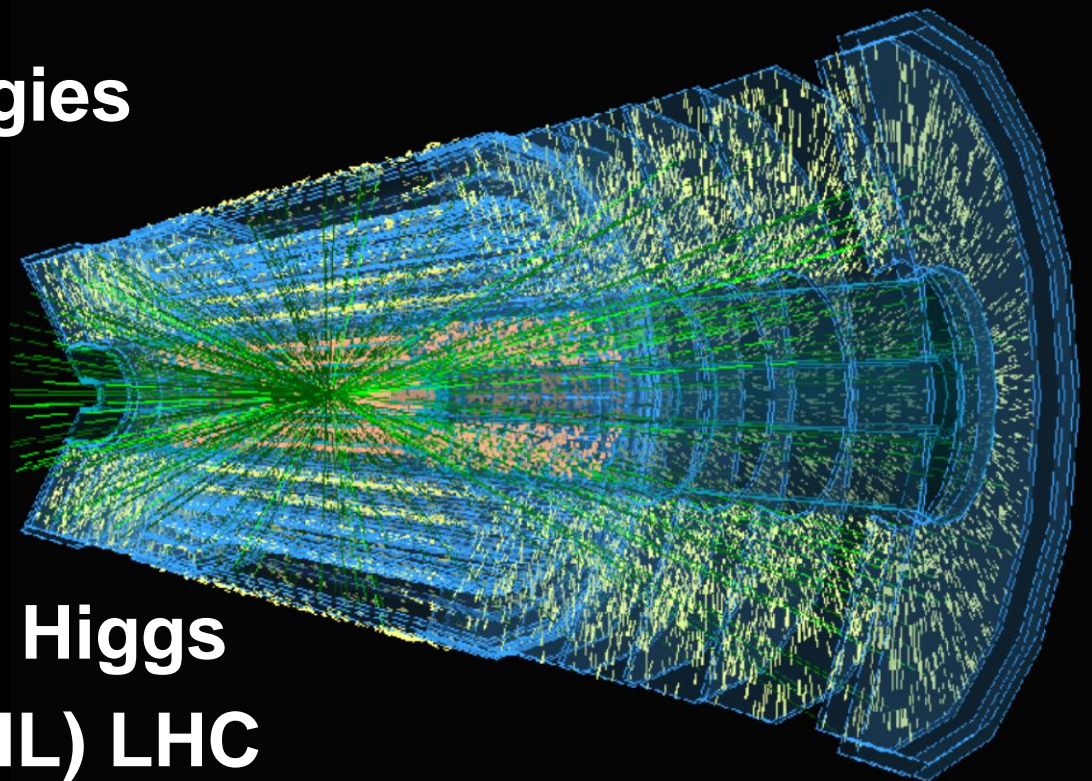# Detectors and Electronics for 21st Century Instrumentation: What have we Learnt? Where should we Focus?

Phil Allport

(ATLAS Collaboration, RD50 Collaboration, PRaVDA and Liverpool University)

10/07/13

- **Introduction**
- **Detector Technologies**
  - **Particle Physics**
  - **Medical Imaging**
  - **Security**
- **Digression:**

    ATLAS and the Higgs
- **High-Luminosity (HL) LHC**
- **Conclusions**

The Challenges

- Detectors are typically required to provide for a system of i particles: (t_i, x_i, y_i, z_i) and $(E_i, p_{xi}, p_{yi}, p_{zi})$; the position of each particle at a particular time and the corresponding energy and momentum.

- We often need to cope with many particles per cm^2 per second (high particle fluxes), many different particle types (different masses etc) and constraints of cost, accessibility, operating environment (*incl* temperature, pressure etc), implied radiation levels over long operation periods, data transmission and data storage limitations …

- Usually a system of detectors is needed so that the different components have to perform their function while minimally interfering with the function of the other parts

- The requirements always push in the direction of improved position, time, energy and momentum resolution with clearer particle identification (or background rejection) and real-time pattern recognition and data processing

- At the same time many application demand affordable large area coverage

Particle Detectors

- **Tracking** detectors focus on measuring $(t, x_{i1}, y_{i1}, z_{i1})$, $(t, x_{i2}, y_{i2}, z_{i2})$, $(t, x_{i3}, y_{i3}, z_{i3})$, ... $(t, x_{in}, y_{in}, z_{in})$ for the *i* charged particles at a given time, t, and the quantities $(E_i, p_{xi}, p_{yi}, p_{zi})$; and charge are derived from linking the hits for each particle and tracking its path, combined with additional information from the tracking and other detectors.

- A very powerful technique to measure momentum is to track in a known magnetic field where the curvature is proportional to 1/p.
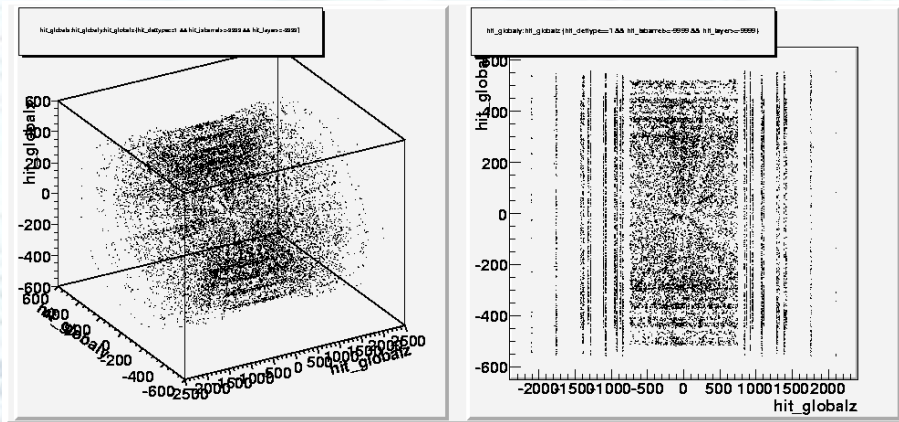
Join the dots and fit for curves (seen end-on) in a solenoid magnetic field
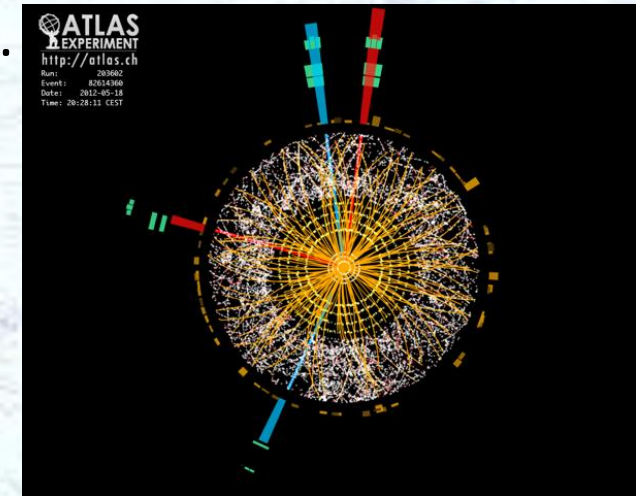
- As the particle traverses the full detector system (including the tracker) the pattern of energy loss in different media provides information on the particle type (and therefore mass).

- Where massive detectors stop the particle entirely (**electromagnetic** and **hadronic calorimeters**) they directly provide **E** and also the energies and directions of the **neutral** particles.
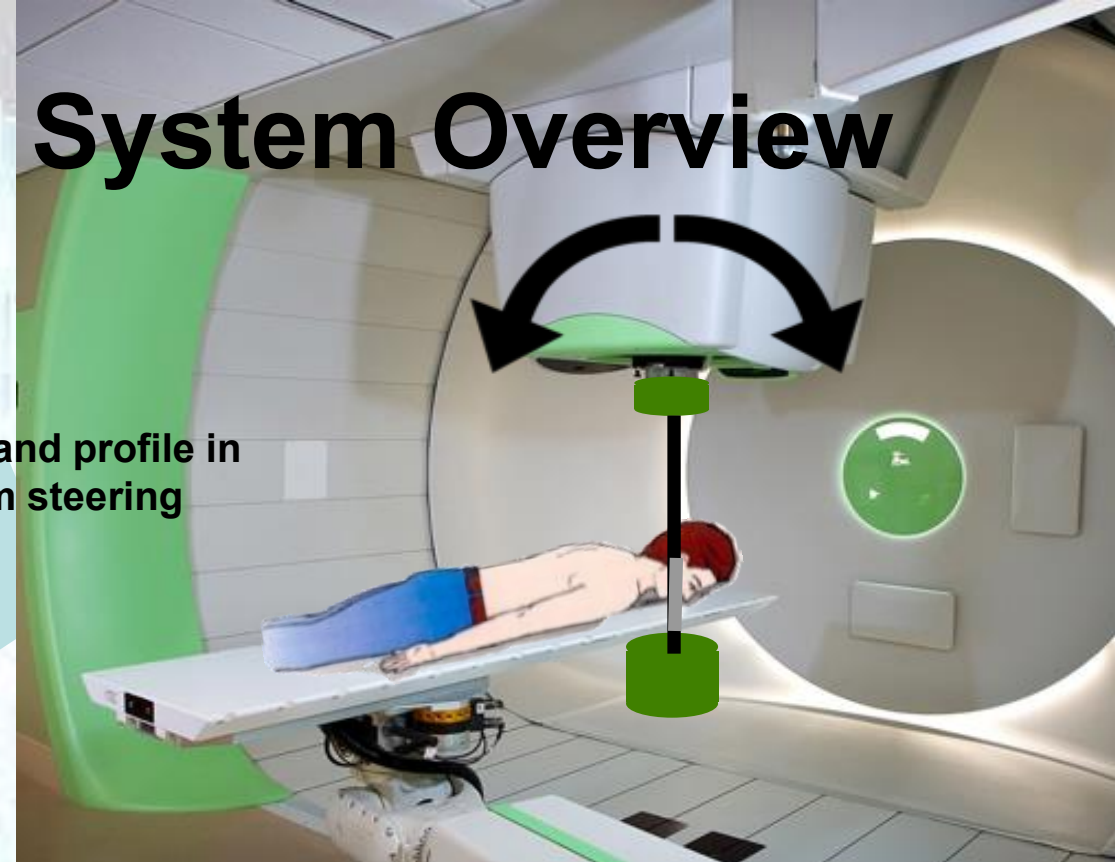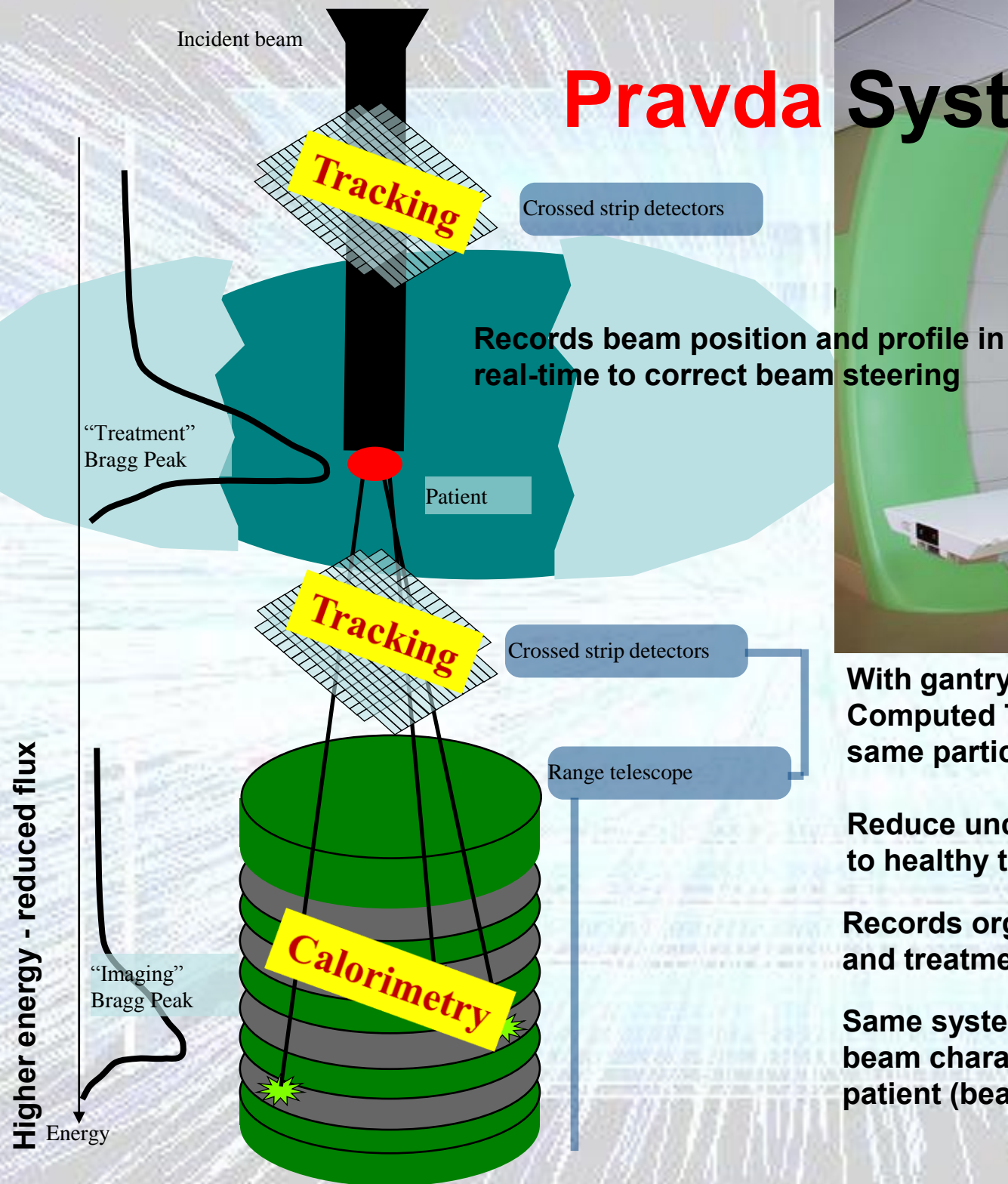
3

Pravda

Proton Radiotherapy Verification and Dosimetry Applications

– Integrated computed tomography and dosimetry instrumentation for proton therapy

wellcome trust

UNIVERSITY OF LINCOLN

ICR — The Institute of Cancer Research

UNIVERSITY OF SURREY

UNIVERSITY OF LIVERPOOL

NHS — University Hospitals Birmingham

UNIVERSITY OF BIRMINGHAM

isdi

Pravda System Overview

Incident beam

Tracking

Crossed strip detectors

Records beam position and profile in real-time to correct beam steering

"Treatment" Bragg Peak

Patient

Tracking

Crossed strip detectors

Range telescope

Higher energy - reduced flux

"Imaging" Bragg Peak

Calorimetry

Energy

With gantry movement permit full proton-Computed Tomography (pCT) scan using same particle type as for treatment.
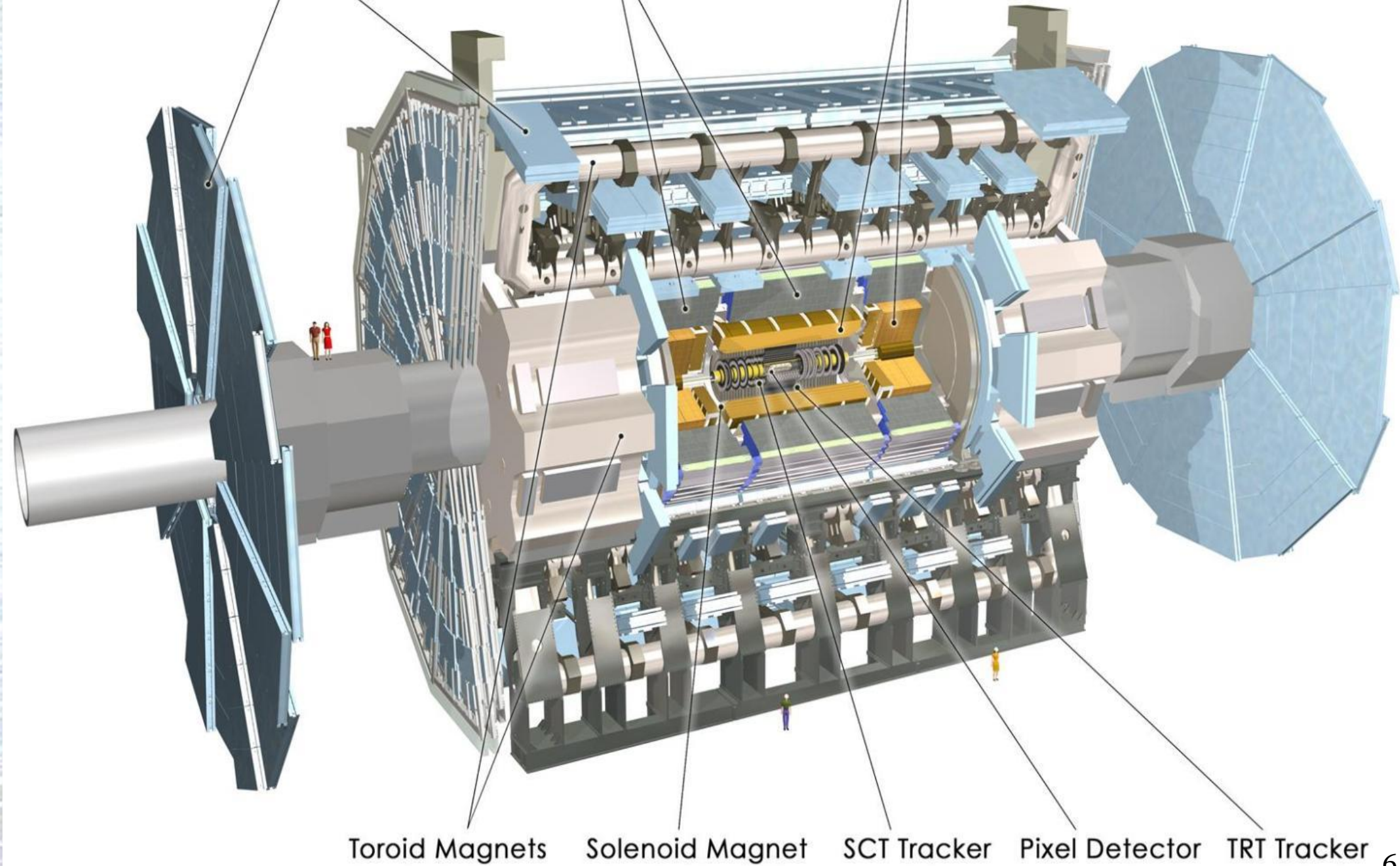
Reduce uncertainties and hence less damage to healthy tissue.

Records organ position prior to treatment, and treatment dose.

Same system can be used for detailed beam characterization in absence of patient (beam monitoring).
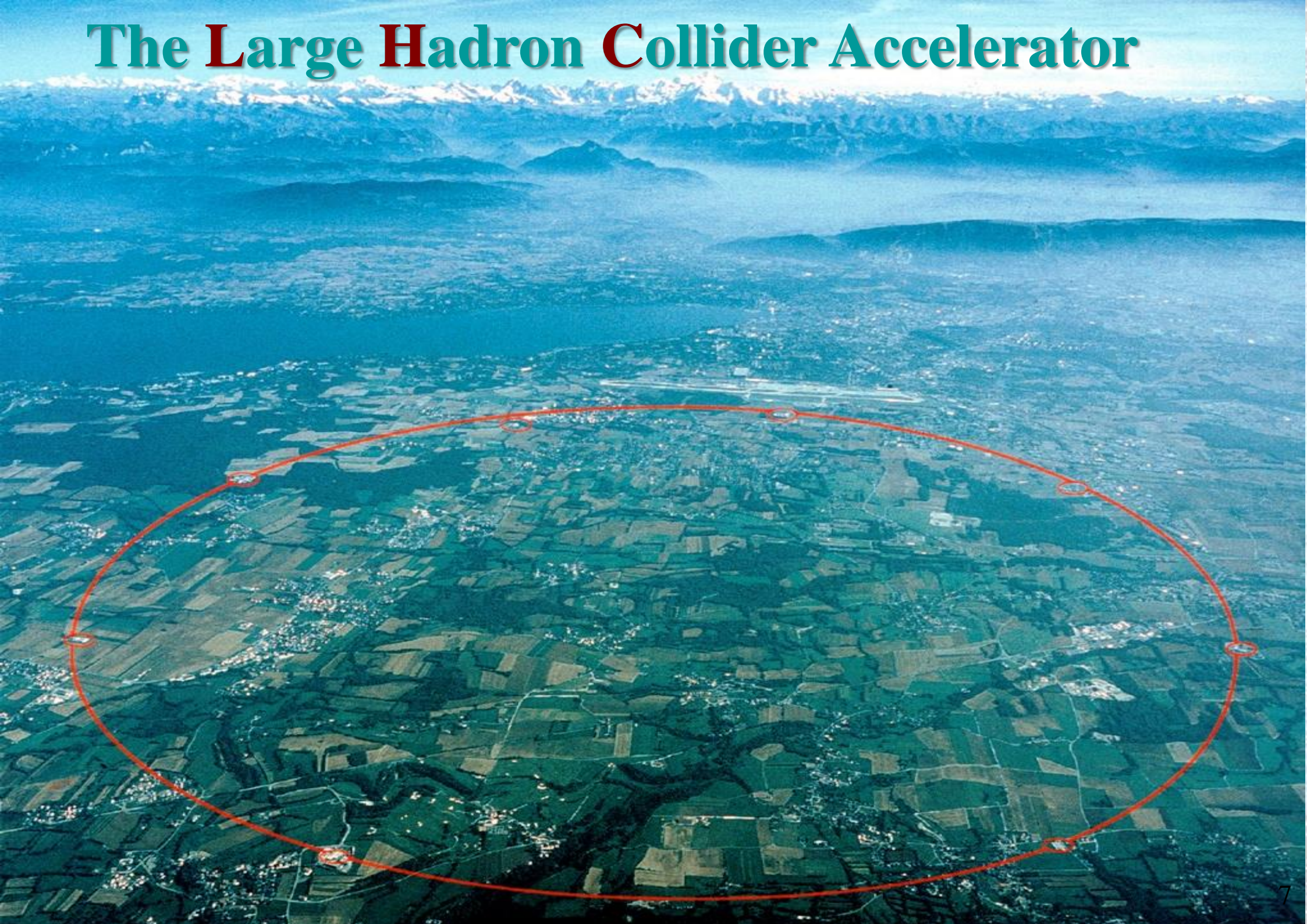
5

Muon Detectors

Tile Calorimeter

Liquid Argon Calorimeter

Toroid Magnets

Solenoid Magnet

SCT Tracker

Pixel Detector

TRT Tracker
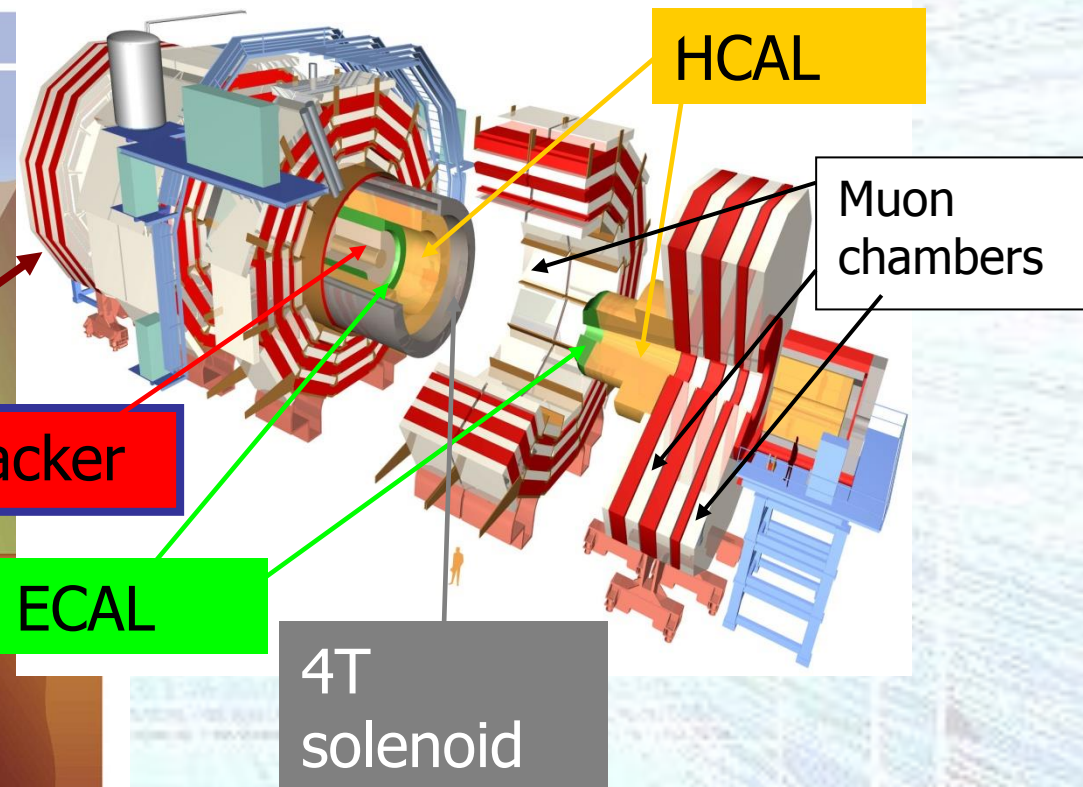
6

The Large Hadron Collider Accelerator
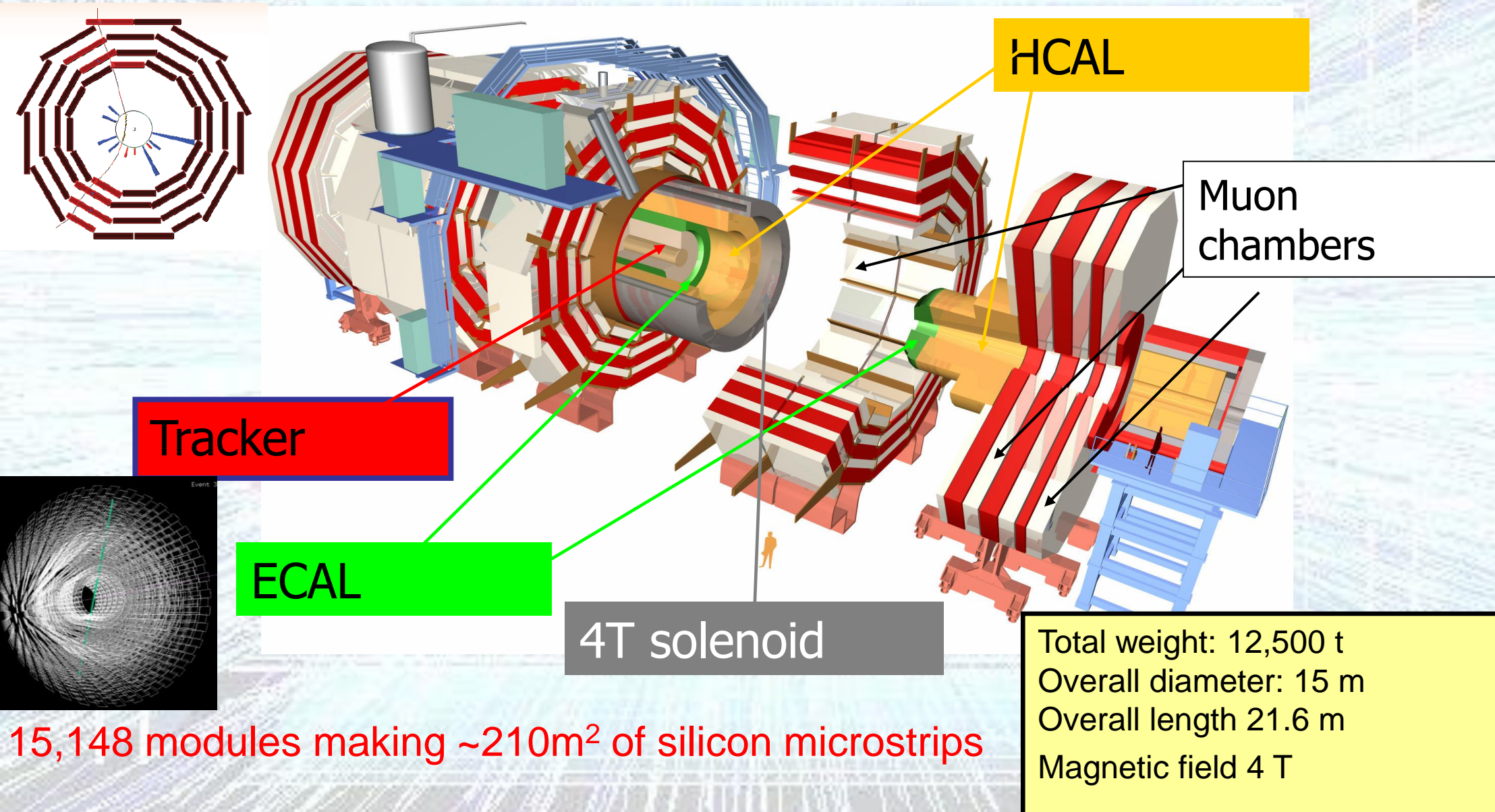
Experiments at the LHC

Collider Experiments

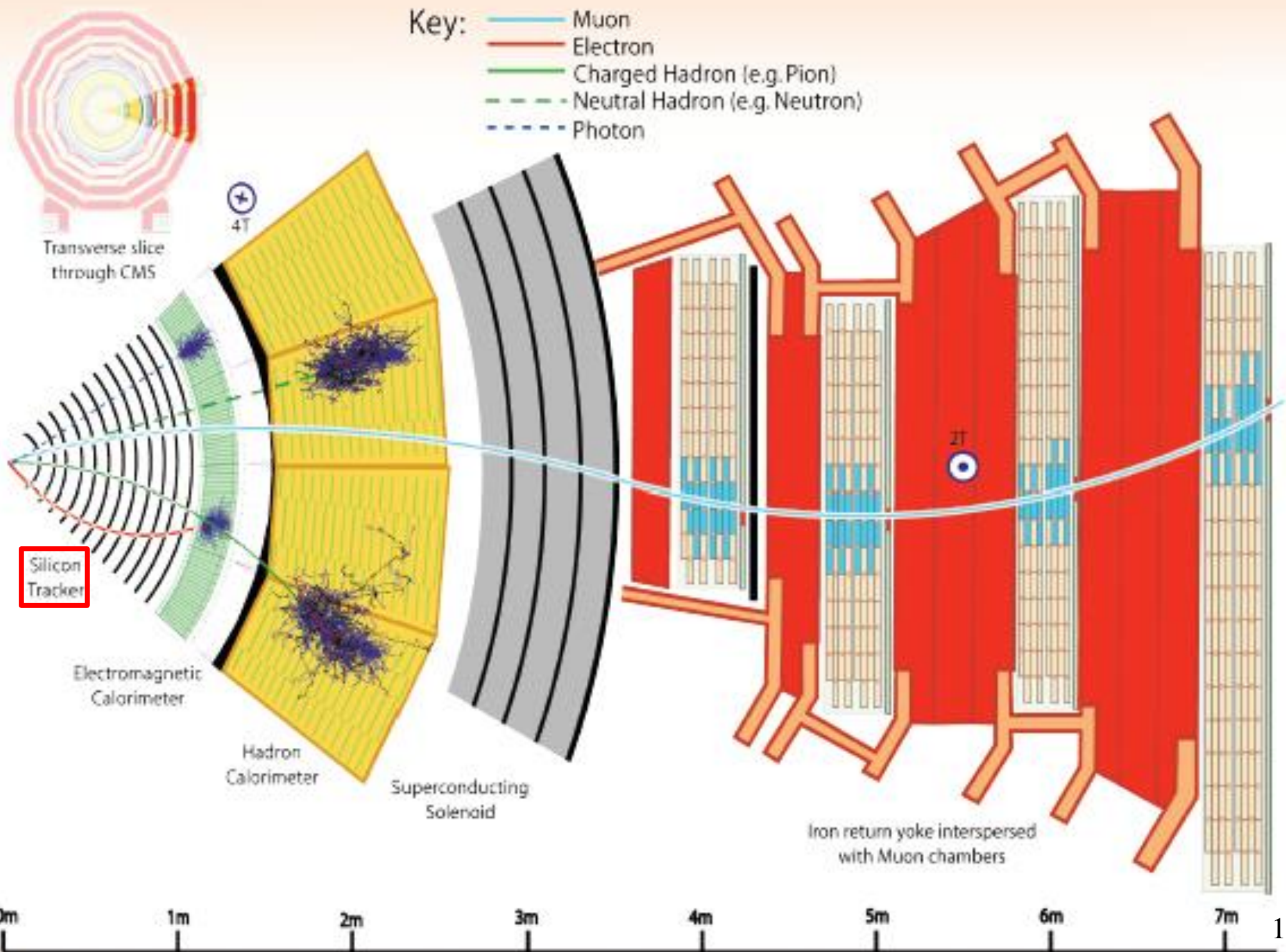CERN Geneva

The Large Hadron Collider 14 TeV: Proton on Proton
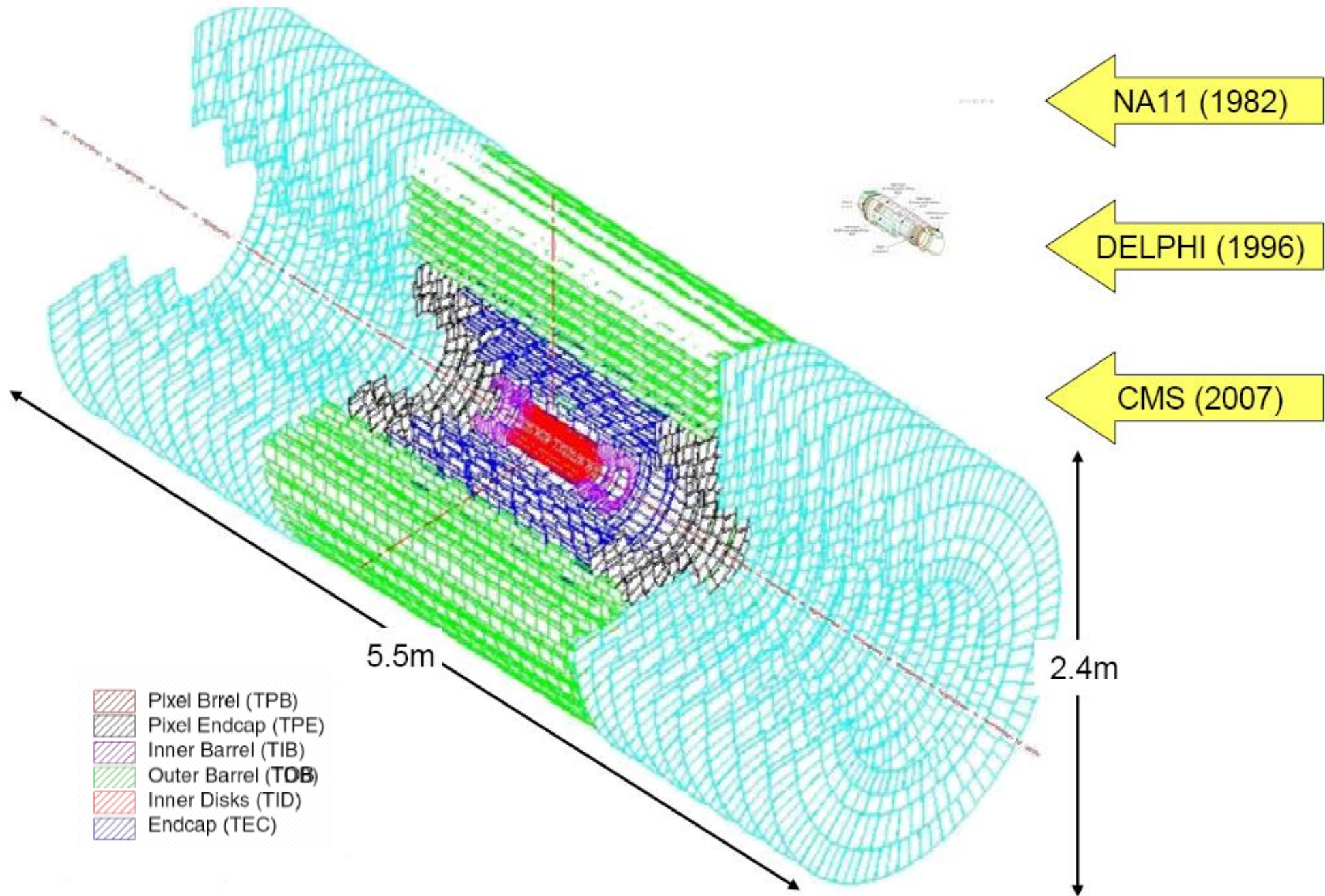
2 Giant General Purpose Detectors at the LHC

HCAL

Muon chambers

Tracker

ECAL

4T solenoid

The "Compact" Muon Spectometer

40 - V10/09/97

CMS: The Compact Muon Solenoid

HCAL

Muon chambers

Tracker

ECAL

4T solenoid

15,148 modules making ~210m² of silicon microstrips

Total weight: 12,500 t
Overall diameter: 15 m
Overall length 21.6 m
Magnetic field 4 T

Key:
- Muon
- Electron
- Charged Hadron (e.g. Pion)
- Neutral Hadron (e.g. Neutron)
- Photon

Transverse slice through CMS

4T

Silicon Tracker

Electromagnetic Calorimeter

Hadron Calorimeter

Superconducting Solenoid

2T

Iron return yoke interspersed with Muon chambers

0m   1m   2m   3m   4m   5m   6m   7m

10

CMS Silicon Tracker: Largest Ever Built

NA11 (1982)

DELPHI (1996)

CMS (2007)

5.5m

2.4m

Pixel Brrel (TPB)
Pixel Endcap (TPE)
Inner Barrel (TIB)
Outer Barrel (TOB)
Inner Disks (TID)
Endcap (TEC)

11

Silicon Trackers: Time Evolution
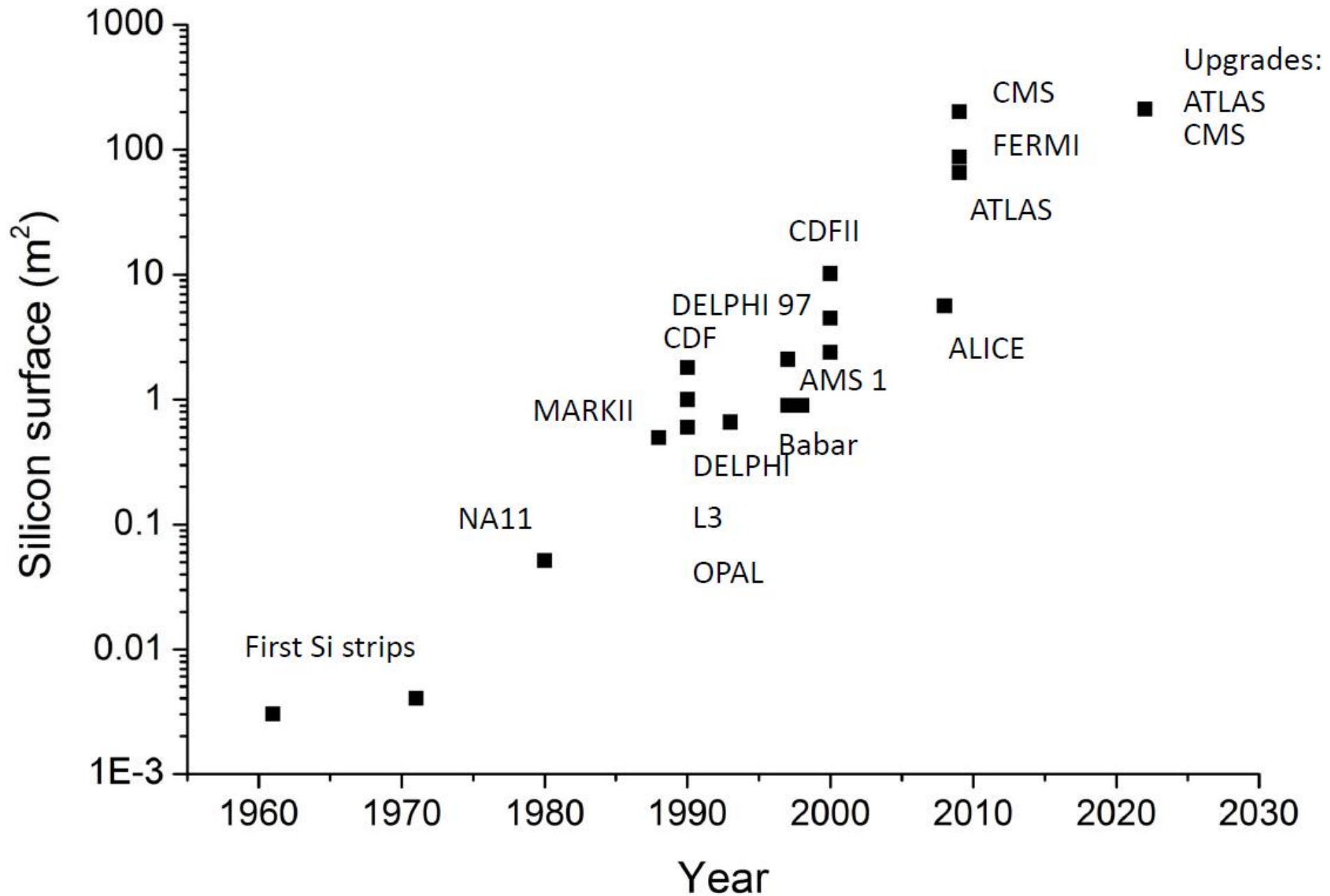
Silicon Trackers: Time Evolution
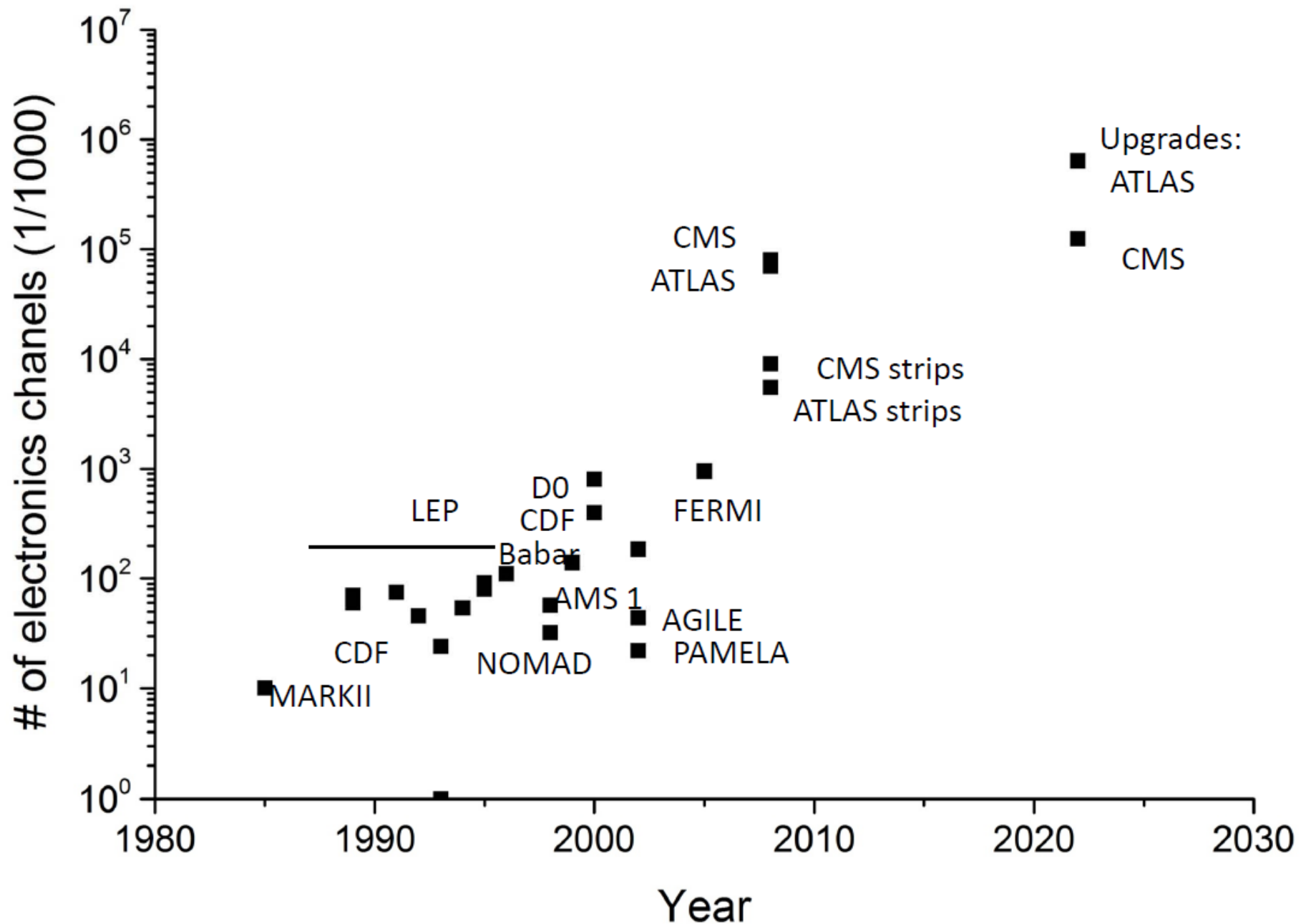
The Data Deluge

- Billions of particles (or even billions of collisions with many hundreds of particles produced in each) per second recorded in many millions to billions of channels presents a further challenge.

- In many cases to store all the possibly relevant data that the sensor system can provide is unrealistic and, as the rates of particles to be handled increases, becomes also undesirable.

- Three approaches can be considered to deal with this.
  1. Do as much as possible on the detector to reduce the data to be transmitted to just the most important information (feature extraction and/or background rejection)
     - A relatively easy first step is to set a threshold and to discard all channel information below that threshold (zero-suppression).
     - Typically further processing requires application specific hardware, often custom (ASIC) chips and/or powerful reconfigurable electronics (FPGA) and/or embedded processors
  2. Have many thousands of very fast (multi-Gb/s) data links to external processing farms using more commercially standard high-speed computing farms which perform initial data processing tasks and greatly reduce the ultimate data storage requirements
  3. Both

- Many subject areas still end up with many Peta-byte per year to be available for analysis and with data processing requirements for such large data sets
  - However, since $1000 \times$ Gb/s implies Tb/s, this still requires factors of 10^4-10^6 reduction in the volume of data to be kept compared with the volume coming of the detector system.

Experiments at the LHC
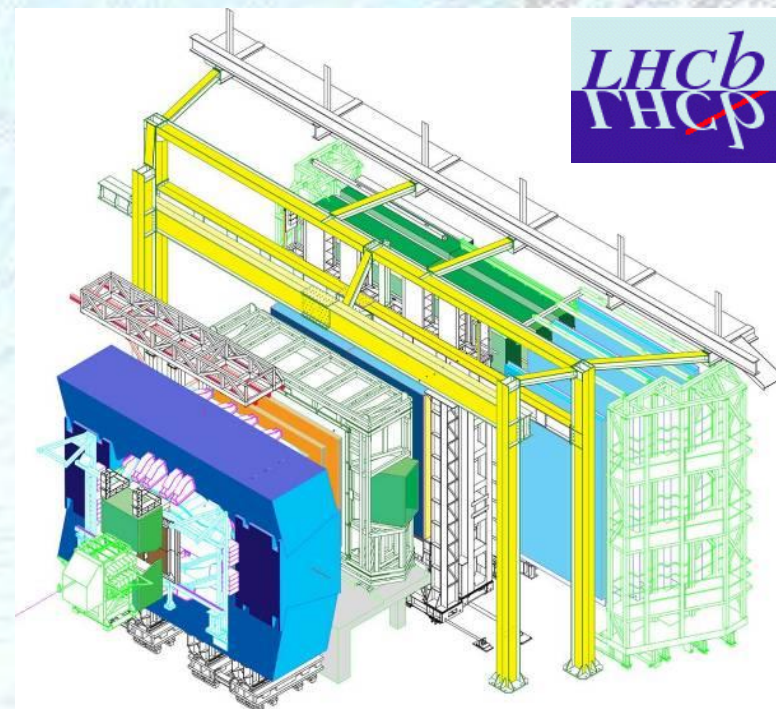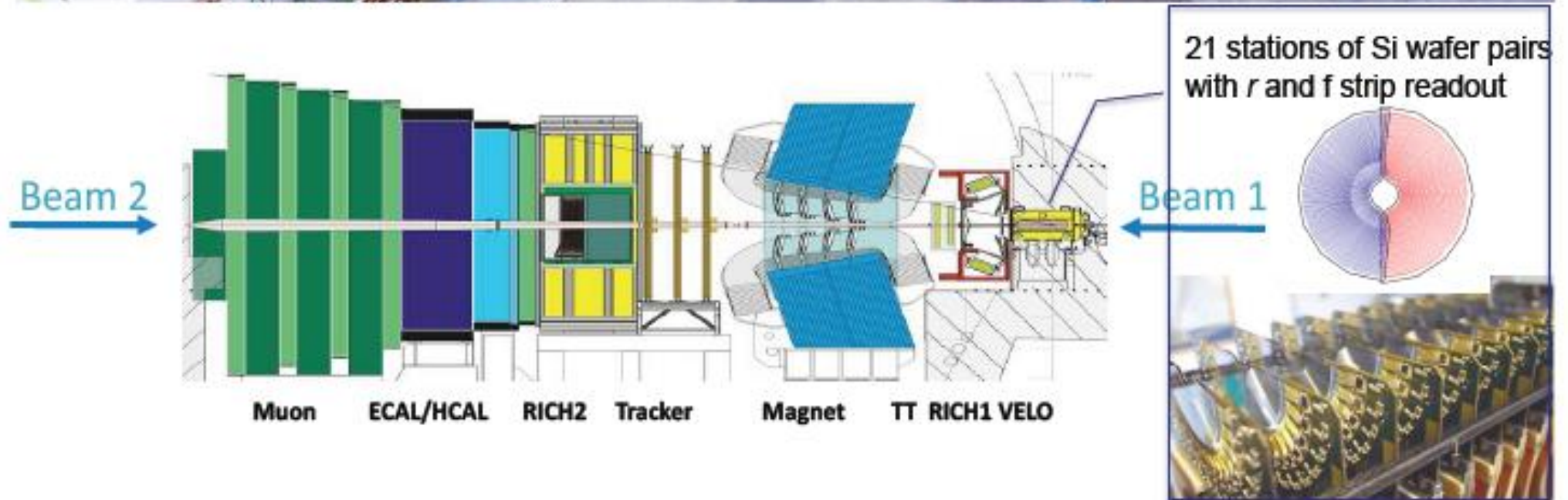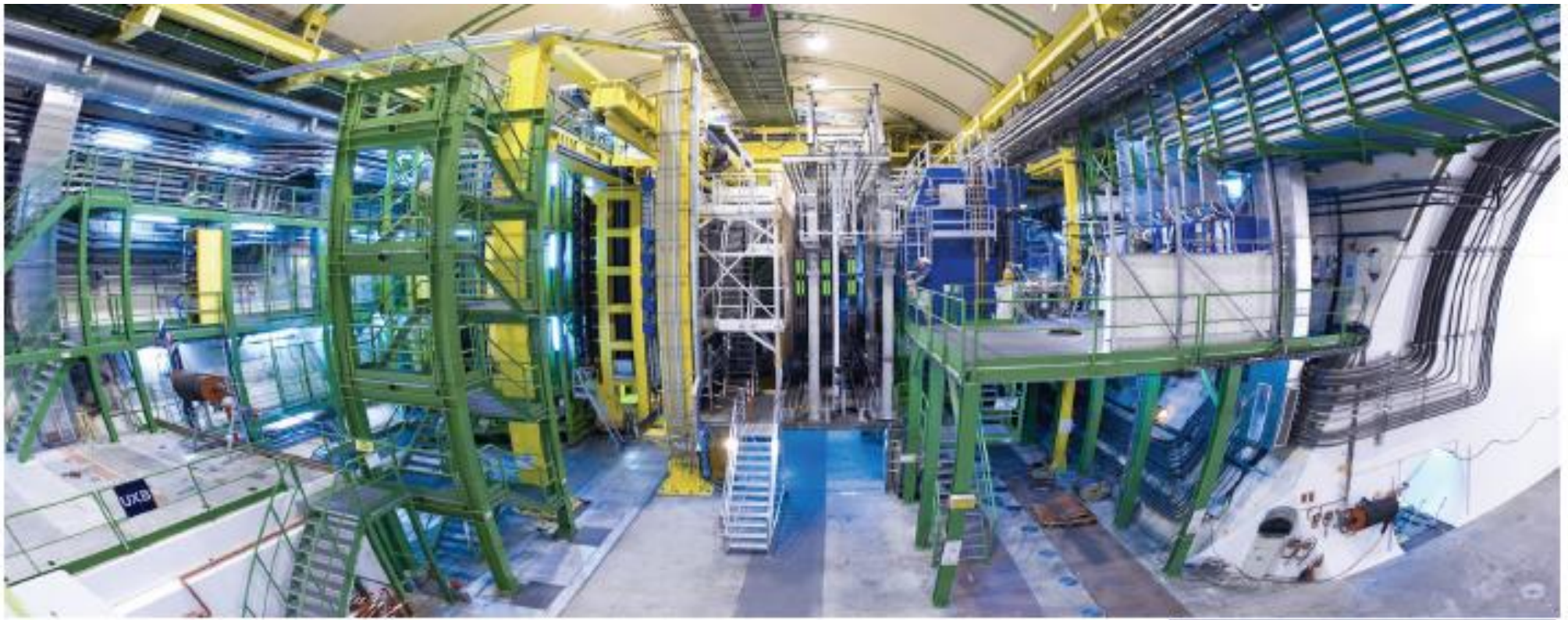
Collider Experiments
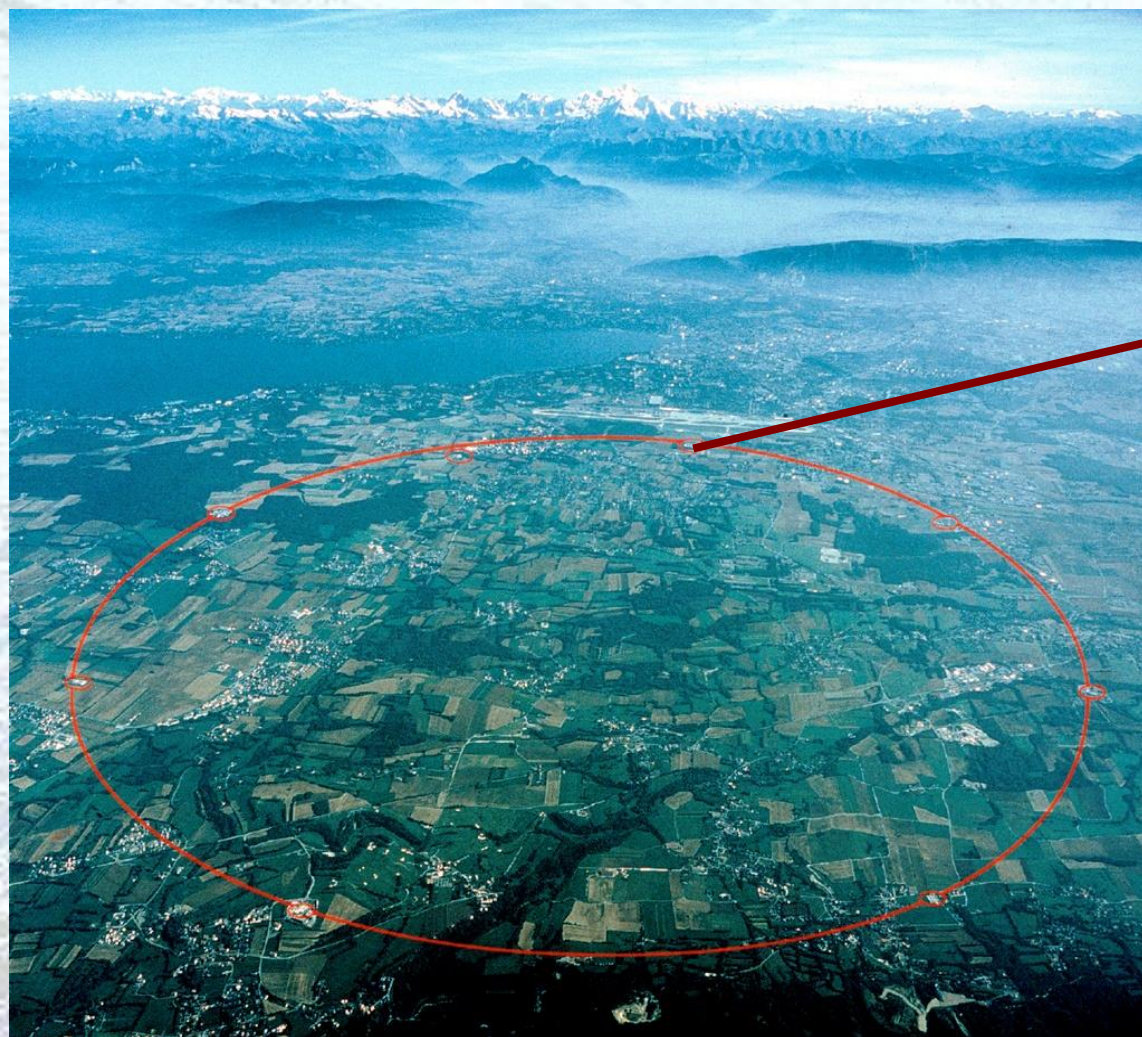
LHCb

High Statistics B Physics

Sensitivity to new physics through being sensitive to subtle effects or rare phenomena

Complementary physics reach to ATLAS and CMS

21 stations of Si wafer pairs with *r* and *f* strip readout

Beam 2 → ← Beam 1

Muon ECAL/HCAL RICH2 Tracker Magnet TT RICH1 VELO

Physics of Micro-strip Silicon Detectors

- Highly segmented silicon detectors have been used in Particle Physics experiments for over 40 years

- **The principle application has been to detect the passage of ionising radiation with high <u>spatial</u> resolution and good efficiency.**

- **Segmentation → position**
- **Depletion depth → efficiency**
- **$(W_{Depletion} = \{2\rho\mu\varepsilon(V_{ext} + V_{bi})\}^{½})$**

Resistivity

Mobility

Applied Voltage

Pitch ~ 50μm

p$^+$ in n$^-$

Resolution ~ 5μm

- **~80e/h pairs/μm produced by passage of minimum ionising particle, 'mip'**

17
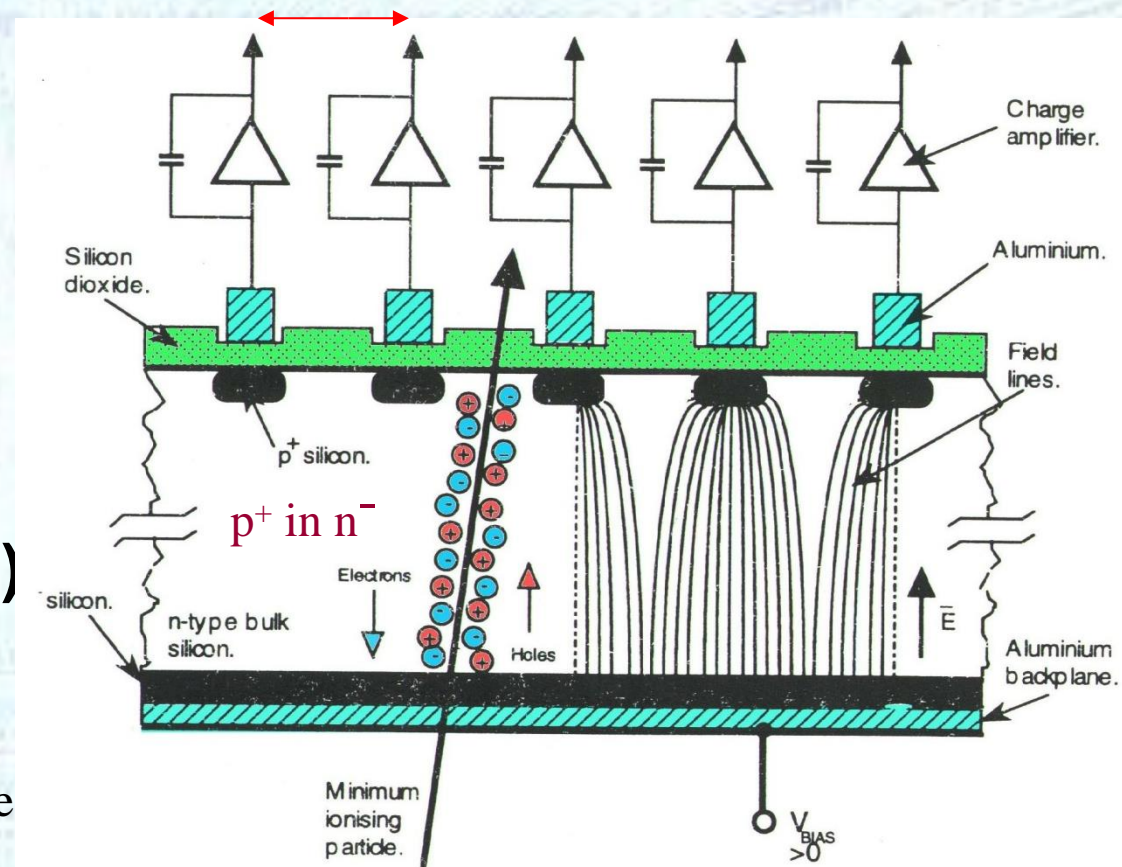
Highly Segmented Silicon Detectors

- Nearly all early applications of silicon micro-strip detectors were to detect and measure particles with pico-second (10^{-12}) lifetimes such that (taking account of special relativity) $\beta\gamma c\tau \geq 300\mu m$

- This meant the primary goal was to locate primary (collision) and secondary
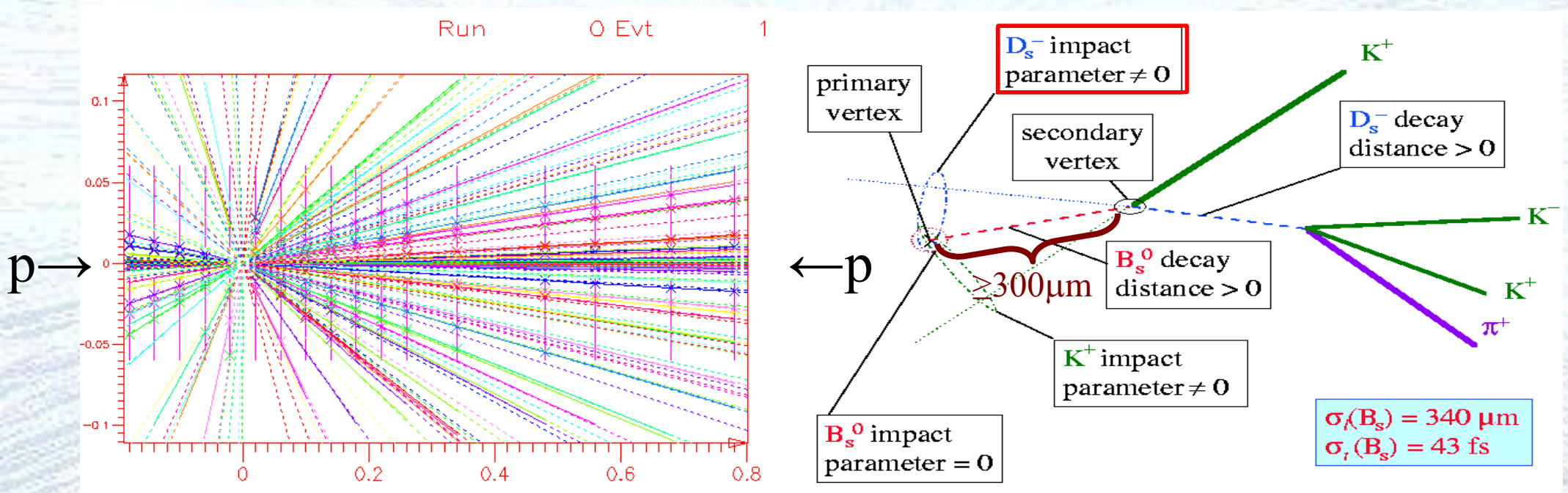
- A key limitation in tracking comes from the tracker material itself

Multiple scattering: $\theta_{rms} = \dfrac{13.6\text{MeV}}{\beta cp} z \sqrt{\dfrac{x}{X_0}} \left(1 + 0.038 \ln\left(\dfrac{x}{X_0}\right)\right)$ x material thickness X_0 radiation length
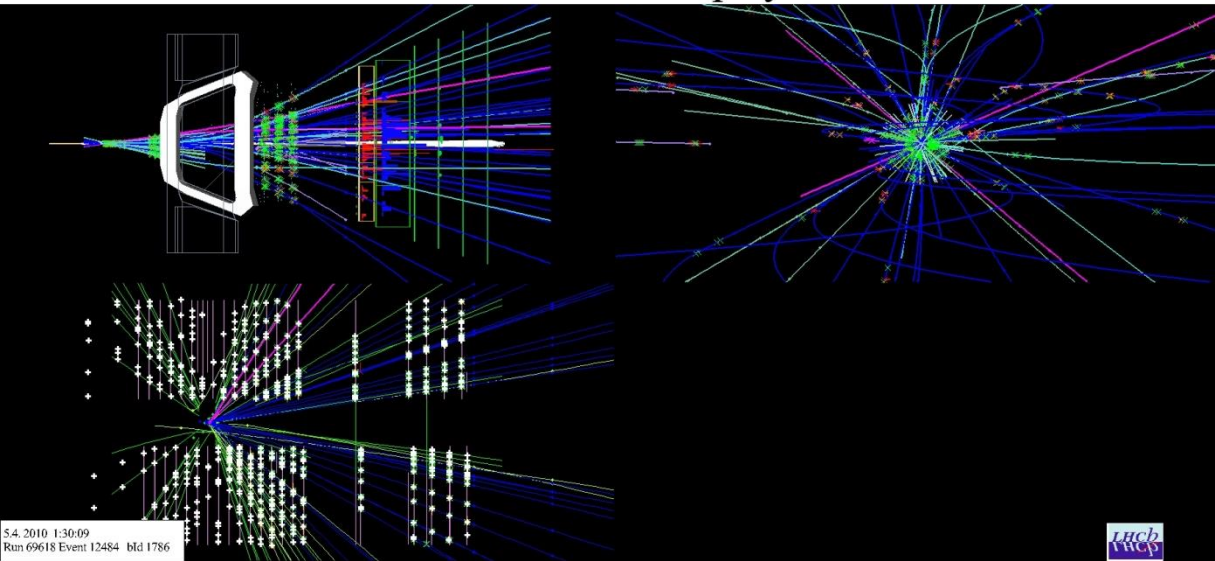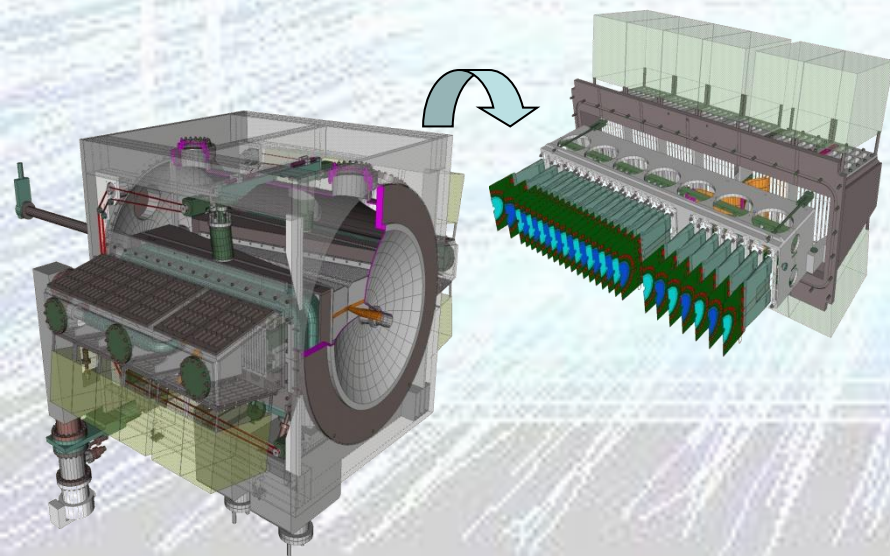
LHCb Vertex Locator: VELO
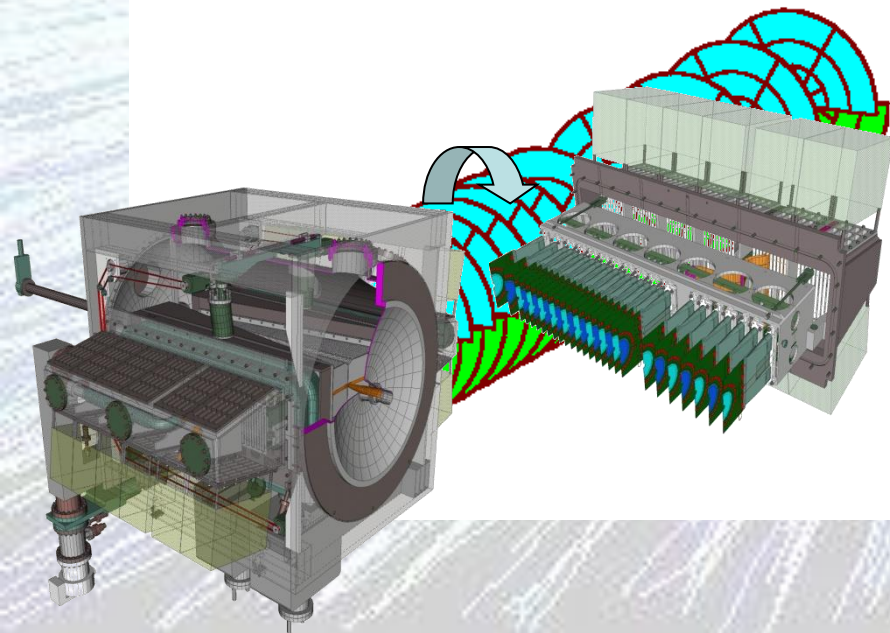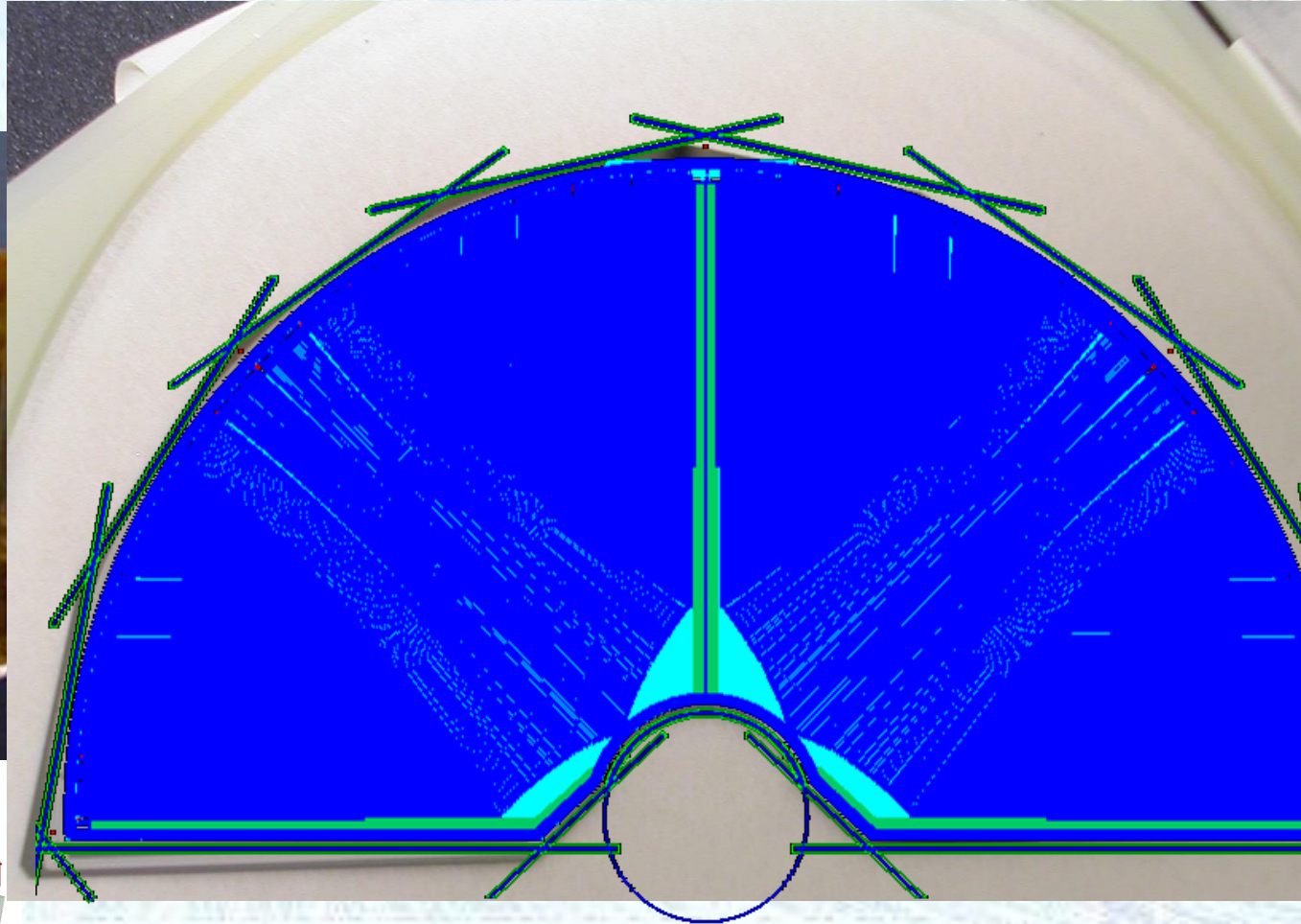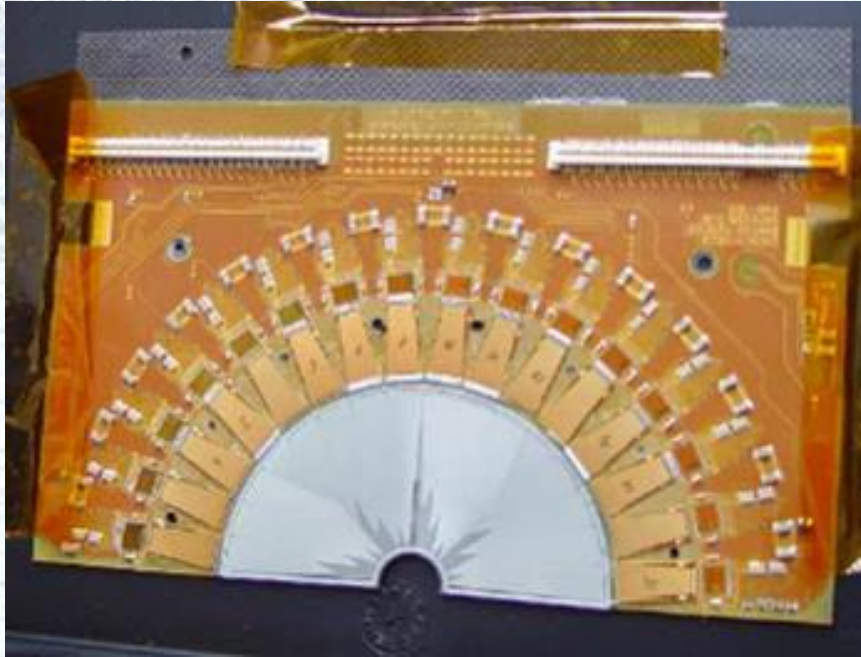
At the LHC B-mesons are mostly produced in pairs going predominantly near the beam axis (forward region)
LHCb observes 10^{12} b-pairs /year and the detector is optimized to study B-mesons and record as many rare decays as possible.
B decays are identified using the fact that their lifetime of 10^{-12} s makes it possible (with accurate enough tracking) to see that some tracks come from a displaced vertex.

LHCb Vertex Locator: First B Event
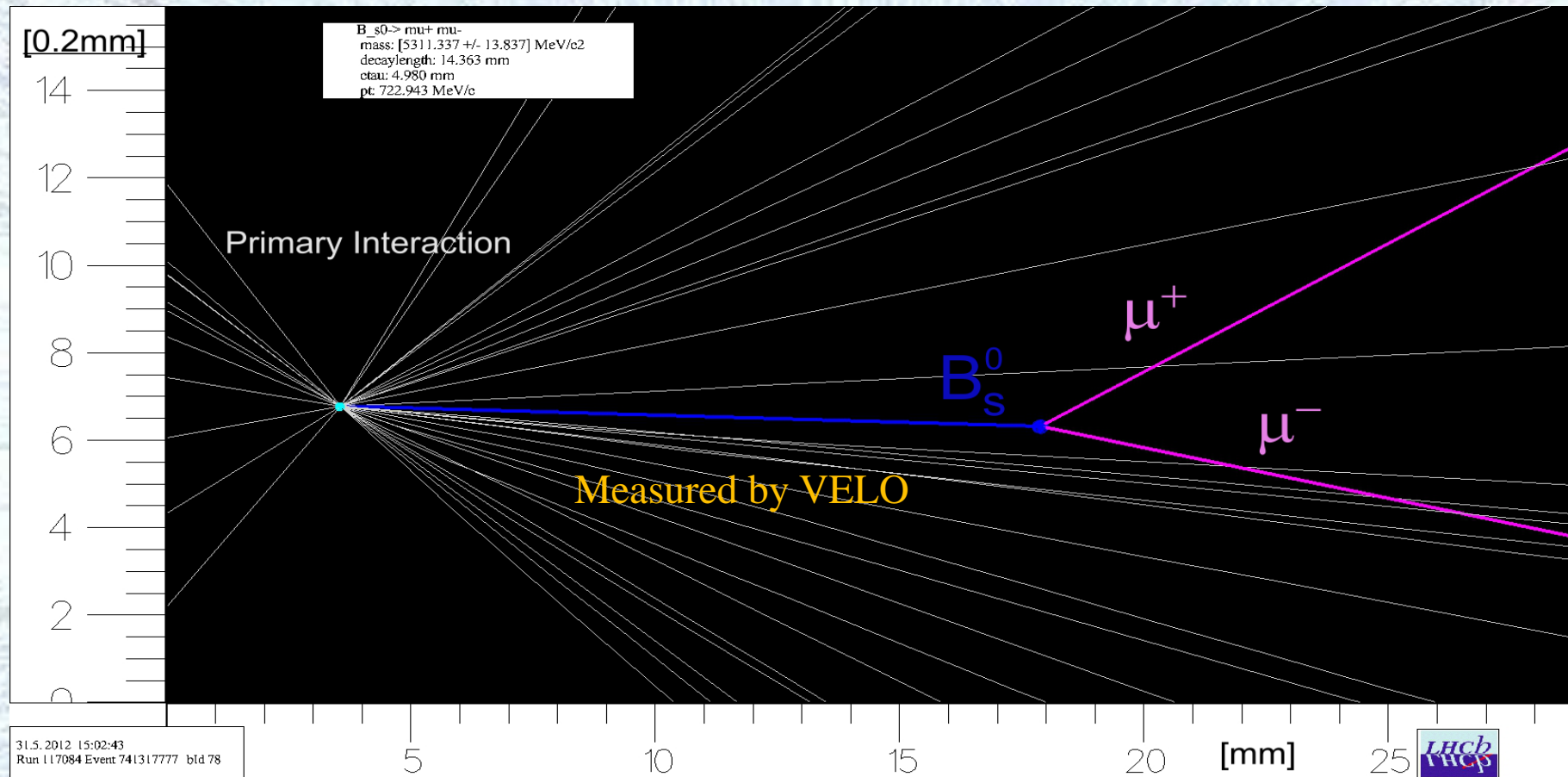
LHCb Event Display

$B^+ \rightarrow J/\Psi K^+$

XY Projection

[mm]

Tracks from primary vertex

Primary vertex

B^+

μ^+

B decay vertex

J/Ψ

K^+

μ^-

5.4. 2010 1:30:09
Run 69618 Event 12484 bId 1786

$\mathbf{B_s^0}$ impact
parameter = 0

Tracks from PV are forced to come from PV

At the LHC B-mesons are mostly produced in pairs going predominantly near the beam axis (forward region)
LHCb observes 10^{12} b-pairs /year and the detector is optimized to study B-mesons and record as many rare decays as possible.
B decays are identified using the fact that their lifetime of 10^{-12} s makes it possible (with accurate enough tracking) to see that some tracks come from a displaced vertex.
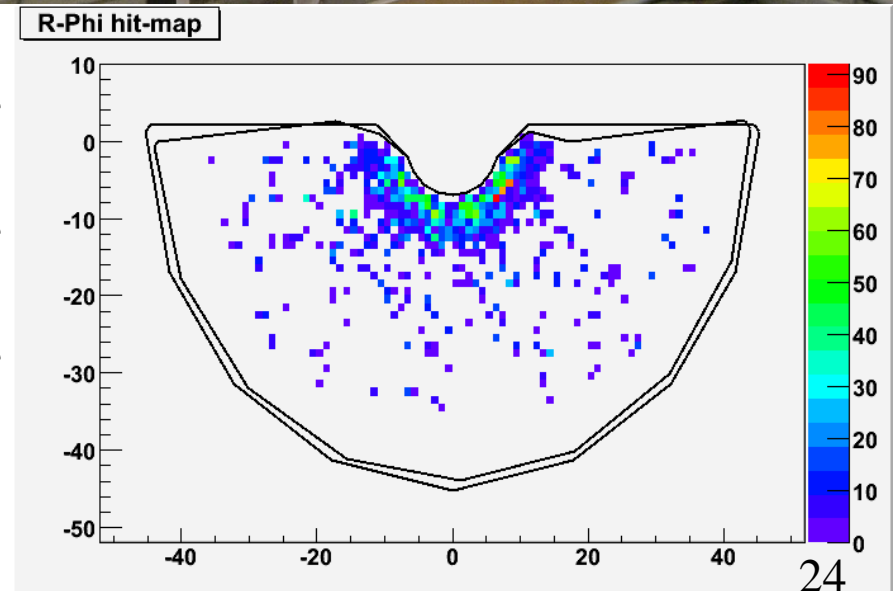
20

LHCb Vertex Locator: $B_S \to \mu\mu$

B_s0-> mu+ mu-
mass: [5311.337 +/- 13.837] MeV/c2
decaylength: 14.363 mm
ctau: 4.980 mm
pt: 722.943 MeV/c

[0.2mm]

Primary Interaction

B_S^0

Measured by VELO

μ^+

μ^-

31.5.2012 15:02:43
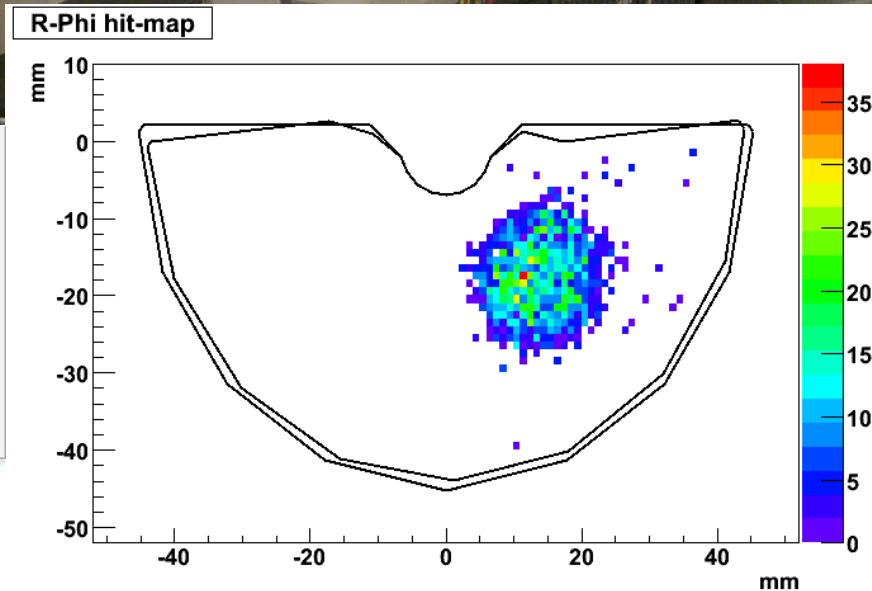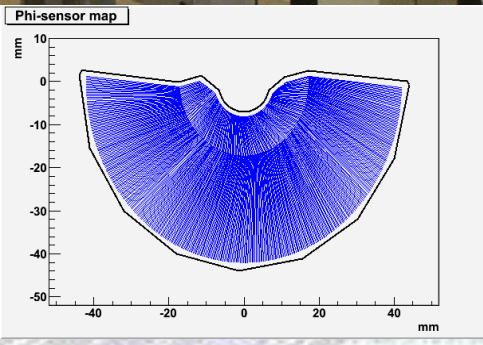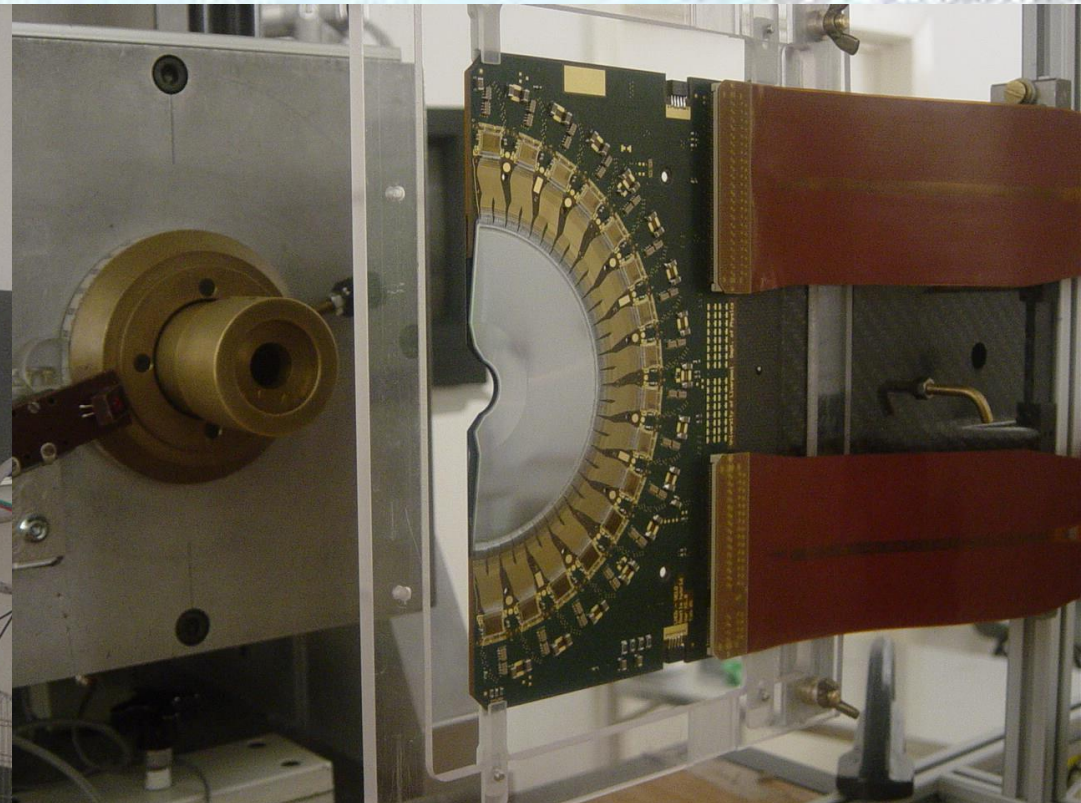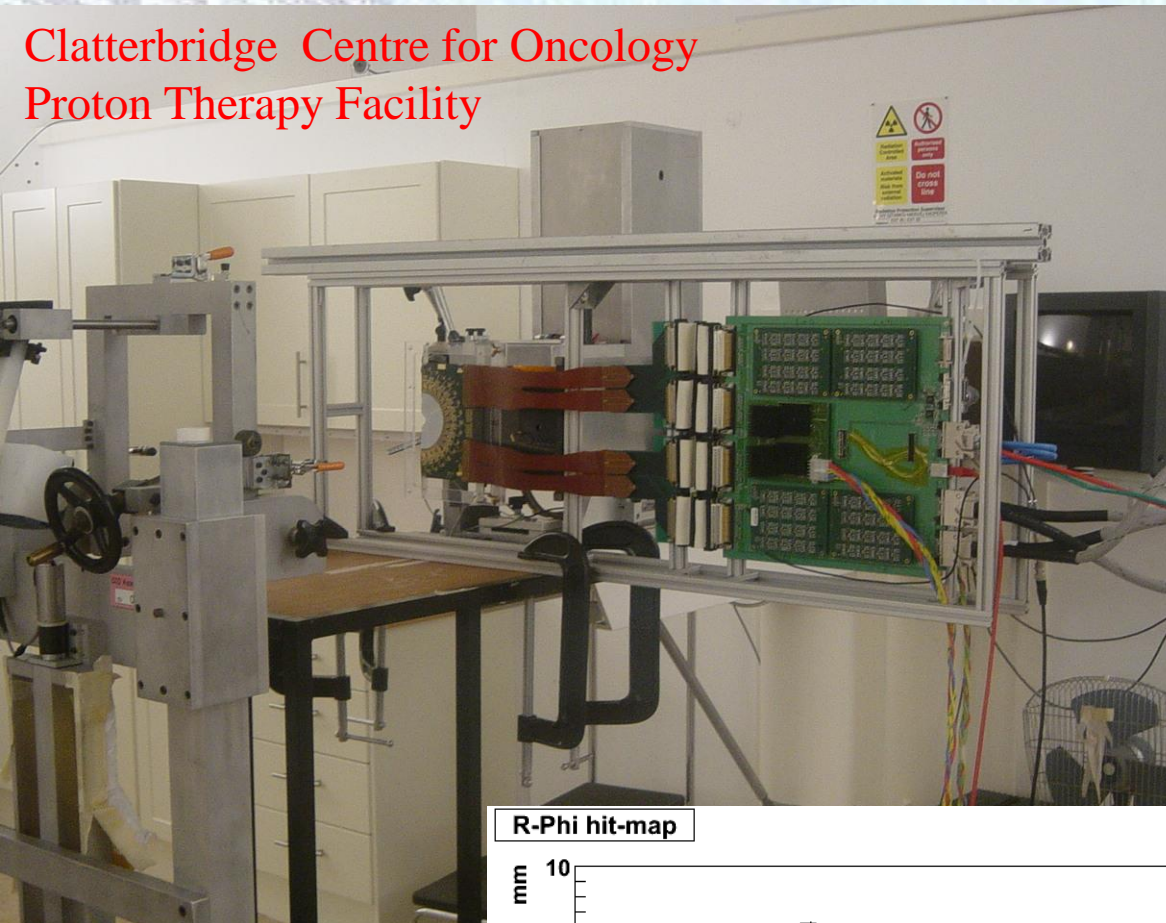Run 117084 Event 741317777 bld 78

[mm]

Measuring decays fractions at 10^{-9} level to give sensitivity to subtle effects that can be predicted by new physics
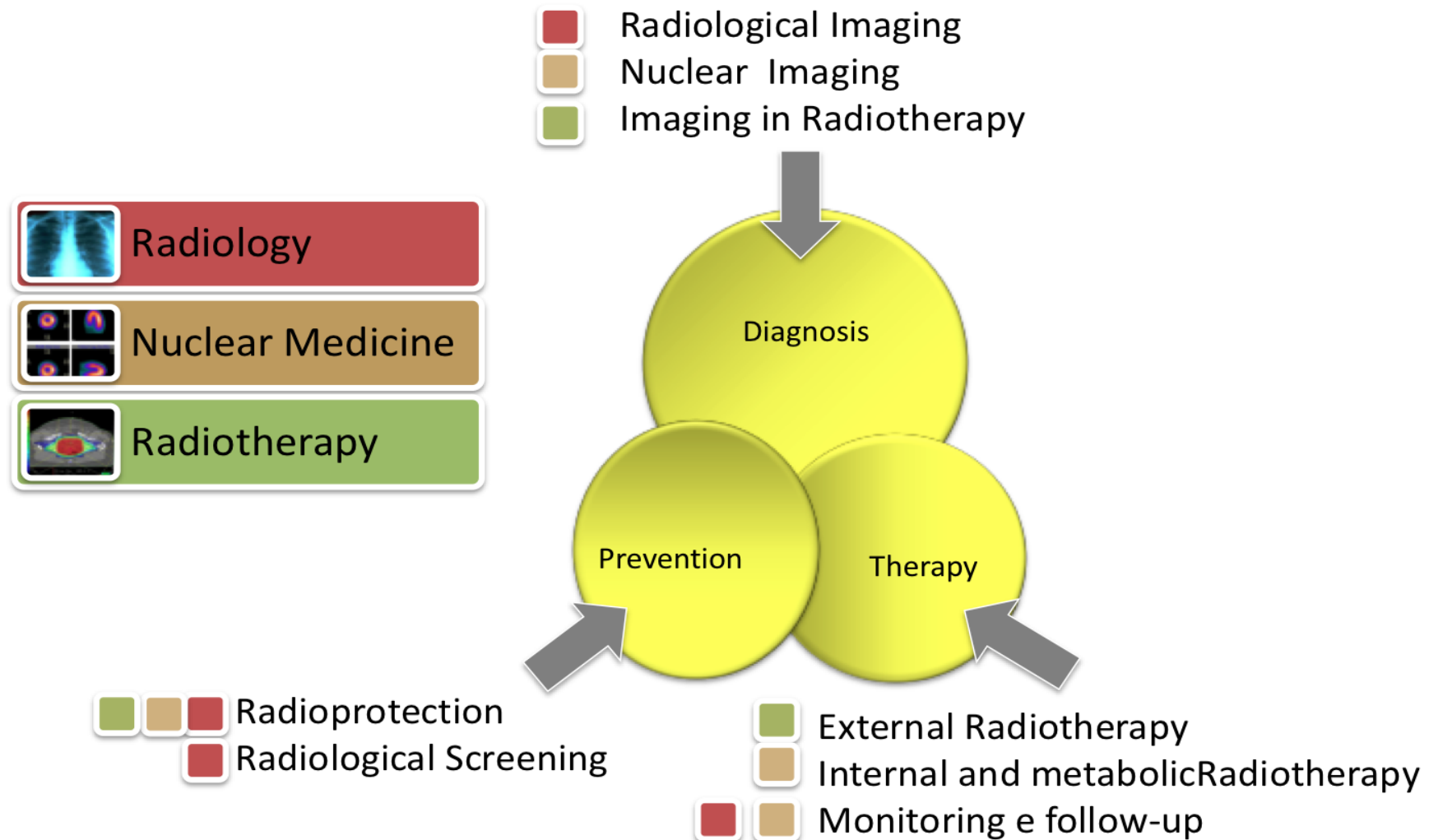
21
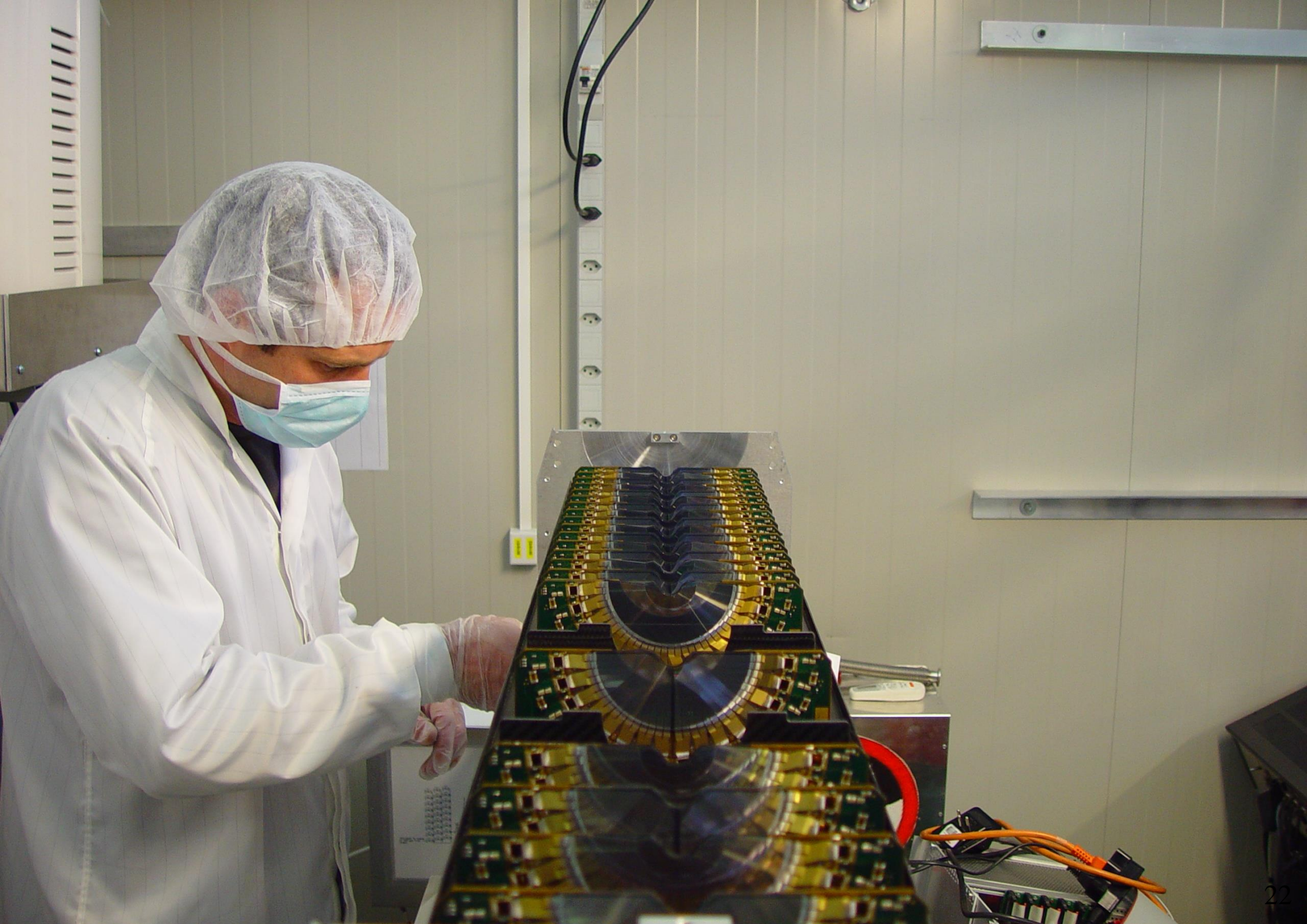
LHCb Vertex Locator: Beam Halo Monitor

Clatterbridge Centre for Oncology
Proton Therapy Facility

LHCb Back-to-Back
Sensor Module

Medical Imaging Today

Radiological Imaging
Nuclear Imaging
Imaging in Radiotherapy

Radiology

Nuclear Medicine

Radiotherapy

Diagnosis

Prevention

Therapy

Radioprotection
Radiological Screening

External Radiotherapy
Internal and metabolicRadiotherapy
Monitoring e follow-up

Different Points of view

- **Medical point of view**
  - Application driven
  - Diagnosis or intervention
  - Morphological/functional /combined imaging
  - Parameter requirements (size, spe... contrast... dose..)
  - Workflow

And the economical point of view…

  - ...view
  - Technology driven
  - Wavelength (X-rays, gamma rays, Visible light, NIR, Terahertz…)
  - Feasibility determined by available sources, materials, electronics, computing power

26
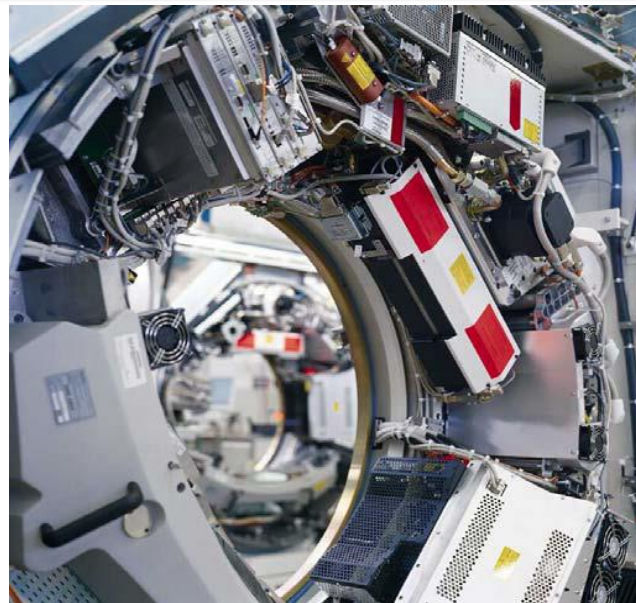
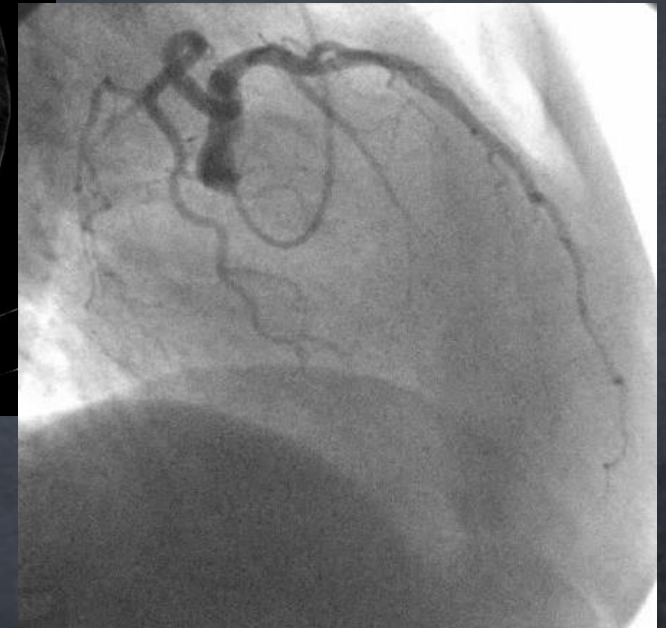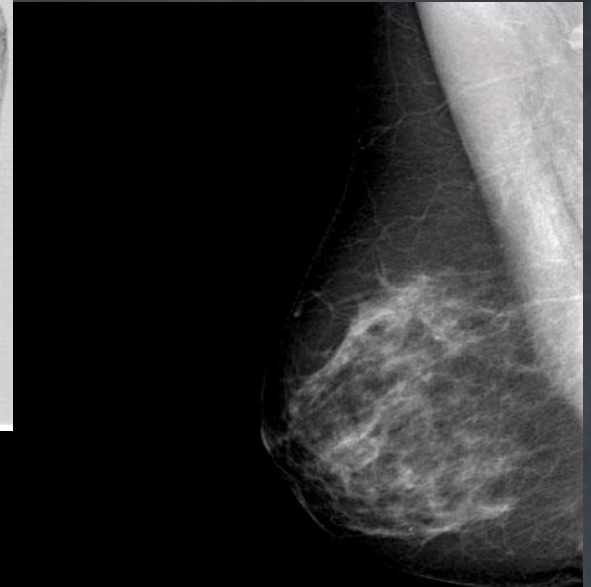## Radiological Imaging

General radiography

Angiography

Digital Subtraction Angiography (DSA)

Mammography

Computed Tomography (CT)

Cardiology (fluoroscopy)

M. Giuseppina Bisogni, Pisa University and INFN Pisa

Requirements for X-ray detectors

	Radio-graphy	Angio-graphy	Mammo-graphy	Biopsy	CT
Detector size (cm^2)	43 x 43	30 x40	18 x 24 24 x 30	5 x 9	4 x 70 (curved)
Pixel (μm)	125–165	150–400	50–100	<50	500
Resolution	12 bits	12 bits	12 bit	16 bit	20 bit
Frame rate	Single shot < 1 s	< 2-30 f/s 15-60 f/s (cardio)	Single shot < 1s	Single shot < 1 s	2000-6000 f/s

Digital Radiography Today

- aSi:H Flat Panels technology firstly introduced in early '90s

- First devices commercially available in 2000 (GE Senographe)

- State-of-the-art X-ray imaging is done with flat-panel detectors (aSi:H or aSe, TFT read-out)
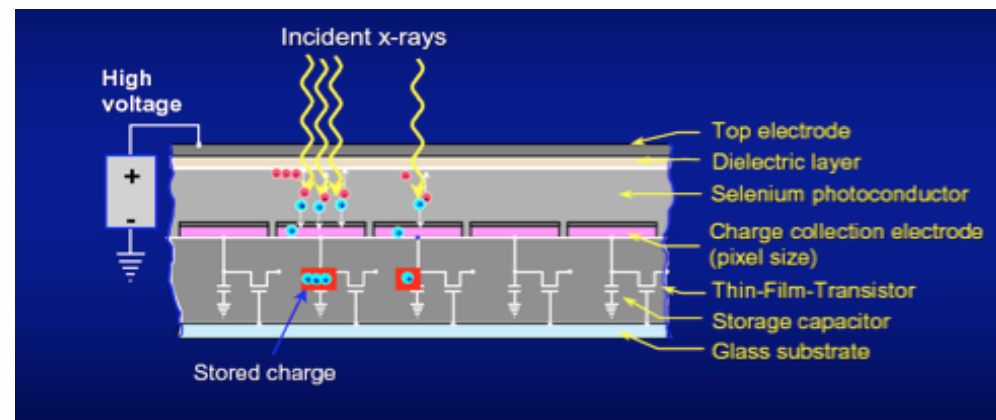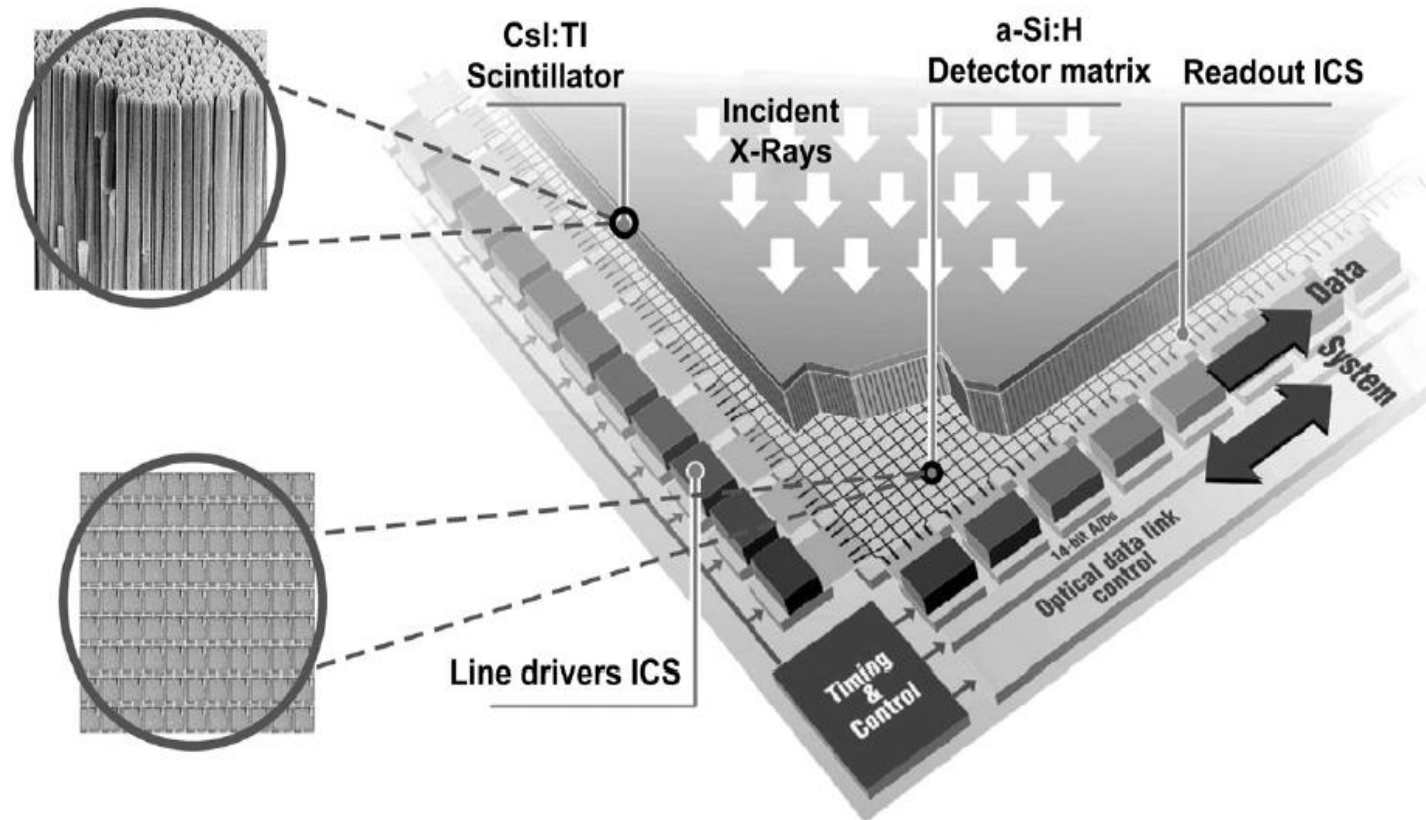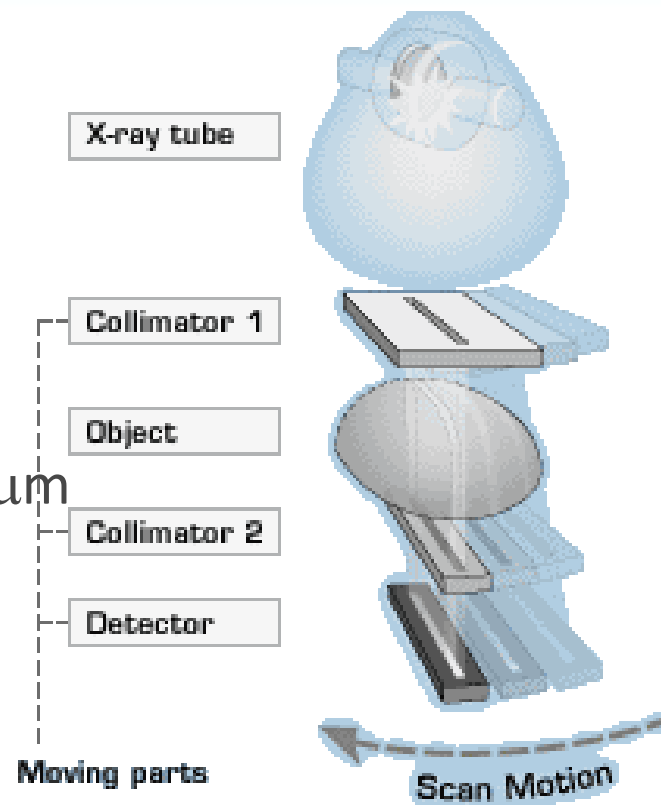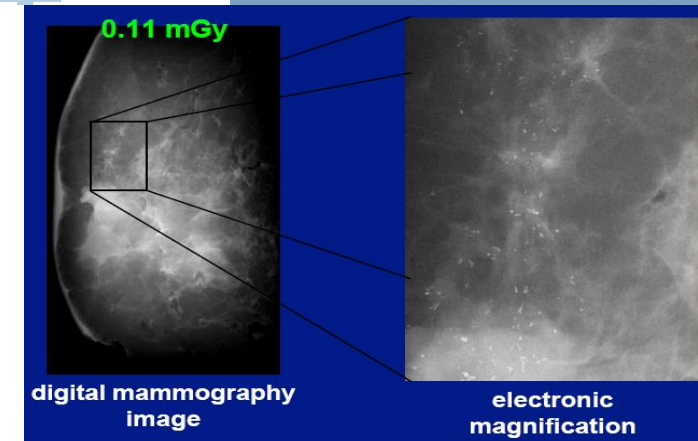
Sectra MicroDose™

Now Philips MicroDose

Mammography

- – Si strip detectors, 768 strips, 50 μm pitch, 21 detector rows
- – slight fan-out (to compensate beam divergence), 2 cm long
- – 500 μm thick
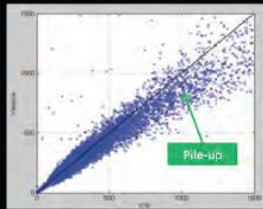- – "quasi" edge-on (4º- 4.5º tilt angle)
- – ~90% efficiency @ 30 keV

X-ray tube

Collimator 1

Object

Collimator 2

Detector

Moving parts

Scan Motion

- • ASIC:
- • 128 channels
- • counting rate per pixel: >1 MHz

0.11 mGy

digital mammography image

electronic magnification

M. Giuseppina Bisogni,
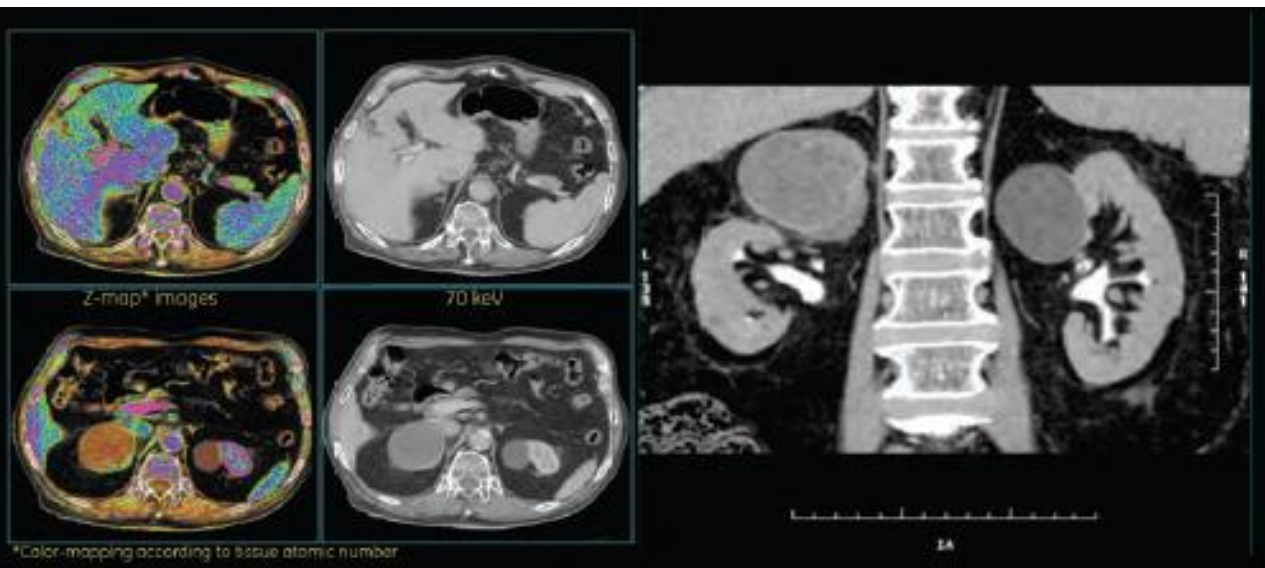Pisa University and INFN Pisa

Low Dose CT

Experimental validation of photon counting vs. conventional CT acquisition. The impact of "zero electronic noise" is apparent in ultra-low dose CT acquisitions.

At high doses the "pile-up" effect makes counting individual photons difficult and lowers efficiency of photon counting detector.

Color Imaging

Photon Counting Prototype Clinical Study: Full FOV abdominal imaging. Improvements in material decomposition allow for Z-map images that are color coded according to tissue atomic number. Efficient energy separation allows for true mono-energetic images.

By *Tibor Duliskovich, MD, Medical Director CT, GE Healthcare* "Photon Counting: A New CT Technology Just Over the Horizon", 2011

31

Requirements for Medical Imaging

(With many thanks to **Juan José Vaquero**, Departamento de Bioingeniería e Ingeniería Aeroespacial, Universidad Carlos III de Madrid for his help with these slides)

Here focus on radiation detectors for medical imaging: mainly gamma-rays for PET and SPECT, although some of the ideas may apply to x-ray imaging

Three specific drivers discussed here:

1. Better specifications
2. Multimodality
3. Real-time imaging

There are many other generic drivers, but those apply to all the fields, not just medical imaging (cost, size, power requirements…)
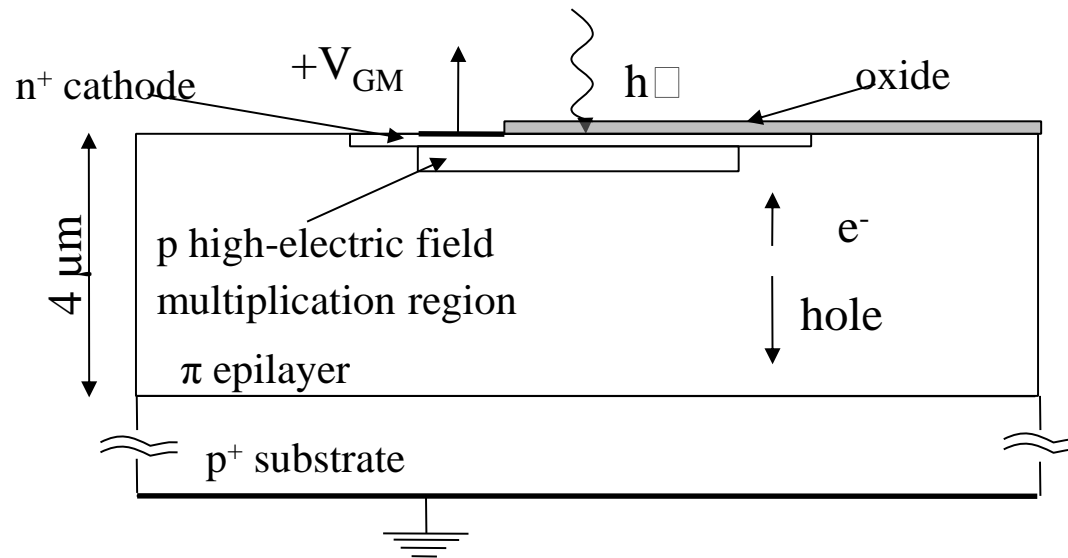
1st driver: Need for Better Specifications

- **GRANULARITY: the higher the granularity the better the sensitivity, resolution (space, energy and time)**

- **Best detector:**
  One (scintillator) crystal for one photodetector for one signal channel
- **Positron range in biological tissue is the limiting factor in maximum spatial resolution. This means it should be possible to use that less that one mm square crystals. A typical preclinical (rodents) PET scanner may have a 10 cm axial FOV and a 10 cm transaxial FOV. If the detectors were placed just at the edge of the FOV, then we will need more than 31 thousand detector channels.**

- **Although this may be doable in HEP experiments, at least for preclinical systems, these should be "table-top" instruments. Unless these detectors are miniaturized and the their data is processed in real time, the resulting systems size will be unusable in a preclinical lab, not mentioning the cost.**

- **For commercial systems, some high level of on-detector data processing is also extremely advantageous.**

Silicon PhotoMultiplier: The Ultimate dream?
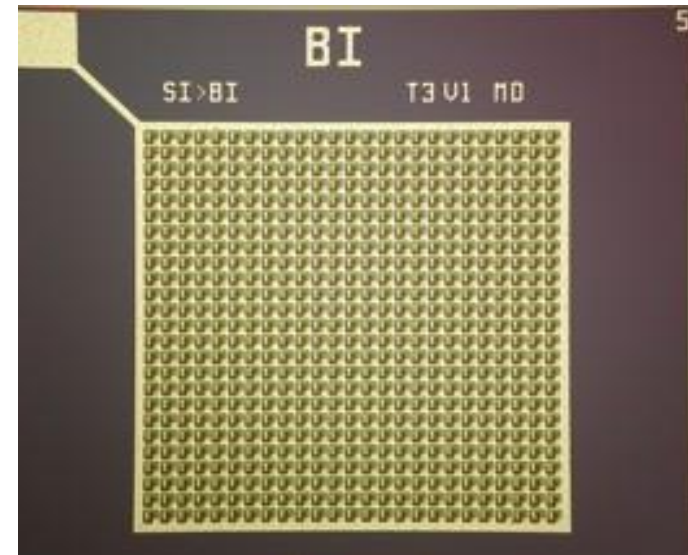
SOLID STATE PHOTODETECTOR ➔   SiPM: **Multicell Avalanche Photodiode** working in limited Geiger mode

n⁺ cathode $+V_{GM}$ h☐   oxide

p high-electric field multiplication region

π epilayer

4 μm

p⁺ substrate

e⁻

hole

- 2D array of microcells: structures in a common bulk.

- Vbias > Vbreakdown: high field in multiplication region

- Microcells work in Geiger mode: the signal is independent of the particle energy

- The SiPM output is the sum of the signals produced in all microcells fired.

-The photon is absorbed and generates an electron/hole pair

-The electron/hole diffuses or drifts to the high-electric field multiplication region

-The drifted charge undergoes impact ionization and causes an avalanche breakdown.

-Resistor in series to quench the avalanche (limited Geiger mode).

As produced at FBK-irst,Trento, Italy➔

➔**High gain** ➔**Low noise** ➔ **Good proportionality if $N_{photons} \ll N_{cells}$**

PMTs vs solid state photodetectors

|	PMT	APD	SiPM
Gain	10^5-10^7	10^2	10^5-10^6
Dynamic range	10^6	10^4	10^3/mm
Excess Noise Factor	0.1-0.2	>2	1.1-1.2
Rise time	<1 ns	2-3 ns	~1 ns
Dark current	<0.1 nA/cm^2	1-10 nA/mm^2	0.1-1 MHz/mm^2
QE @ 420 nm	25%[a]	60-80%	<40%[b]
Bias voltage	~800-2000 V	~100-1500 V	~30-50 V
Temperature coefficient	<1 %/K	2-3 %/K	3-5 %/K
Magnetic susceptibility	Very high (mT)	No	No

DPC: Front-end Digitization by Integration of Single Photon Avalanche Diodes & CMOS

analog SiPM

$(Ta=25\ °C, M=7.5 \times 10^5)$

Number of photons
1
2
3
4
5
6
7
8
9
10

Time

www.hamamatsu.com
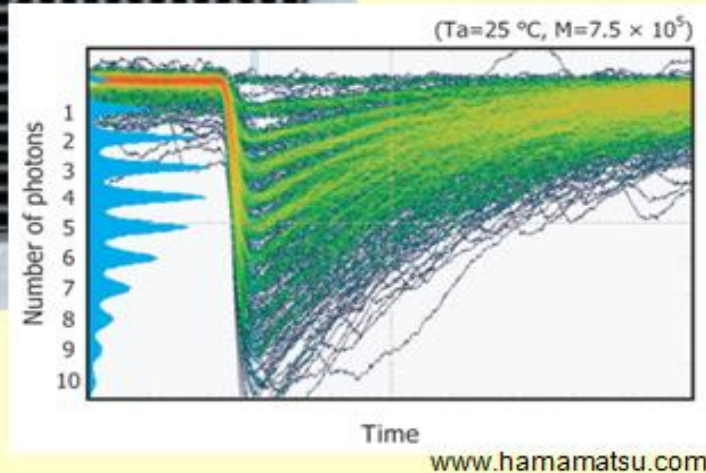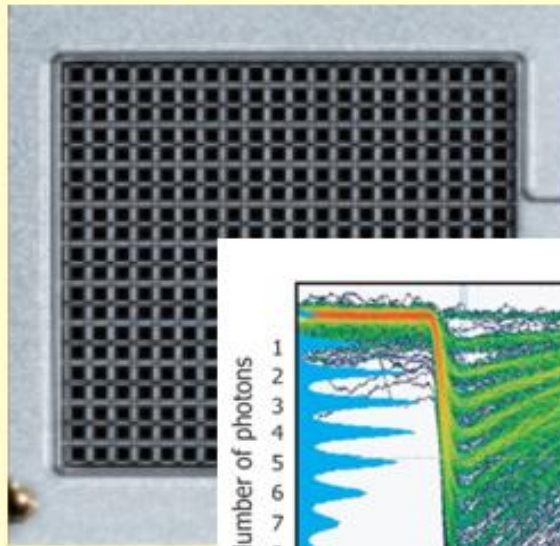
Summing all cell outputs leads to an analog output signal and limited performance

Digital Photon Counter (DPC)

TDC and photon counter

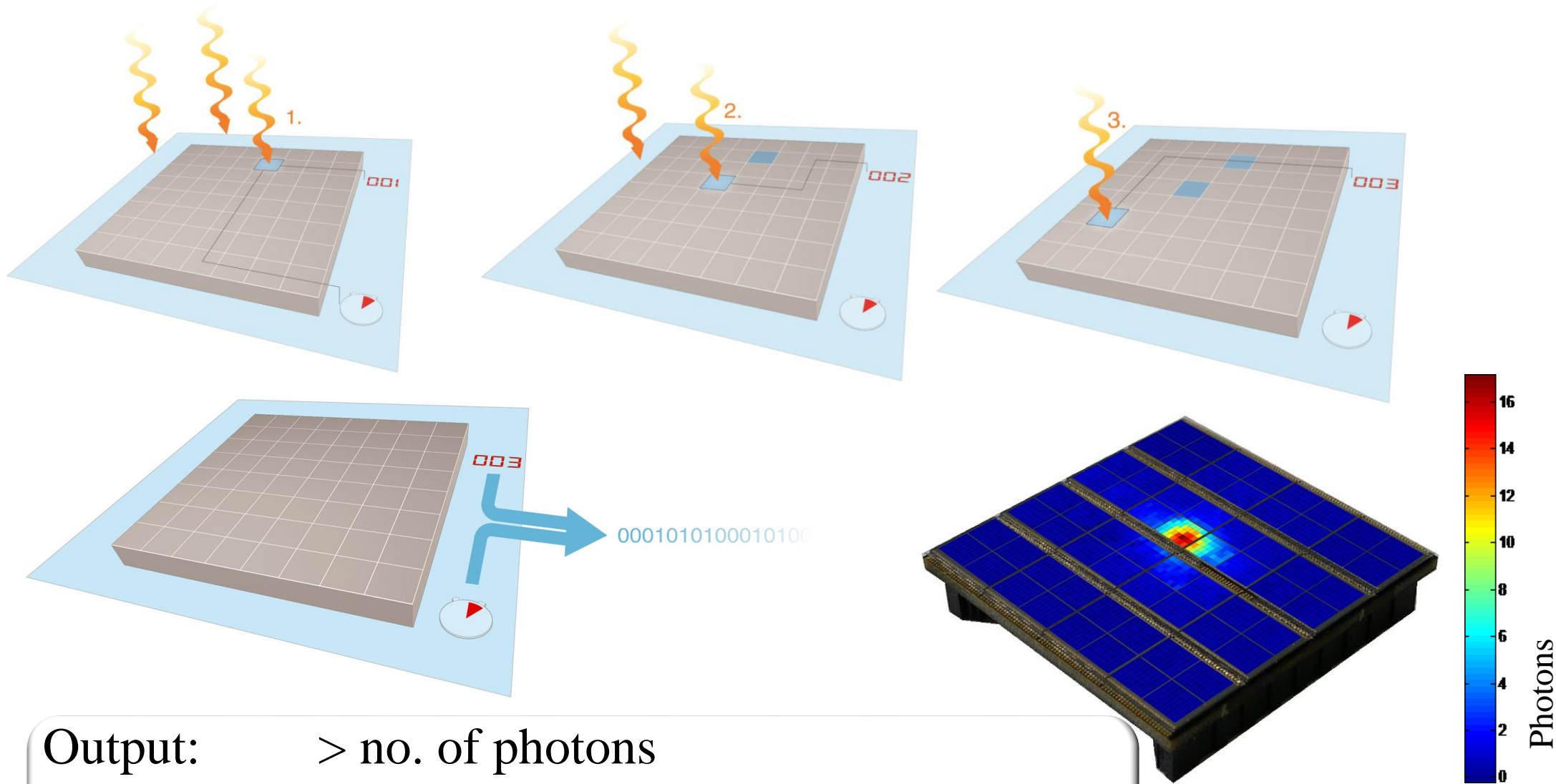Digital Cells

Digital output of
• Number of photons
• Time-stamp
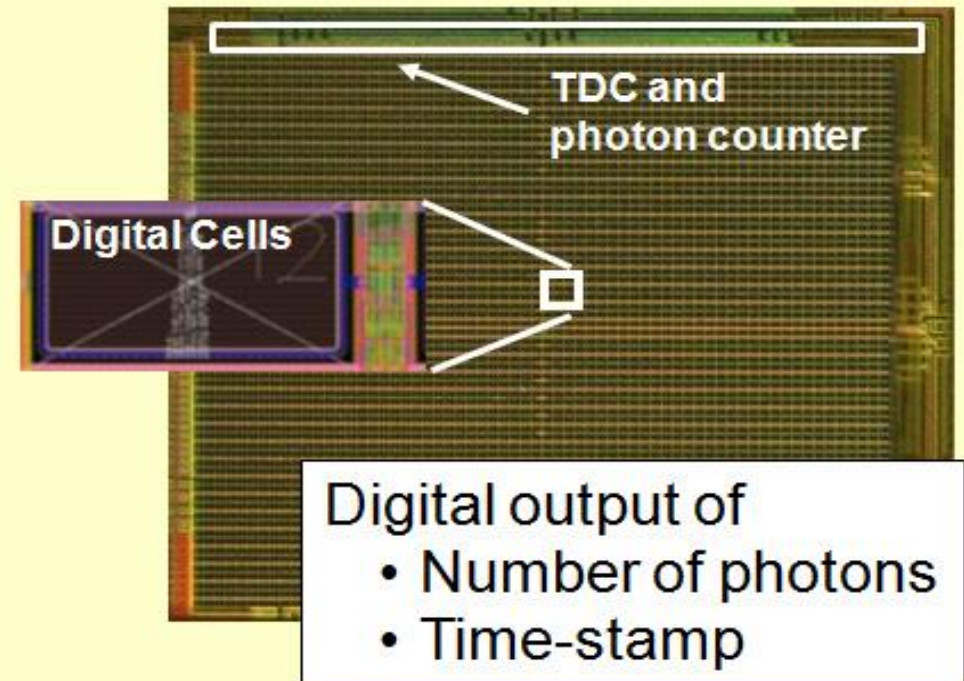
Integrated readout electronics is the key element to superior detector performance

*With thanks to **York Haemisch**, Business Development Manager. Senior Director Corporate Technologies*

DPC: Now Photons are <u>Counted</u> Directly
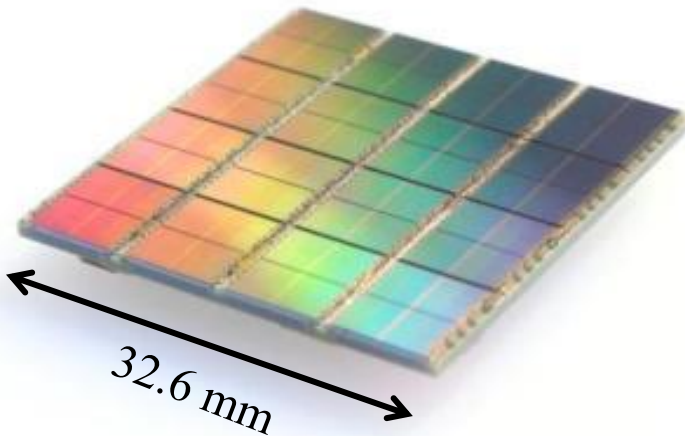

Output: > no. of photons
             > time stamp(s)
No analog post-processing necessary!

DPC is an Integrated "Intelligent" Sensor

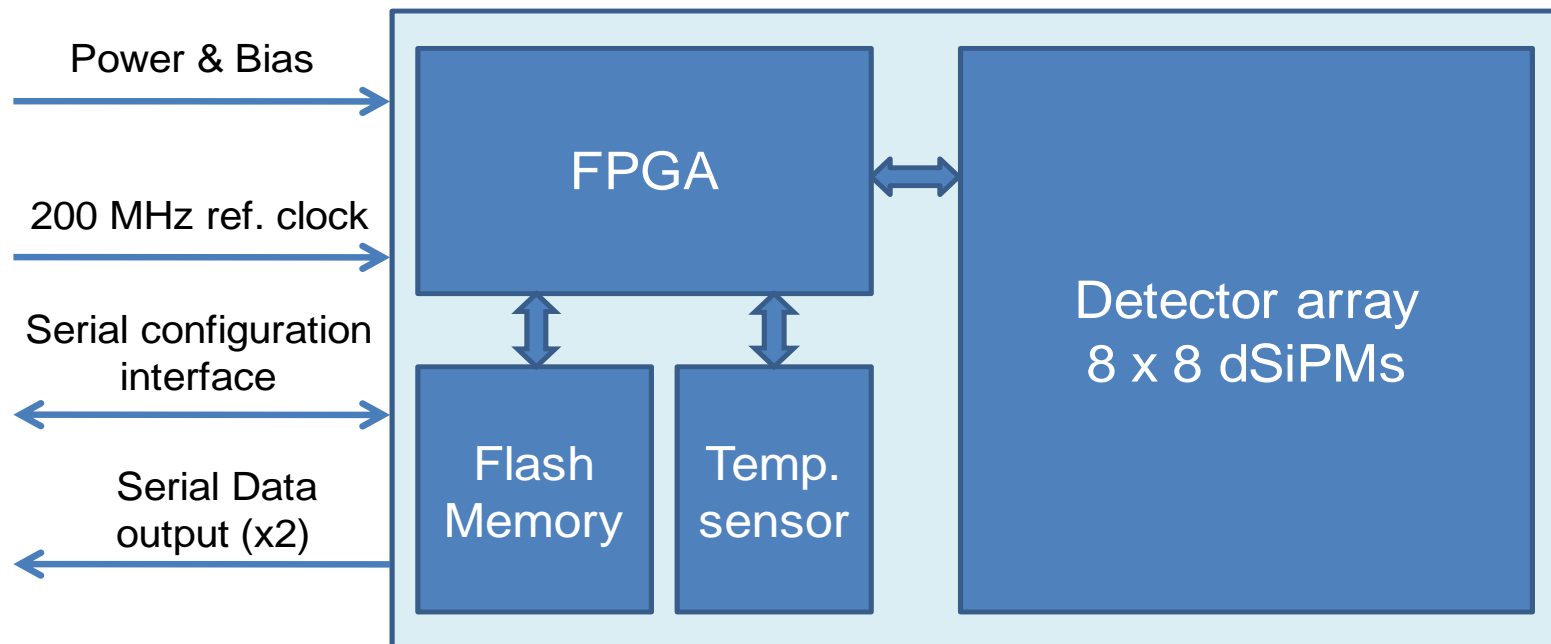DPC3200-22-44
DPC6400-22-44

32.6 mm

FPGA
- Clock distribution
- Data collection/concentration
- TDC linearization
- Saturation correction
- Skew correction

Flash
- FPGA firmware
- Configuration
- Inhibit memory maps

Power & Bias →

200 MHz ref. clock →

Serial configuration interface ↔

Serial Data output (x2) ←

FPGA

Flash Memory

Temp. sensor

Detector array
8 x 8 dSiPMs

2nd Driver: Multimodality

- Different detector technologies for different types of radiation have to share the same space and Field of View.
- They may interfere one with each other.
- This is a typical layout in which radiation PET detectors and their electronics (blue, green and red) and to share the space with the MRI RF coil and electronics. This is not yet a solved problem.
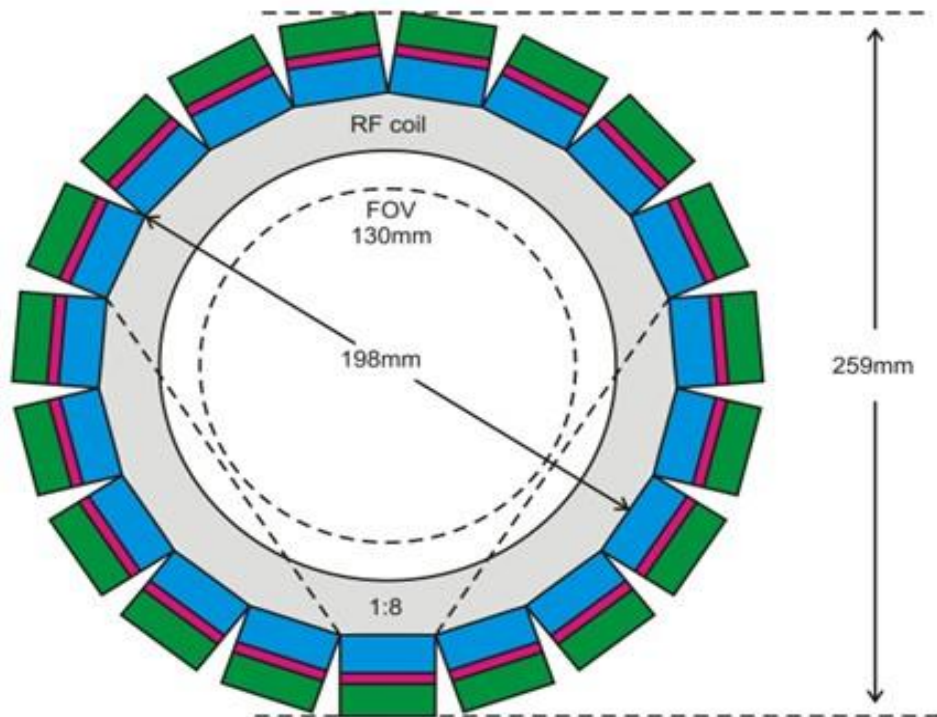
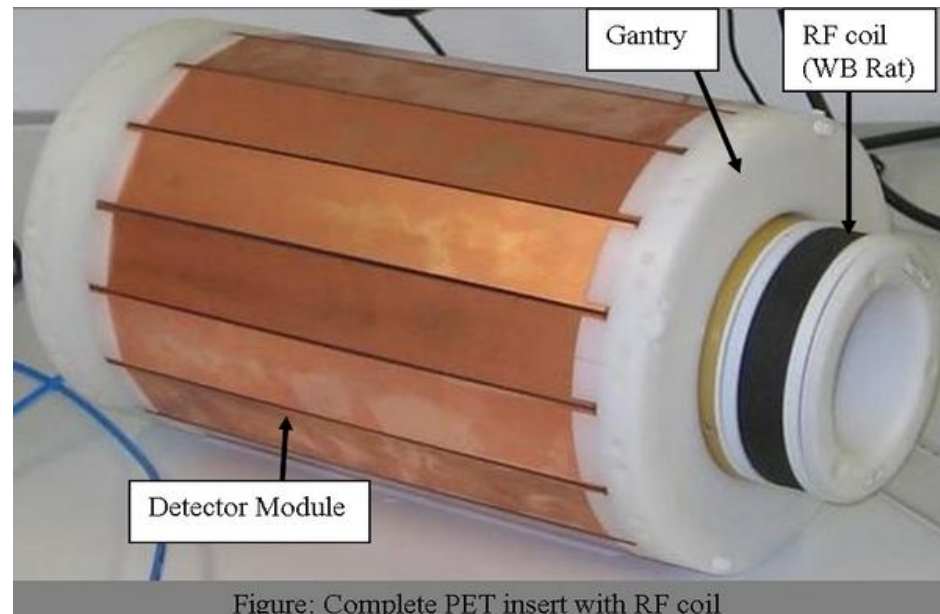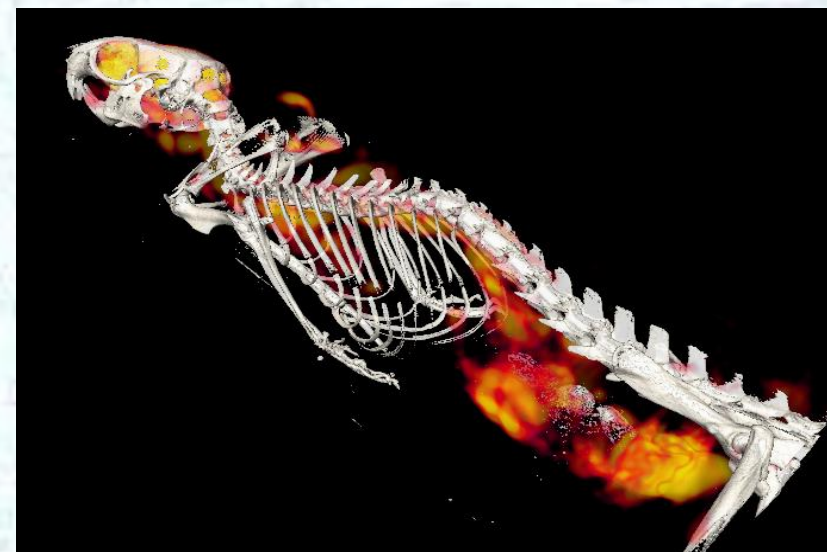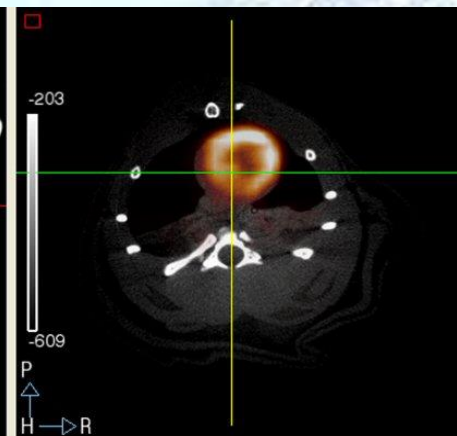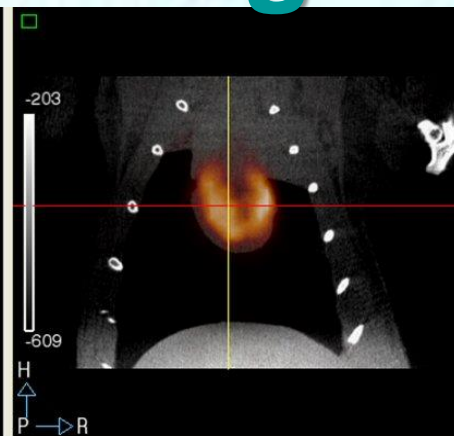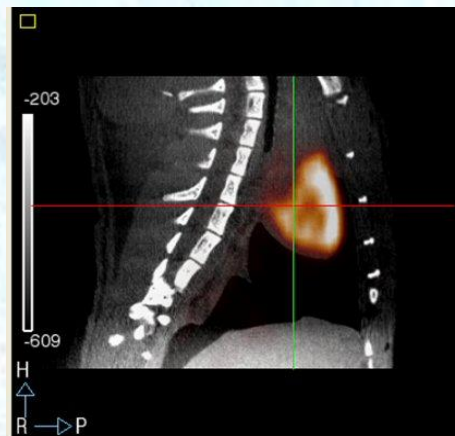PET ring for 40cm bore magnet: mice, rats and rabbits
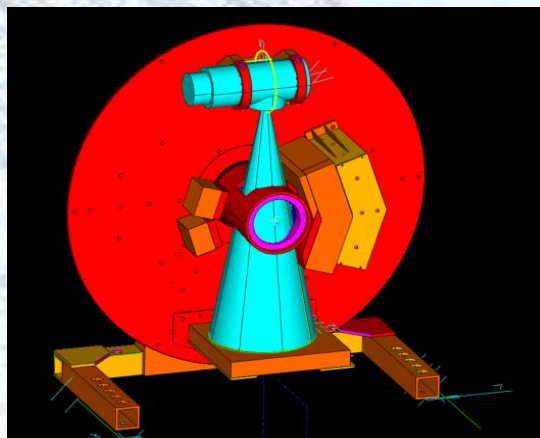
Figure: Complete PET insert with RF coil
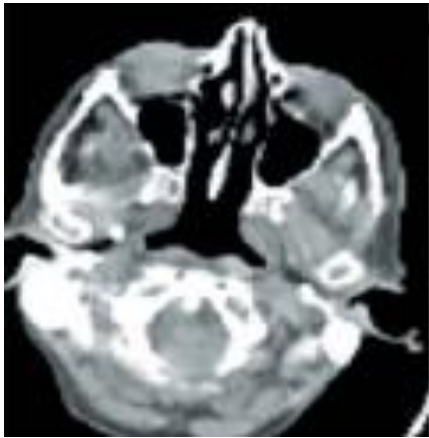
PET-CT Hybrid Systems: Preclinical Imagers
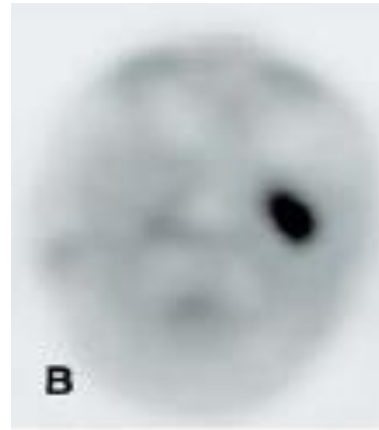

IEEE Trans Nuc Sci (2009)

Patent PCT/ES/2006/070160,

Nuclear medicine imaging techniques (PET and SPECT) and X-ray radiology are intrinsically complementary.

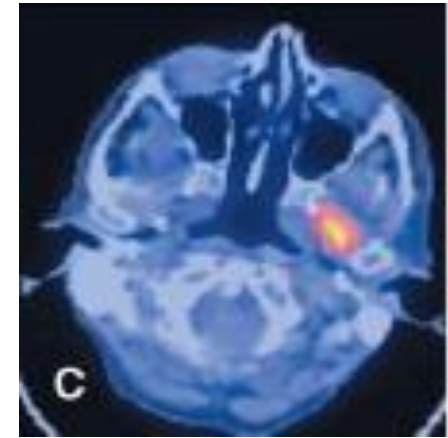| CT	PET	PET/CT

A CT image precisely displays the body's anatomy but does not reveal the body's functional chemistry

A PET scan reveals areas of abnormal activity but the exact location is unknown

The information is combined

- The history of combined PET/MR dates back to the mid 1990s even before the advent of PET/CT.

- One of the limitations of CT is the poor imaging of soft tissues

- Standalone MRI systems reveal structure and function, but cannot provide insight into the physiology and/or the pathology at the molecular level

- A combined PET/MR system provides both the anatomical images from MRI and the quantitative capabilities of PET.

TAC   PET   PET/TAC   MRI   PET   PET/MRI
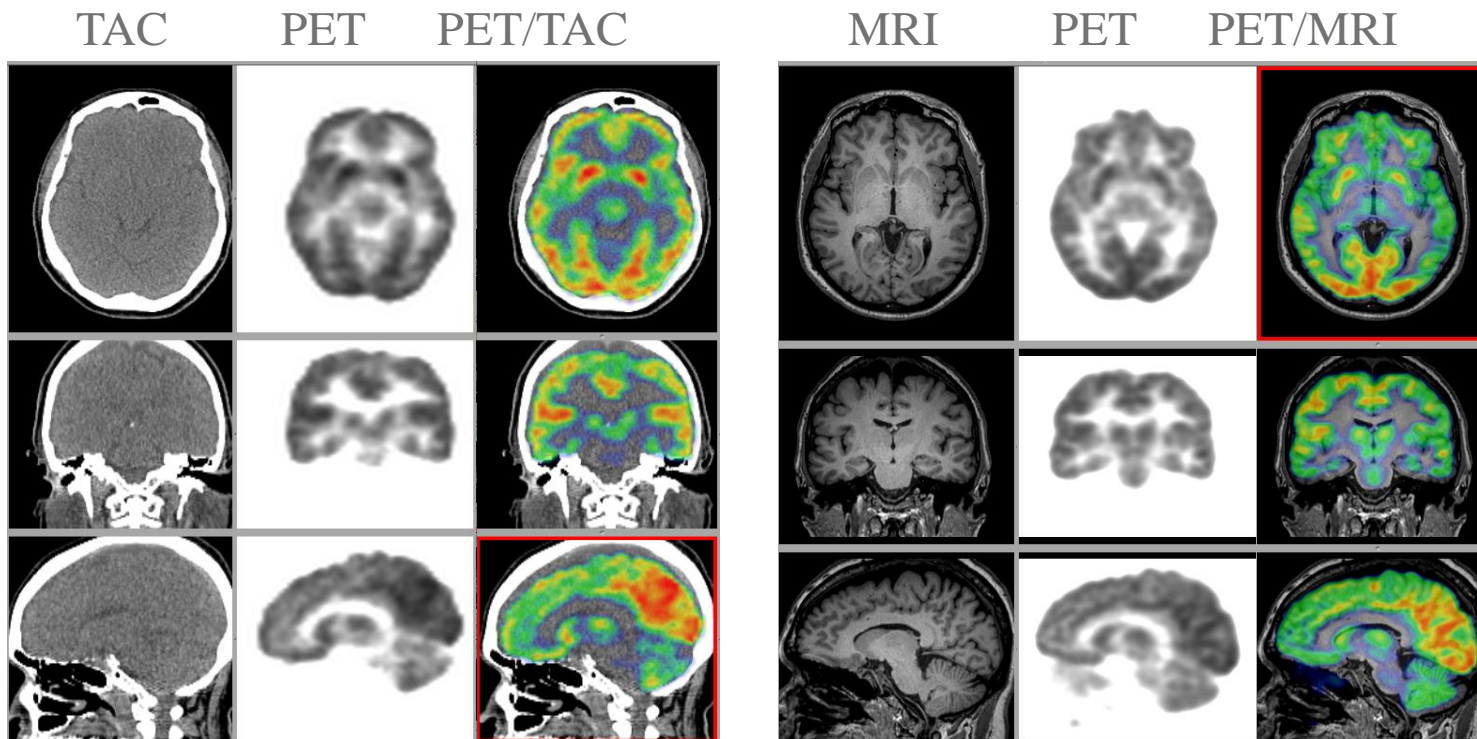
In addition, such a system would allow exploiting the power of MR spectroscopy (MRS) to measure the regional biochemical content and to assess the metabolic status or the presence of neoplasia and other diseases in specific tissue areas.

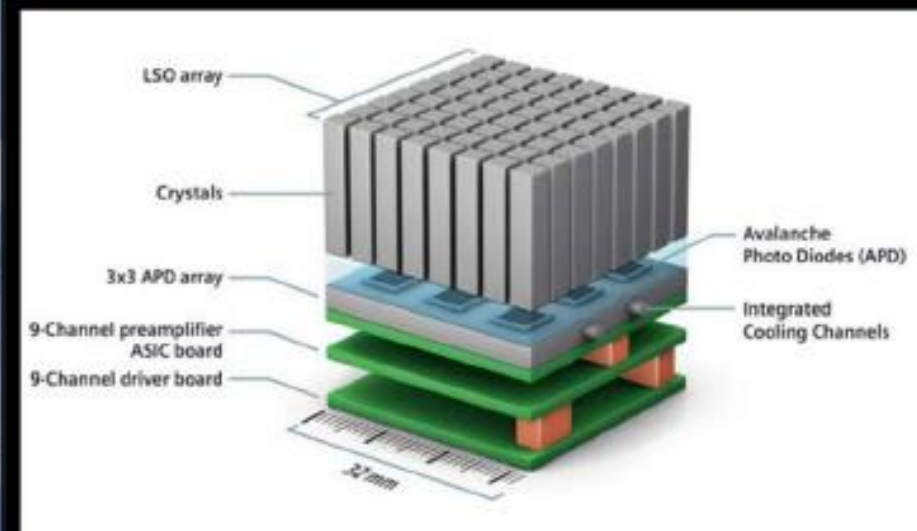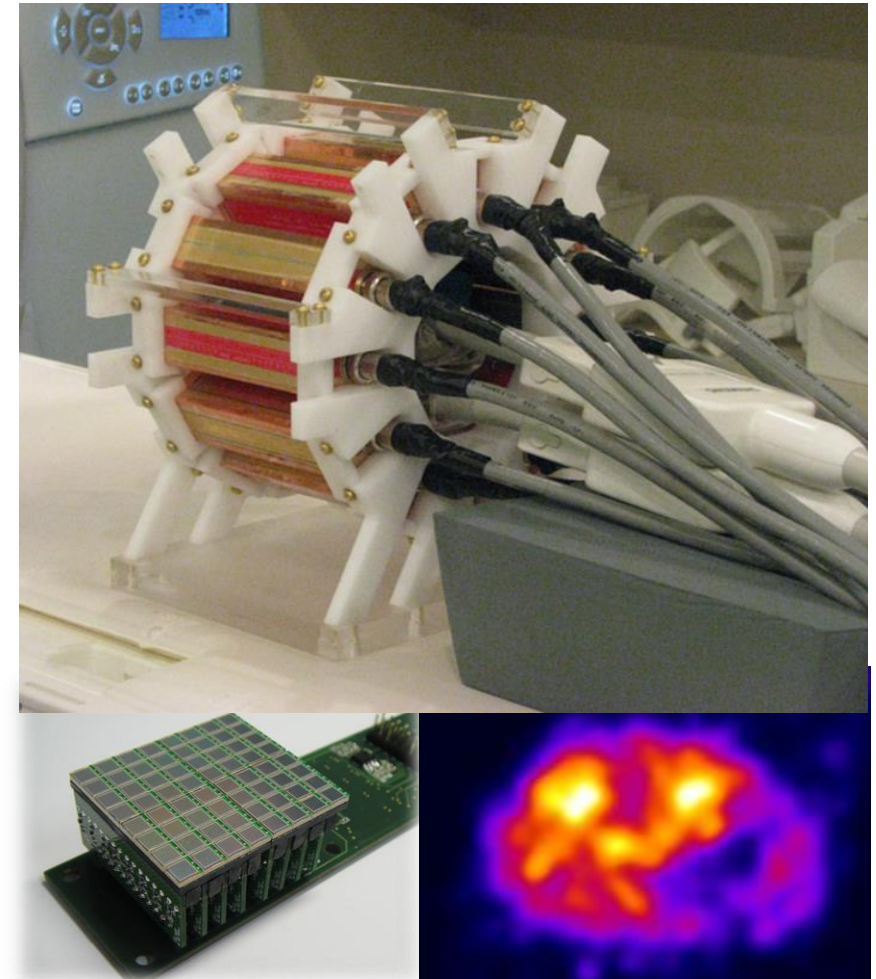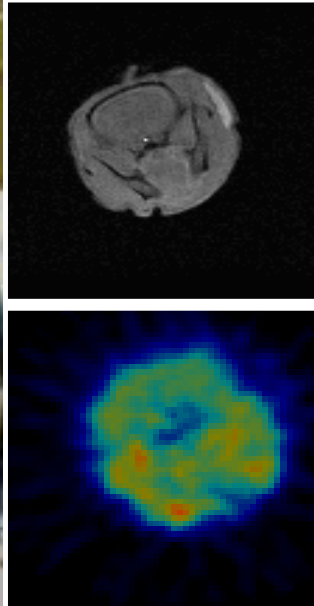# Current PET/MR Configurations

Separated Gantries
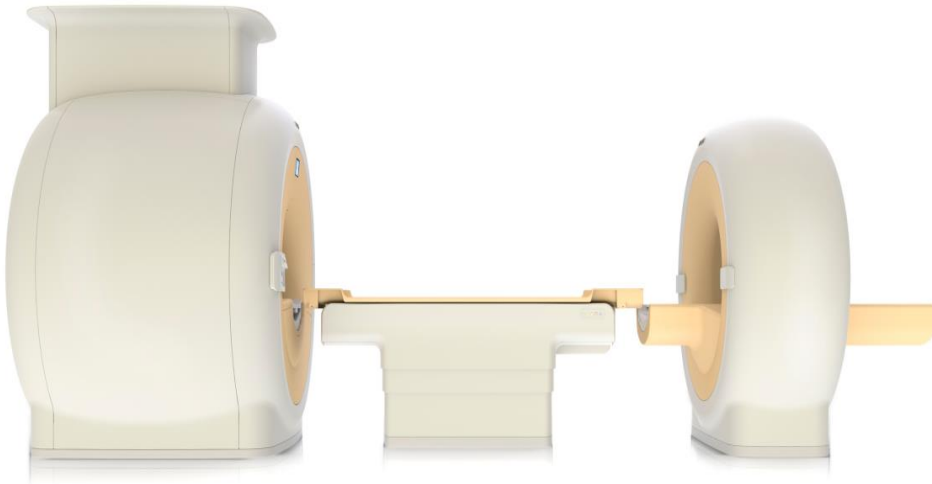
Integrated Gantries

Philips MR/PET

Siemens mMR Biograph

Siemens Biograph mMR based on APD technology

Courtesy of Seiichi Yamamoto
Kobe University

Courtesy of Jae Sung Lee,
Seoul National University

Human TOF PET/MRI based on SiPMs

Optical → Array with 22 x 22 LYSO pixels

Analog → SiPM-Tile: 4x4 monolithic SiPM arrays with 2x2 SiPMs

Analog/Digital → ASIC-Tile: 2x 32 Channel TDC/ADC

Digital → Interface-Tile: 64 channel FPGA pre-processing

Gradient   PET-Ring   Gradient
RF-Coil
RF-Screen
Magnet
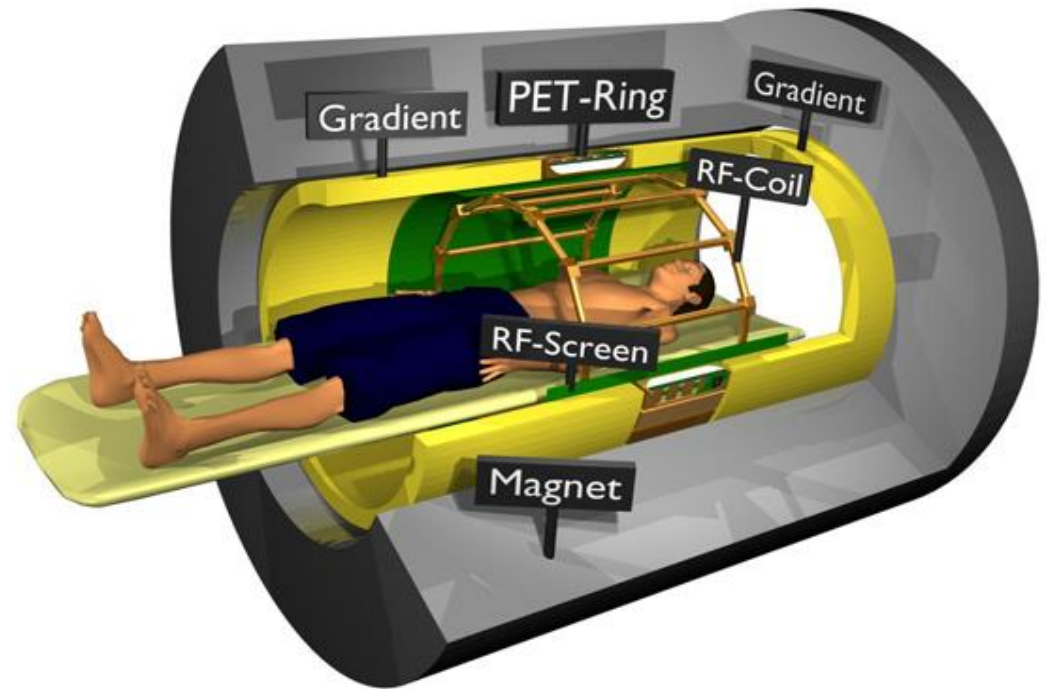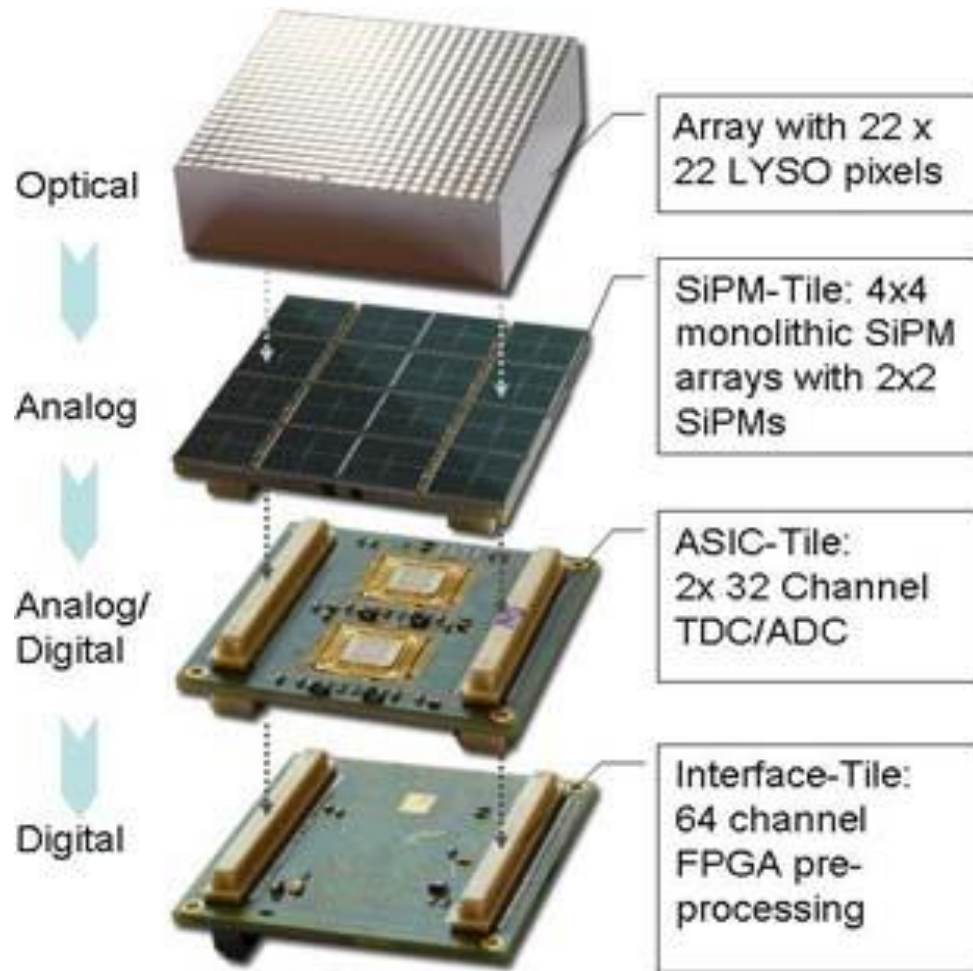
Also a dSiPM-based version

M. Giuseppina Bisogni,
Pisa University and INFN Pisa

46

3rd Driver: Real-time Imaging

- There are several in-vivo application that will benefit enormously if real-time imaging detectors where available. Here there are two examples.

- Intraoperative gamma imagers are commonly used in several surgical procedures. However, its integrations with advance applications like image-guided surgical systems requires to add real-time space tracking and co-registration with preoperative imaging.

- This is an example of a intraoperative gamma-imager that can be tracked in the operating theatre, tested with a torso phantom. It is mandatory to miniaturize the camera and boost its signal processing capabilities in order for widespread use in clinical practice.

Universidad Carlos III de Madrid

47
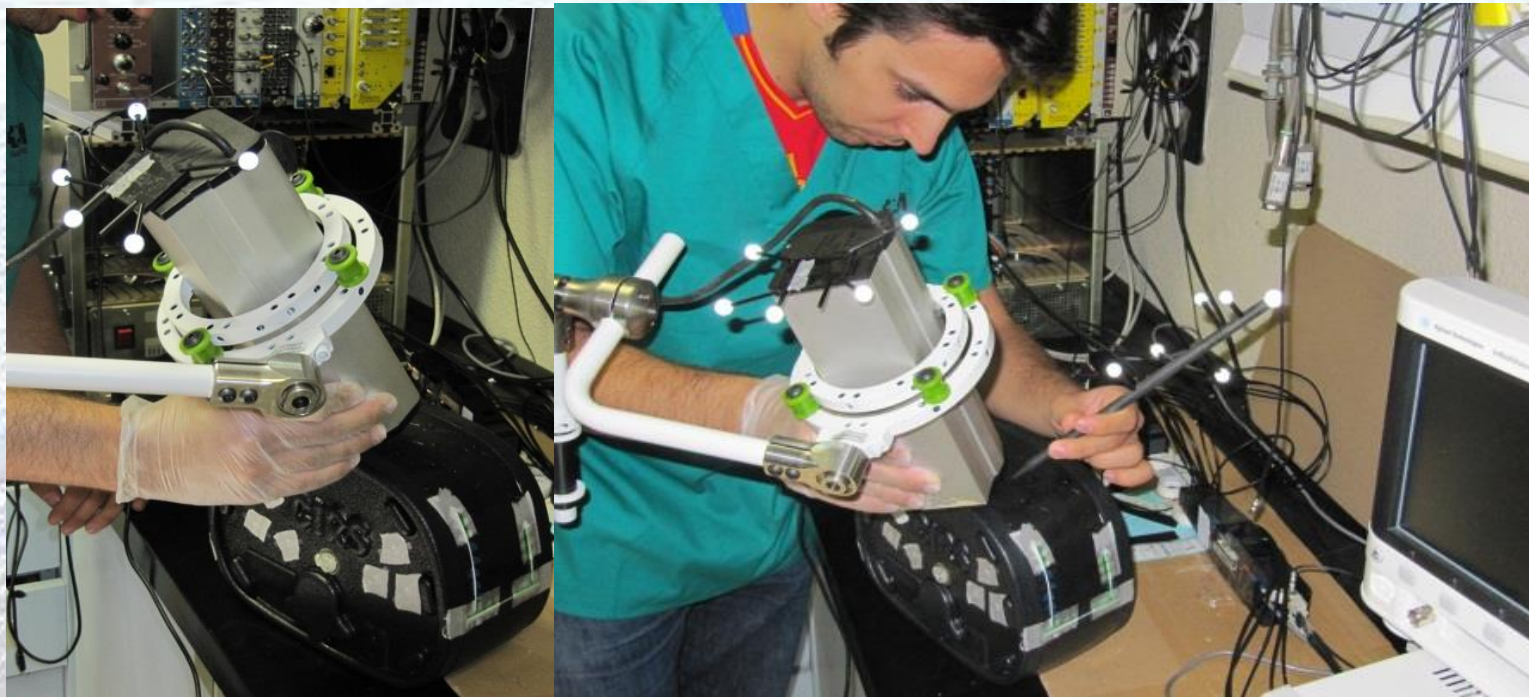
3rd Driver: Real-time Imaging, Preclinical Applications

Imaging animals requires anesthesia. It is well know that this may impact studies involving the brain, and therefore systems to allow the free movement of the animal while scanning have been devised. Imagers can track the position of the animal and compute the projections in a normalized framework that will allow tomographic reconstruction free of movement artifacts. To synchronize the camera with the motion tracker requires a powerful signal processor. Intelligent sensors aware of their relative position can alleviate the post-processing and produce better results.

This is becoming more and more ubiquitous.
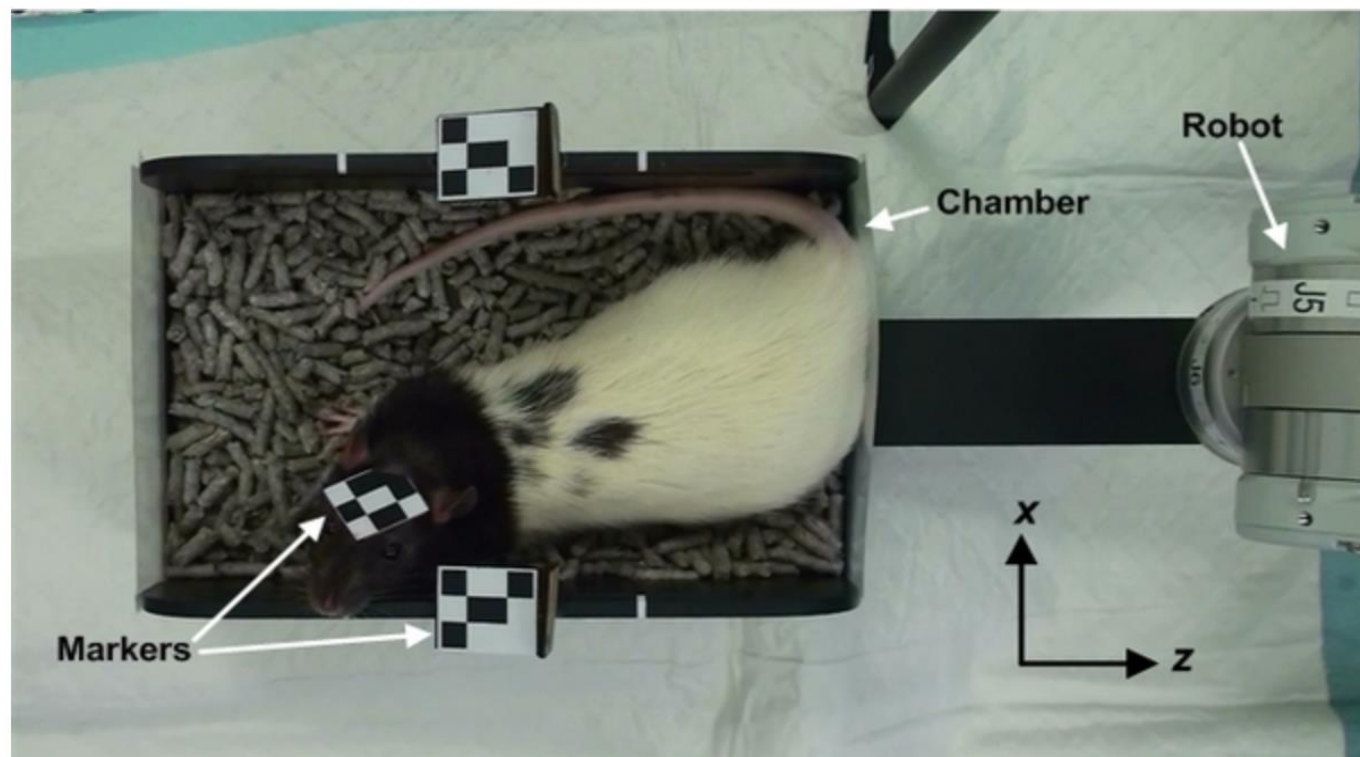
Freely moving rat inside the motion-adaptive chamber. The chamber attaches to a robot and is adjusted in the horizontal (x-z) plane to maintain the head near the centre of the scanner FOV. Here, attached markers on the head and chamber are being used for motion tracking.

More on Single Photon Emission Computed Tomography (SPECT)

SPECT

8 mSv typical dose

< collimator

Position sensitive light detector
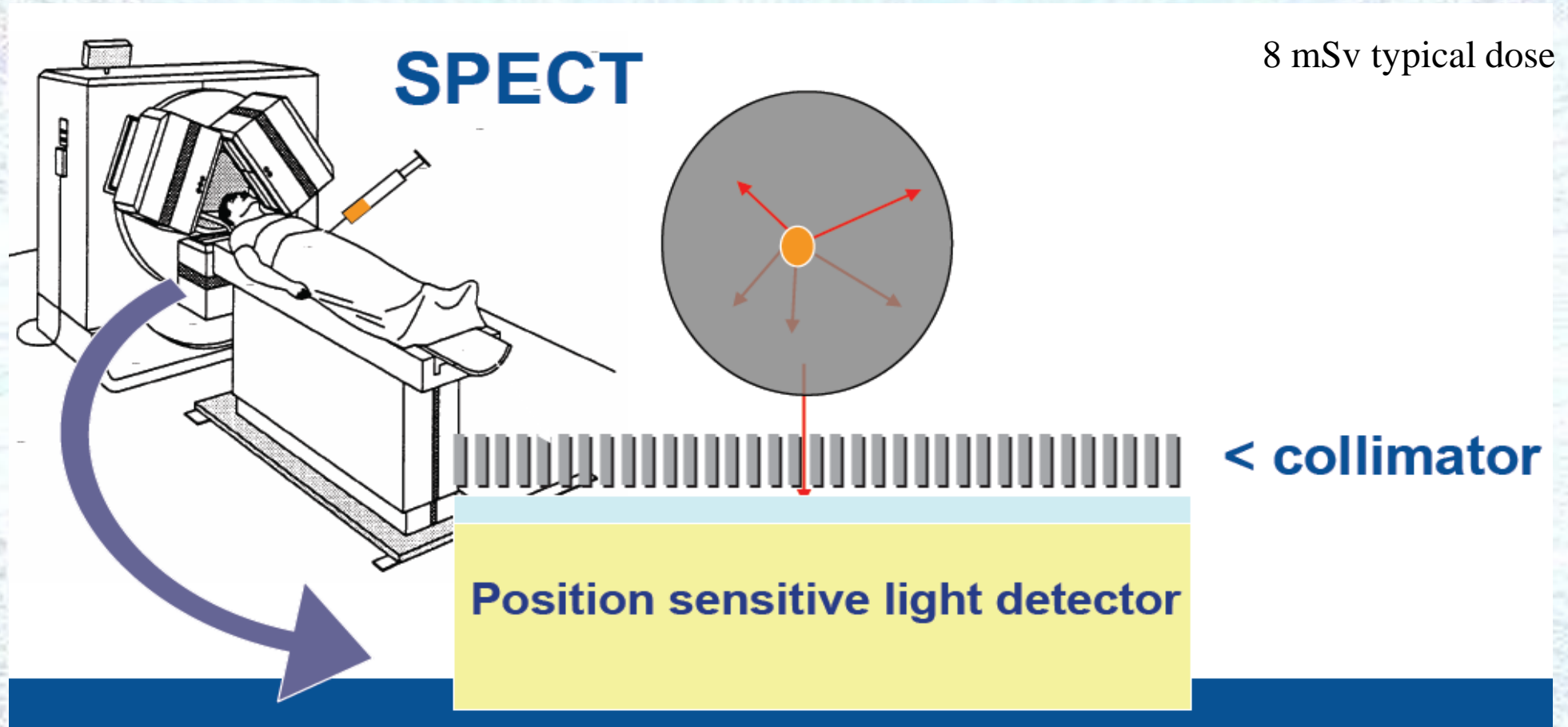
Functional imaging modality

(With many thanks to **Andy Boston**, Nuclear Structure, University of Liverpool)

SPECT : Problems/Opportunities

Technical

- Collimator Limits Spatial Resolution & Efficiency
- Collimator is heavy and bulky
- Energy of radioisotope limited to low energy

- NaI:Tl Dominant for >40 Years...
- MRI $\rightarrow$ Existing PMTs will not easily operate

- Would like to be able to image a larger fraction of events.

Common radionuclides: ^{99m}Tc, ^{123}I, ^{131}I
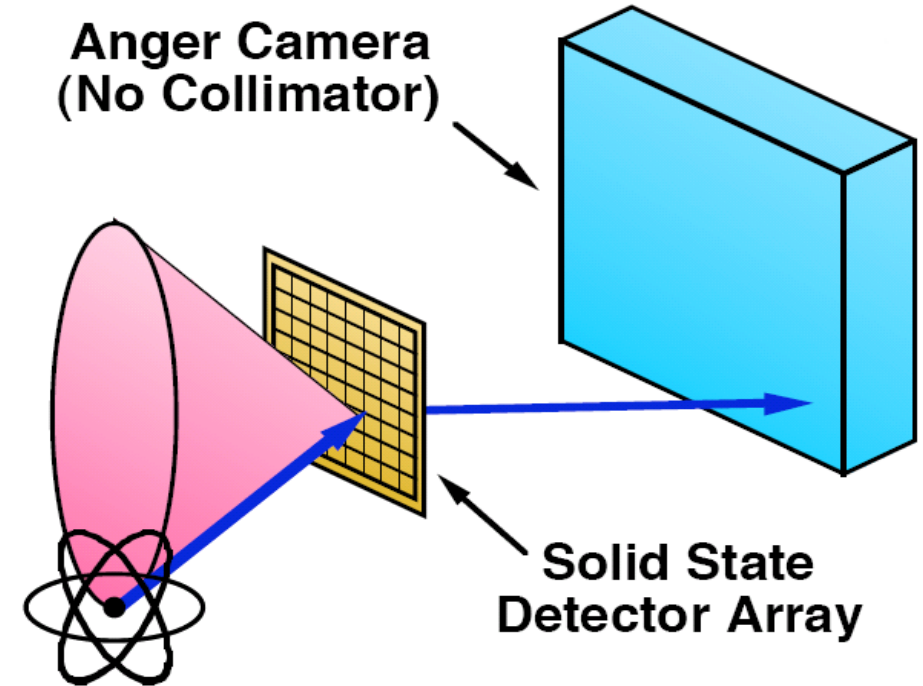
Scatter | True | Other
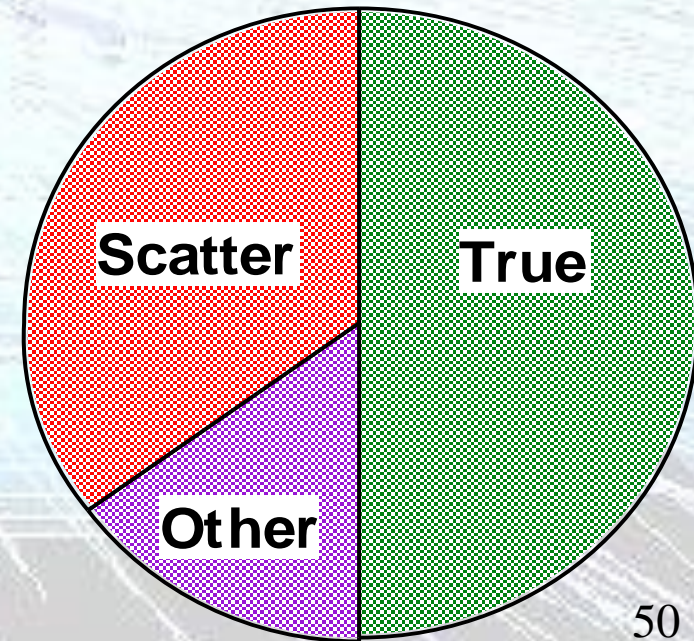
ProSPECTus: Compton Imaging

- Radical change → No mechanical collimator
- Utilising semiconductor sensors
- Segmented technology and PSA and digital electronics (AGATA)
- Image resolution 7-10mm → 2-3mm
- Efficiency factor ~10 larger
- Simultaneous SPECT/MRI

AGATA
(Advanced GAmma
Tracking Array)

Anger Camera
(No Collimator)
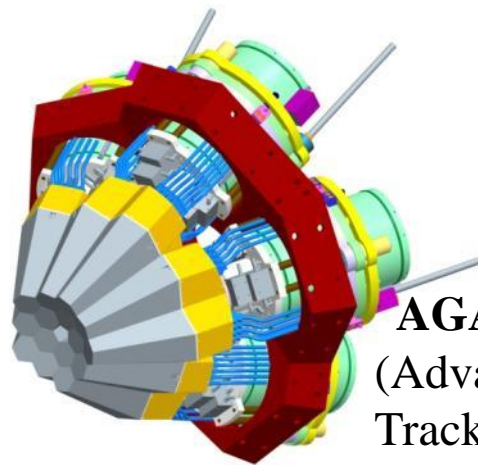
Solid State
Detector Array

ProSPECTus: Compton Imaging

Conventional SPECT

Compton camera

Source

E_0
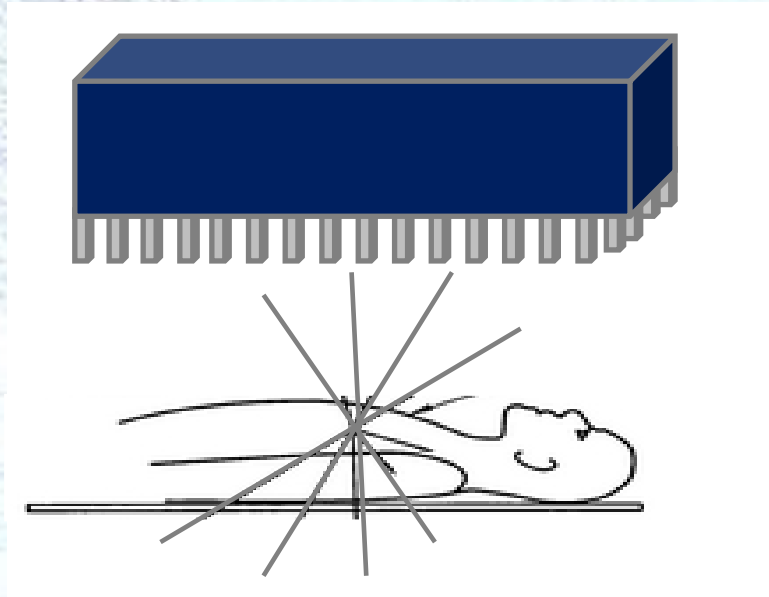
- Gamma rays detected by a gamma camera
- Inefficient detection method
- Incompatible with MRI
- 2D information
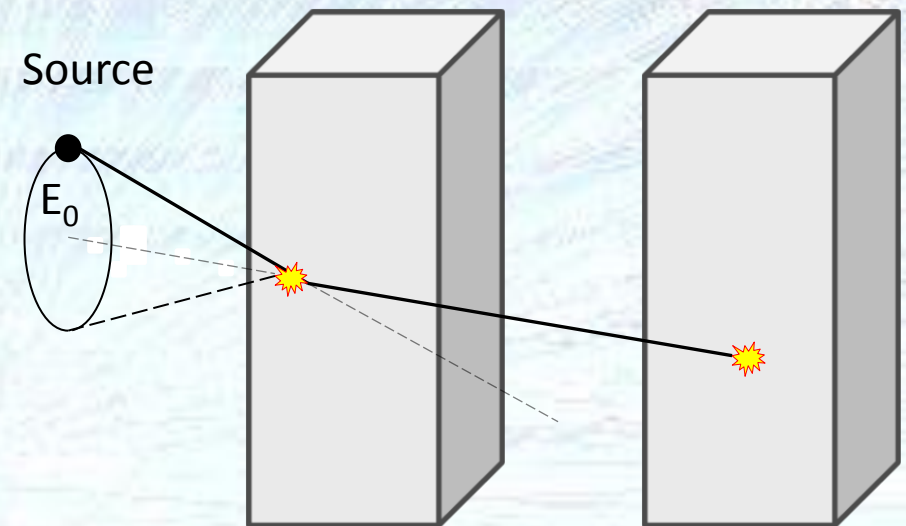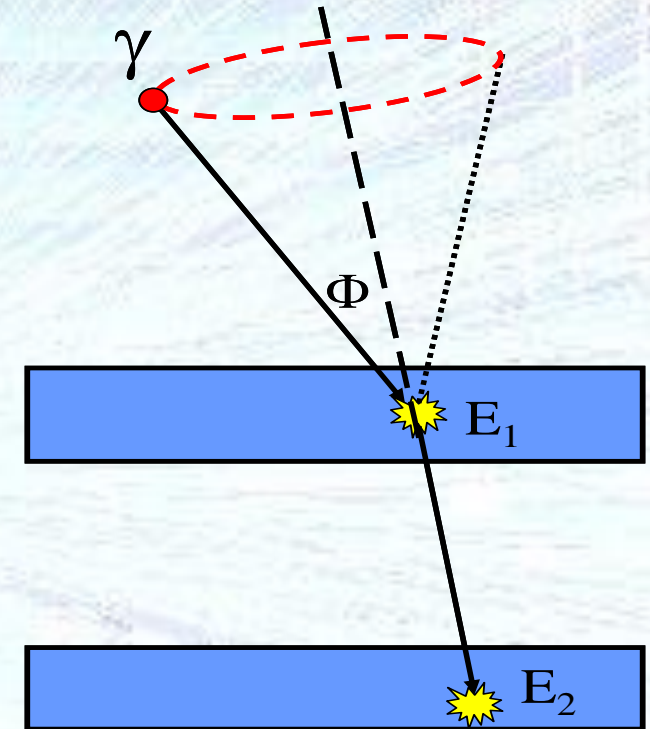
- Gamma rays detected by a Compton camera
- Positions and energies of interactions used to locate the source
- 3D information.

Factors that limit the performance of a Compton Imager:
Energy resolution, Detector position resolution, Doppler Broadening

52

Research : Compton Imaging

o Compton *Cones of Response* projected into image space

$$\cos\phi = 1 - m_e c^2 \left(\frac{1}{E_2} - \frac{1}{E_1 + E_2} \right)$$

Research : Compton Imaging

o Compton *Cones of Response* projected into image space

$$\cos\phi = 1 - m_e c^2 \left(\frac{1}{E_2} - \frac{1}{E_1 + E_2} \right)$$

o Compton *Cones of Response* projected into image space

$$\cos\phi = 1 - m_e c^2 \left(\frac{1}{E_2} - \frac{1}{E_1 + E_2} \right)$$

Research : Compton Imaging

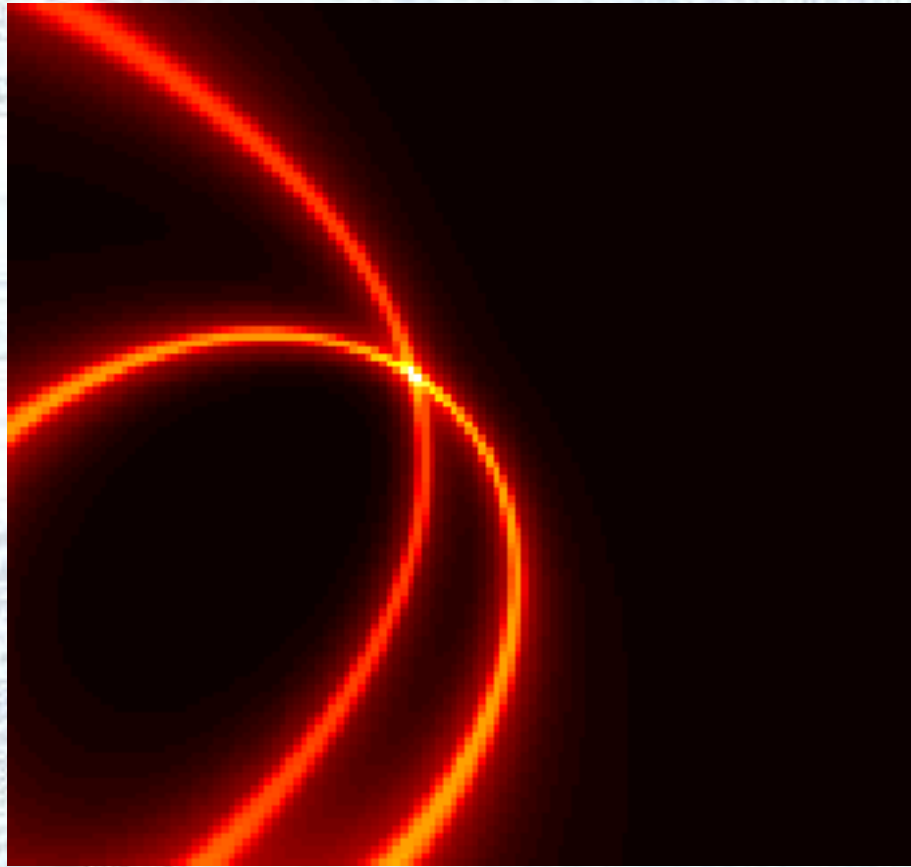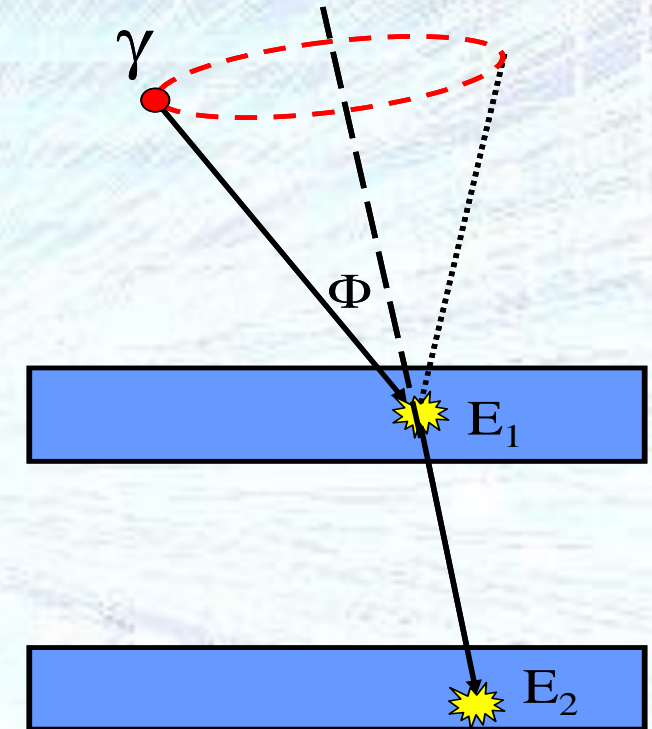o Compton *Cones of Response* projected into image space

$$\cos\phi = 1 - m_e c^2 \left(\frac{1}{E_2} - \frac{1}{E_1 + E_2} \right)$$
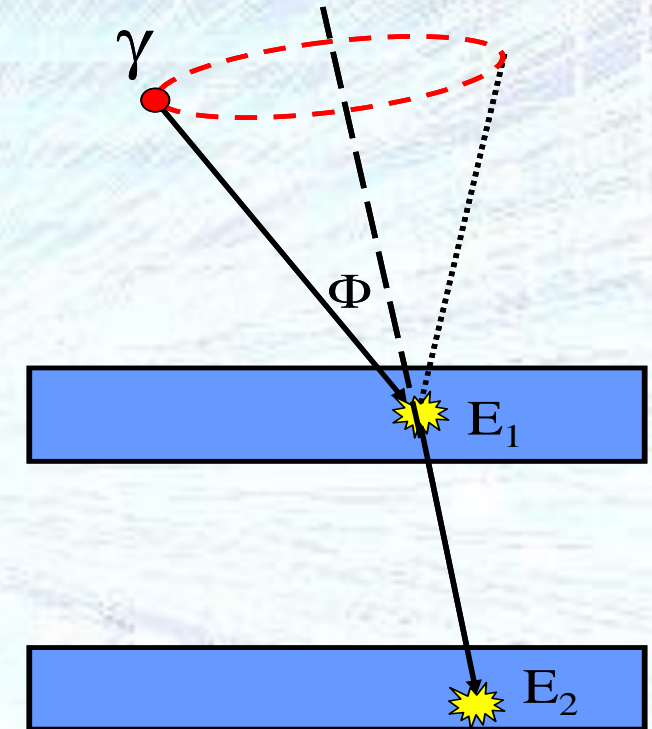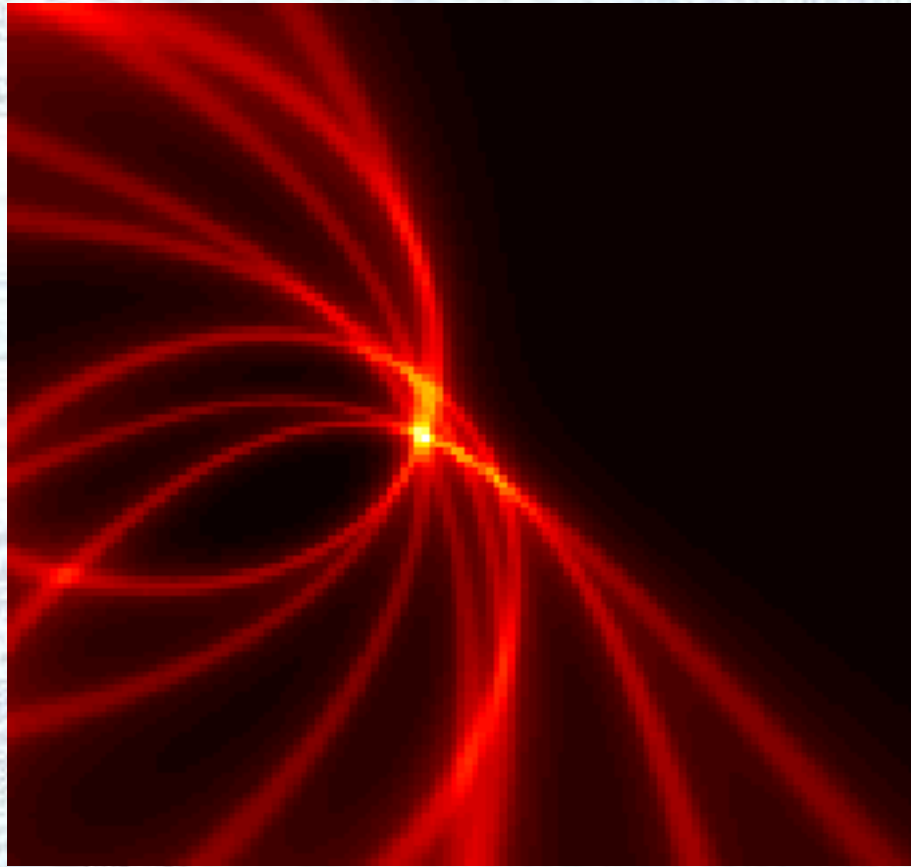
Research : Compton Imaging

○ Compton *Cones of Response* projected into image space
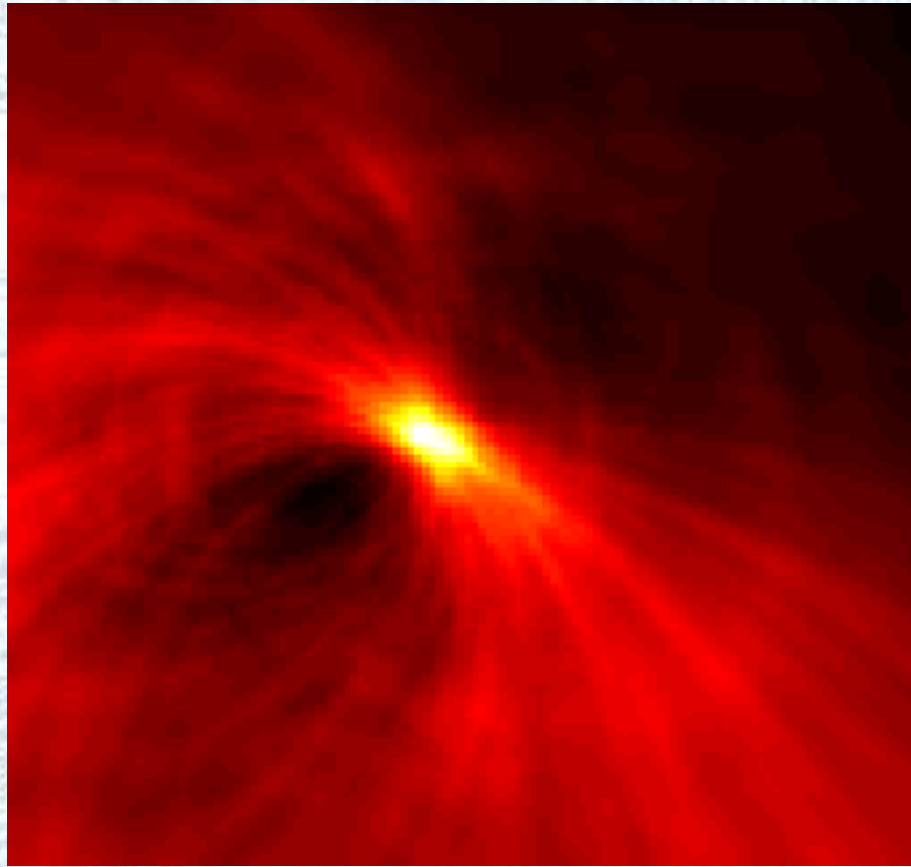
$$\cos\phi = 1 - m_e c^2 \left(\frac{1}{E_2} - \frac{1}{E_1 + E_2} \right)$$

System Configuration

GEANT4 simulations L. Harkness

1cm   2cm

141keV

5cm   2cm

Si(Li)   Ge
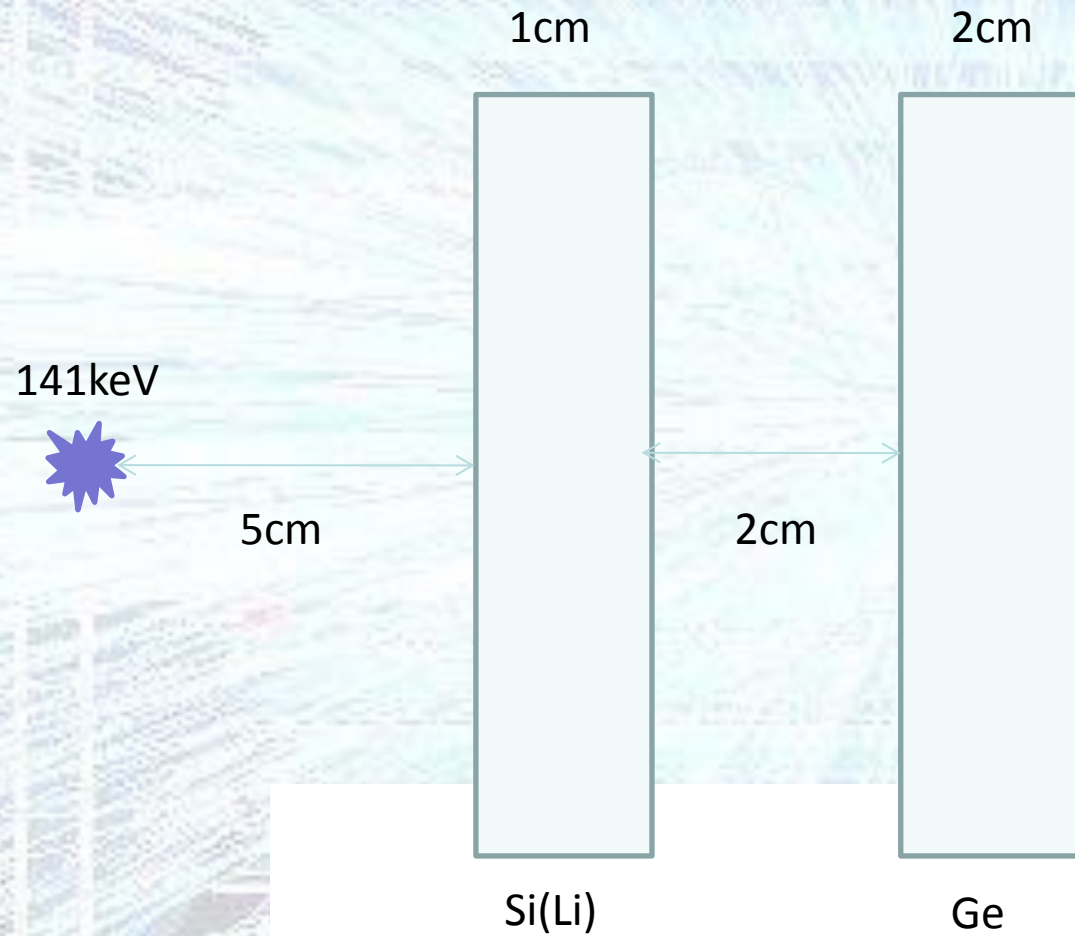
Ortec & SemiKon

Ingredients of γ-Tracking

AGATA ADVANCED GAMMA TRACKING ARRAY

1 Highly segmented HPGe detectors
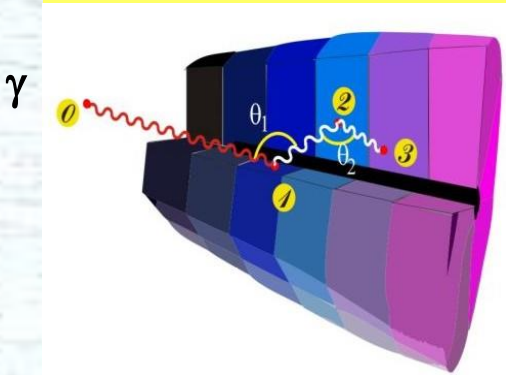
2 Digital electronics to record and process segment signals

3 Pulse Shape Analysis to decompose recorded waves

Identified interaction points

$$(x,y,z,E,t)_i$$

4 Reconstruction of tracks e.g. by evaluation of permutations of interaction points
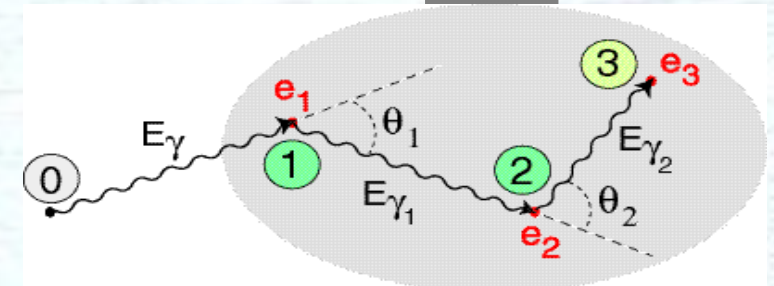
reconstructed γ–rays

Uniformity of Response for Planar Germanium Crystals

Am-241 AC x-y surface intensity distribution
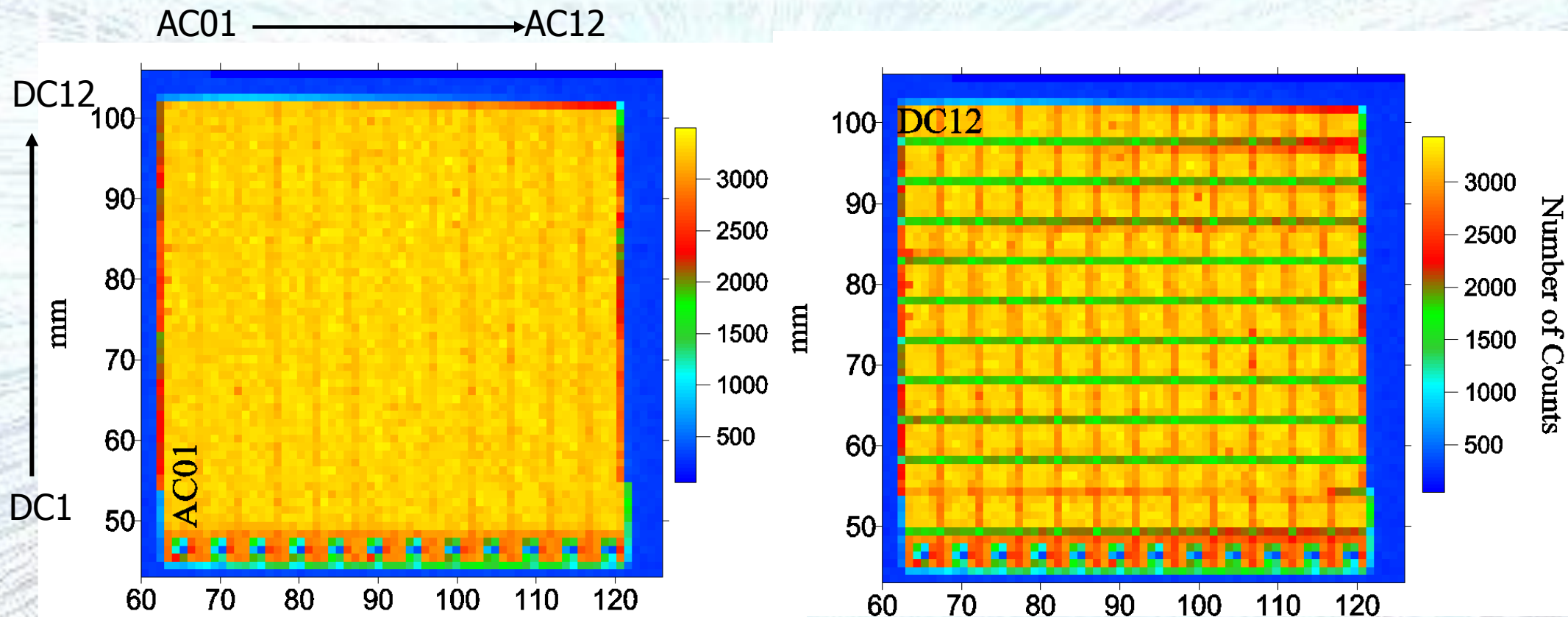
Use of Pulse Shape Response

"superpulse" pulse shapes for ^{137}Cs (662 keV) events versus depth

Compton Imaging

~7° Angular Resolution FWHM, central position
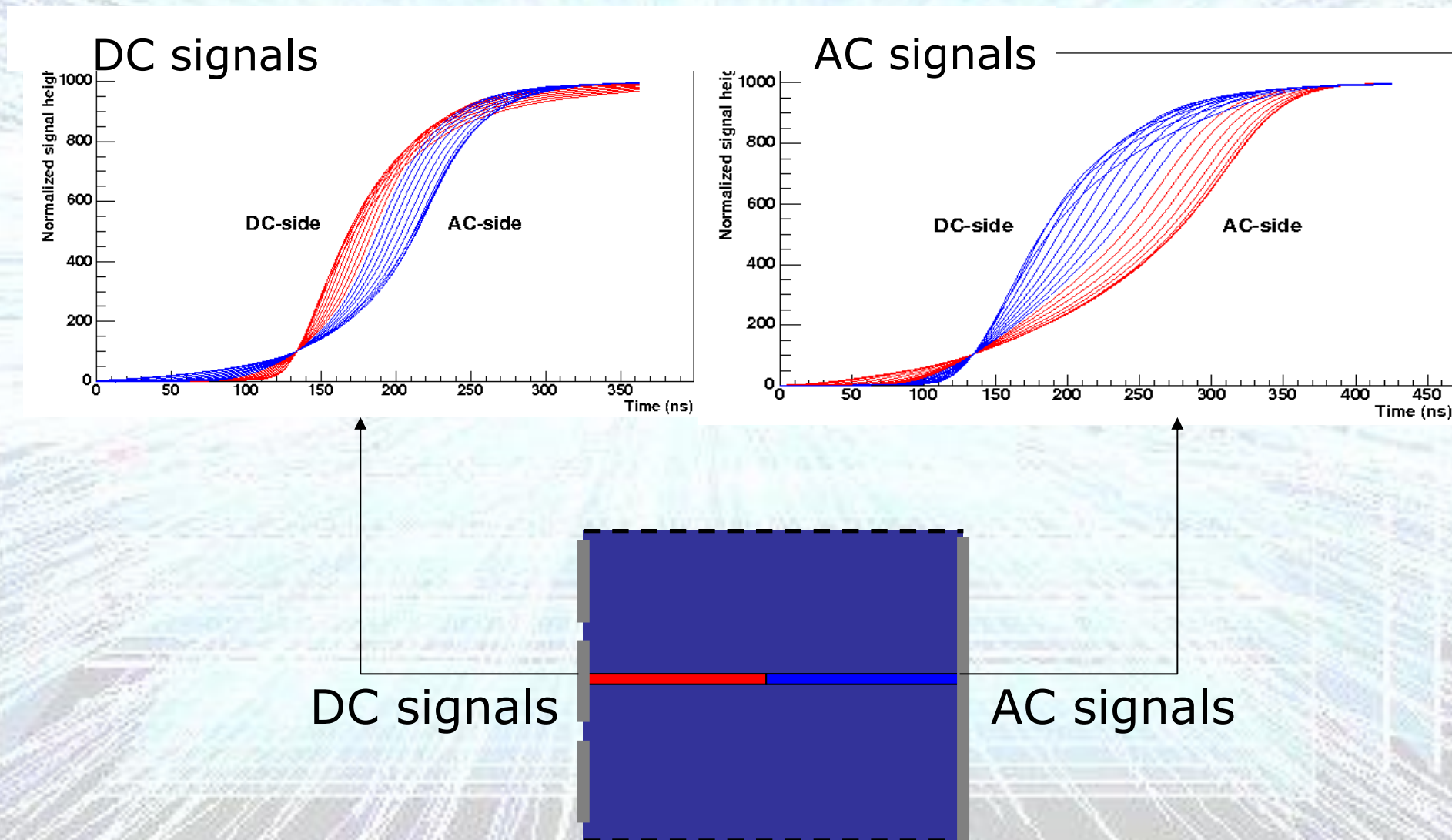
Multi-nuclide imaging

¹⁵²Eu
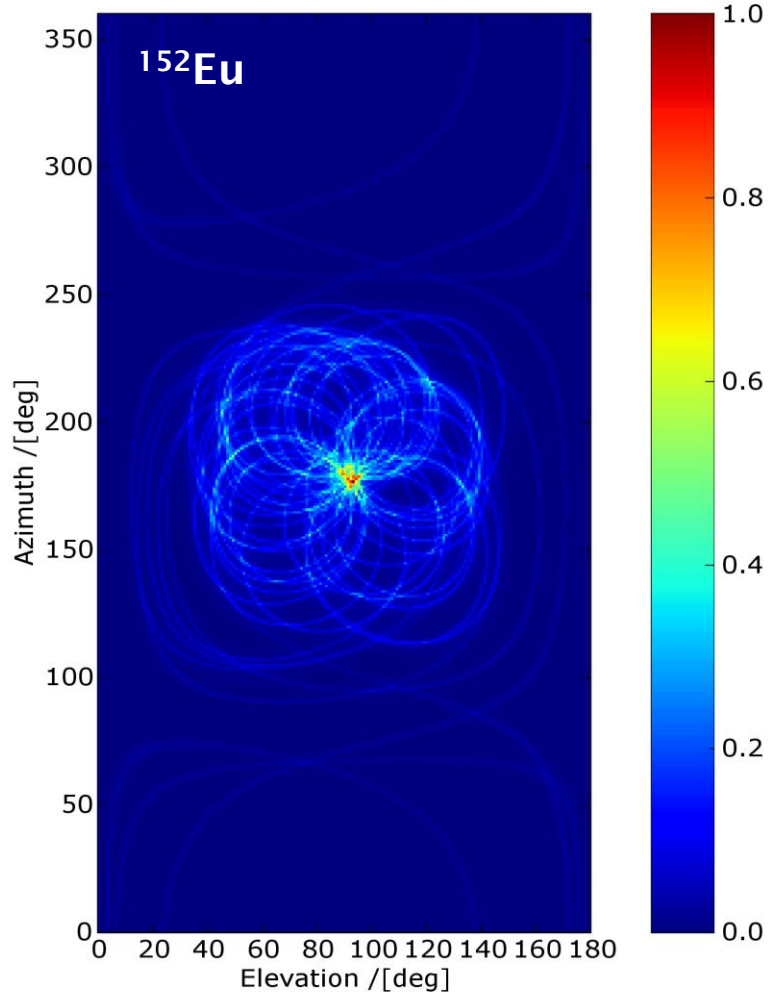
No PSA (5x5x20)

Cone back projection

¹⁵²Eu E = 1408 keV

²²Na E = 1274 keV

2cm source separation
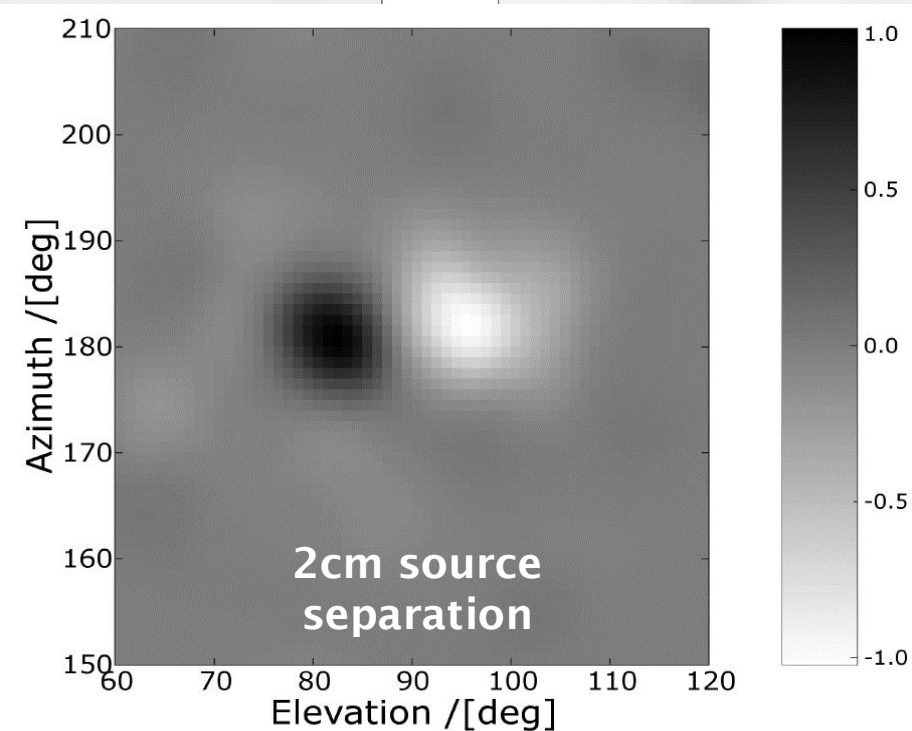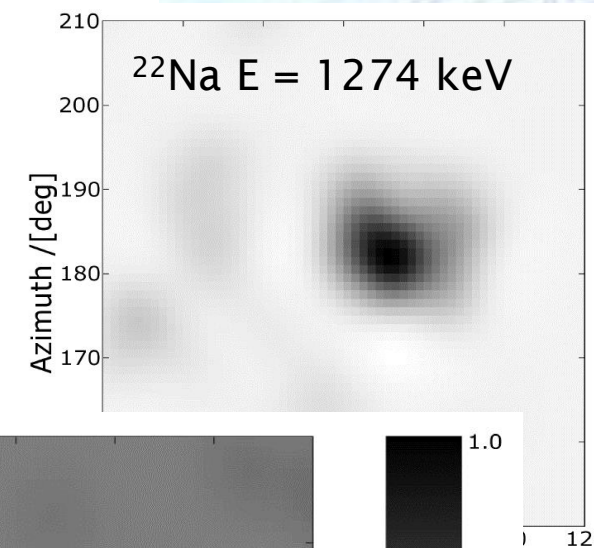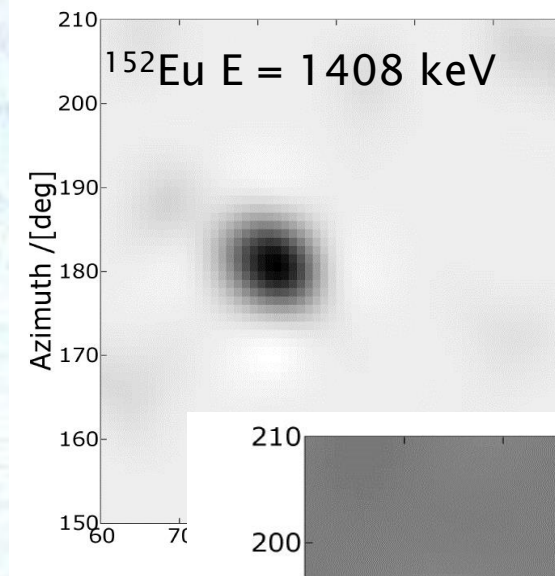
MRI Compatibility & Status

- Test existing gamma-ray detector in an MRI scanner

- Does the detector cause distortions in the MRI image? No

- Does the MRI system degrade the detector performance? In certain positions (which can be minimised)

- Encouraging results!
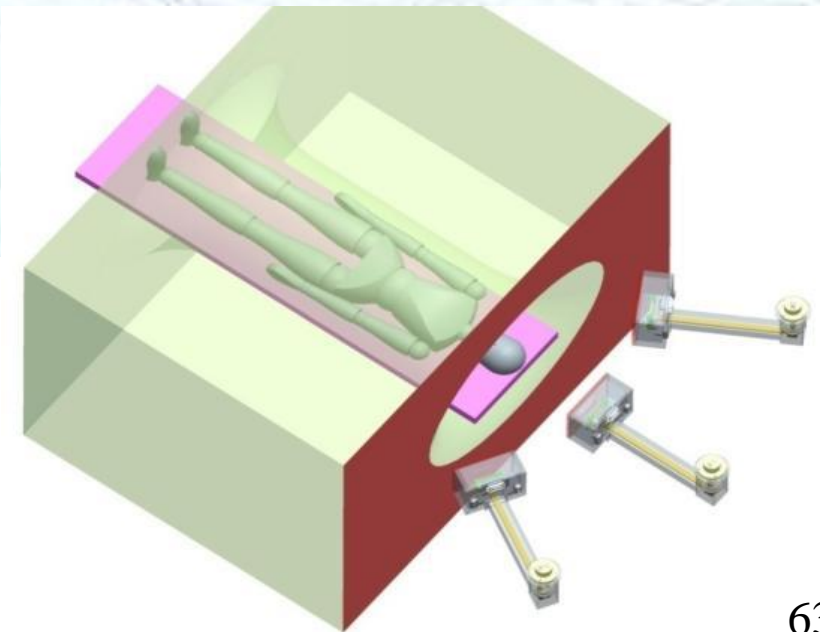
Radioactive Source Location and Identification

Courtesy K. Vetter LBL (work @ LLNL)

- The ability to locate and identify radioactive material with high precision
- Quantification of waste into low/intermediate/high brackets
- Wide range of activities from ~37kBq -> MBq
- There are many open challenges and opportunities

Si(Li) + Ge Cryogenic Solutions
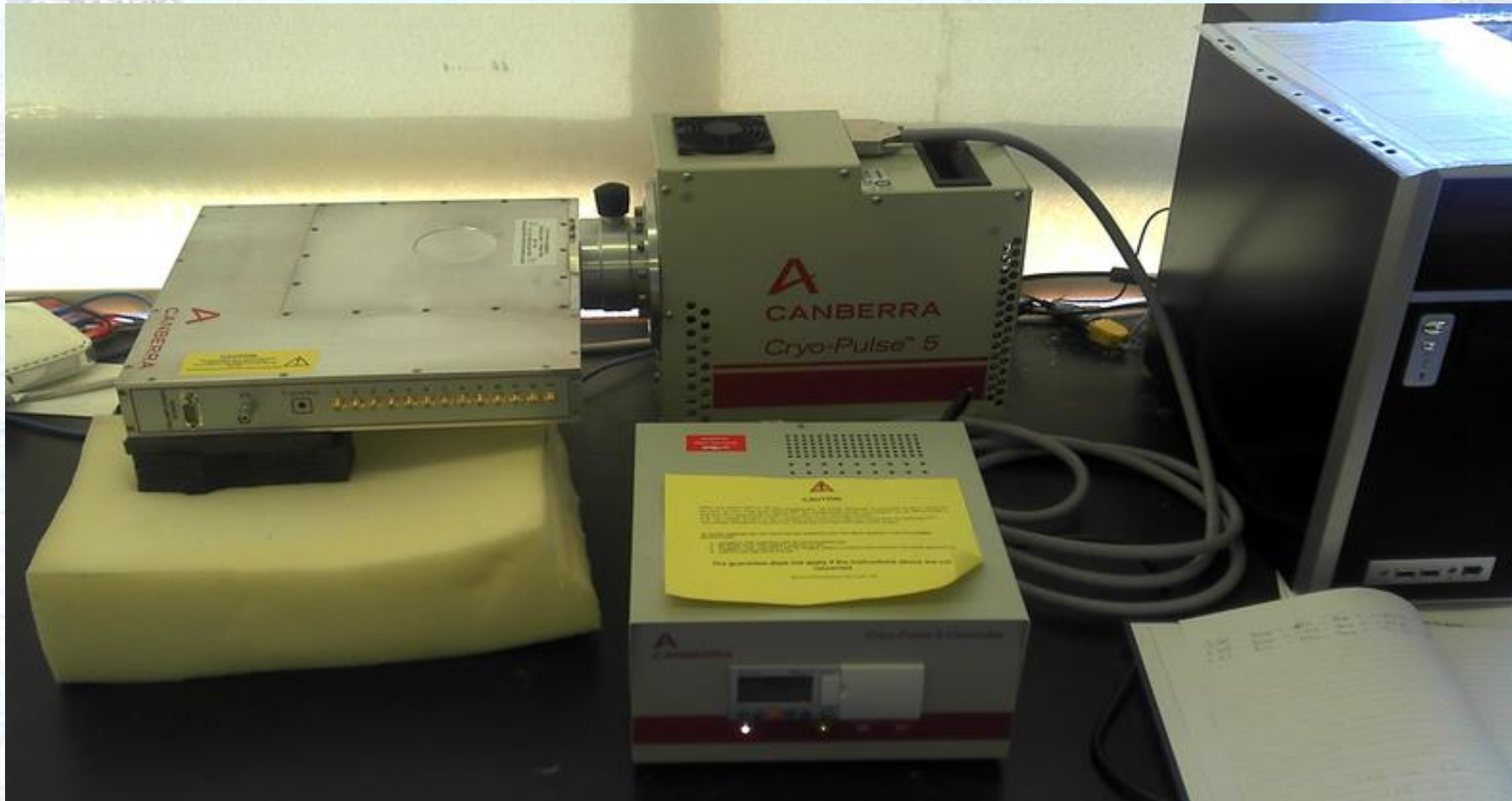
- Mechanically cooled
- Battery powered
- Work in collaboration with industry

CZT Room temperature: PorGamRayS

A portable gamma-ray spectrometer with Compton imaging capability (60keV – 2MeV)
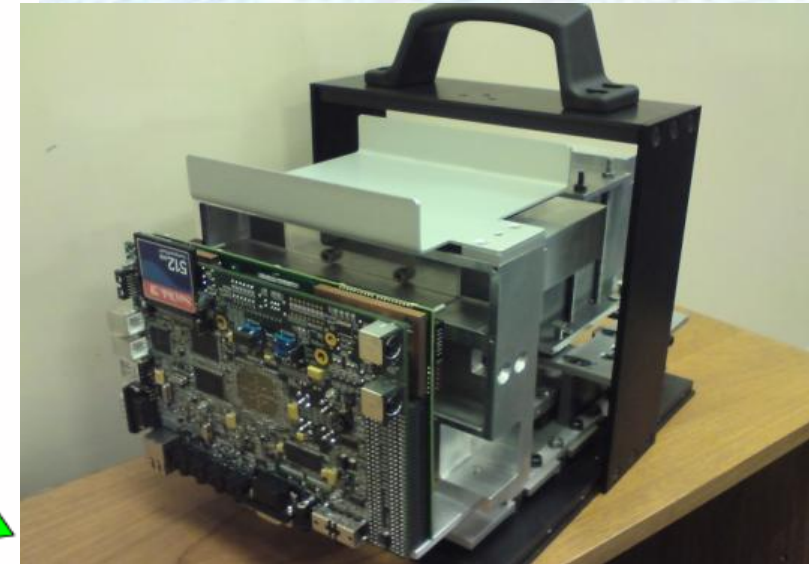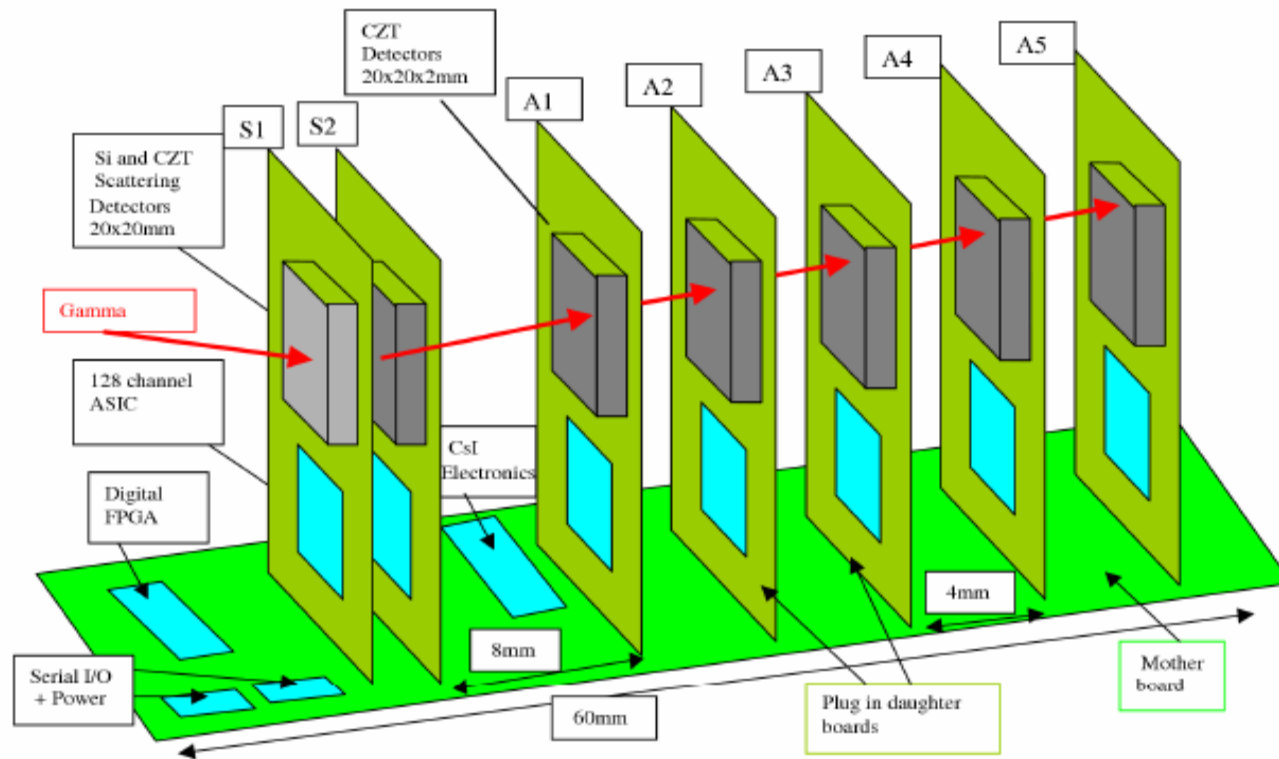
Gamma-ray spectroscopy/imaging with CZT detectors. **Pulse Shape Analysis** to refine spatial resolution and correct charge collection issues

^{137}Cs example image with CBP

XY slice through Z = 175
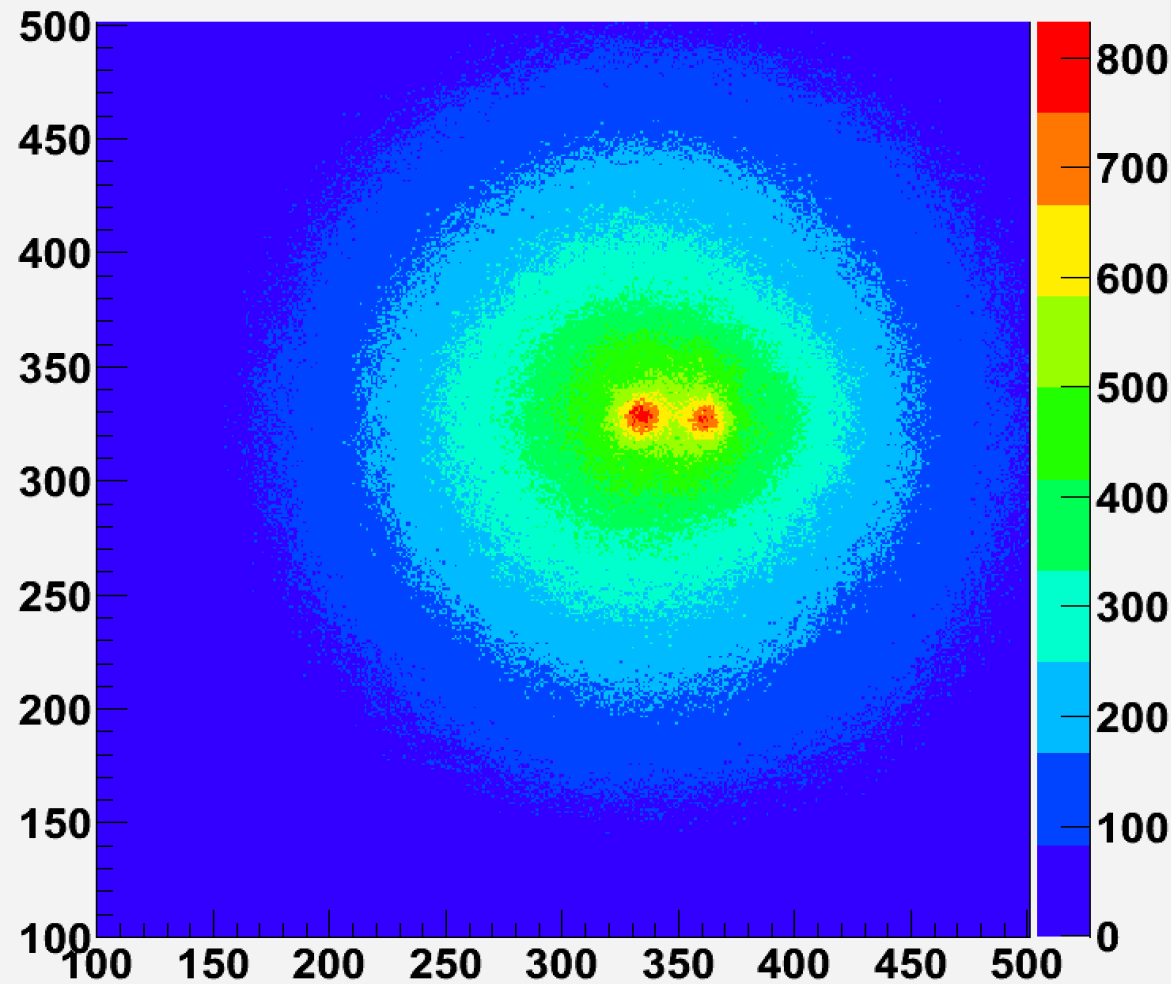
Fit to X slice through Z = 175, Y = 328, ChiSq/DOF = 191.55

FWHM X1 = 19 mm
- Data
- Total Fit
- Peak 1
- Peak 2
- Background

y_slice_fit

File Edit View Options Tools
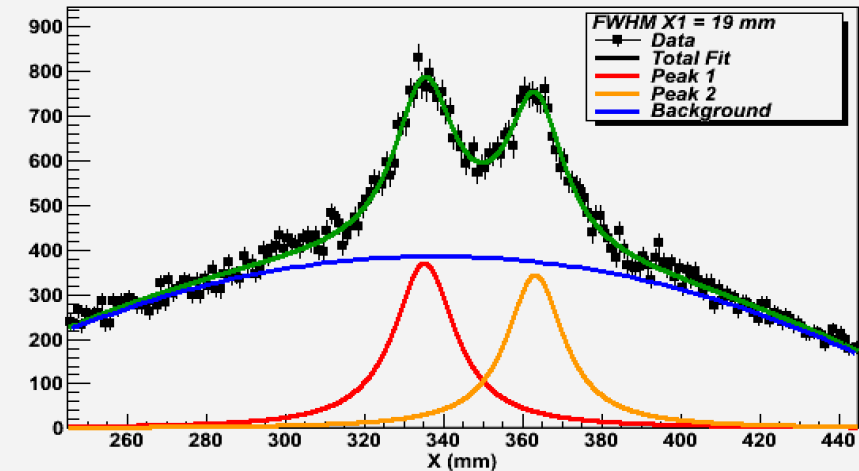
Fit to Y slice through Z = 175, X = 333, ChiSq/DOF = 538.86

FWHM Y = 38 mm
- Data
- Total Fit
- Peak
- Background
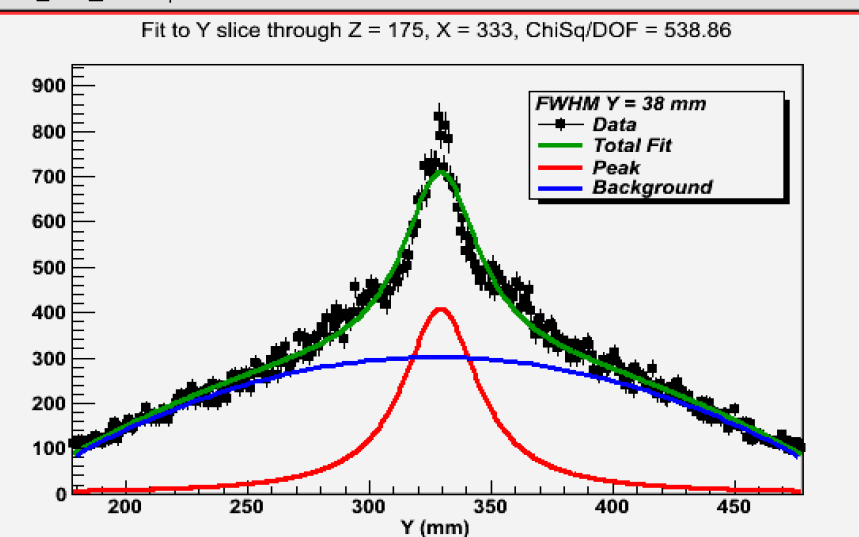
370 kBq @ 5cm standoff   19mm FWHM

^{133}Ba example image with CBP

XY slice through Z = 145 Compression = 1

Addback spectrum comparing fold 1 only with fold 1 and 2

- Fold 1 and 2 events
- Fold 1 events only

Counts

Energy (keV)

Fit to X slice through Z = 145, Y = 335, ChiSq/DOF = 183.54 Compression = 1

FWHM X = 19 mm
- Data
- Total Fit
- Peak
- Background

X (mm)
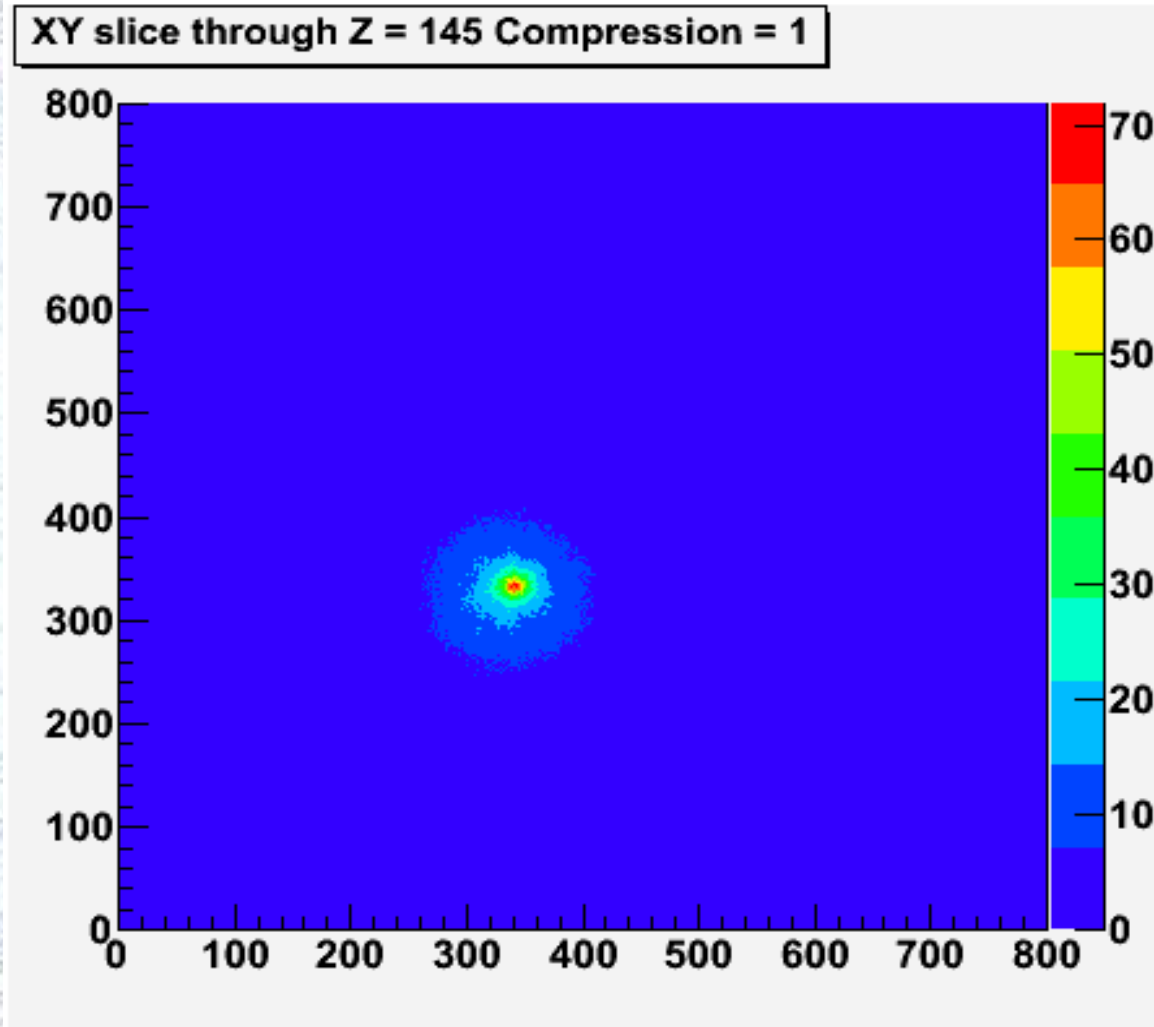
340 kBq @ 5cm standoff
19mm FWHM

68
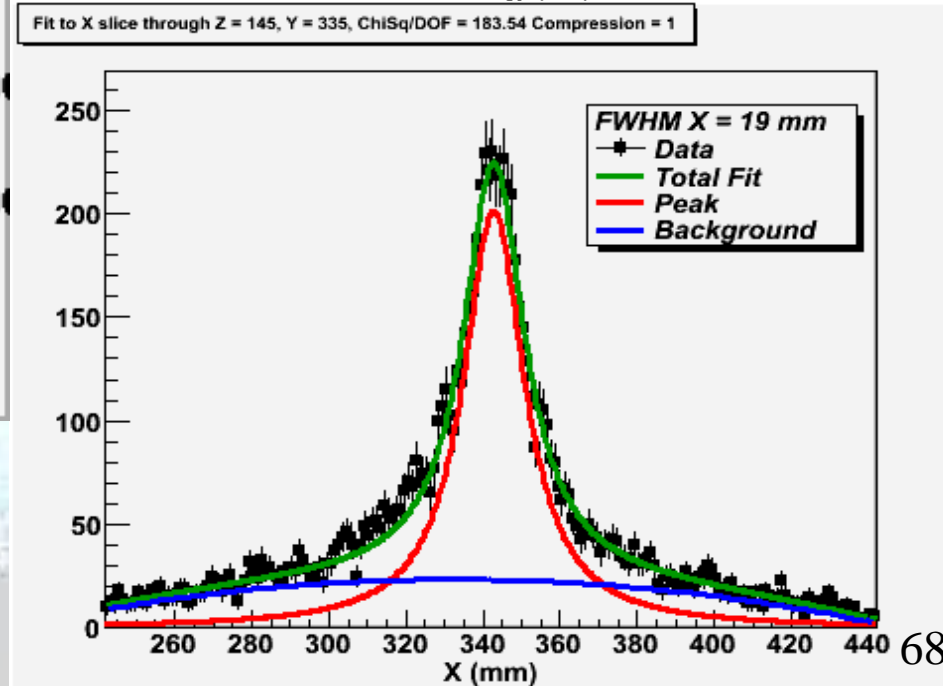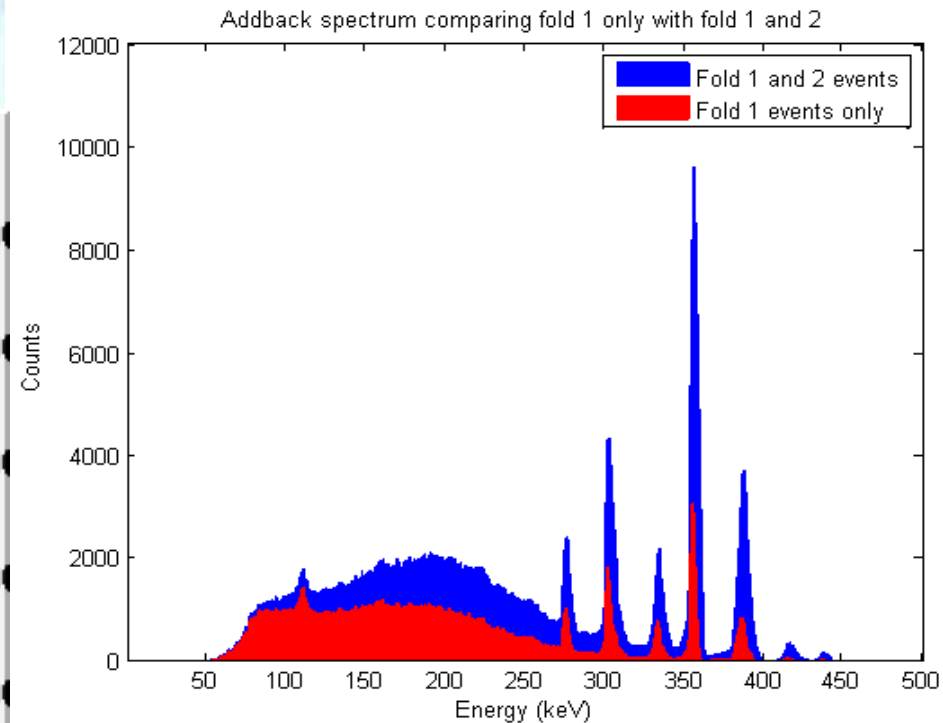
Stereoscopic Optical Image Fusion

1.5m standoff

A Compton Camera provides 3D source location

Utilise a 3D optical imager
Bubblebee 3 camera head

Depth
X: -0.15758 m
Y: -0.0087582 m
Z: 0.45933 m

Radiometric
Counts: 8

POINT GREY
Innovation in Imaging

Digression on the ATLAS Role in the Higgs Discovery
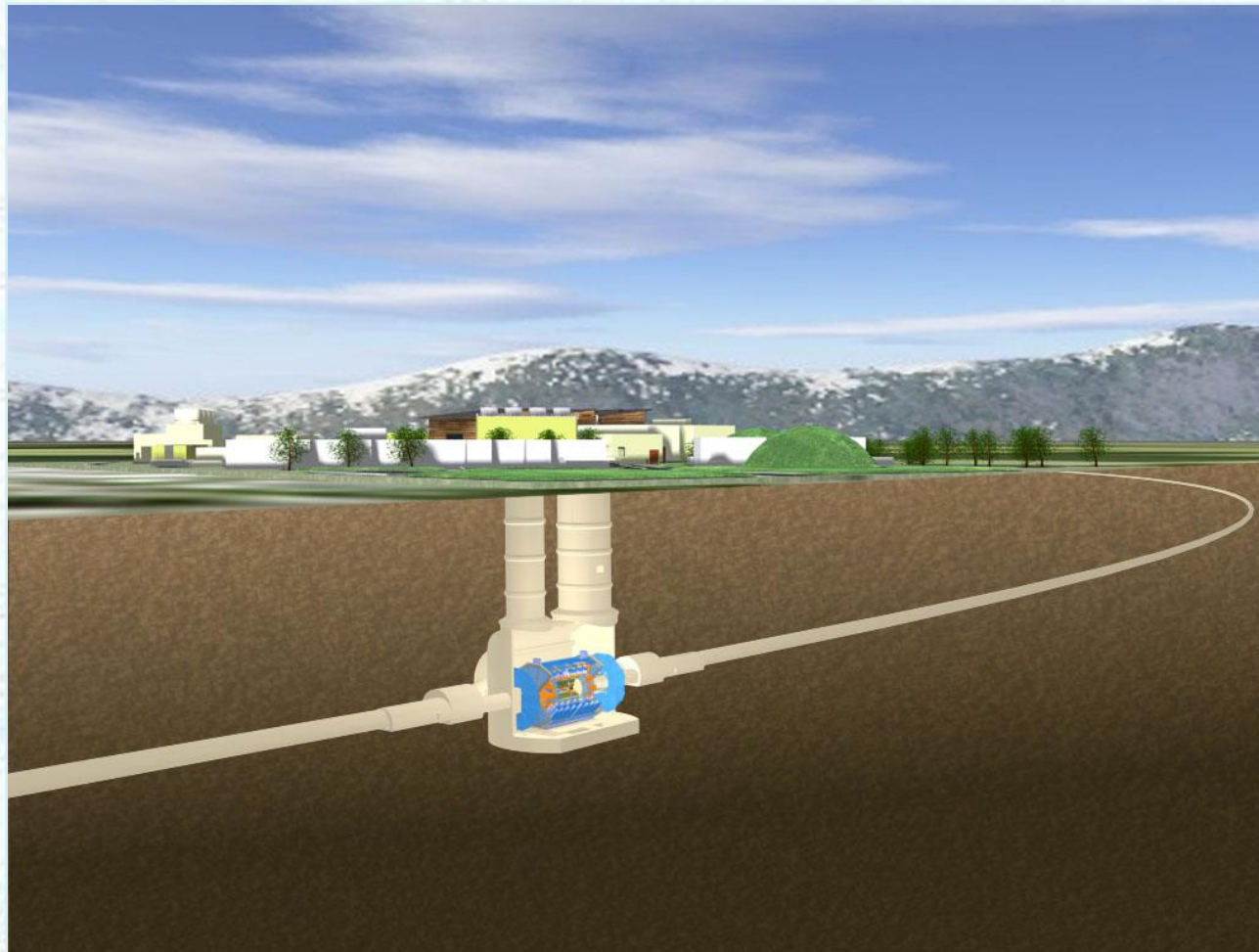
Experiments at the LHC

Building 40 at CERN

ATLAS

CMS
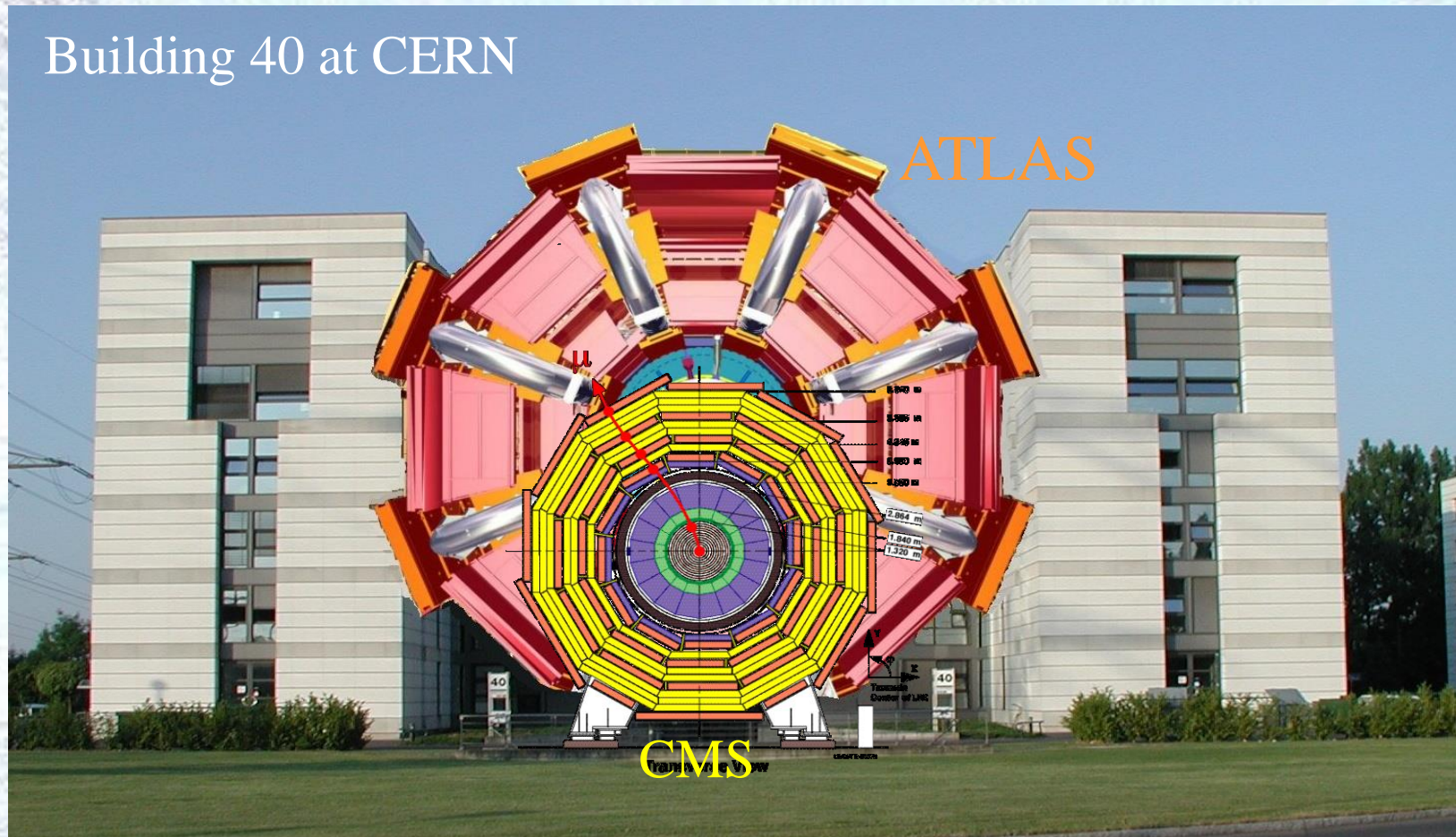
- **ATLAS, CMS, ALICE and LHCb**
- **Detector Technologies**
  - **Noble gases, scintillators, crystals, Cherenkov, …**
  - **Silicon Microstrip Tracking Detectors**

Experiments at the LHC

Collider Experiments

CERN Geneva

The Large Hadron Collider 14 TeV: Proton on Proton

2 Giant General Purpose Detectors at the LHC

ATLAS

ATLAS: Inner Tracking Detectors

Muon Detectors

Tile Calorimeter

Liquid Argon Calorimeter

25 m

45 m

Toroid Magnets   Solenoid Magnet   SCT Tracker   Pixel Detector   TRT Tracker

73

ATLAS Inner Detector

R = 1082 mm

TRT

R = 554 mm
R = 514 mm

SCT

R = 443 mm

R = 371 mm

R = 299 mm

25 m

R = 122.5 mm
Pixels
R = 88.5 mm
R = 50.5 mm

R = 0 mm

TRT — Straw tubes

SCT — Silicon strip

Pixels — Silicon pixel
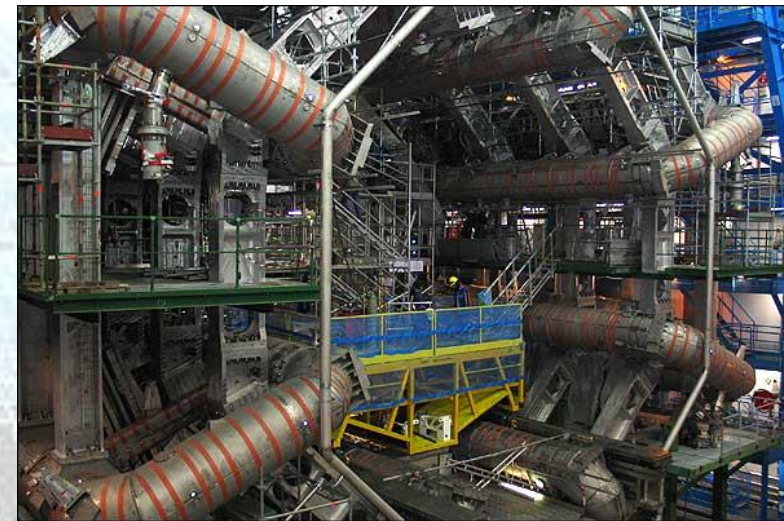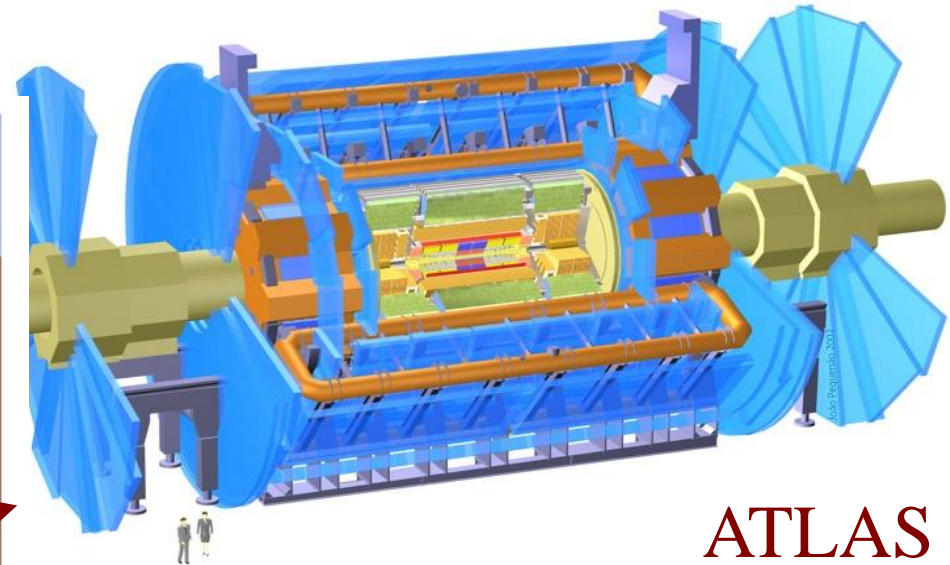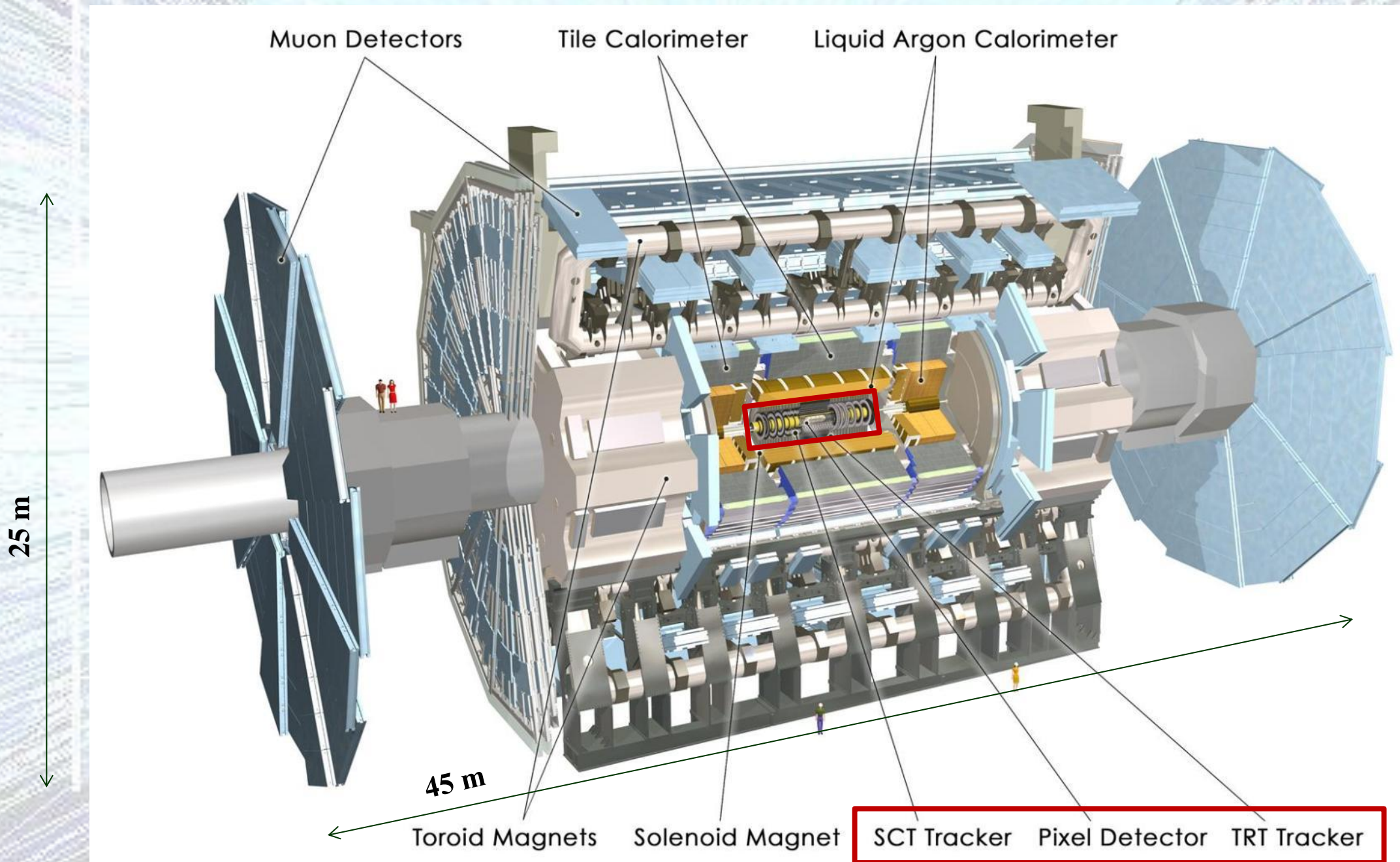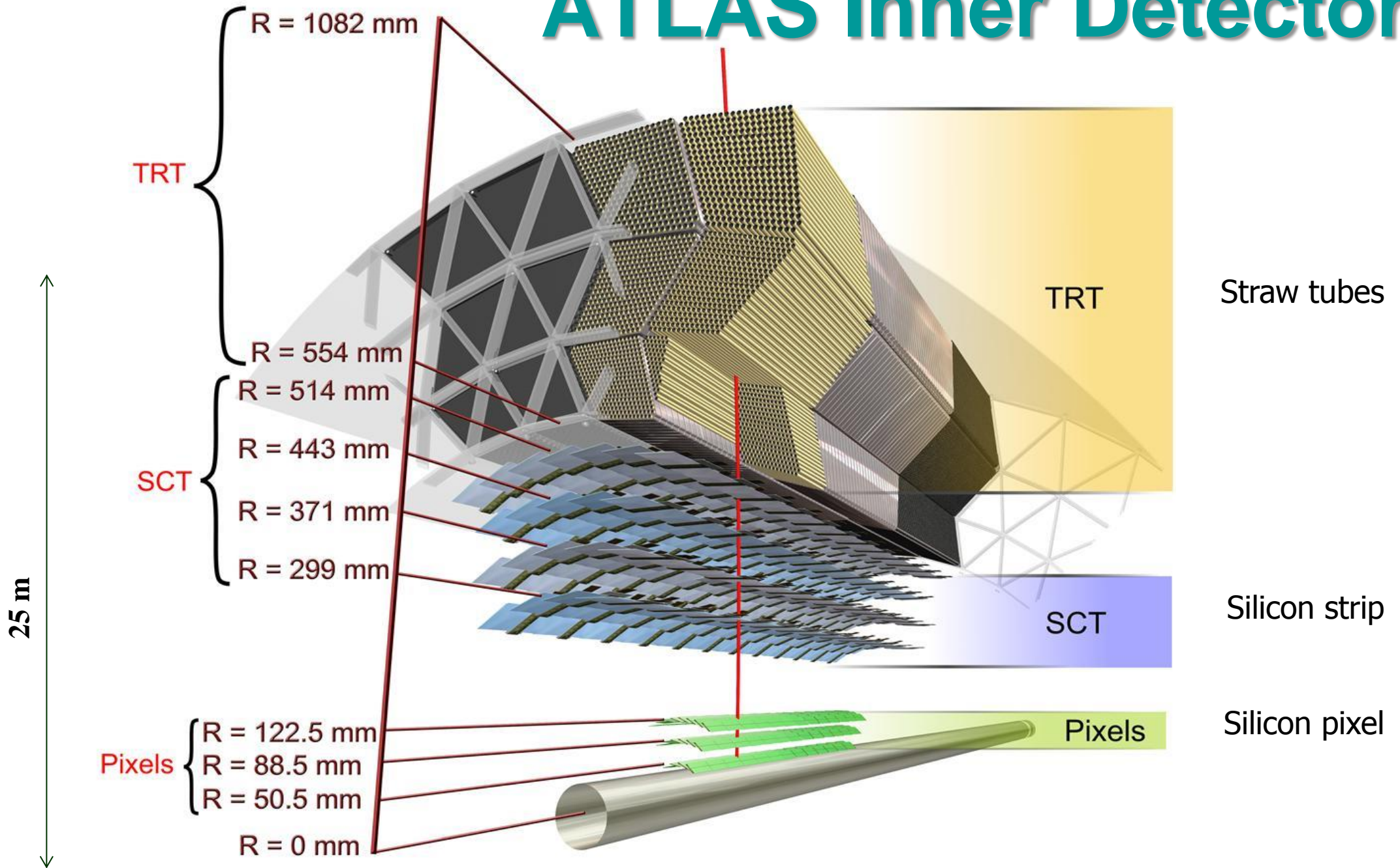
SCT Tracker   Pixel Detector   TRT Tracker

ATLAS: Inner Tracking Detectors

Muon Detectors — Tile Calorimeter — Liquid Argon Calorimeter

25 m

45 m

Toroid Magnets — Solenoid Magnet — SCT Tracker — Pixel Detector — TRT Tracker
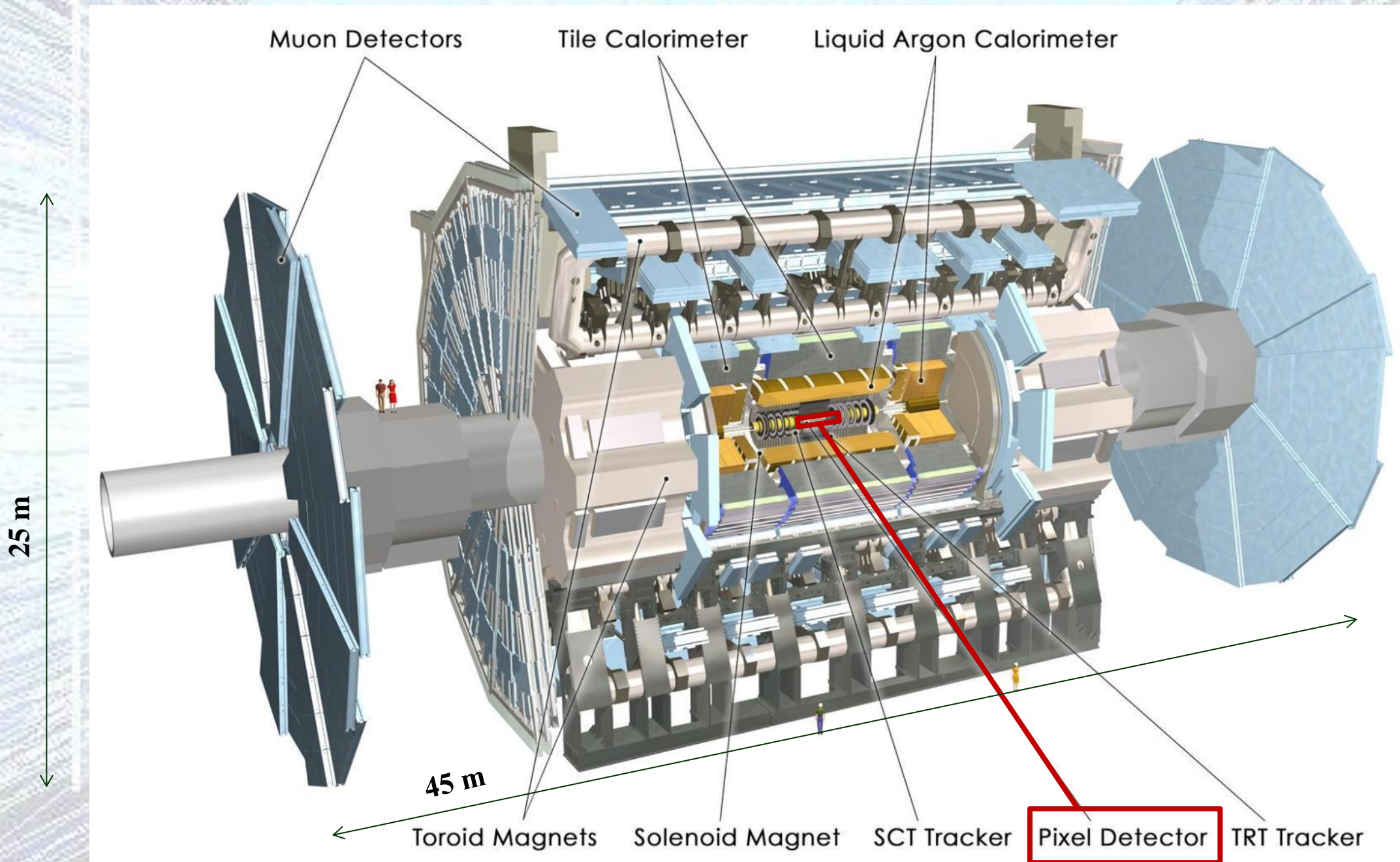
The ATLAS Pixel Detector
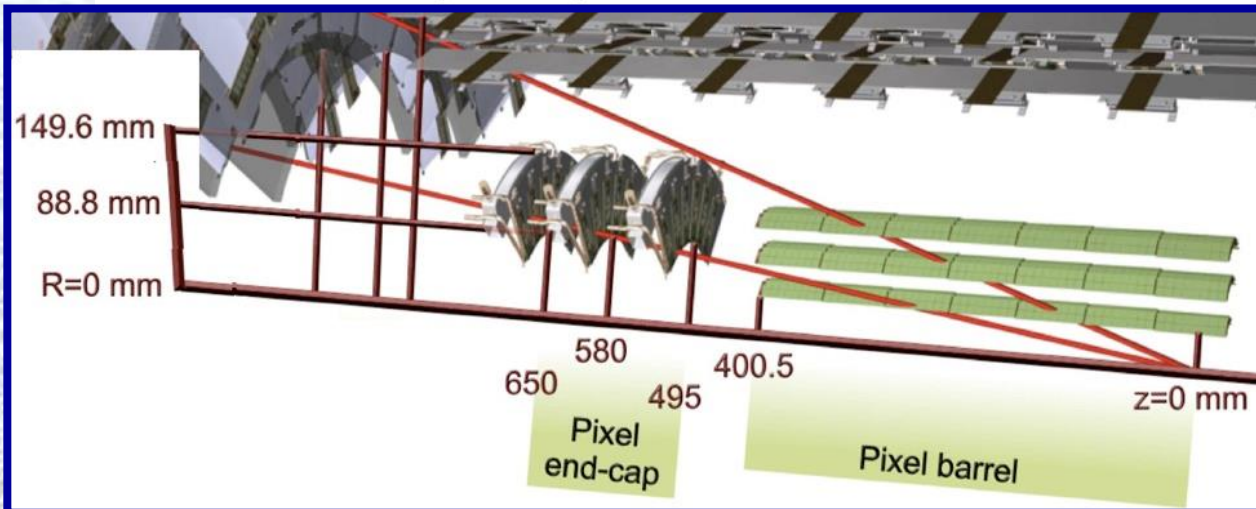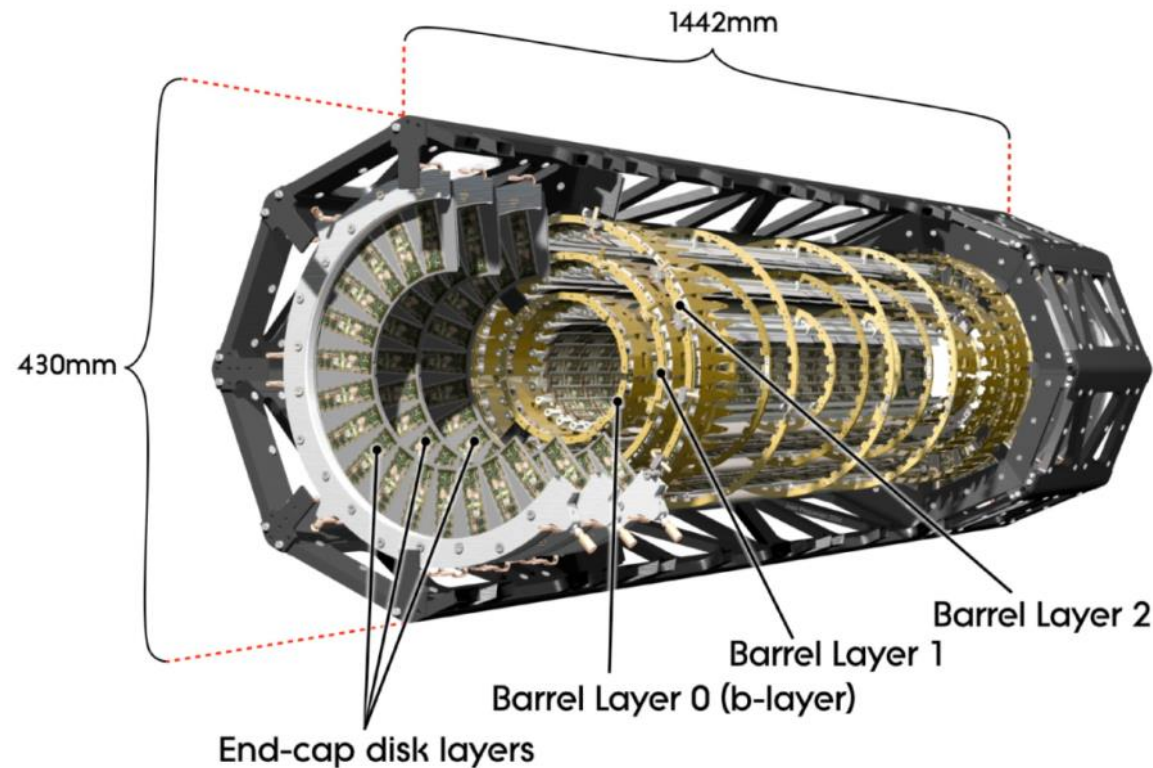
- **Three barrel layers:**
  - R= 5 cm (B-Layer), 9 cm (Layer-1), 12 cm (Layer-2)
  - modules tilted by 20º in the Rφ plane to overcompensate the Lorentz angle.
- **Two endcaps:**
  - three disks each
  - 48 modules/disk
- **Three precise measurement points up to $|\eta|$<2.5:**
  - RΦ resolution:10 μm
  - η (R or z) resolution: 115 μm
- 1456 barrel modules and 288 forward modules, for a total of 80 million channels and a sensitive area of 1.7 m².
  - Environmental temperature about -10 ºC
  - 2 T solenoidal magnetic field.

ATLAS Silicon Strip Detectors
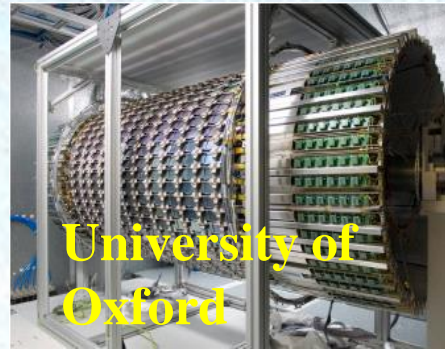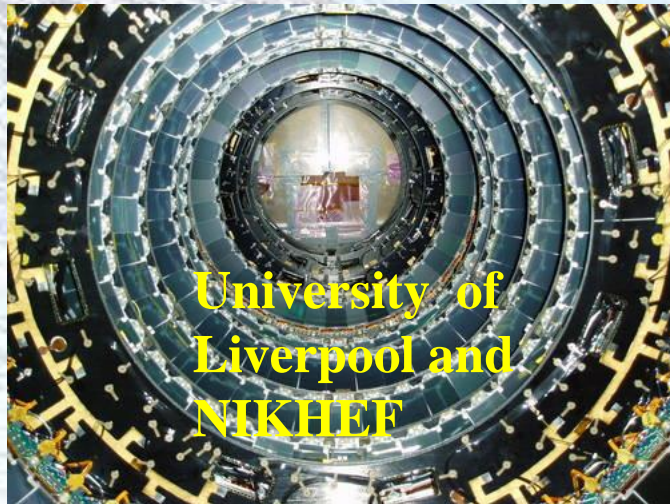
4 barrels (2112 modules) and 2×9 disc end-caps (1976 modules)

610,000cm^2 of silicon micro-strips
~20,000 separate 6cm×6cm sensors

University of Liverpool and NIKHEF

University of Oxford

ATLAS

Z→μμ and 25 pile-up
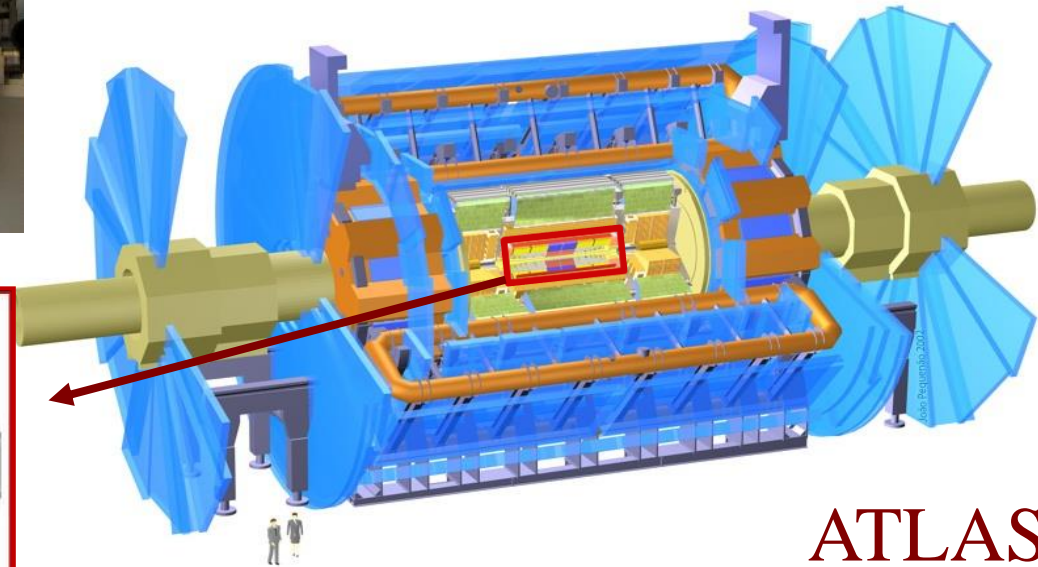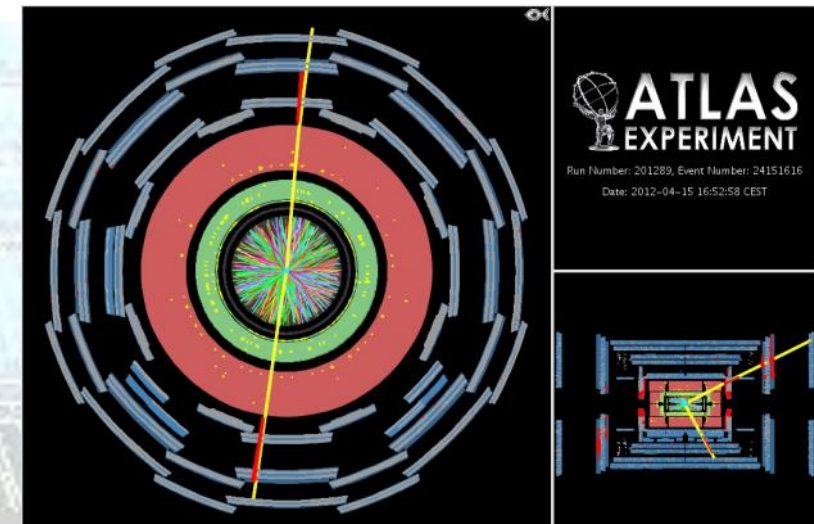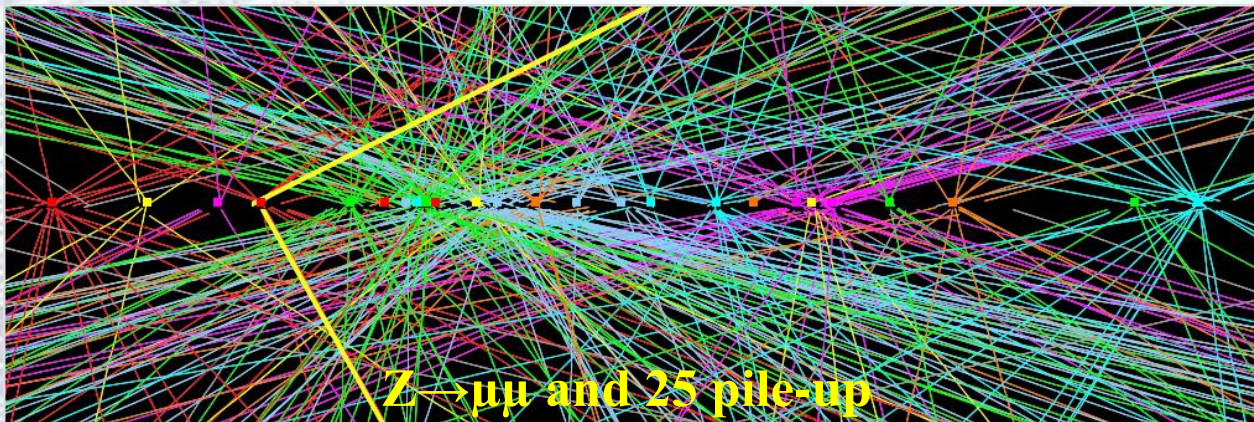
Current SCT ATLAS Module Designs

ATLAS Tracker Based on
Barrel and Disc Supports
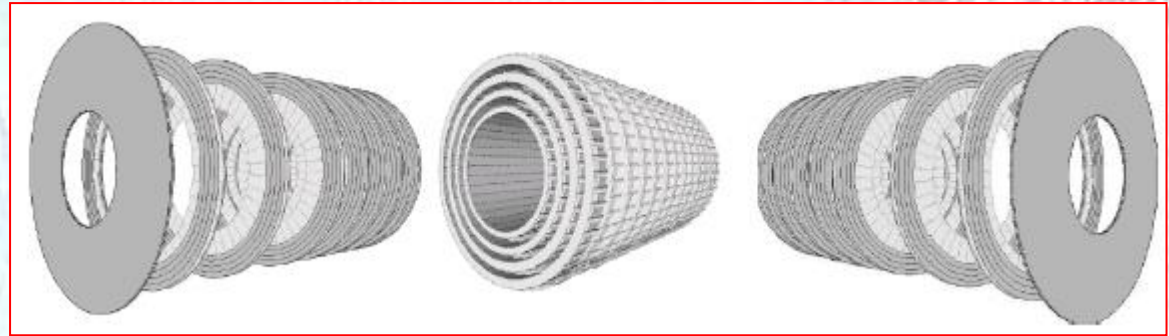
Effectively two styles of double-sided modules (2×6cm long)
each sensor ~6cm wide (768 strips of 80μm pitch per side)
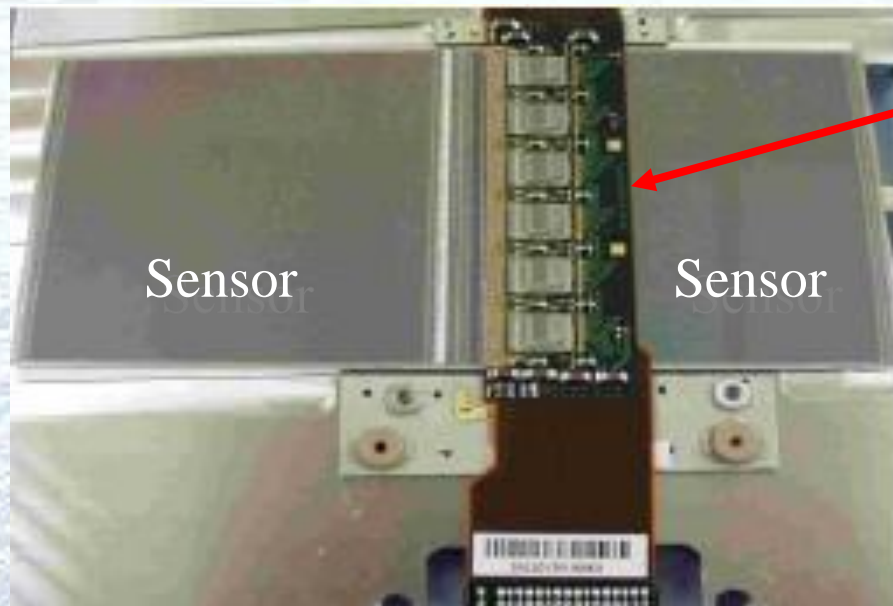
Hybrid cards carrying read-out chips and multilayer interconnect circuit

Sensor   Sensor
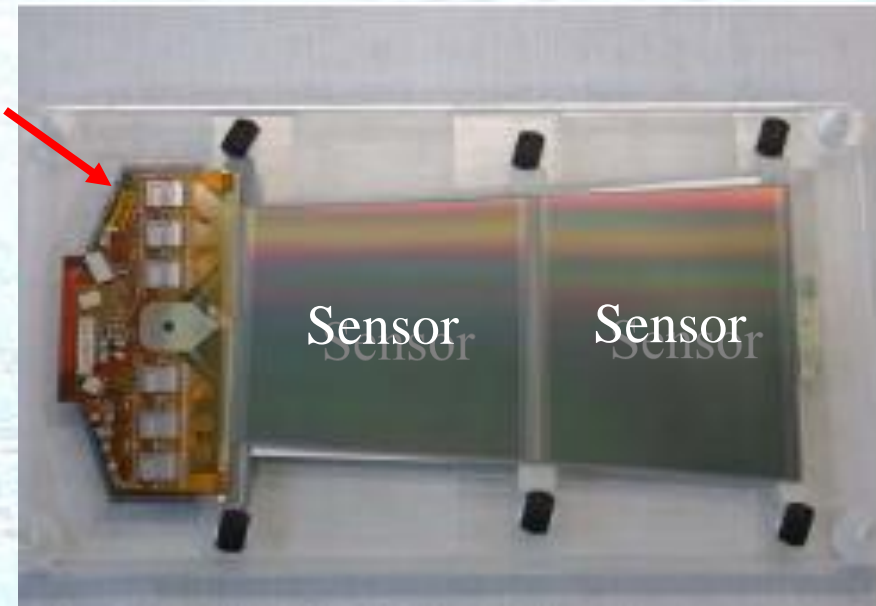
Sensor   Sensor

Barrel Modules
(Hybrid bridge above sensors)

Forward Modules
(Hybrid at module end)

ATLAS Silicon Strip Detectors

Designed to record each separate collision at 40 million collisions per second.
Measure where particles go with 10μm precision (15 million strips).
Has to withstand radiation of $10^{14}n_{eq}/cm^2$ and 100kGy.

2012 (8TeV running) Higgs candidate to 4 muons showing importance of forward tracking

Run: 204769
Event: 71902630
Date: 2012-06-10
Time: 13:24:31 CEST

6.2m

2.1m

Barrel semiconductor tracker
Pixel detectors
Barrel transition radiation tracker
End-cap transition radiation tracker
End-cap semiconductor tracker
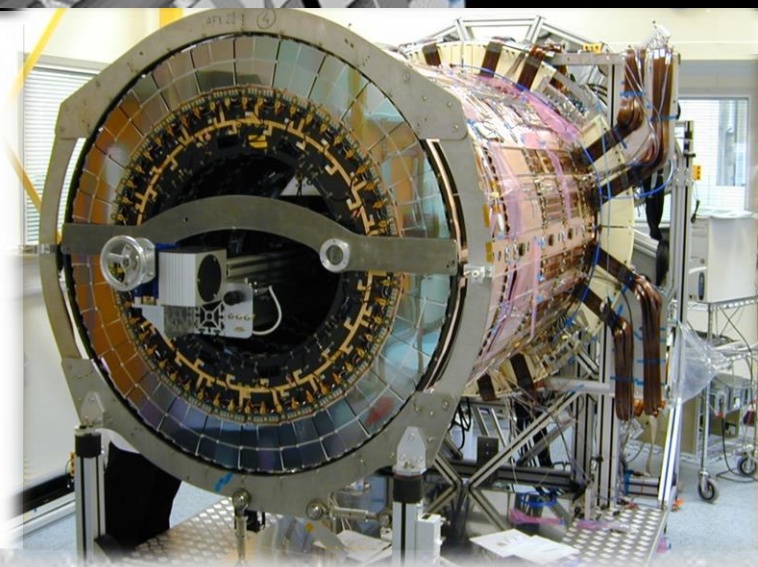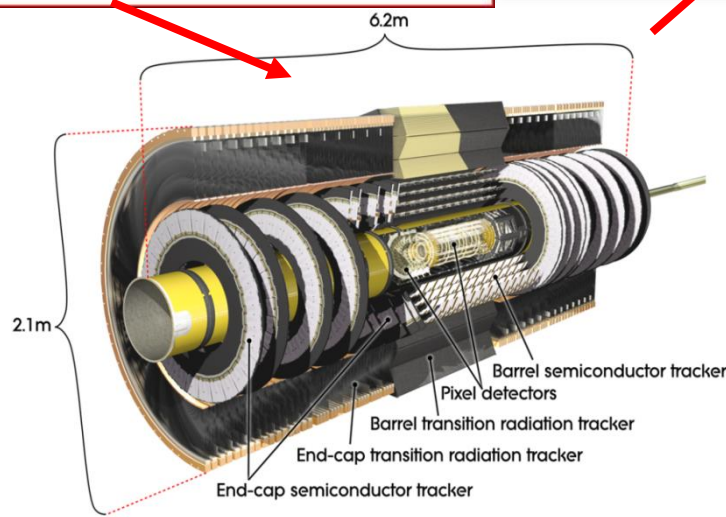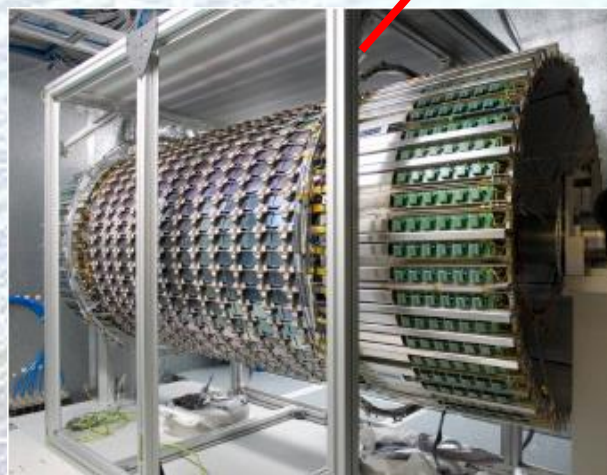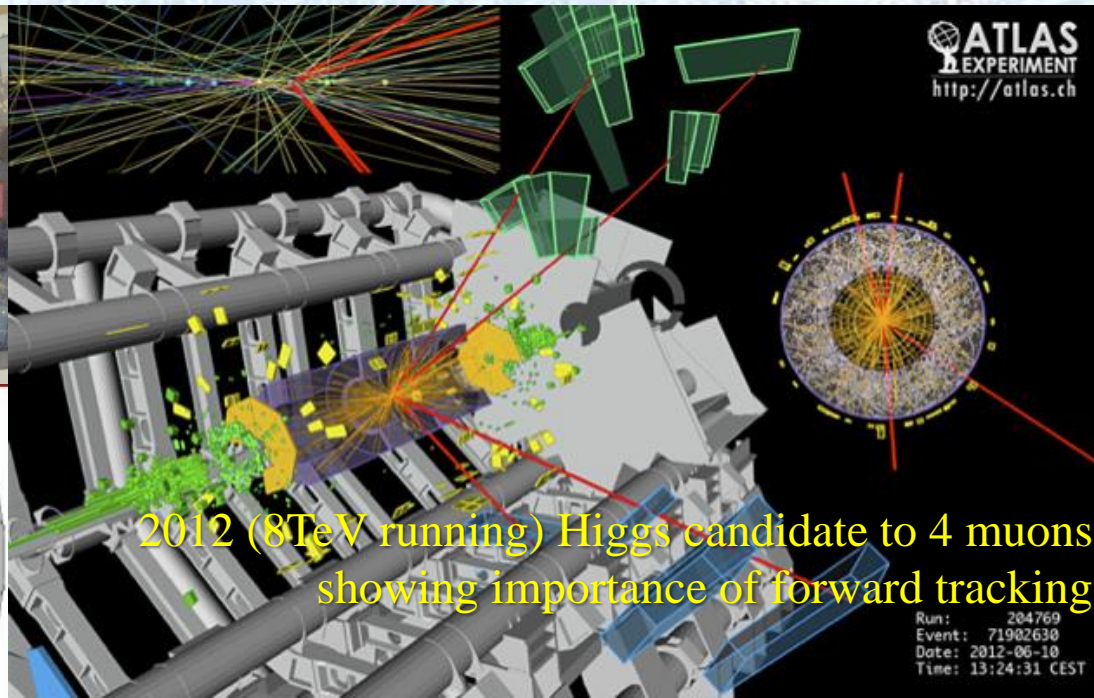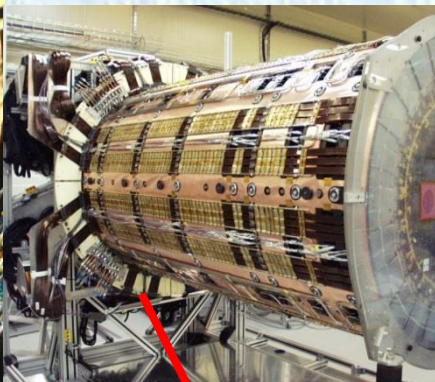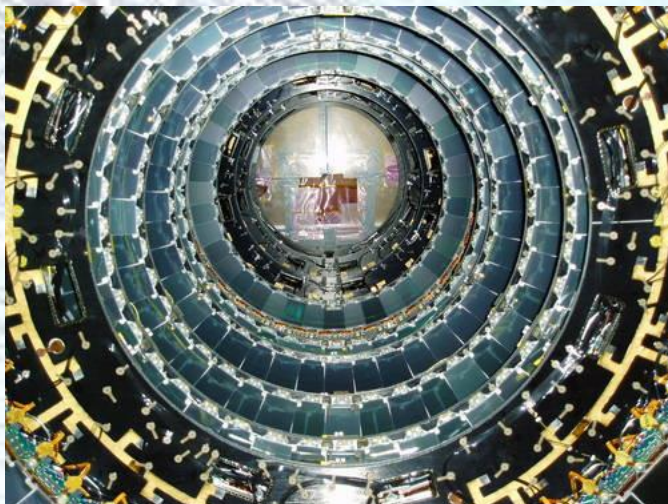
Physics Reach at the LHC

The challenge of the LHC is to cope with proton-proton collisions at rates giving up to 10^{16} collision events per year, but where only a tiny fraction can be sensibly recorded

Most collisions give "low p_T" events that do not correspond to the proton's constituents undergoing the head-on collisions which have the energies to make new particles

A multi-level "trigger" quickly identifies signatures of high-energy constituent collisions and gives $\times 10^{-5}$ data reduction

Even then, many tens of millions of Gigabytes per year need storing and processing:

$\rightarrow$ Worldwide LHC Computing Grid (WLCG over 150,000 processors at over 170 sites in 36 countries http://lcg.web.cern.ch/LCG/public/)
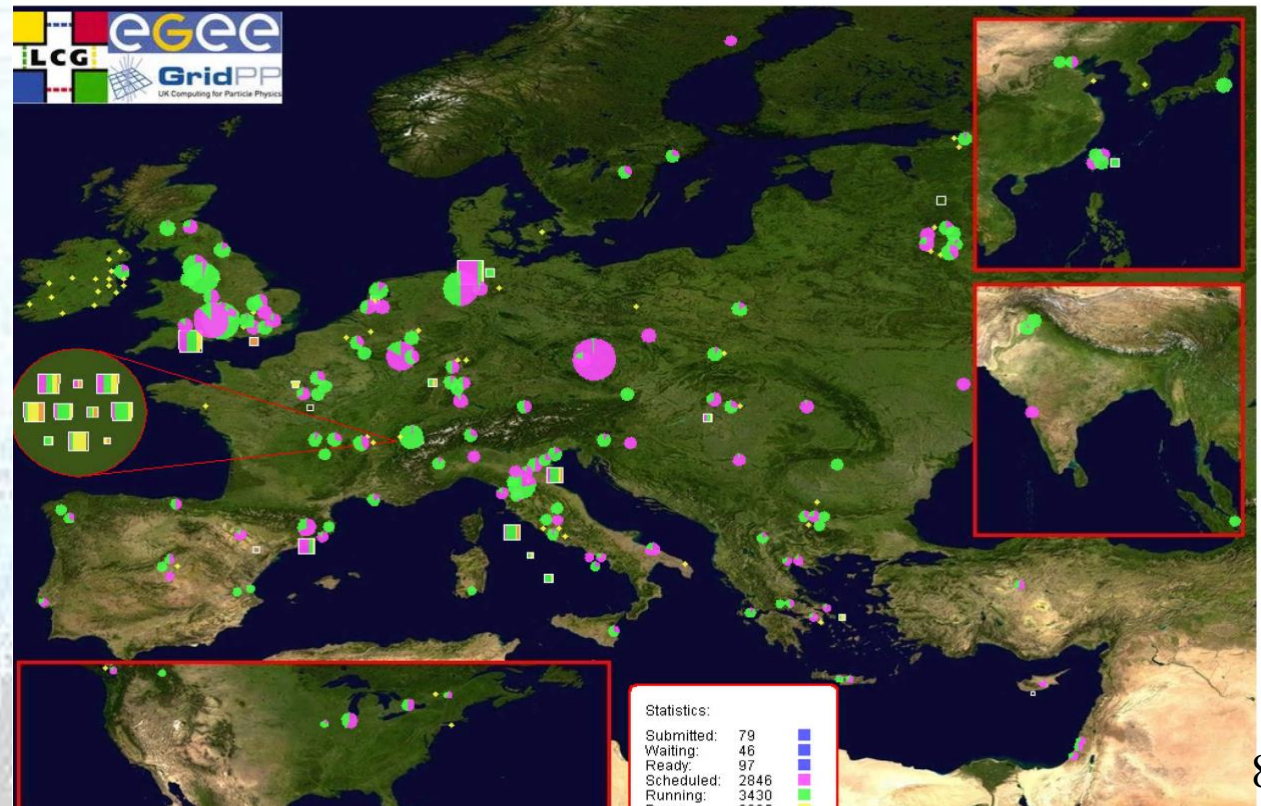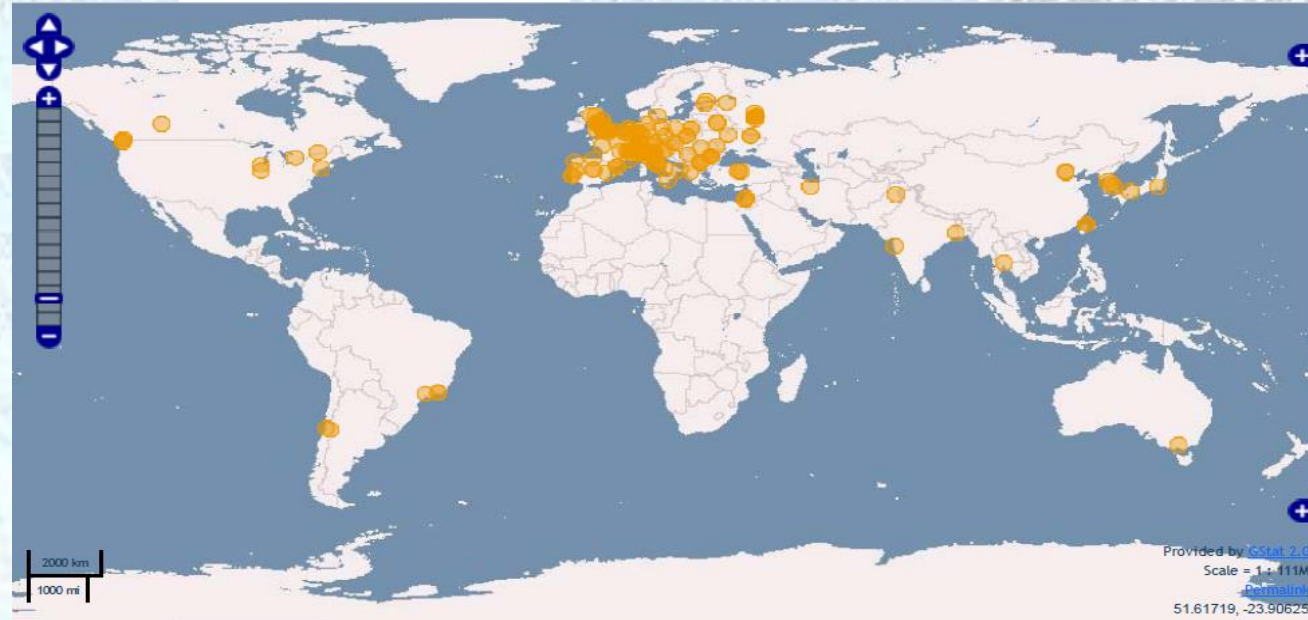
LHC Computing (CERN Director General)

After filtering, CERN detectors select ~200 interesting collisions per second.

Several MBs of data to be stored for each collision...

➡ more than 25 Petabytes/year of data!

8 Megabyte (8MB)
A digital photo

1 Gigabyte (1GB)
= 1000MB
A DVD movie

1 Terabyte (1TB)
= 1000GB
World annual
book production

> 25 Petabytes (25PB)
= 25000TB
Annual LHC data output

CERN, home of the World Wide Web, is a driving force
in Grid Computing

Discovery of the Higgs at the LHC

- Prior to the LHC start-up all we knew: Higgs mass > 114 GeV
- After 2 years of successful LHC operation, last July ATLAS and CMS announced the discovery of a new Higgs-like boson
- Clearest in γγ, ZZ
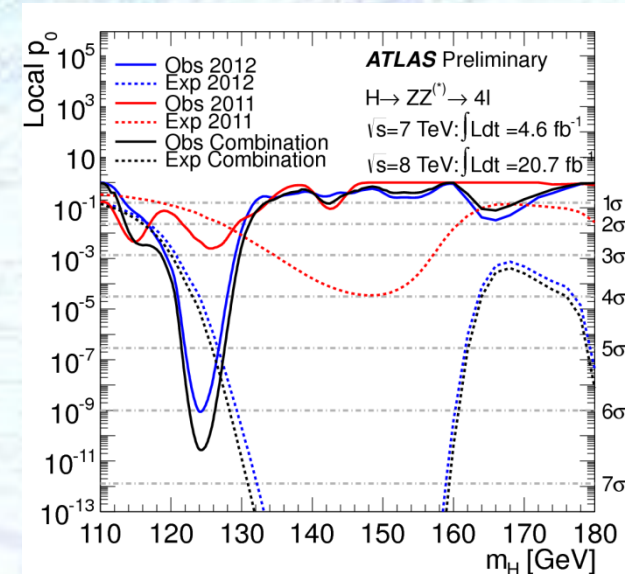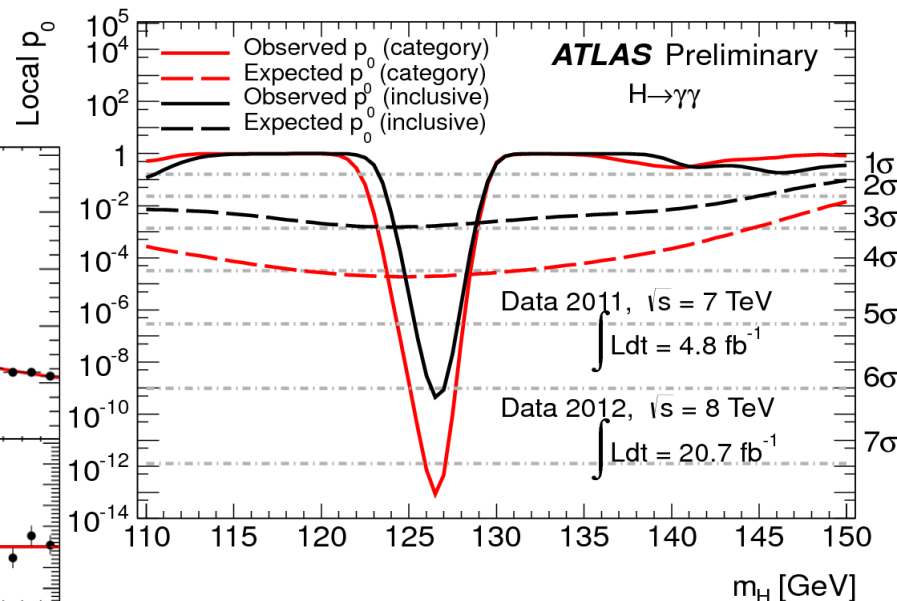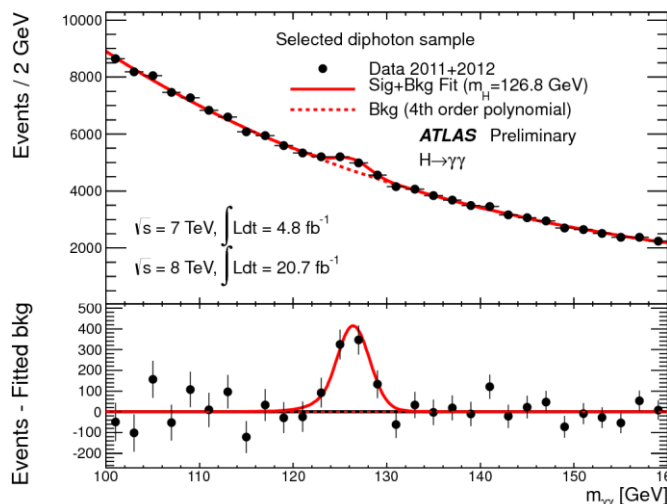
- It is unique amongst the particles we know (spin-0)
  - neither a force (spin-1) nor matter (spin-½) particle
- It is key to the way the universe works
- It is stepping stone to a deeper understanding
- Measuring its properties is now our highest priority
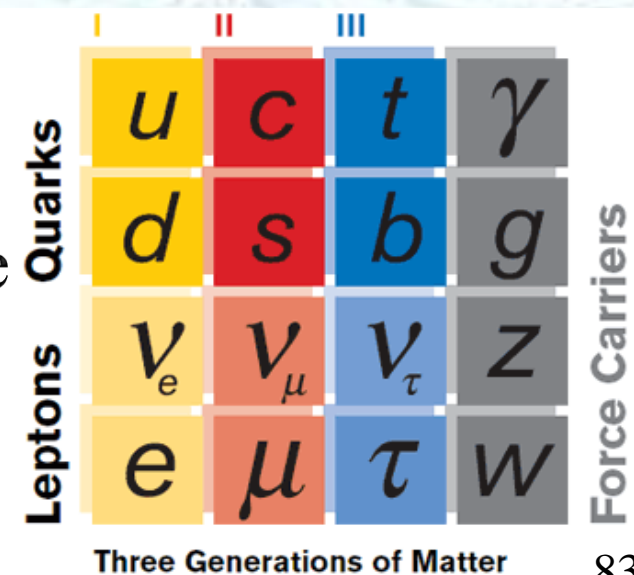
Discovery of the Higgs at the LHC
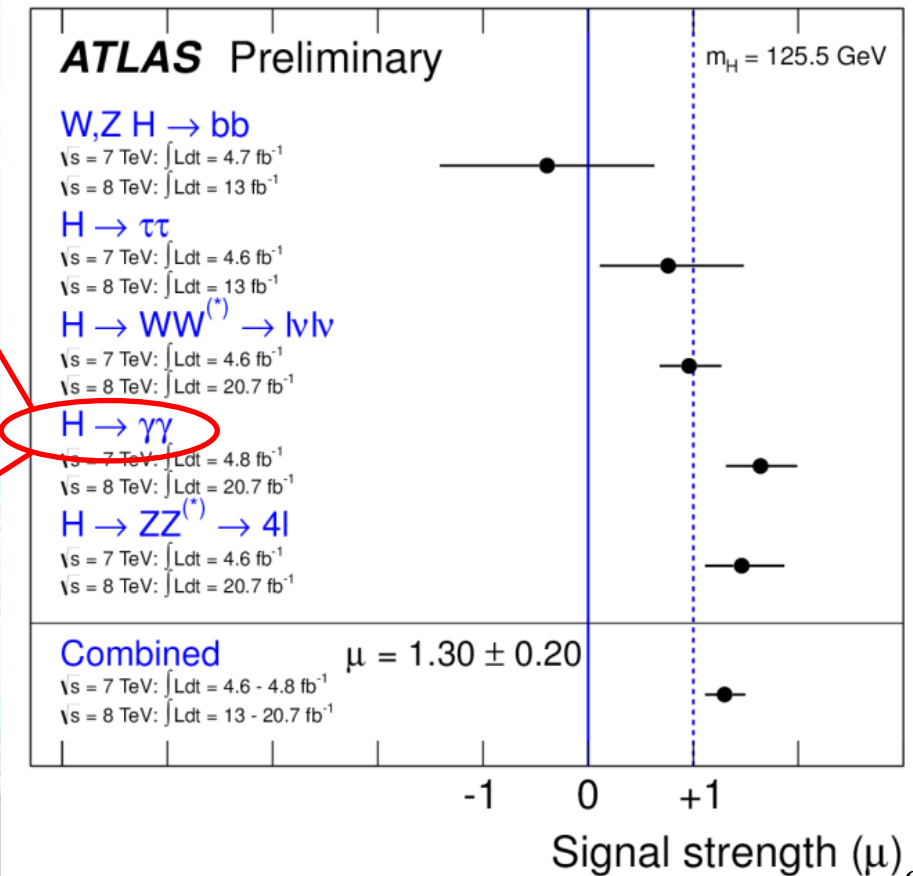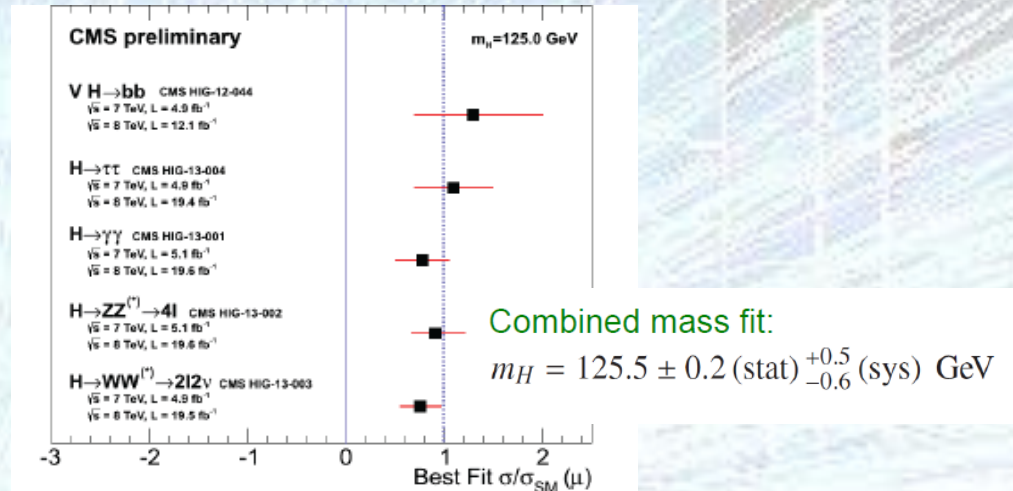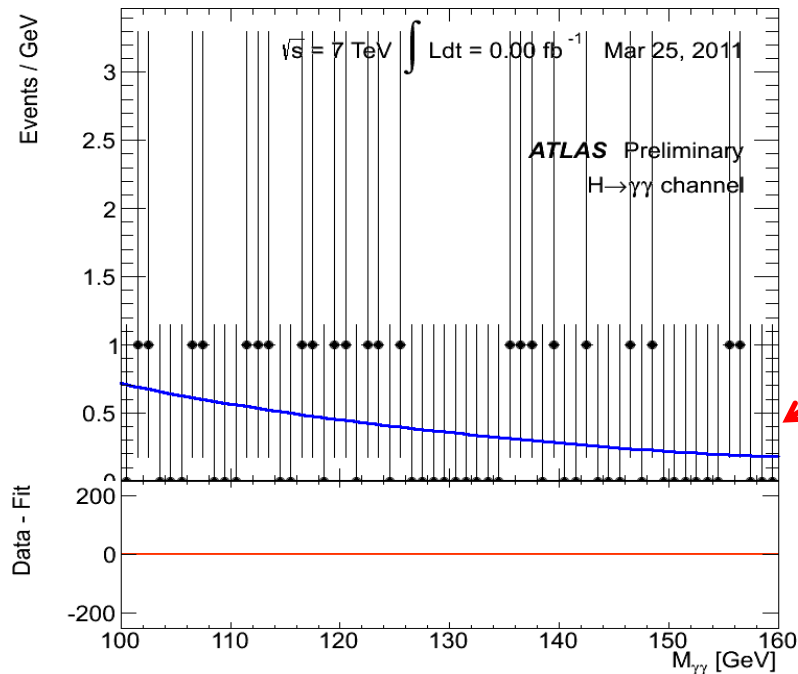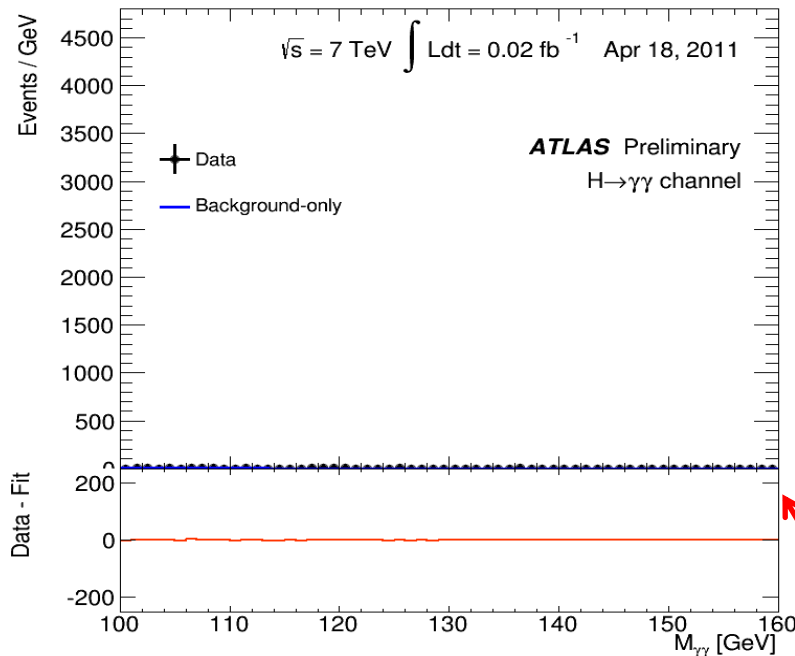
Discovery of the Higgs at the LHC
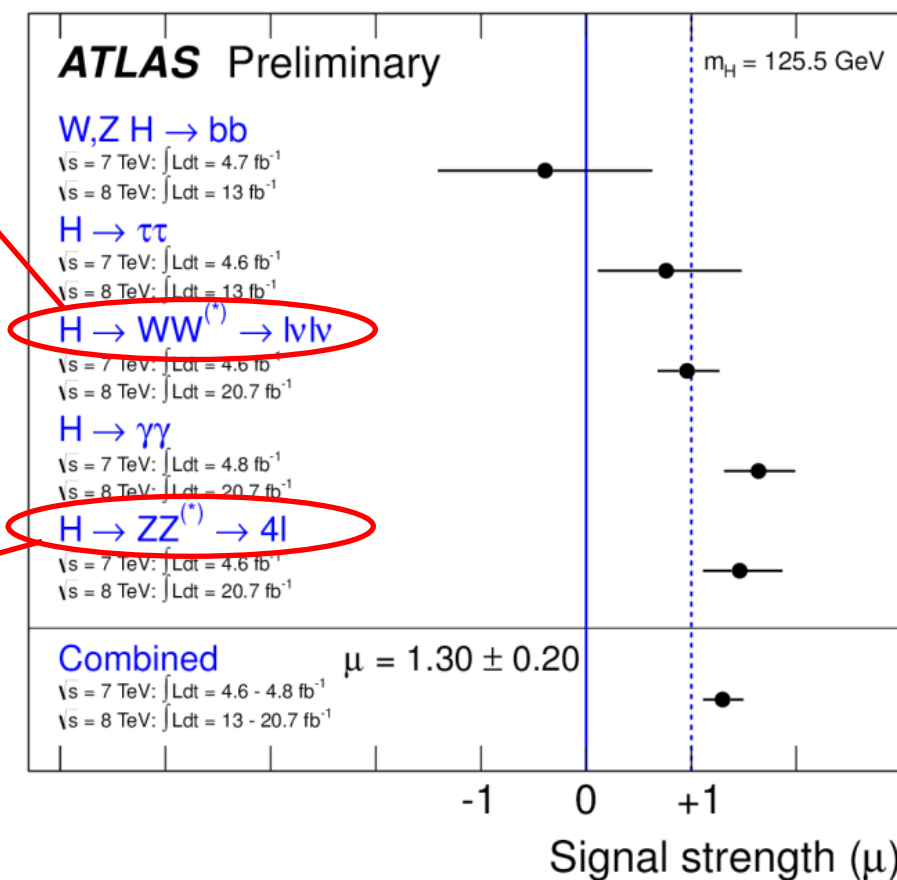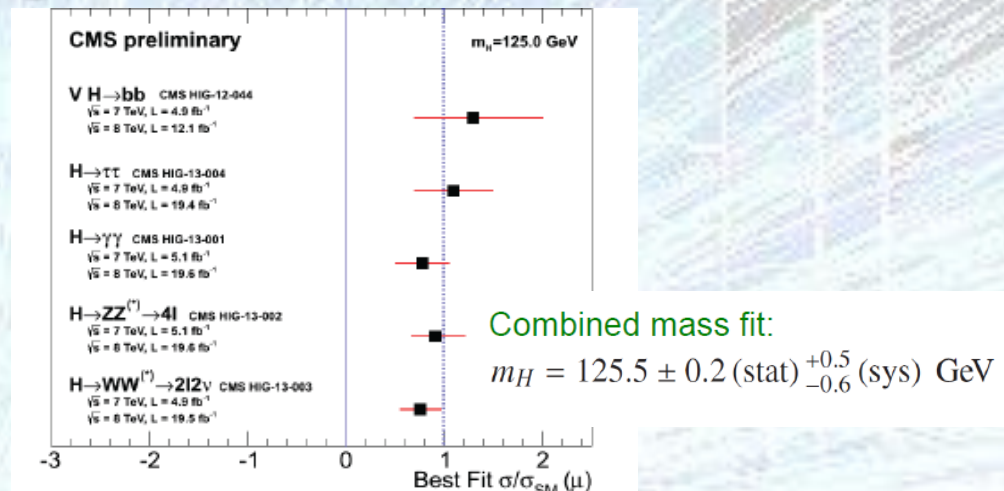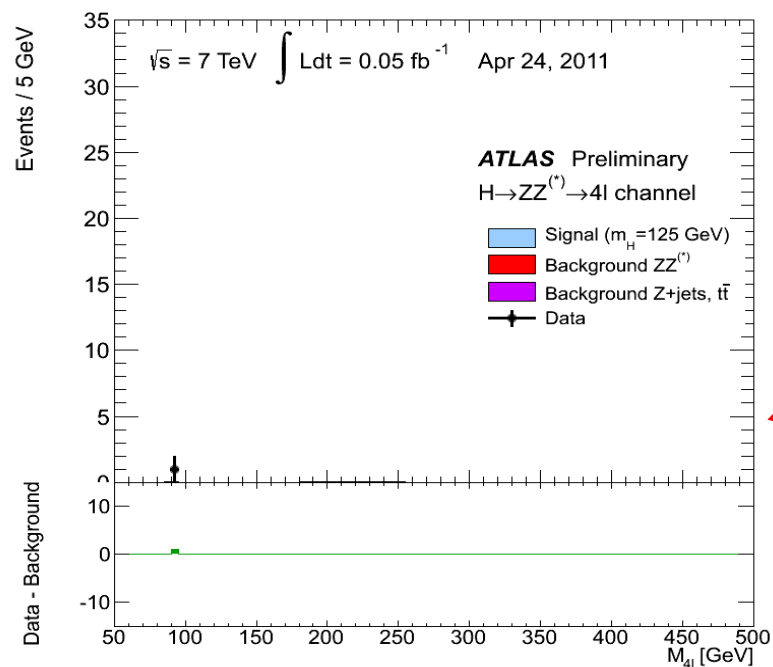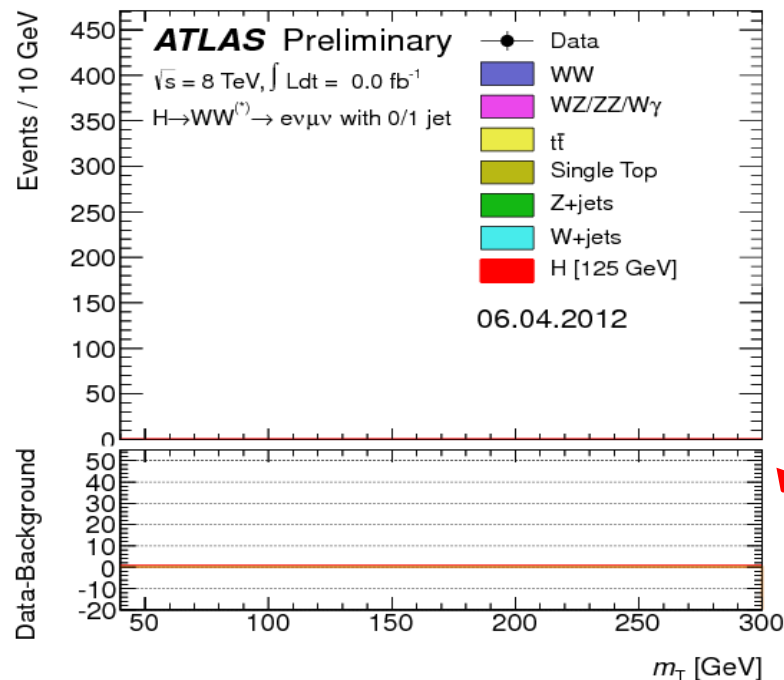
Discovery of the Higgs at the LHC
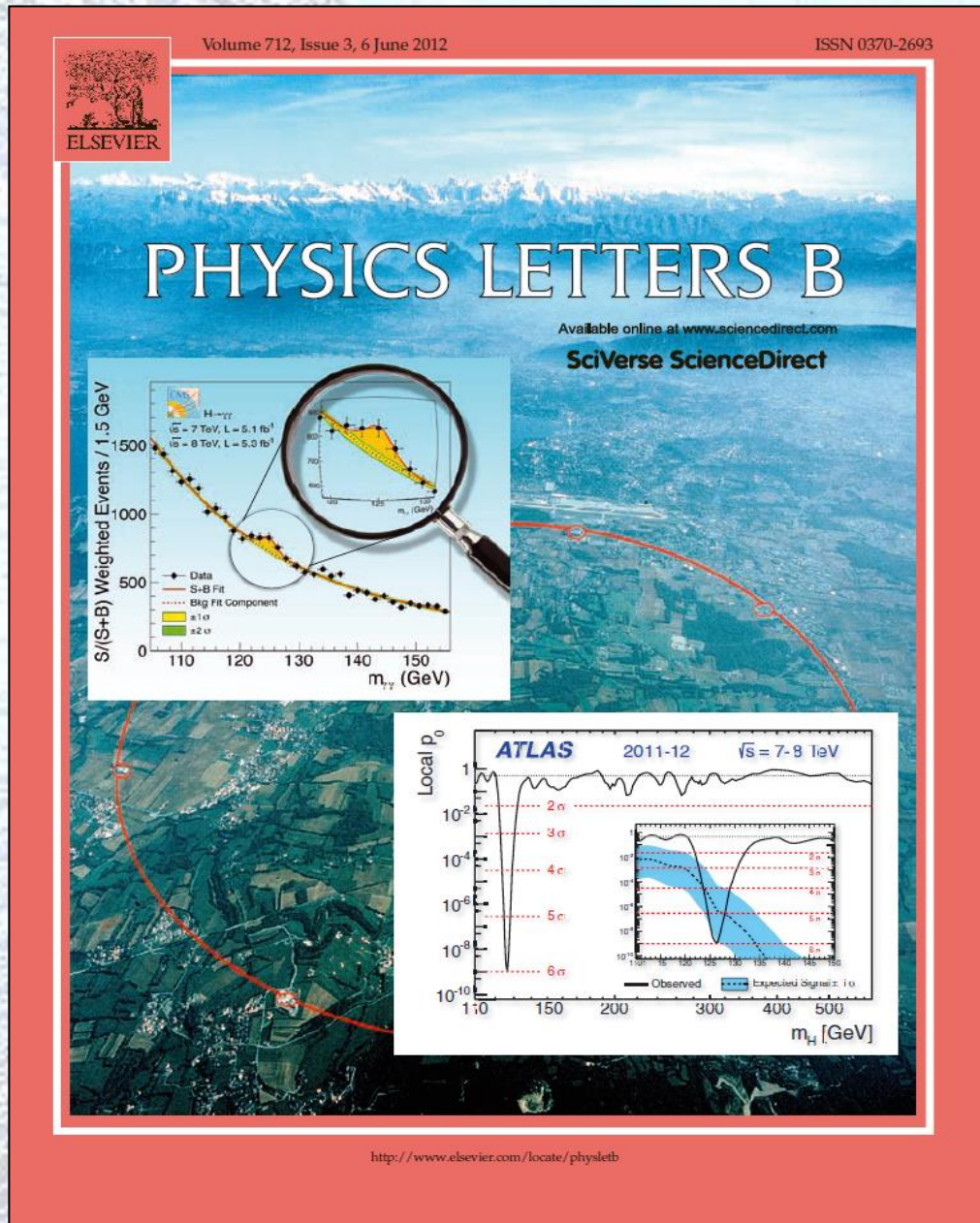
The Higgs: Next Steps at the LHC

- Is this the particle proposed by Peter Higgs?
  - precision measurements of mass, spin and decays
- Are there more Higgs bosons?
- Can Higgs decays help us find dark matter?

- Deep questions in physics remain: unification of forces, nature of dark matter and dark energy, matter/anti-matter asymmetry.

- LHC programme only just begun (1% of data collected at half the final energy). A rich 20 year programme is still ahead.

- Many theories anticipate further discoveries that are in reach at the LHC.

- Whilst direct searches for new states provide the most convincing discoveries, indirect searches involving the highest possible statistical precision at either the LHC or through other rare decay facilities will provide complementary studies
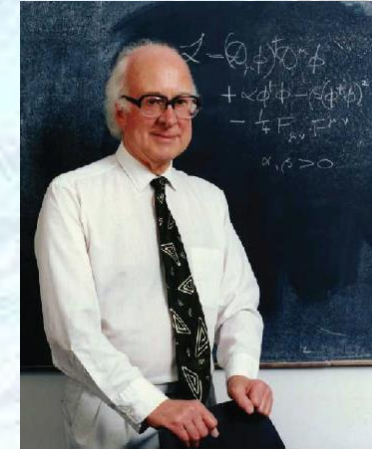
LHC and HL-LHC Timeline

(See for example DG presentation of 6th April 2013)

2009

Start of LHC

Run 1: 7 and 8 TeV centre of mass energy, luminosity ramping up to few 10^{33} cm^{-2} s^{-1}, few fb^{-1} delivered

2013/14

LHC shut-down to prepare machine for design energy and nominal luminosity

Run 2: Ramp up luminosity to nominal (10^{34} cm^{-2} s^{-1}), ~50 to 100 fb^{-1}

2018

Injector and LHC Phase-I upgrades to go to ultimate luminosity

Run 3: Ramp up luminosity to 2.2 x nominal, reaching ~100 fb^{-1} / year accumulate few hundred fb^{-1}

~2022

Phase-II: High-luminosity LHC. New focussing magnets for very high luminosity with levelling

Run 4: Collect data until > 3000 fb^{-1}

2030

https://cds.cern.ch/record/1551933/files/Strategy_Report_LR.pdf?version=1.

ESWG: *"Europe's top priority should be the exploitation of the full potential of the LHC, including the high-luminosity upgrade of the machine and detectors with a view to collecting ten times more data than in the initial design, by around 2030"*

Main Upgrade Motivations for Phase-II

- The much larger data set allows unique access to rare processes either involving already known particles, the newly found Higgs-like particle, or indeed any further higher mass states discovered during the rest of this decade.

- The HL-LHC programme also offers significant increases in mass reach over that achieved at LHC. For example, the mass reach for SUSY particles ("charginos" and heavy "neutralinos") with ×10 data increases from 500 GeV to ~1 TeV.

- **The relatively low mass of the Higgs-like particle means that it decays to particles with a fairly soft momentum (p_T) spectrum, mandating the use of relatively open (low p_T threshold) Level-1 triggers to collect events as inclusively as possible.**

- From measurement, we have already established the unique nature of this new fundamental particle
  - ➢ We have shown it cannot be spin-1: "force particle" or a spin-½ : "matter particle"
  - ➢ If it is the Higgs of the Standard Model, this points to a spin-0 field permeating all space accounting for the known fundamental particle masses
  - ➢ If not, the prospects are even more exciting

ATLAS Simulation, 14 TeV
— WH
— SUSY-direct-gaugino
— t$\bar{t}$
L1(>20)/L1(>30)
~ 1.3 -1.8
(with offline cuts)

true muon p_T [GeV/c]
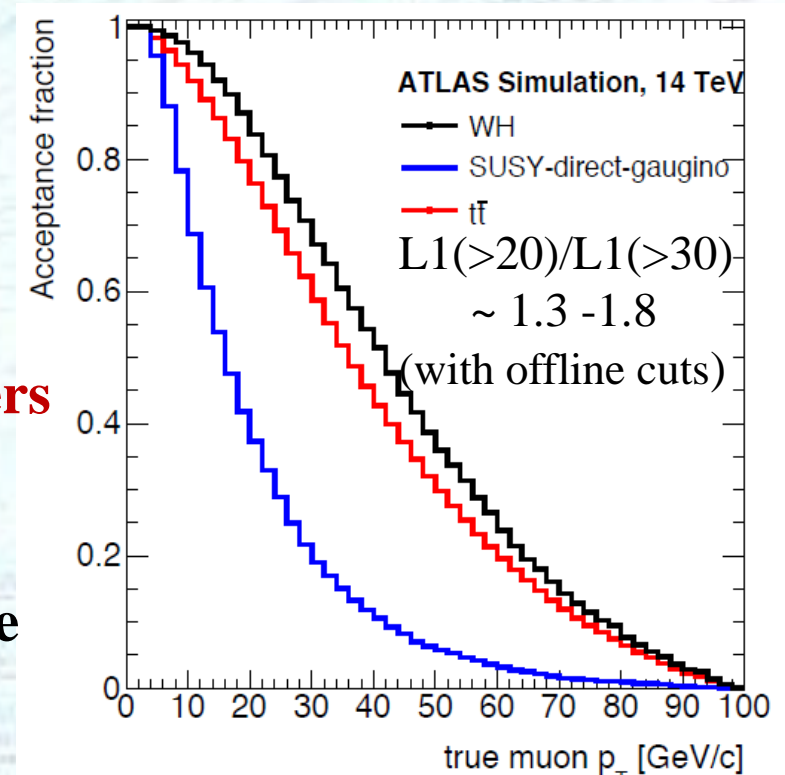
Acceptance vs muon momentum threshold

89

ATLAS: Limits from Data to 2012

H→Zγ Search

Possible new physics in rare/forbidden Higgs decays
Search for H→Zγ (Z→ℓℓ)
- σ·B similar to H→ZZ→4ℓ, but much worse S/B
- Main backgrounds are Z+γ and Z+jets

Use full 2011+2012 data set

No significant signal

Fit for signal in Δm=$m_{\ell\ell\gamma}$-$m_{\ell\ell}$

For m_H=125 GeV @ 95%CL:
σ(H → Zγ)<18.2·σ(H → Zγ)$_{SM}$
(Expected 13.5)

H→µµ Search

Search for small resonance on top of Drell-Yan background
- Enhance S/B by req. p_T(µµ)>15 GeV & splitting in central/non-central µµ
- Background modeled with Breit-Wigner+exponential

Central µµ category

No significant signal

For m_H=125 GeV @ 95% CL:
σ(H → µµ)<9.8·σ(H → µµ)$_{SM}$
(Expected 8.2)

Invisible Higgs Search

Search for invisible decays in ZH prod.
- Suppress Z background with E_T^{miss}>90 GeV
- Require boosted Z and back-to-back with E_T^{miss}
- Veto events with jets
- Main backgrounds: ZZ, WZ and WW

Final E_T^{miss} distribution

Limit on σ·B(ZH→ℓℓinv)

For m_H=125 GeV and SM σ(ZH):
B(H→invisible)<65% @ 95%CL
(Expected: 84%)

Direct Gaugino Search

Natural SUSY requires light $\chi^{\pm}_1$, χ^0_1
χ^0_1 good candidate for dark matter
Search for decays in to τ's and E_T^{miss}
- ≥2 τ_{had}, no e/µ, no (b-)jet, no Z, E_T^{miss}>40 GeV
- Discriminate using stransverse mass, m_{T2}
- Data-driven estimate of multi-jets & W+jets

Limits are set in scenarios with light τ

90

ATLAS: Higgs Spin/CP Properties

- Establish the nature of this particle by determining the spin/CP quantum numbers → already disfavour non 0^+ hypotheses with at least > 2 σ.

- Even better separation from 0^-, spin 1 and spin 2 with large datasets and higher energy. Similarly with 300 fb^{-1} @ 14 TeV spin/CP quantum numbers of non-mixed states can be established with a significance > 5 σ.

- With 3000 fb^{-1}, **clean channels** and **rare couplings** can be studied.

ttH, H → γγ for top yukawa couplings

Rare decays: H → μμ
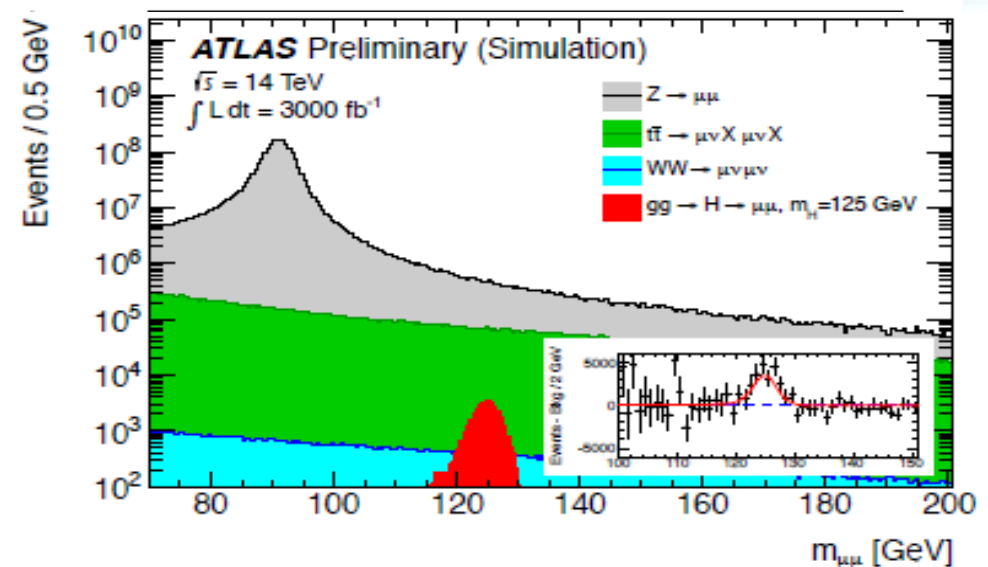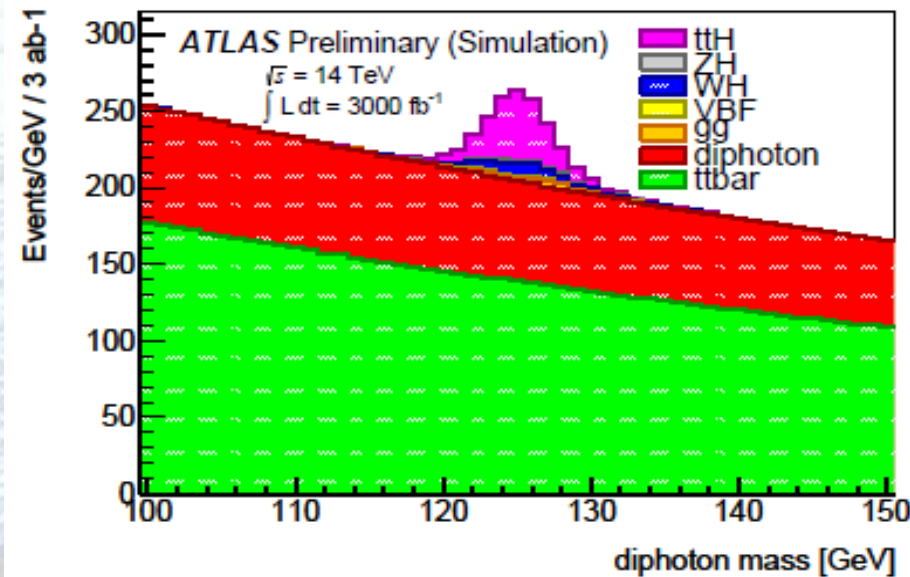
Small signal-to-background ratio (~ 0.2%) but narrow signal peak → expected signal significance > 6

ATLAS: Higgs Coupling Parameters

- For a given production and decay mode, $\sigma \times BR$ is assumed to be proportional to $\Gamma_i \Gamma_j / \Gamma_H$
- The coupling fit parameters are chosen as

$$\frac{\Gamma_W}{\Gamma_Z}, \frac{\Gamma_\gamma}{\Gamma_Z}, \frac{\Gamma_\tau}{\Gamma_Z}, \frac{\Gamma_\mu}{\Gamma_Z}, \frac{\Gamma_t}{\Gamma_g}, \frac{\Gamma_Z}{\Gamma_g} \text{ and } \frac{\Gamma_g \cdot \Gamma_Z}{\Gamma_H}$$

Expected precision on signal strength at 300 and 3000 fb-1

Phase-I: 10-60 (80)%
Phase-II: 10-30%

(*) only vector boson fusion taken into account
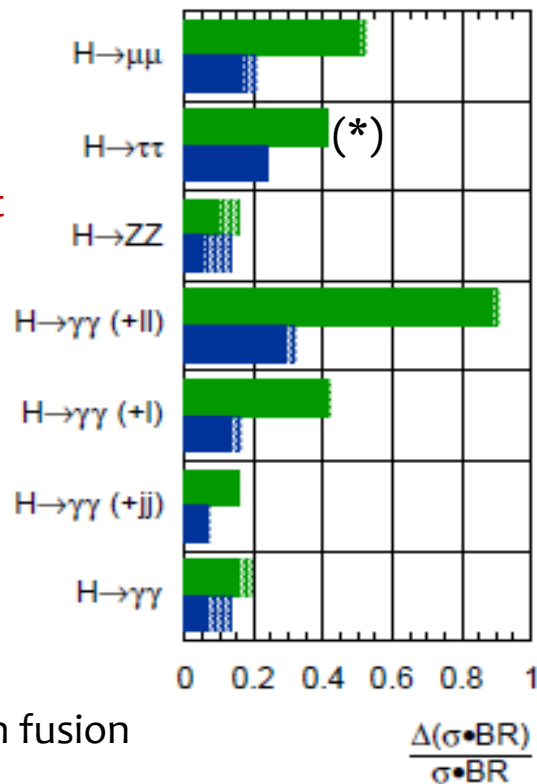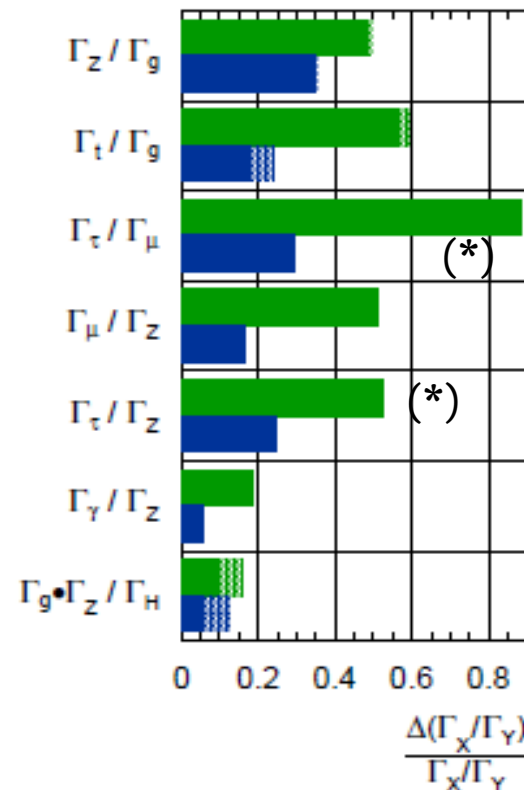
Expected precision on ratios of Higgs partial widths

Also in progress (see back-up):

Studies on **trilinear self-coupling** (λ_{HHH}) relevant to determine SM parameters and nature of higgs mechanism:
- Most promising channels: **HH → bbγγ** and **HH → bbττ**

ATLAS Preliminary (Simulation)
$\sqrt{s}$ = 14 TeV; $\int Ldt$=300 fb^{-1}; $\int Ldt$=3000 fb^{-1}

$H\to\mu\mu$, $H\to\tau\tau$ (*), $H\to ZZ$, $H\to\gamma\gamma$ (+ll), $H\to\gamma\gamma$ (+l), $H\to\gamma\gamma$ (+jj), $H\to\gamma\gamma$

$\frac{\Delta(\sigma \cdot BR)}{\sigma \cdot BR}$

ATLAS Preliminary (Simulation)
$\sqrt{s}$ = 14 TeV; $\int Ldt$=300 fb^{-1}; $\int Ldt$=3000 fb^{-1}

Γ_Z/Γ_g, Γ_t/Γ_g, Γ_τ/Γ_μ (*), Γ_μ/Γ_Z, Γ_τ/Γ_Z (*), Γ_γ/Γ_Z, $\Gamma_g \cdot \Gamma_Z/\Gamma_H$

$\frac{\Delta(\Gamma_X/\Gamma_Y)}{\Gamma_X/\Gamma_Y}$

2009	2010	2011	2012	2013	2014	2015	2016	2017	2018	2019	2020	2021	2022	2023	...	2030
	Phase 0			LS1		Phase I,II			LS2	Phase II			LS3			

"Phase-0" upgrade: consolidation
$\sqrt{s} = 13\sim14$ TeV, 25ns bunch spacing
$L_{inst} \simeq 1 \times 10^{34}$ cm^{-2}s^{-1} ($\mu \simeq 27.5$)
$\int L_{inst} \simeq 50$ fb^{-1}

"Phase-I" upgrades:
ultimate luminosity
$L_{inst} \simeq 2\text{-}3 \times 10^{34}$ cm^{-2}s^{-1} ($\mu \simeq 55\text{-}81$)
$\int L_{inst} \gtrsim 350$ fb^{-1}

"Phase-II" upgrades:
$L_{inst} \simeq 5 \times 10^{34}$ cm^{-2}s^{-1} ($\mu \simeq 140$) w. leveling
$\simeq 6\text{-}7 \times 10^{34}$ cm^{-2}s^{-1} ($\mu \simeq 192$) no level.
$\int L_{inst} \simeq 3000$ fb^{-1}

ATLAS has devised a 3 stage upgrade program to optimize the physics reach at each Phase

- New Insertable pixel b-layer (IBL)
- New Al beam pipe
- New pixel services
- New evaporative cooling plant
- Consolidation of detector elements (e.g. calorimeter power supplies)
- Add specific neutron shielding
- Finish installation of EE muon chambers staged in 2003
- Upgrade magnet cryogenics

- New Small Wheel (nSW) for the forward muon Spectrometer
- High Precision Calorimeter Trigger at Level-1
- Fast TracKing (FTK) for the Level-2 trigger
- Topological Level-1 trigger processors
- New forward diffractive physics detectors (AFP)

- All new Tracking Detector
- Calorimeter electronics upgrades
- Upgrade part of the muon system
- Possible Level-1 track trigger
- Possible changes to the forward calorimeters

93

ATLAS: New All-silicon Inner Tracker

Long Barrel Strips

Short Barrel Strips

Forward Strips

Barrel pixel

Microstrip Stave Prototype

Serial Powered "Stavelet"

Baseline layout of the new ATLAS inner tracker for HL-LHC
Aim to have at least 14 silicon hits everywhere (robust tracking)

1 MeV neutron equivalent fluence

charged particle fluence

14 TeV collisions; integrated luminosity = 3000fb⁻¹

Quad Pixel Sensor Wafer
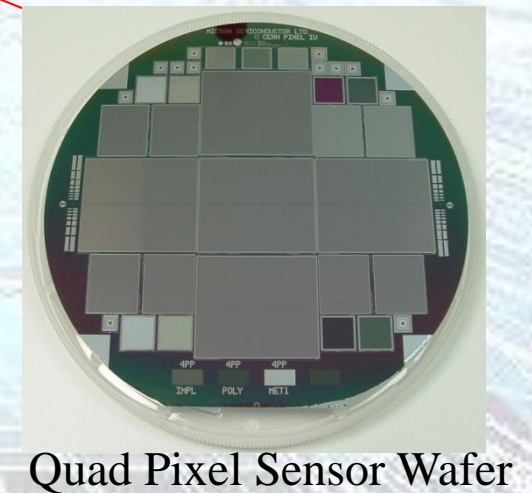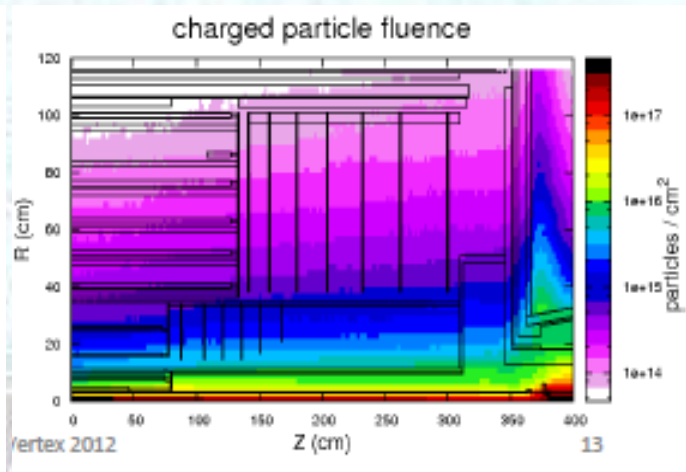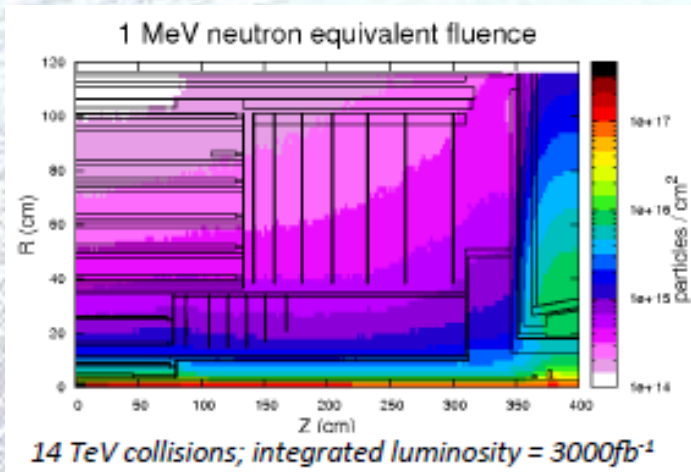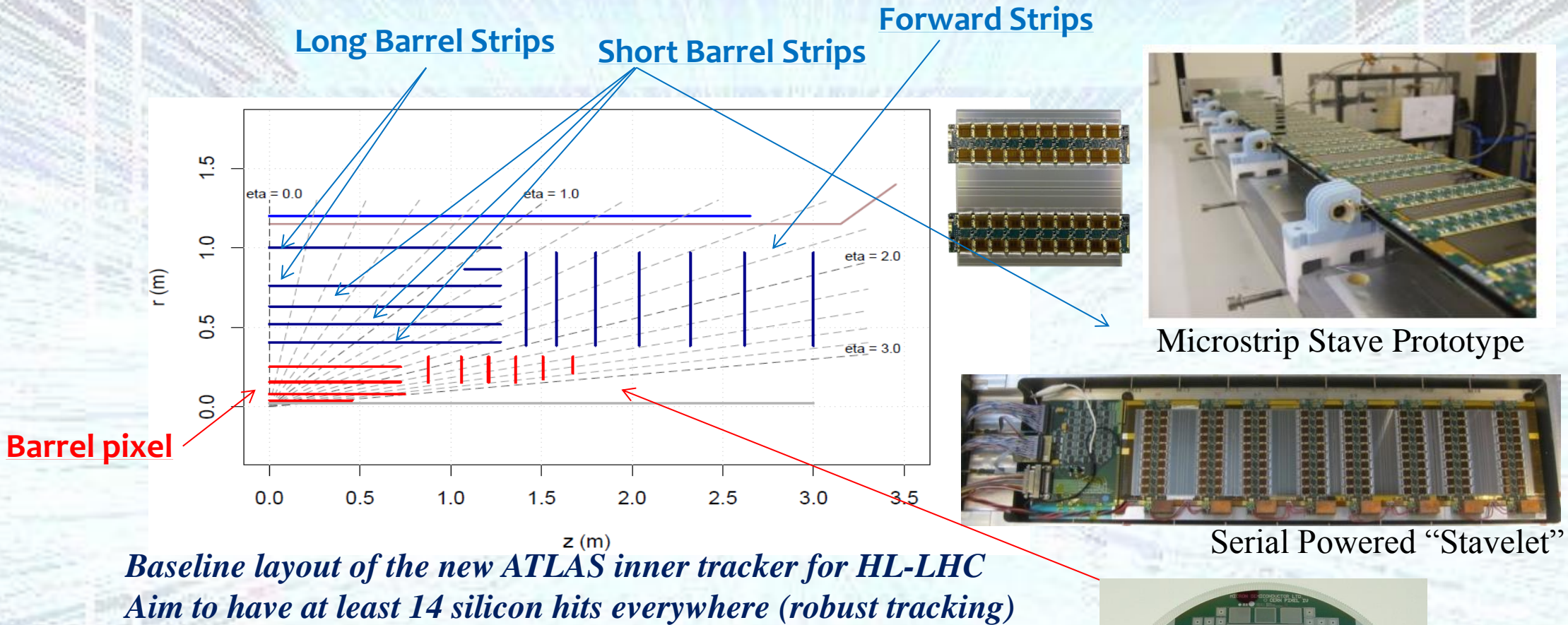
Upgrade Strip Module Irradiation

AL Foil

AL Foil
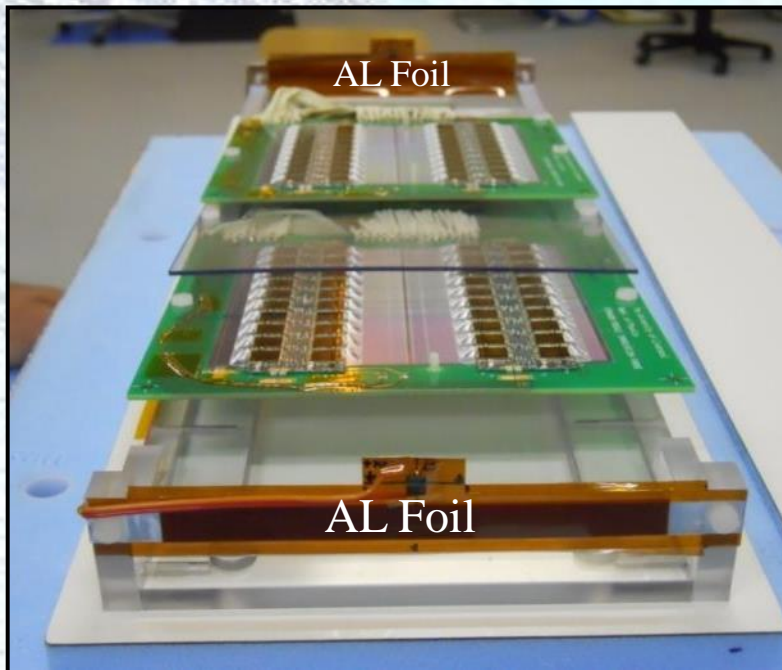
- **Irradiated at CERN-PS irradiation facility**
  - **Module biased, powered, and clocked during irradiation**
  - **Total dose of 1.9×10^{15} n_{eq} cm^{-2} delivered**
    - Max predicted fluence is 5.3×10^{14} n_{eq} cm^{-2} (barrel) and 8.1×10^{14} n_{eq} cm^{-2} (endcap)
- **Sensor and module behave as expected**
- **Noise increase consistent with shot noise expectations**
- **Signal over noise at two times 3000fb^{-1} expected dose should be 12-16 in highest fluence region**

Specification for Strip Sensors

(500 V)
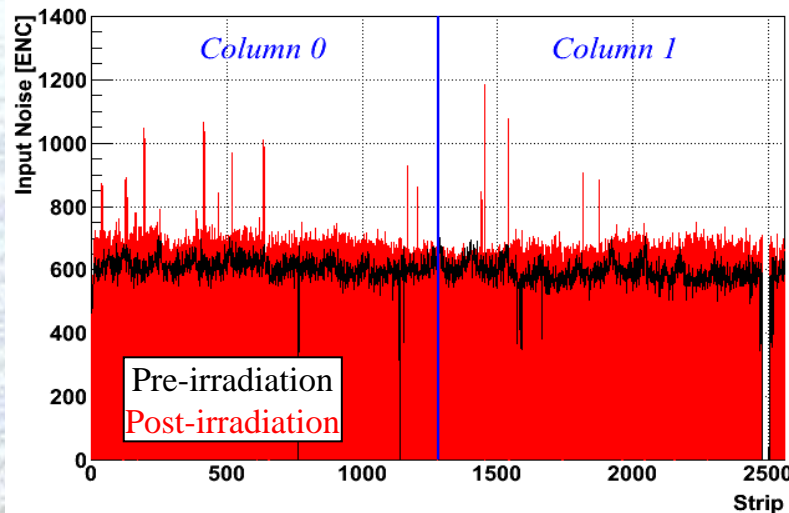
Noise	Column 0	Column 1
Pre-Irrad	610 e$^-$	589 e$^-$
Post-Irrad	675 e$^-$	650 e$^-$
Difference	65 e$^-$	61 e$^-$
Expected	670 e$^-$	640 e$^-$

New All-silicon Inner Tracker

Pixel Detector

- **Pixel sensors in several technologies proved to high doses (planar/3D/diamond shown to $2\times10^{16}n_{eq}$/cm^2)**
- **IBL pixel (50×250μm) OK for outer pixel layers, but can go down to 25μm×125μm pixels with 65 nm CMOS**
- **Test structures in 65nm produced and even studies after irradiation**
- **Larger area sensors (n-in-p) quads/sextuplets produced on 150mm diameter wafers with several foundries**
- **Quad pixel module produced, being tested and results look promising**
- **Prototyping of local supports for various concepts has been carried out**
- **A number of support designs and service routings have been studied**

Quad module prototype

FE-TC4-P1 demonstrator

ATLAS: New All-silicon Inner Tracker

R&D and Performance

- **Silicon strip prototyping at a fairly mature stage with 7 sites having module production capability (Longest lead-time: ATLAS ID TDR published 1997 http://atlas.web.cern.ch/Atlas/GROUPS/INNER_DETECTOR/TDR/tdr.html)**
- **Upgrade pixel module prototypes based on 130nm FE-I4 (IBL) ASIC**
- **Detailed performance up to 200 "pile-up"**

$$\theta_{rms} = \frac{13.6\,\text{MeV}}{\beta cp}\, z\, \sqrt{\frac{x}{X_0}}\, \left(1 + 0.038 \ln\left(\frac{x}{X_0}\right)\right)$$
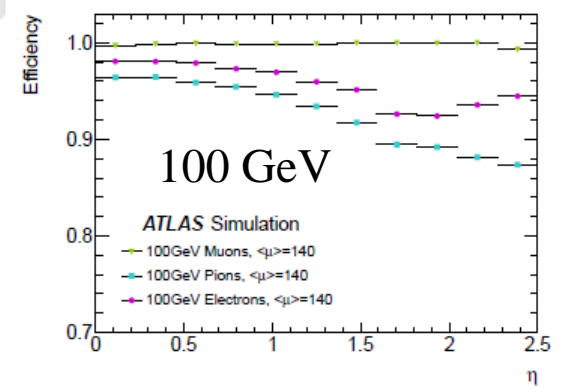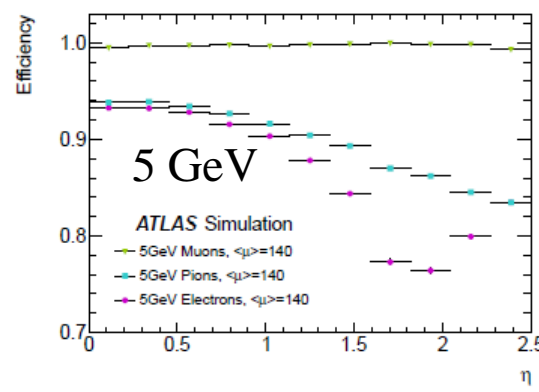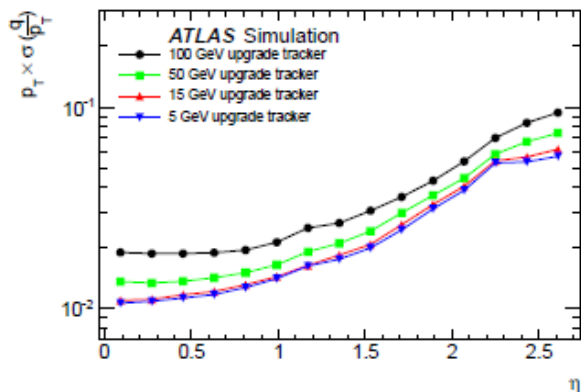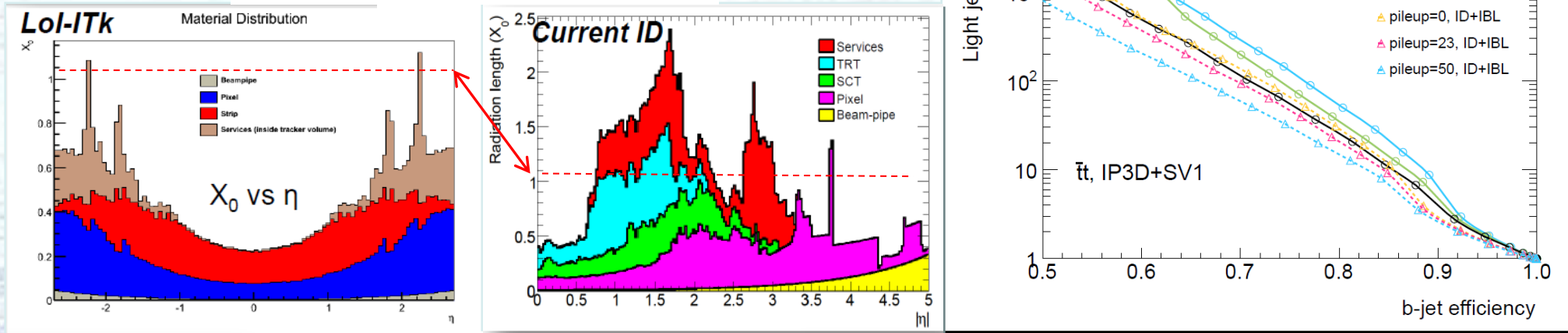
ATLAS: Phase-II Split TDAQ L1 Scheme

Simulation studies show that including a track trigger complements muon and EM triggers

➤ **Improves muon P_T resolution**

➤ **Improves EM identification by matching to track**

Implemented as 2-level scheme reusing Phase-I L1 trigger improvements for new L0

FTK technology could be used to perform fast track fit in L0 defined Region of Interest (RoI)
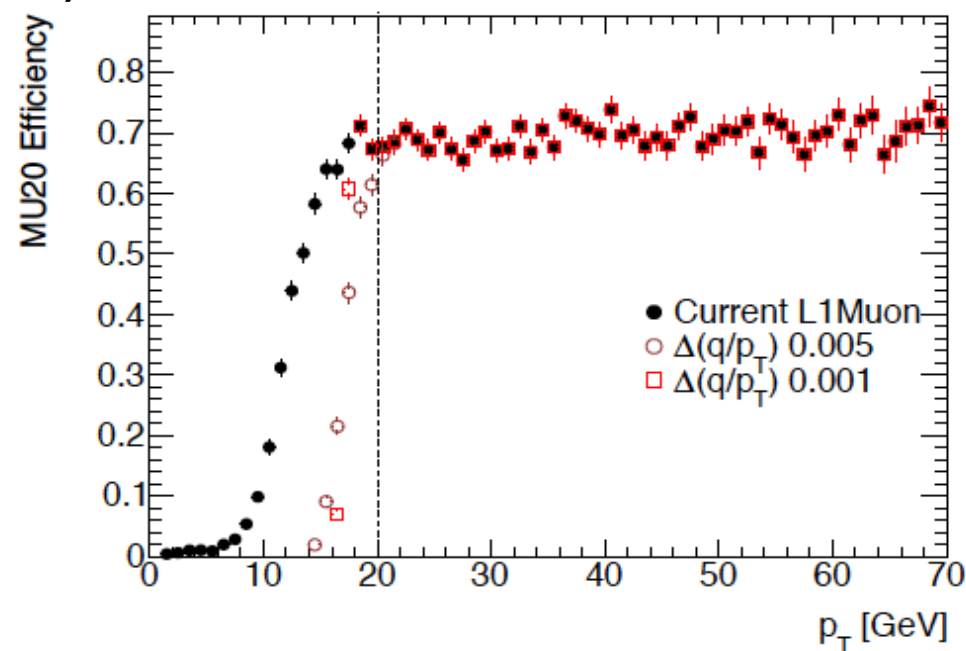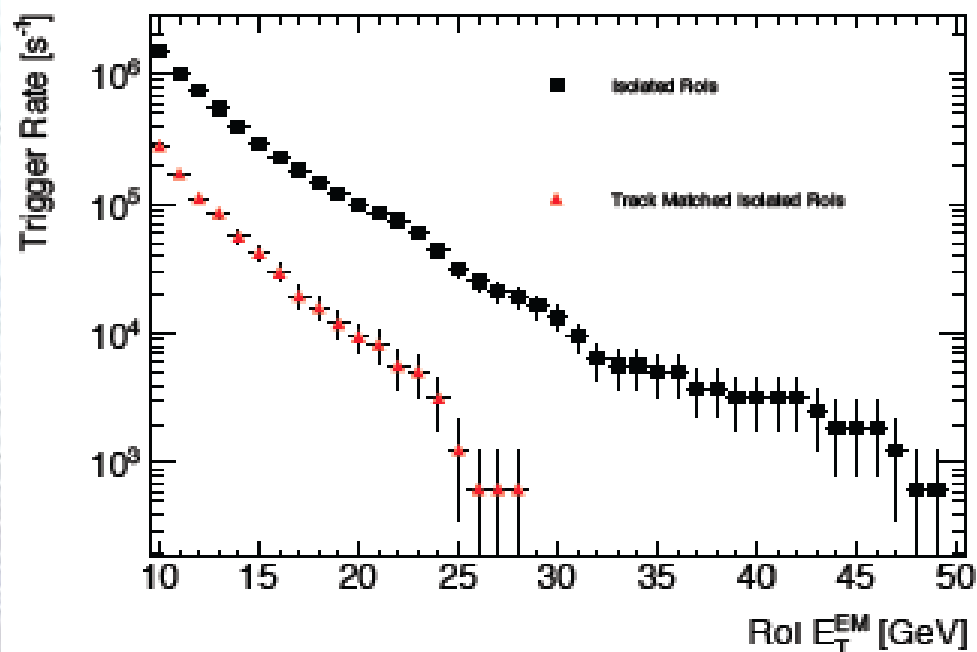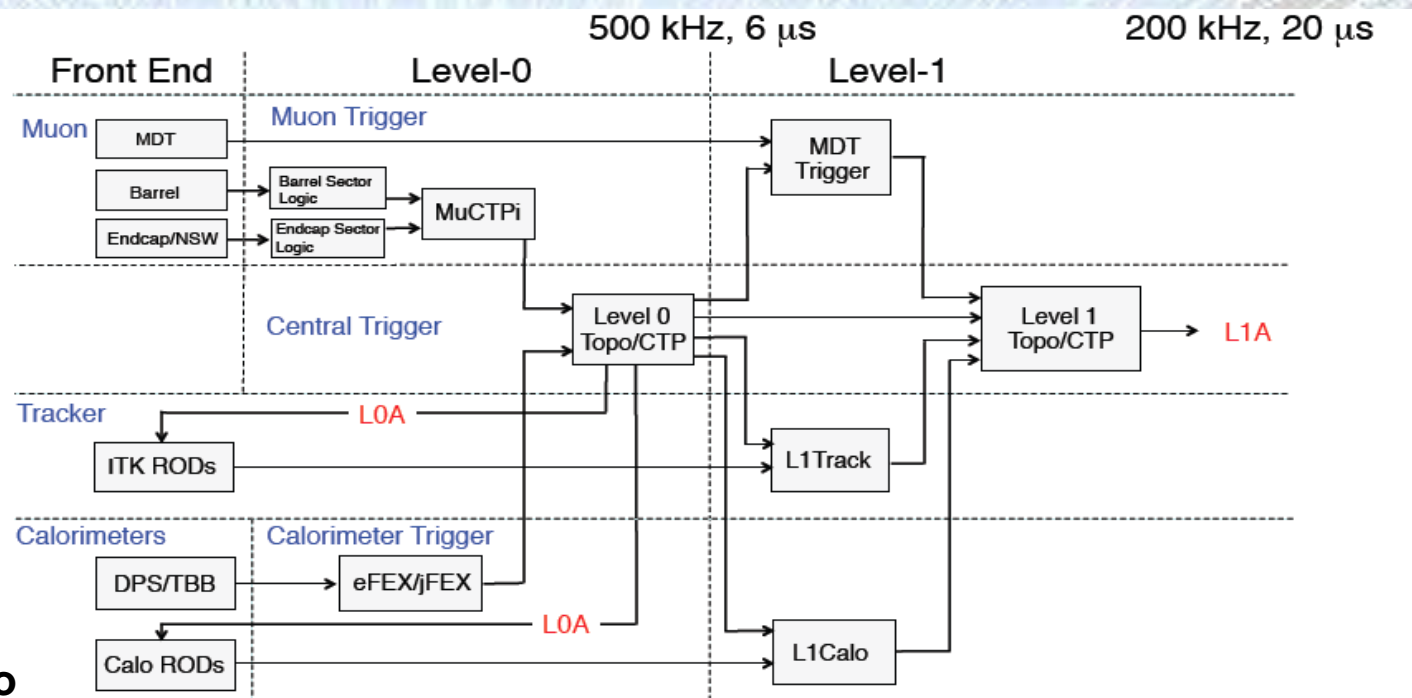
Fast TracKer (FTK)

- **Rapid pattern recognition**
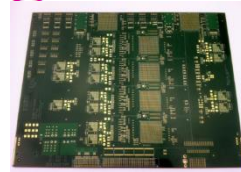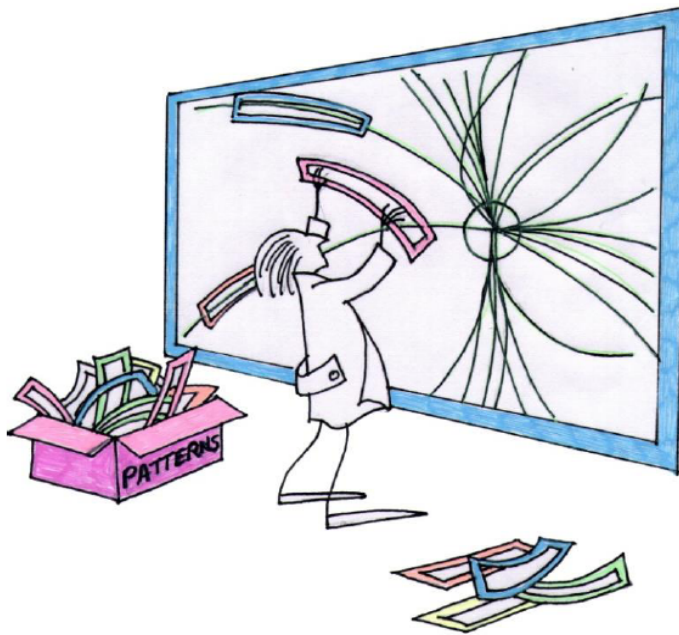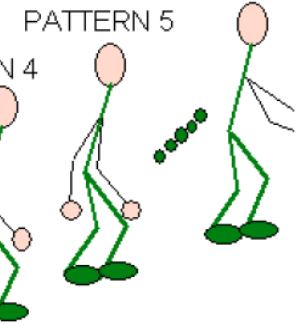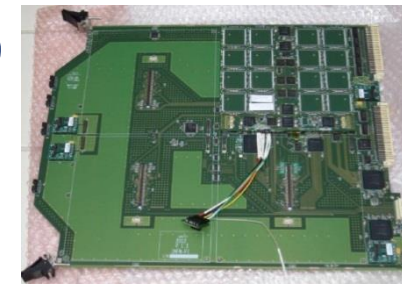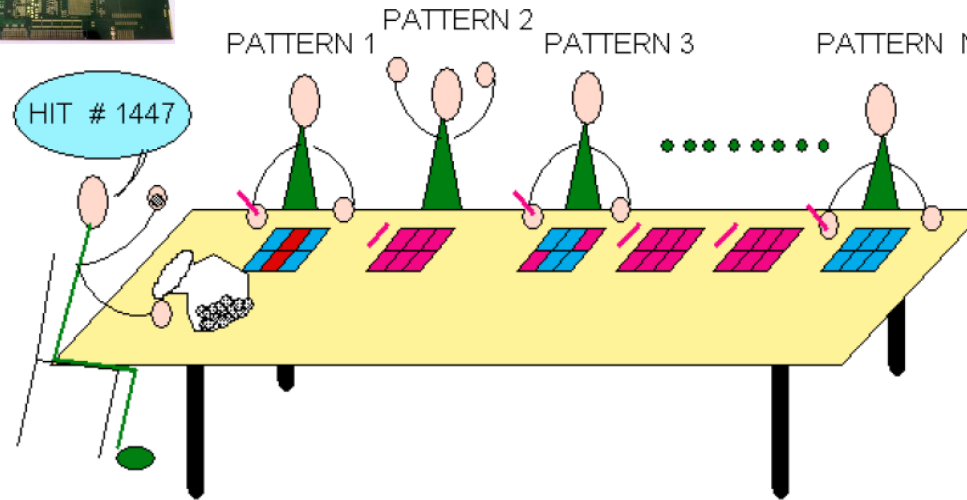
- A pattern consists of a Super-Strip in each layer (10s of pixels/strips wide).
- Uses HEP-specific content addressable memory (CAM) custom chip.
- Patterns determined from full ATLAS simulation.
- $\sim 10^9$ patterns see each hit almost simultaneously.
- When hits have all been sent off detector, pattern recognition is $\sim$ done.
  - $\rightarrow$ This is then followed by FPGA based track fitting (1 fit/ns)

Designed for installation before Phase-I, but as an aid to the Level-2 Trigger.
For Phase-II need to speed up to fit tracks in RoI as input to Level-1.

CMS: "Long-Barrel" Double-Stack Concept

- Layout optimized for L1 track finding. Geometry helps to keep problem "local"
- Within double-stack, each lower module is combined with two upper modules to form "Tracklets"
- Tracklets in each "super-layer" are extrapolated to the other two super-layers
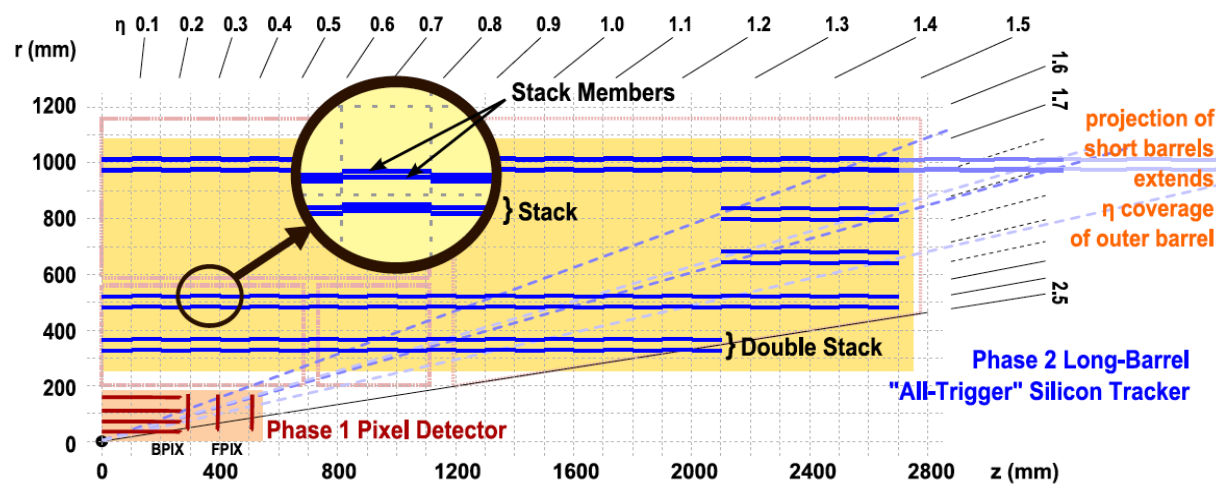
6 long layers = 3 Super layers

φ arrangement within double-stack layer

Common supporting mechanics
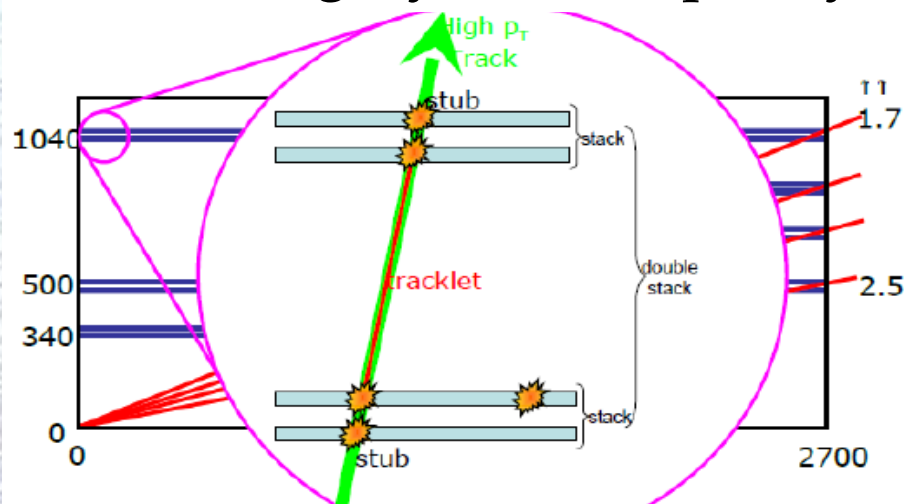
Pairs of stubs are combined to form "tracklets"

Self-contained φ sectors.
Each sector needs to be combined with the two neighbouring sectors (left and right) to "contain" ~2.5 GeV tracks.

15 degree sector

100
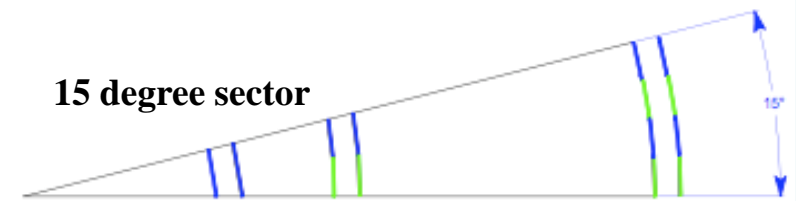
CMS: Phase-II Requirements and Guidelines

- ➢ **Radiation hardness**
  - ⊙ **Ultimate integrated luminosity considered ~ 3000 fb^{-1}**
    - ★ To be compared with original ~ 500 fb^{-1}

- ➢ **Resolve up to ~200 collisions per BX, with few % occupancy**
  - ★ Higher granularity

Strip-Strip Module

- ➢ **Improve tracking performance**
  - ⊙ **Improve performance @ low p_T , reduce particle interaction rates**
  - ⊙ **Reduce material in the tracking volume**
  - ⊙ **Improve performance @ high p_T**
    - ★ Reduce average pitch

Pixel-Strip Module

- ➢ **Tracker input to Level-1 trigger**
  - ⊙ **μ, e and jet rates would become unacceptably large at high luminosity**
    - ★ Even considering "phase-1" trigger upgrades
    - ★ Performance of selection algorithms degrades with increasing pile-up
  - ⊙ **Add tracking information at Level-1**
    - ★ Move part of HLT reconstruction into Level-1!
  - ⊙ **Objective:**
    - ★ Reconstruct "all" tracks above 2 - 2.5 GeV
    - ★ Identify the origin along the beam axis with ~ 1 mm precision
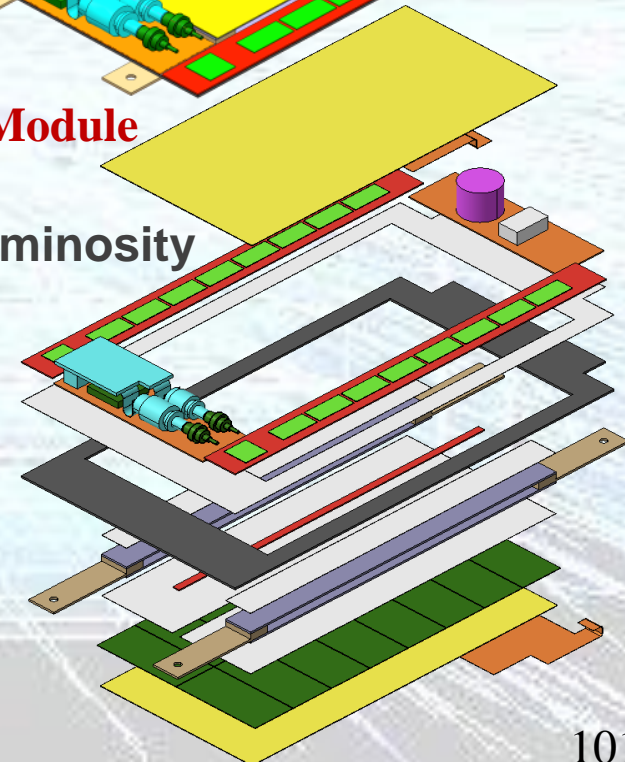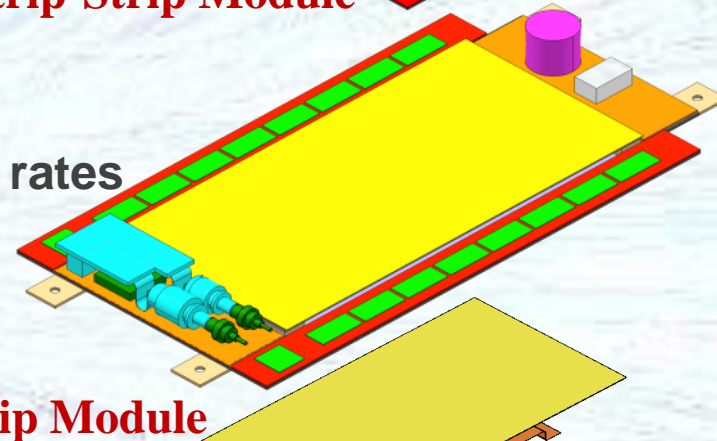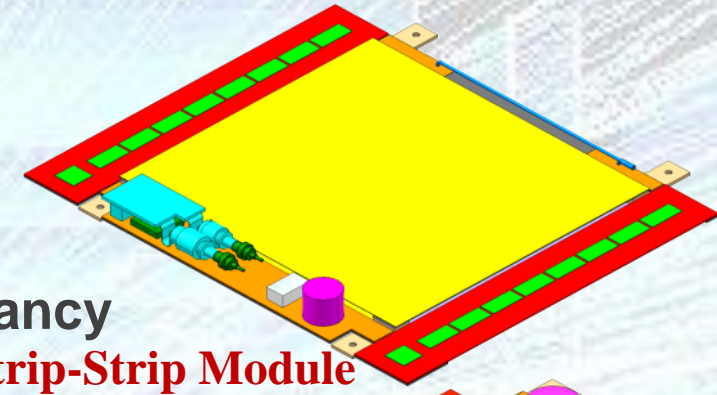
Other Projects: The ILC

31 km
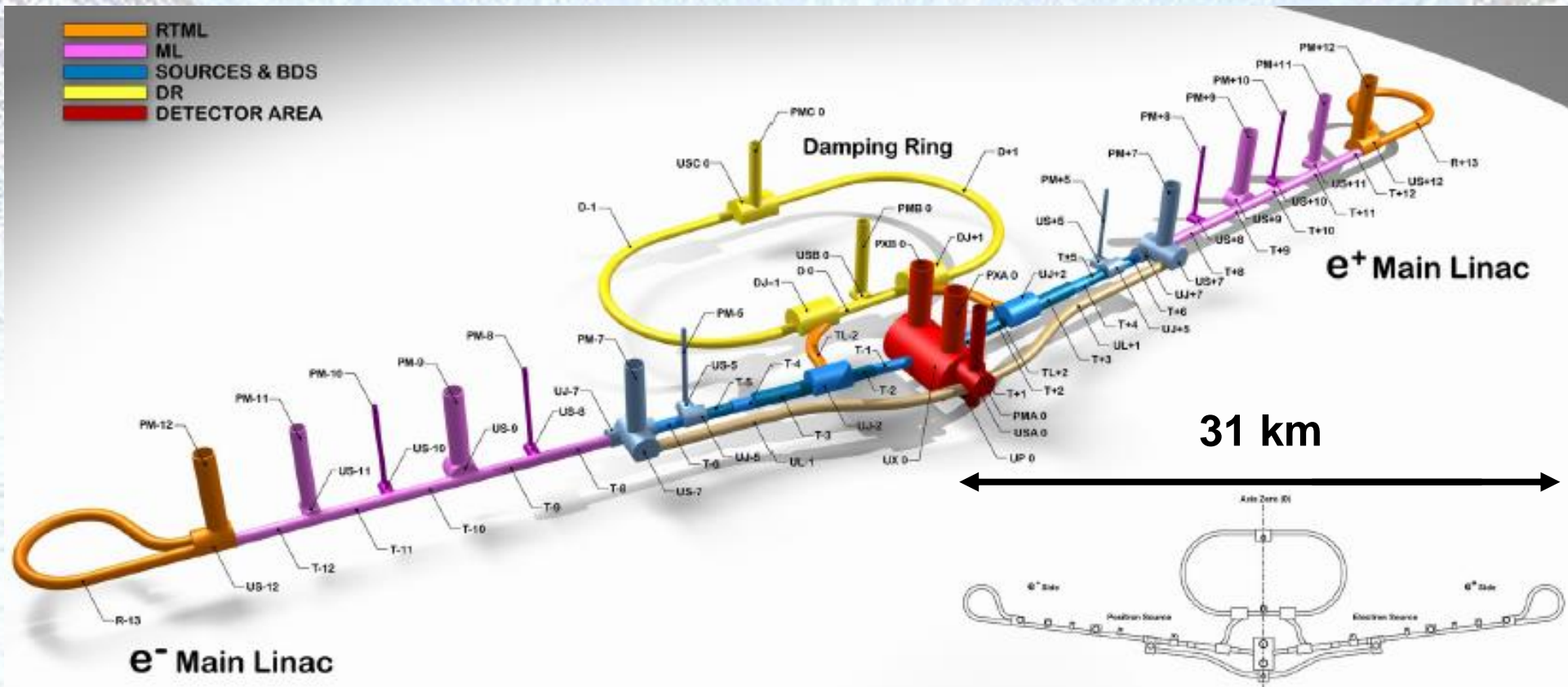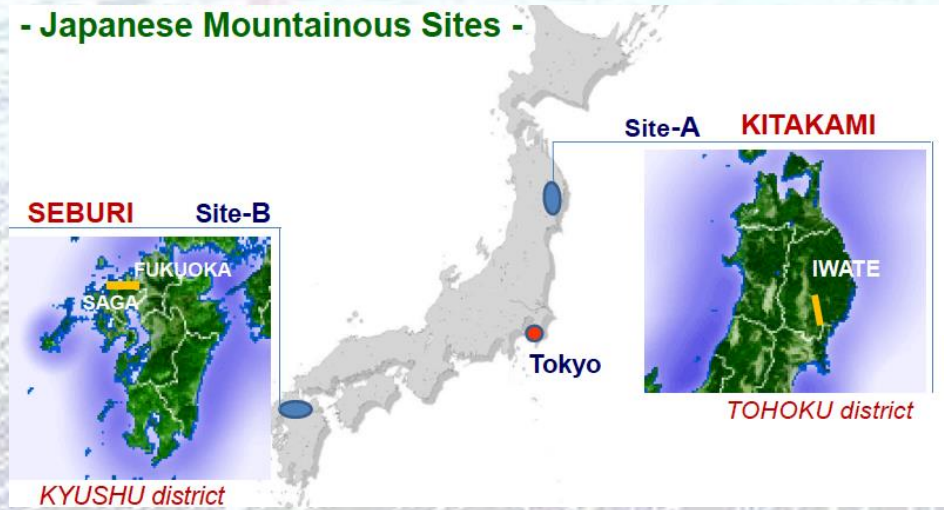
Proposed Update of the European Strategy for Particle Physics

e) There is a strong scientific case for an electron-positron collider, complementary to the LHC, that can study the properties of the Higgs boson and other particles with unprecedented precision and whose energy can be upgraded. The Technical Design Report of the International Linear Collider (ILC) has been completed, with large European participation. The initiative from the Japanese particle physics community to host the ILC in Japan is most welcome, and European groups are eager to participate. *Europe looks forward to a proposal from Japan to discuss a possible participation.*

Other Projects: Muon Collider

Muon Collider Conceptual Layout

Project X
Accelerate hydrogen ions to 8 GeV using SRF technology.

Compressor Ring
Reduce size of beam.

Target
Collisions lead to muons with energy of about 200 MeV.

Muon Capture and Cooling
Capture, bunch and cool muons to create a tight beam.

Initial Acceleration
In a dozen turns, accelerate muons to 20 GeV.

Recirculating Linear Accelerator
In a number of turns, accelerate muons up to 2 TeV using SRF technology.

Collider Ring
Bring positive and negative muons into collision at two locations 100 meters underground.

Vladimir Shiltsev

- 3 TeV Muon Collider
- 3 TeV CLIC

Beamstrahlung in any e+e- collider
$\delta E/E \propto \gamma^2$
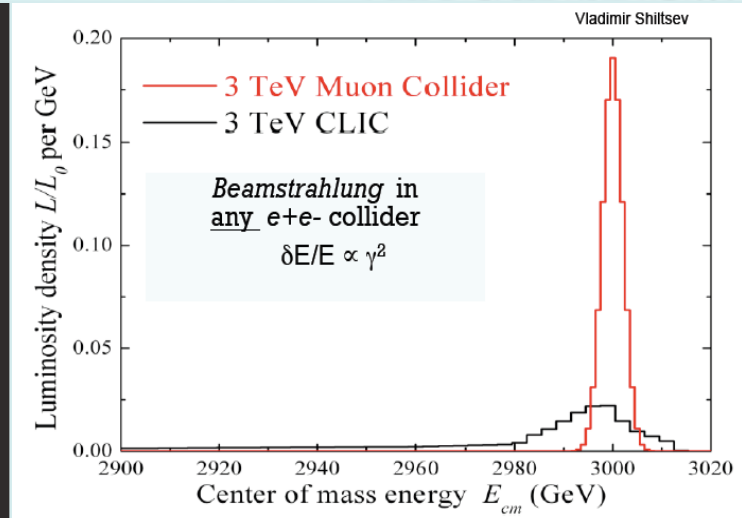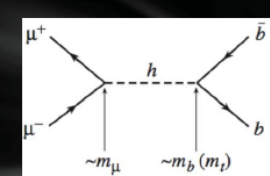
Muon Collider as a Higgs Factory

Resonant Production:

$$\sigma(\mu^+\mu^- \to h \to X) = \frac{4\pi\Gamma_h^2 \mathrm{Br}(h \to \mu^+\mu^-)\mathrm{Br}(h \to X)}{(\hat{s}-m_h^2)^2 + \Gamma_h^2 m_h^2}$$

At the peak with a perfect energy resolution:

$$\sigma_{peak}(\mu^+\mu^- \to h) = \frac{4\pi}{m_h^2}BR(h \to \mu^+\mu^-)$$
$$\approx 41 \text{ pb at } m_h = 125 \text{ GeV}.$$

About 40,000 events produced per fb^{-1}

For muon collider as Higgs factory see https://hepconf.physics.ucla.edu/higgs2013/

cf "LEP-3" (ZH): 250 per fb^{-1} or HL-LHC (3000 fb^{-1}): HZ (Z→e,μ) 10^5 events; HX (H →γγ) 3×10^5 events

Other Projects: 80km Ring
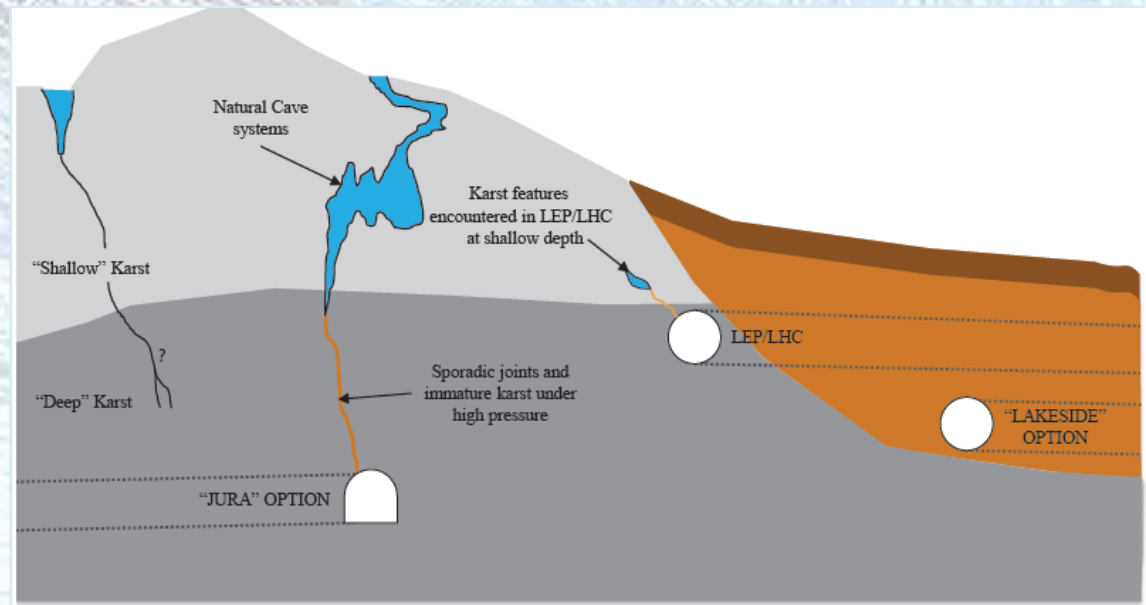
Figure 5: Schematic representation of water inflow problems due to tunnelling in karstic regions of The Jura. Tunnel depths are relative to each other and indicative only.

80 km Jura 80 km Lakeside 47 km Lakeside

HIGH risk = LOW feasibility   LOW risk = HIGH feasibility
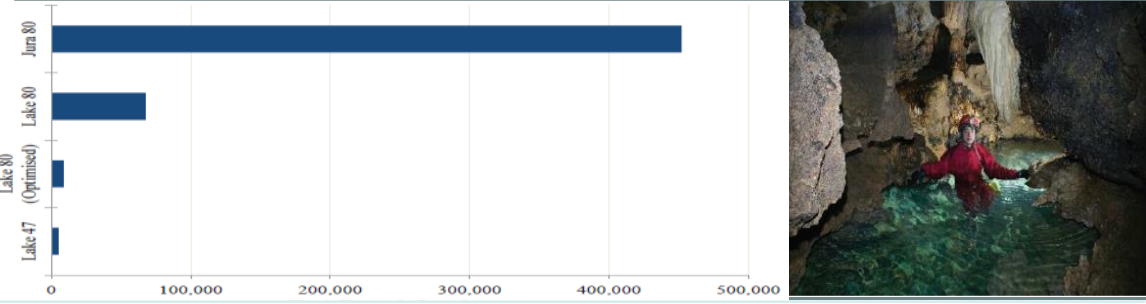
Pre-feasibility study of an 80km tunnel project at CERN

CERN   ARUP   GEOTECHNIQUE APPLIQUEE DERIAZ S.A. GADZ

104
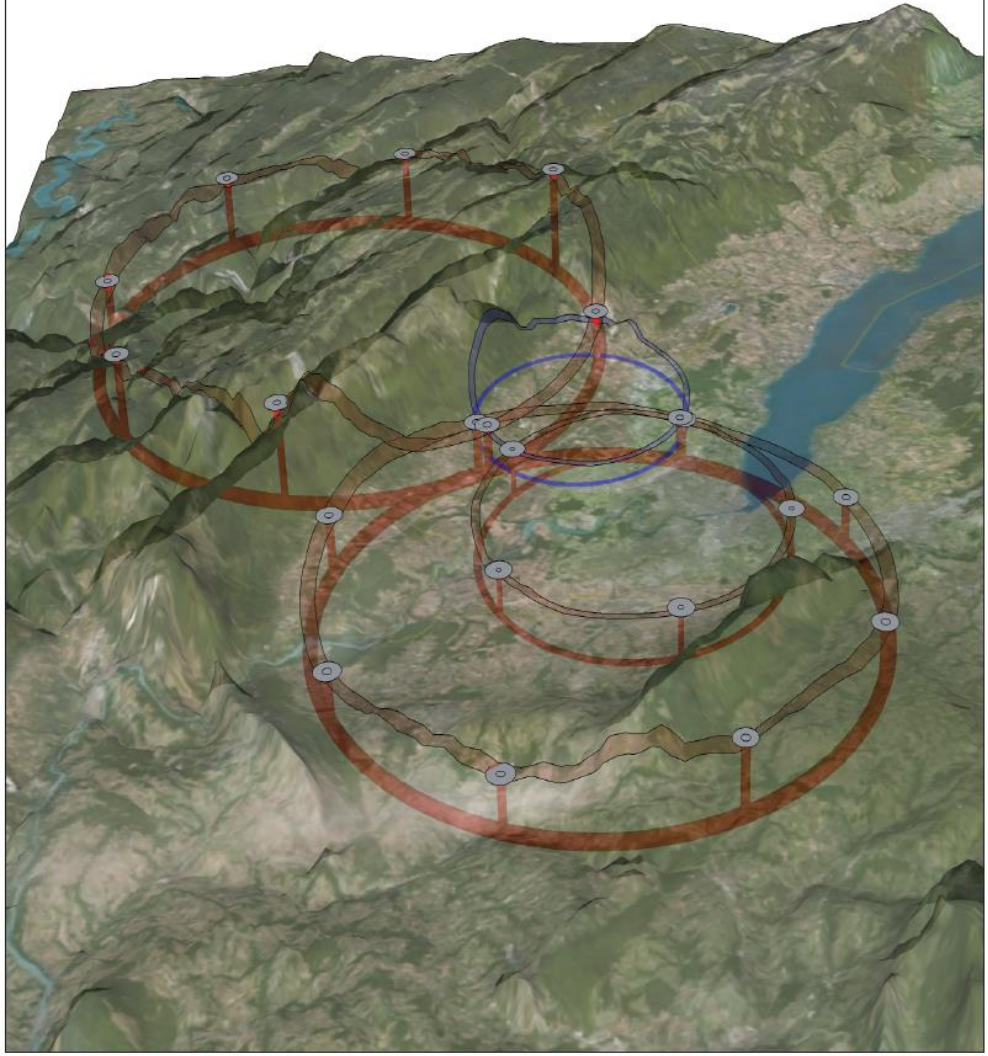
Particle Physics Prospects

- Many aspects not dealt with here, but the key trends for the LHC are radiation hardness, increased granularity and read-out speed (so typically required very numbers of ~10Gbps data links), front-end data reduction and very fast selection of the few per million interesting collisions

- With dedicated detector design (cf CMS Upgrade Tracker) can implement very fast feature extraction to speed up this selection

- More monolithic technologies being explored with same silicon substrate for sensors and the electronics, potentially with embedded cooling. MAPS (CMOS sensor) technology is being exploited (cf Heavy Ion experiments) but use limited by radiation requirements, hence HV-CMOS and 3D integration developments.

- Equally important for many other fields is ultra-precision time resolution.

- The computing and software environment is expected to evolve significantly and this needs to be recognised in longer term planning.

- Many of the challenges discussed are far from unique to particle physics and I apologise that have missed many other areas which are really pushing the technology envelope, as well as many very exciting developments responding directly to commercial requirements.

Future challenges in medical imaging

PAST   PRESENT   FUTURE

MORPHOLOGICAL
- Film (radiography)
- CT
- MRI
- Ultrasound

FUNCTIONAL
- Angiography
- Ultrasound Doppler
- PET/SPECT
- fMRI

HYBRID
- PET/CT
- SPECT/CT
- PET/MRI

MOLECULAR
- PET/SPECT
- MRS
- Optical
- PET/MRI
- MRI/US/CT "contrast enhanced"

XX century   XXI century
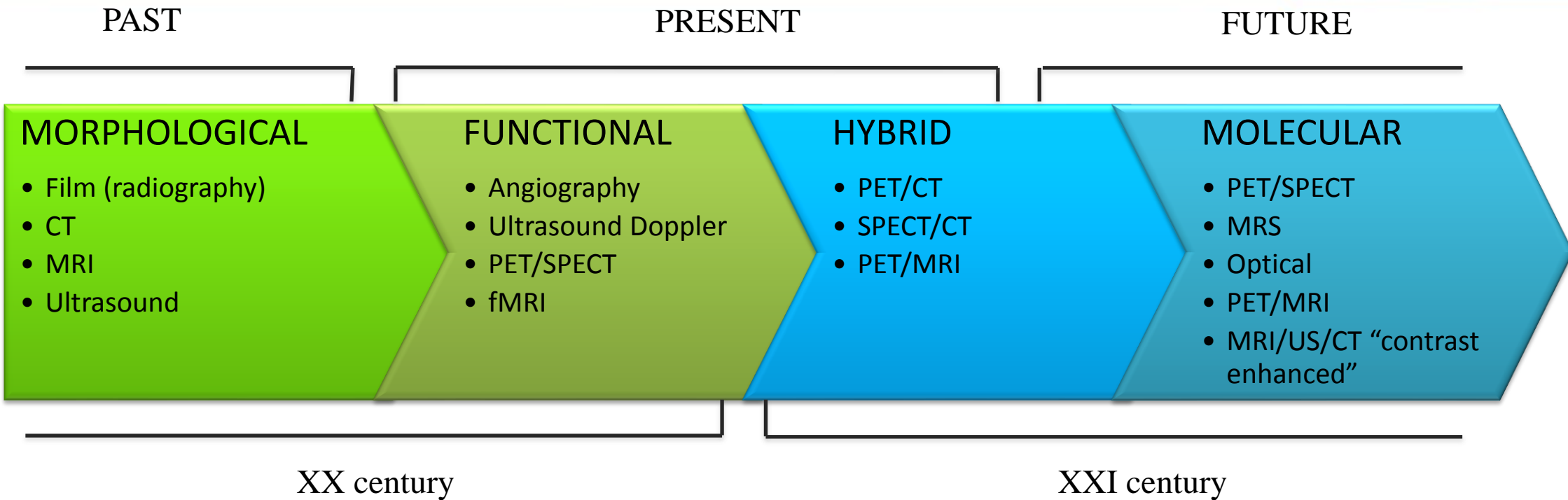
"➔ A *visual representation, characterization, and quantification of biological processes at the cellular and sub-cellular levels within intact living organisms.*"

Sanjiv S.Gambhir

Back-Up
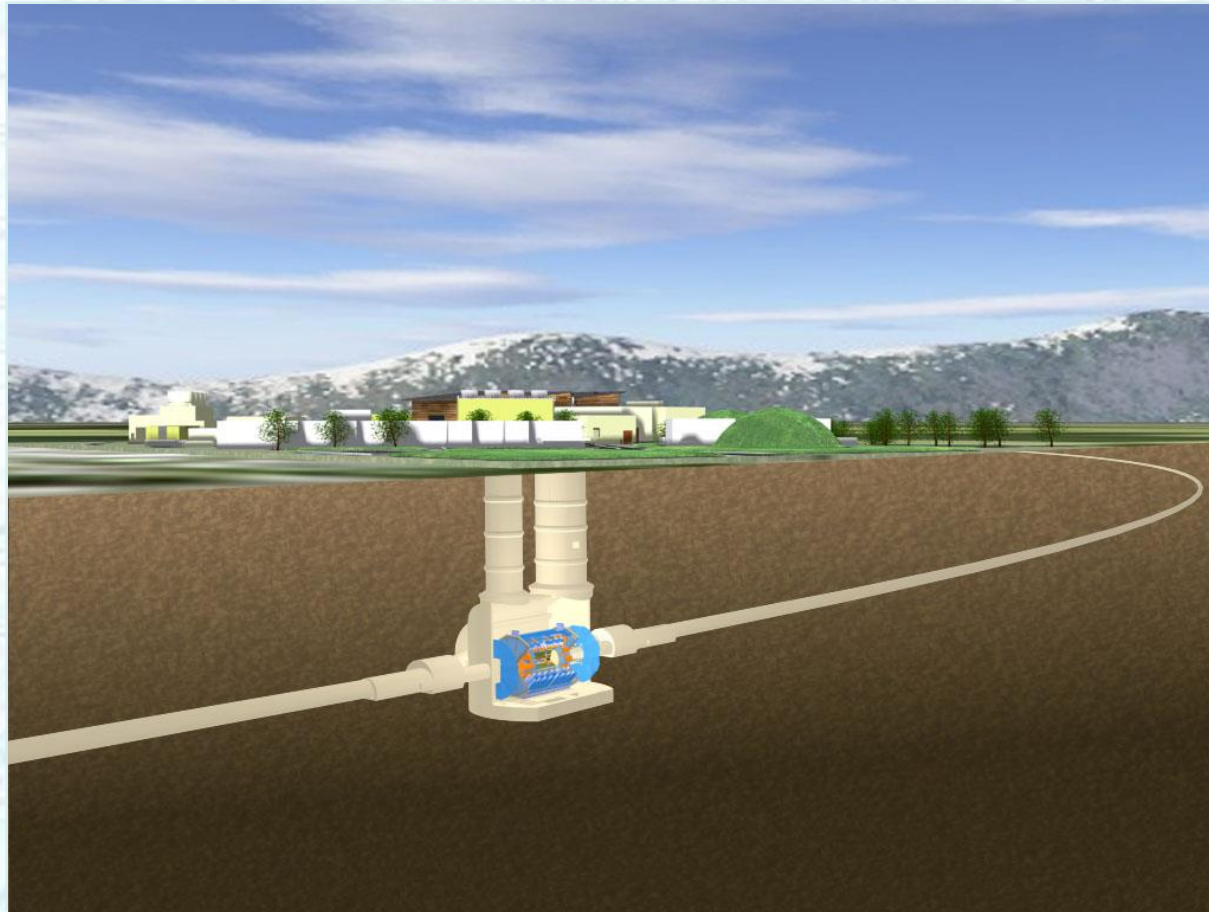
Other Projects: The LHeC

CDR, arXiv:1211.4831 and 5102 http://cern.ch/lhec

60 GeV electron beam energy, L= 10^{33} cm^{-2}s^{-1}, $\sqrt{s}$=1.3 TeV:
Q^2_{max}= 10^6 GeV^2, 10^{-6} < x< 1
Recirculating linac (2 ∗ 1km, 2∗60 cavity cryo modules,
3 passes, energy recovery) and IP with LHC protons/ions
Ring-ring as fall back.

Loss compensation 2 (90m)
Loss compensation 1 (140m)
Linac 1 (1008m)
Matching/splitter (31m)
Injector
Matching/combiner (31m)
Arc 1,3,5 (3142m)
Arc 2,4,6 (3142m)
Bypass (230m)
Linac 2 (1008m)
Matching/combiner (31m)
IP line
Detector
Matching/splitter (30m)
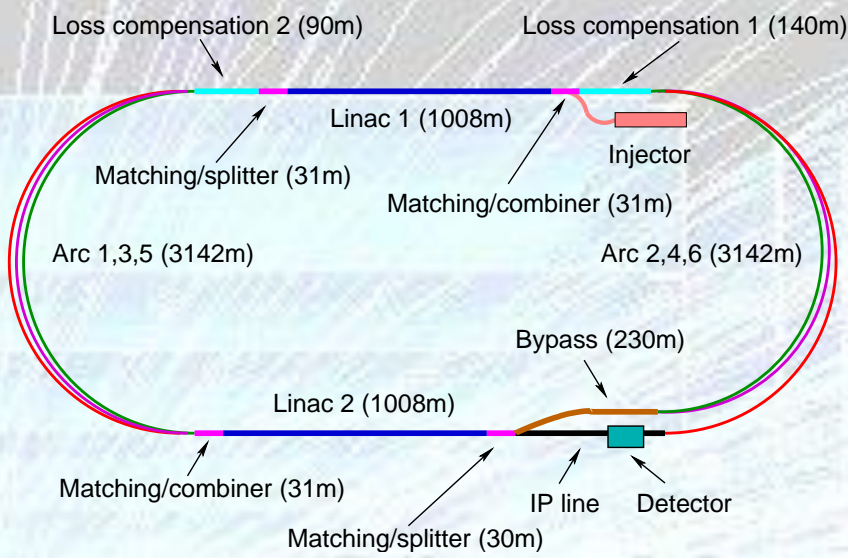
QCD Discoveries	$\alpha_s < 0.12$, $q_{sea} \neq \bar{q}$, instanton, odderon, low x: (n0) saturation, $\bar{u} \neq \bar{d}$
Higgs	WW and ZZ production, $H \to b\bar{b}$, $H \to 4l$, CP eigenstate
Substructure	electromagnetic quark radius, e^*, ν^*, W?, Z?, top?, H?
New and BSM Physics	leptoquarks, RPV SUSY, Higgs CP, contact interactions, GUT through α_s
Top Quark	top PDF, $xt = x\bar{t}$?, single top in DIS, anomalous top
Relations to LHC	SUSY, high x partons and high mass SUSY, Higgs, LQs, QCD, precision PDFs
Gluon Distribution	saturation, $x \approx 1$, J/ψ, Υ, Pomeron, local spots?, F_L, F_2^c
Precision DIS	$\delta\alpha_s \simeq 0.1\%$, $\delta M_c \simeq 3\,\mathrm{MeV}$, $v_{u,d}$, $a_{u,d}$ to $2-3\%$, $\sin^2\Theta(\mu)$, F_L, F_2^b
Parton Structure	Proton, Deuteron, Neutron, Ions, Photon
Quark Distributions	valence $10^{-4} \lesssim x \lesssim 1$, light sea, d/u, $s = \bar{s}$?, charm, beauty, top
QCD	N^{3}LO, factorisation, resummation, emission, AdS/CFT, BFKL evolution
Deuteron	singlet evolution, light sea, hidden colour, neutron, diffraction-shadowing
Heavy Ions	initial QGP, nPDFs, hadronization inside media, black limit, saturation
Modified Partons	PDFs "independent" of fits, unintegrated, generalised, photonic, diffractive
HERA continuation	F_L, xF_3, $F_2^{\gamma Z}$, high x partons, α_s, nuclear structure, ..

Ultra high precision (detector, e-h redundancy)   - new insight
Maximum luminosity and much extended range   - rare, new effects
Deep relation to (HL-) LHC (precision+range) - complementarity

Other Projects: HE-LHC

High Energy LHC
Document prepared for the European HEP strategy update

Table 1: LHC main parameters compared with the HE-LHC with round beams (right column) and flat beam (middle column)

	nominal LHC	HE-LHC	
beam energy [TeV]	7	16.5	
dipole field [T]	8.33	20	
dipole coil aperture [mm]	56	40	
beam half aperture [cm]	2.2 (x), 1.8 (y)	1.3	
injection energy [TeV]	0.45	>1.0	
#bunches	2808	1404	
bunch population [10^{11}]	1.15	1.29	1.30
initial transverse normalized emittance [μm]	3.75	3.75 (x), 1.84 (y)	2.59 (x & y)
initial longitudinal emittance [eVs]	2.5	4.0	
number of IPs contributing to tune shift	3	2	
initial total beam-beam tune shift	0.01	0.01 (x & y)	
maximum total beam-beam tune shift	0.01	0.01	
beam circulating current [A]	0.584	0.328	
RF voltage [MV]	16	32	
rms bunch length [cm]	7.55	6.5	
rms momentum spread [10^{-4}]	1.13	0.9	
IP beta function [m]	0.55	1 (x), 0.43 (y)	0.6 (x & y)
initial rms IP spot size [μm]	16.7	14.6 (x), 6.3 (y)	9.4 (x & y)
full crossing angle [μrad]	285 (9.5 $\sigma_{x,y}$)	175 (12 σ_{x0})	188.1 (12 $\sigma_{x,y0}$)
Piwinski angle	0.65	0.39	0.65
geometric luminosity loss from crossing	0.84	0.93	0.84
stored beam energy [MJ]	362	478.5	480.7
SR power per ring [kW]	3.6	65.7	66.0
arc SR heat load dW/ds [W/m/aperture]	0.17	2.8	2.8
energy loss per turn [keV]	6.7	201.3	
critical photon energy [eV]	44	575	
photon flux [10^{17}/m/s]	1.0	1.3	
longitudinal SR emittance damping time [h]	12.9	0.98	
horizontal SR emittance damping time [h]	25.8	1.97	
initial longitudinal IBS emittance rise time [h]	61	64	~68
initial horizontal IBS emittance rise time [h]	80	~80	~60
initial vertical IBS emittance rise time [h]	~400	~400	~300
events per crossing	19	76	
initial luminosity [10^{34} cm^{-2}s^{-1}]	1.0	2.0	
peak luminosity [10^{34} cm^{-2}s^{-1}]	1.0	2.0	
beam lifetime due to p consumption [h]	46	12.6	
optimum run time t_r [h]	15.2	10.4	
integrated luminosity after t_r [fb^{-1}]	0.41	0.50	0.51
opt. av. int. luminosity per day [fb^{-1}]	0.47	0.78	0.79

Dipole Field for Hadron Collider
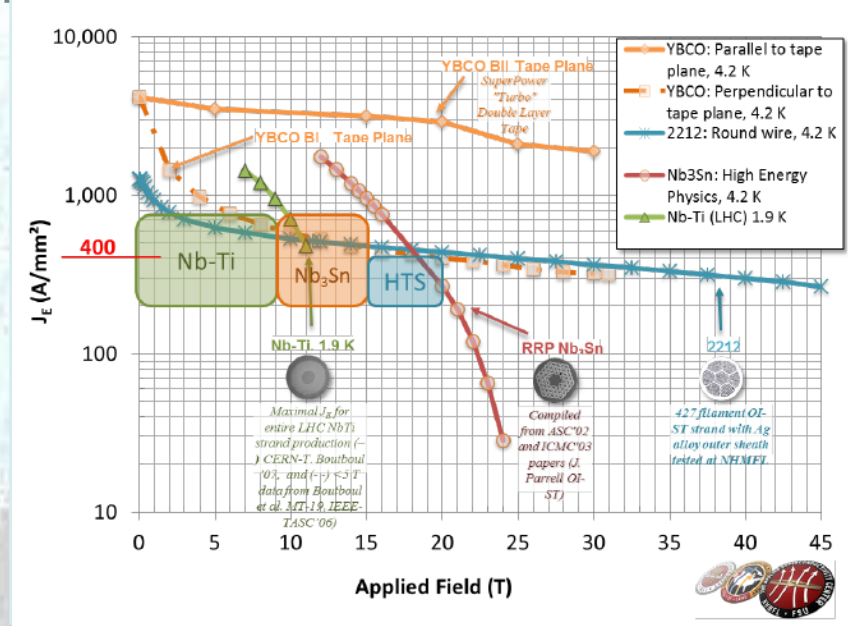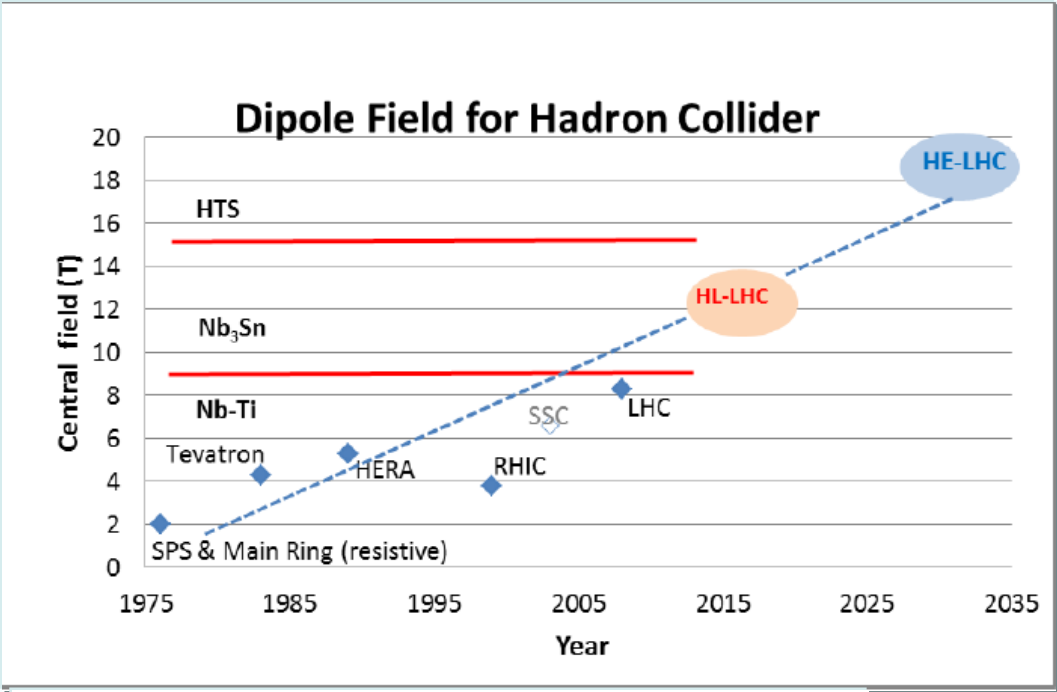
Other Projects: CLIC
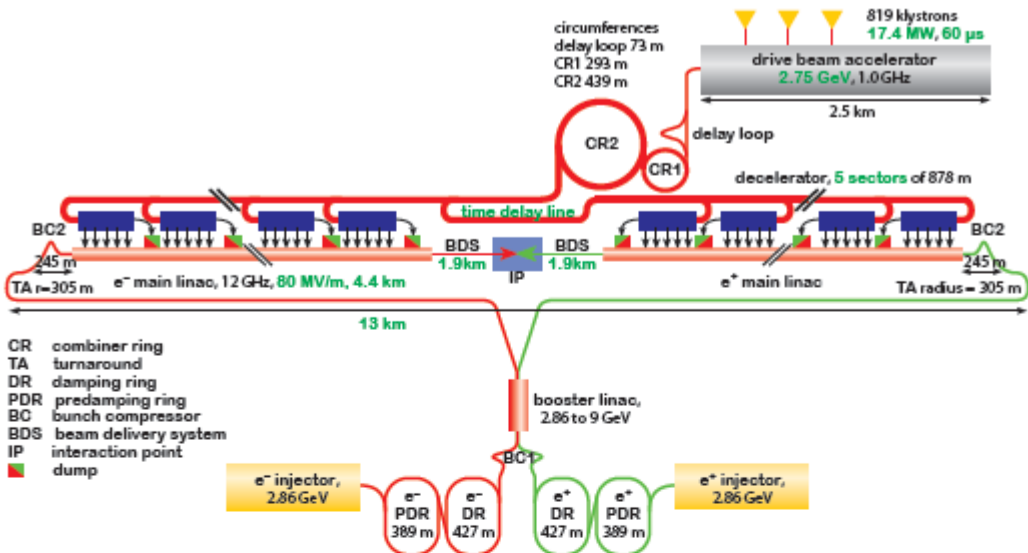
Fig. 1: Overview of the CLIC layout at $\sqrt{s} = 500$ GeV (scenario A).
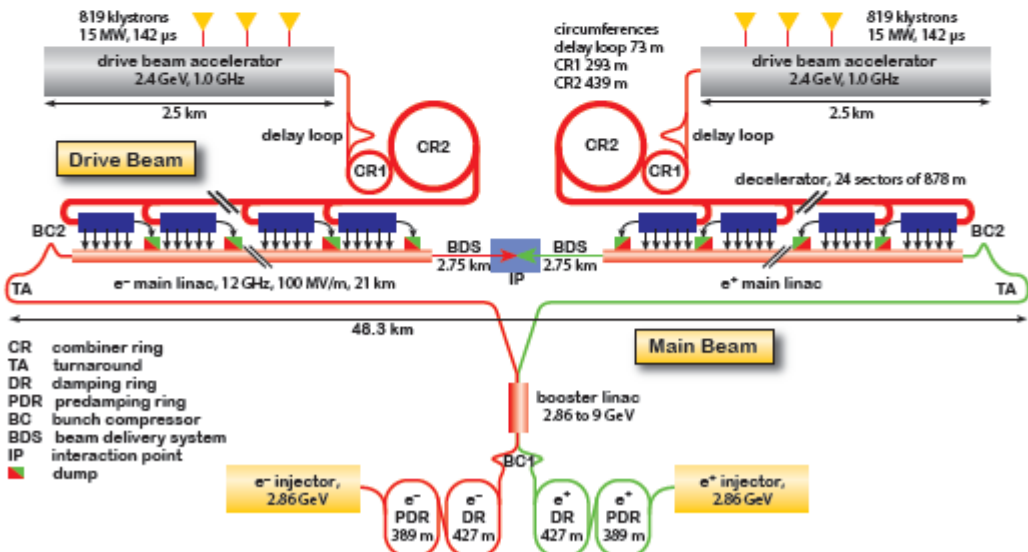
Fig. 2: Overview of the CLIC layout at $\sqrt{s} = 3$ TeV.

CLIC e^+e^- Linear Collider Studies

Input to the update process of the European Strategy for Particle Physics

Table 5: Summary of results obtained in the Higgs studies for $m_H = 120$ GeV. All analyses at centre-of-mass energies of 350 GeV and 500 GeV assume an integrated luminosity of 500 fb^{-1}, while the analyses at 1.4 TeV (3 TeV) assume 1.5 ab^{-1} (2 ab^{-1}).

Higgs studies for $m_H = 120$ GeV

$\sqrt{s}$ (GeV)	Process	Decay mode	Measured quantity	Unit	Generator value	Stat. error	Comment
350	SM Higgs production	$ZH \to \mu^+\mu^- X$	σ	fb	4.9	4.9%	Model independent, using Z-recoil
			Mass	GeV	120	0.131	
500		$ZH \to q\bar{q}q\bar{q}$	$\sigma \times BR$	fb	34.4	1.6%	$ZH \to q\bar{q}q\bar{q}$ mass reconstruction
			Mass	GeV	120	0.100	
500		$ZH, H\nu\bar{\nu}$ $\to \nu\bar{\nu}q\bar{q}$	$\sigma \times BR$	fb	80.7	1.0%	Inclusive sample
			Mass	GeV	120	0.100	
1400	WW fusion	$H \to \tau^+\tau^-$	$\sigma \times BR$	fb	19.8	<3.7%	
3000		$H \to b\bar{b}$			285	0.22%	
		$H \to c\bar{c}$			13	3.2%	
		$H \to \mu^+\mu^-$			0.12	15.7%	
1400 3000	WW fusion	Higgs tri-linear coupling g_{HHH}				~20% ~20%	

Figure labels

CR combiner ring
TA turnaround
DR damping ring
PDR predamping ring
BC bunch compressor
BDS beam delivery system
IP interaction point
■   dump

Most Frequently Used SPECT Radionuclides

$t_{1/2}=65.94h$

$^{99}_{42}Mo$

$^{99}Tc^m$ $t_{1/2}=6.01h$

141 keV

2.1×10^5y

$^{99}_{43}Tc$ >99% $9\times10^{-5}\%$

stable

$^{99}_{44}Ru$
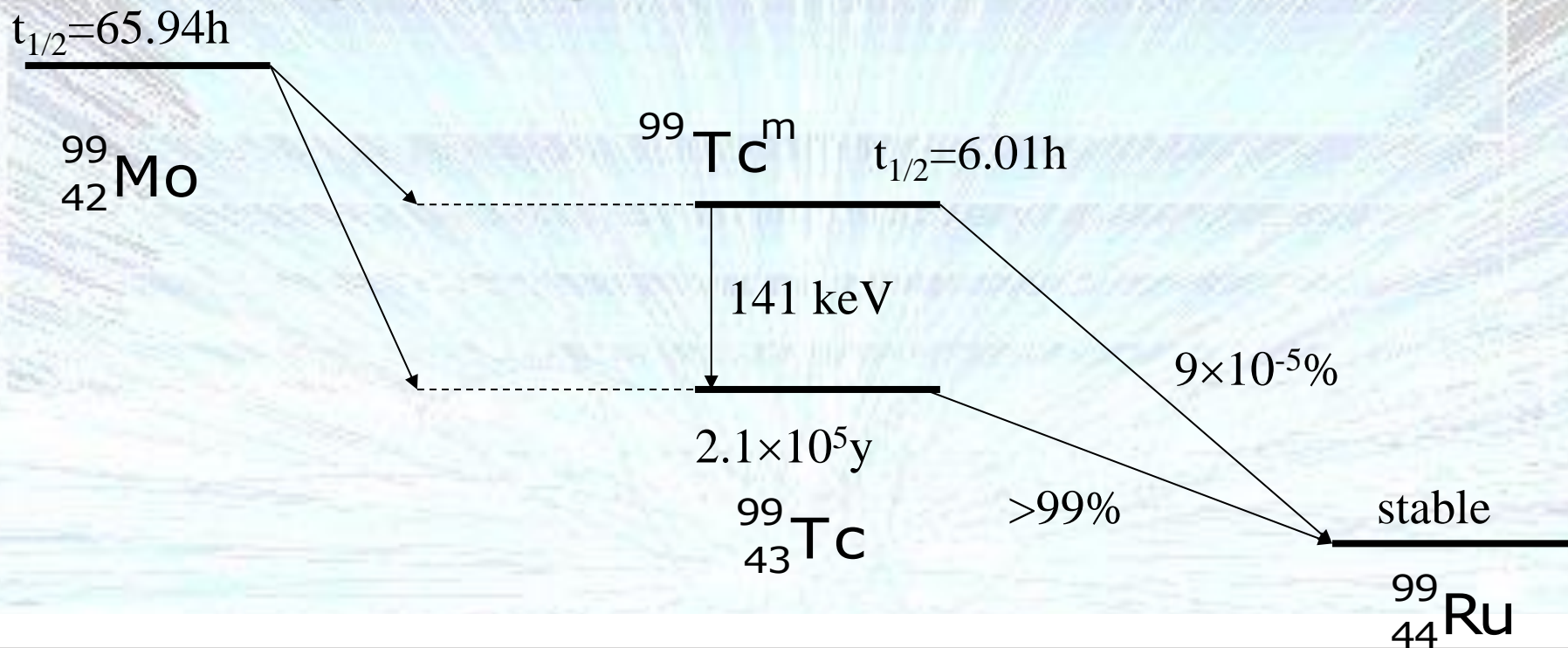
Radioisotope	Energies (keV)	Half Life (Days)	Typical Medical Use
^{99m}Tc	141	0.25	Cancer, liver function, blood flow
^{123}I	159	0.54	Cancer, brain imaging
^{111}In	172, 247	2.80	Cancer, blood flow
^{201}Tl	70, 167	3.00	Blood flow
^{67}Ga	93, 185	3.25	Cancer, blood flow
^{131}I	364, 637	8.00	Thyroid studies

Tomographic Imaging

- The sinogram is what we aim to measure
  - Measure of intensity as a function of projection, θ and position, r
  - Often seen plotted as a 2d grey scale image

x

y

f(x ,y)
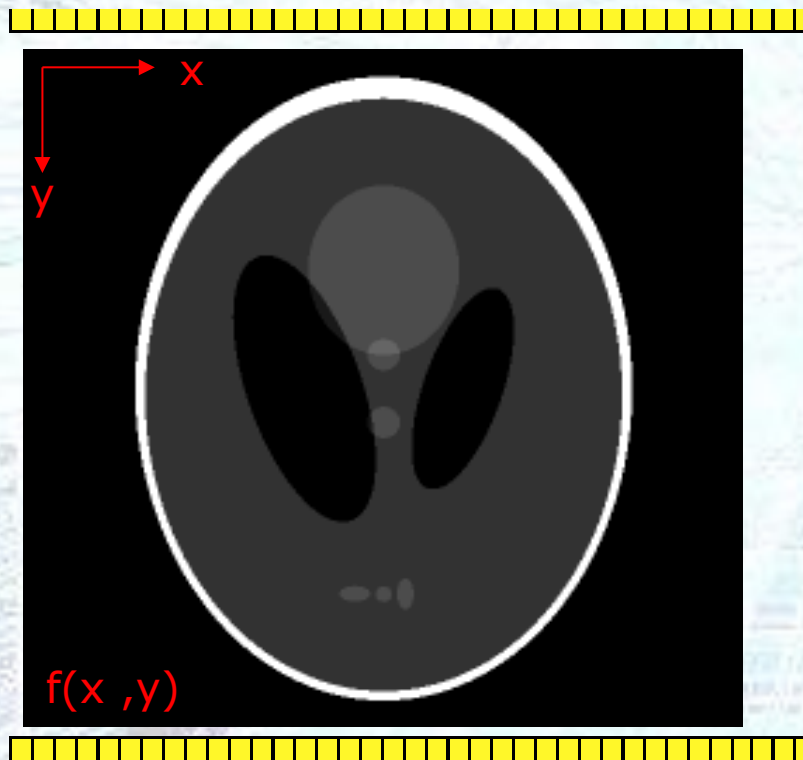
Underlying source distribution
"Shepp-Logan Phantom"
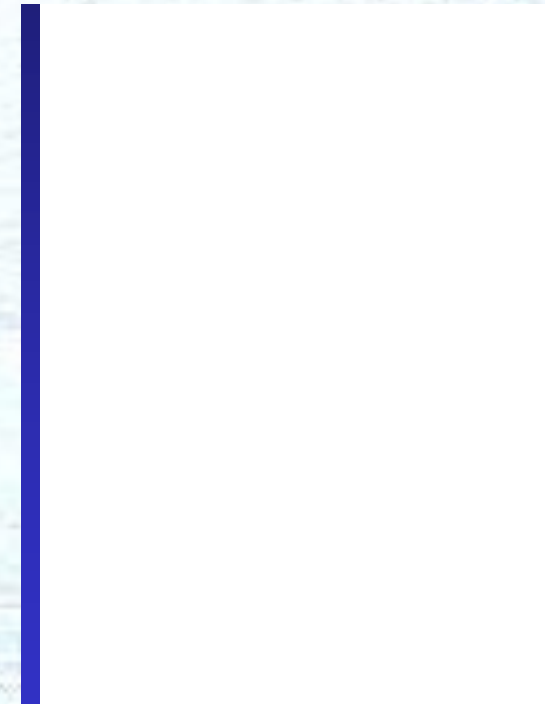
Measured result – **"Sinogram"**
(256 projections, 363 positions per projection)

Note : We measure from 0 to 180°

ATLAS Pixel Module Overview

- **Sensor**
  - 47232 n-on-n pixels with moderated p-spray insulation
  - 250 μm thickness
  - 50 μm (RΦ) $\times$ 400 μm (η)
  - 328 rows (x_{local}) $\times$ 144 columns (y_{local})
- **16 (250nm) FE-I3 chips**
  - bump bonded to sensor
- **Flex Hybrid**
  - passive components
  - Module Controller Chip to perform distribution of commands and event building.
- **Radiation-hard design:**
  - Dose >500 Gy
  - NIEL >10^{15} n_{eq}/cm^2 fluence
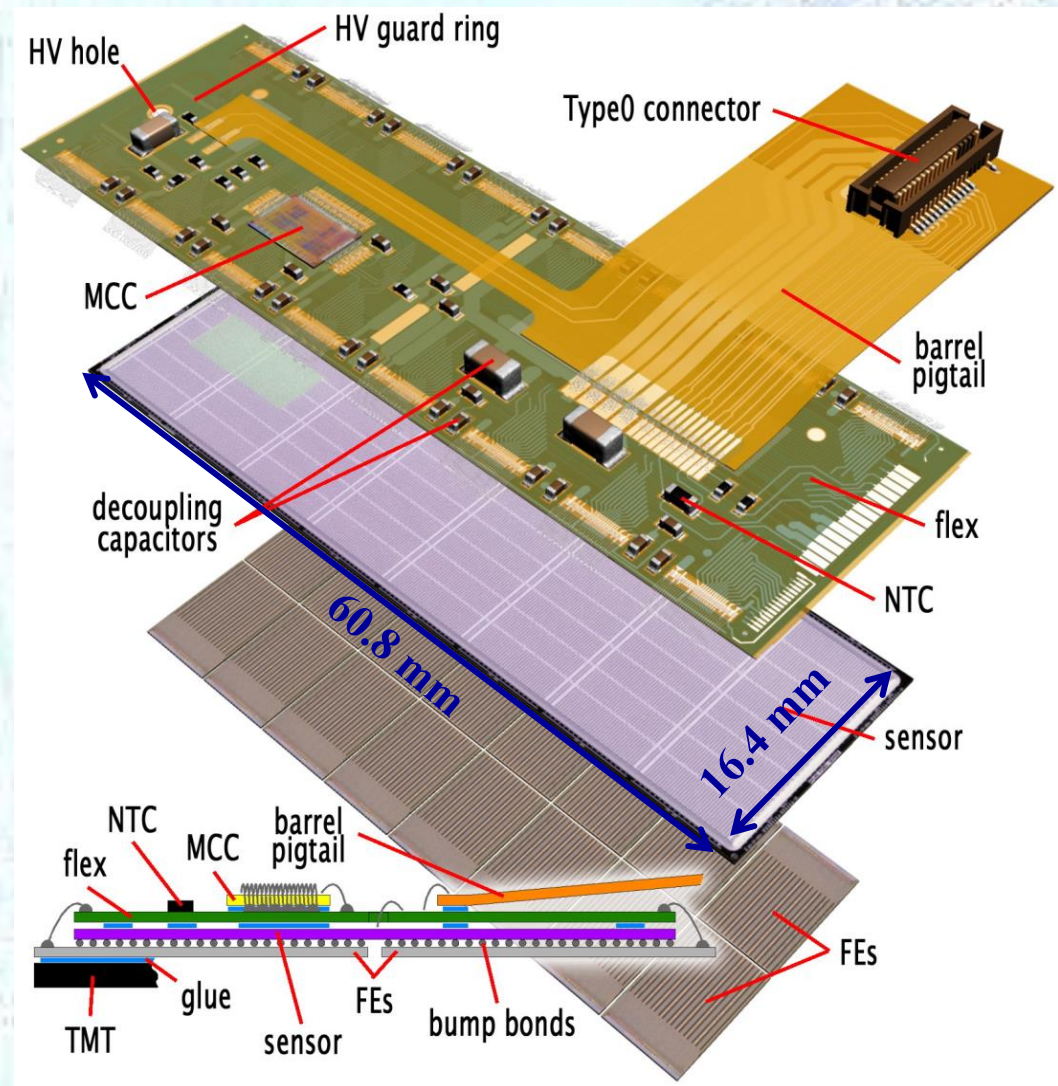
Integrated Luminosity in 2012

Luminosity is measured with forward detectors and calibrated with beam separation scans (Van der Meer)

ATLAS luminosity in 2012

Peak Stable Luminosity Delivered:	7.73×10^{33} cm^{-2}s^{-1}
Max average interactions per bunch crossing:	37
Max Luminosity in fill:	237 pb^{-1}
2011 Luminosity uncertainty:	1.8%
2012 Luminosity uncertainty:	2.8% (prelim.)

arXiv:1302.4393
submitted to EPJC
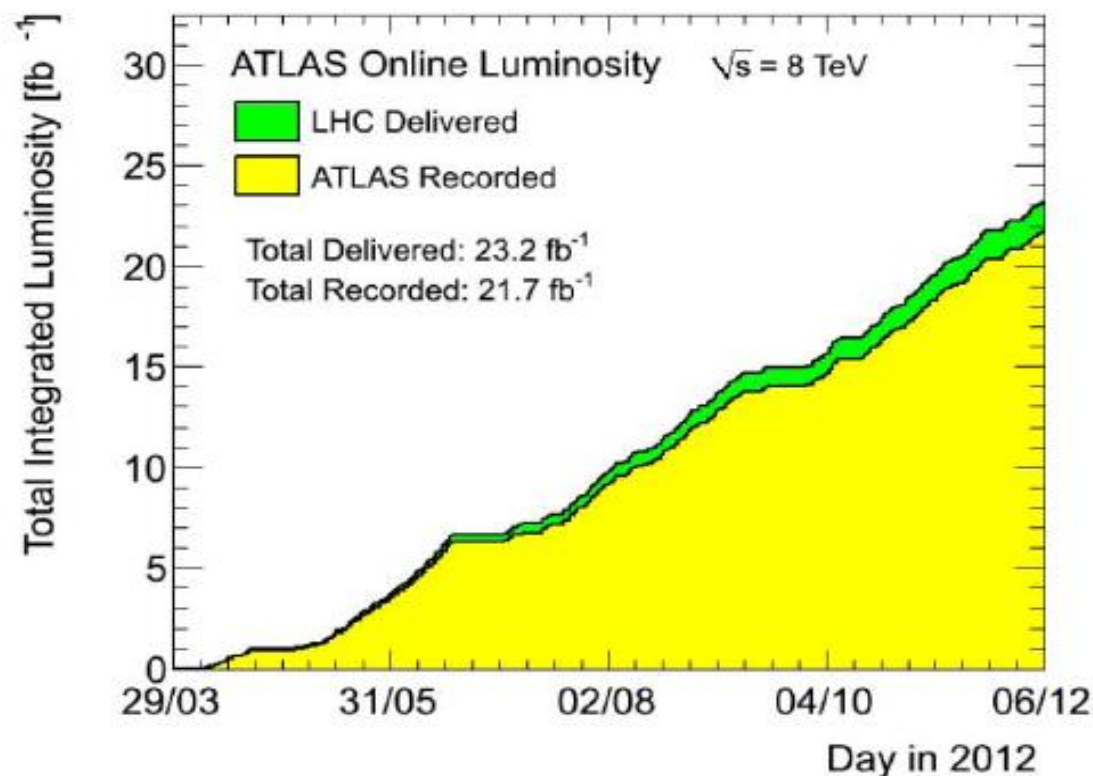
Insertable B-Layer

- New pixel layer around smaller beam pipe
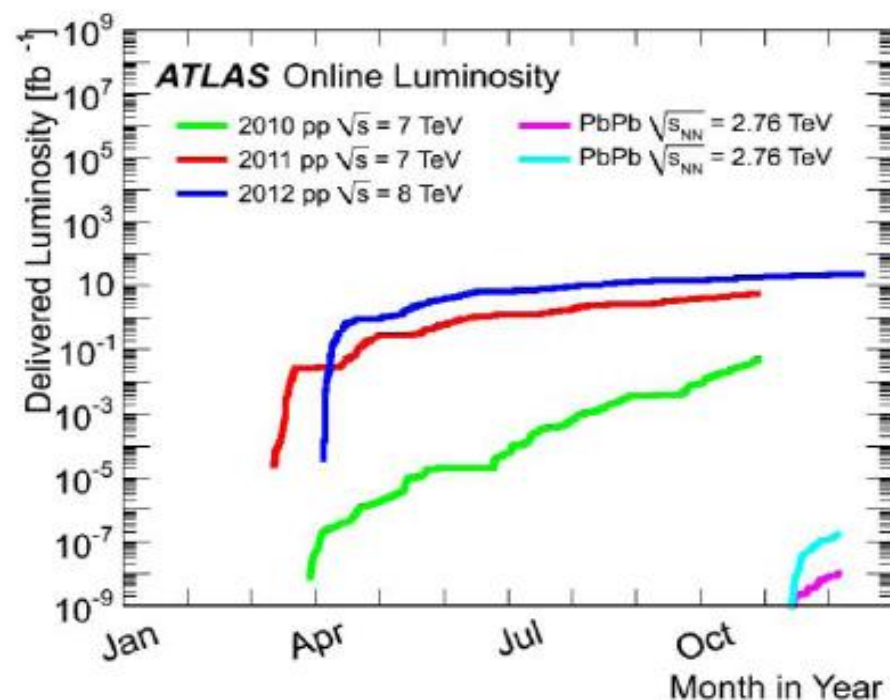- Current pixel package to be brought to surface allowing IBL installation there or later when current pixels reinstalled
  - Latter option assumes IBL support tube inserted anyway at surface
  - New services being installed to fix problems and improve R/O bandwidth
  - New Diamond Beam Monitor also to be installed
- IBL modules and stave status
  - **Sensors & chips done, bump-bonding processing of sensor and electronic wafers completed** - modules production, assembly and qualification underway
  - Focus now on stave assembly
  - **Two prototype staves assembled and under test**

- Integration
  - Test stands prepared for full IBL
  - Integration tooling being finalized and surface building prepared for IBL integration
- Installation
  - **Beam pipe delivered**
  - Installation tooling under final tests
  - Detailed schedule for shutdown has been prepared
- Off-detector
  - Final prototypes completed and being integrated to test stands

Existing B-layer   new beam-pipe

24 mm   33 mm

IBL mounted on beam-pipe
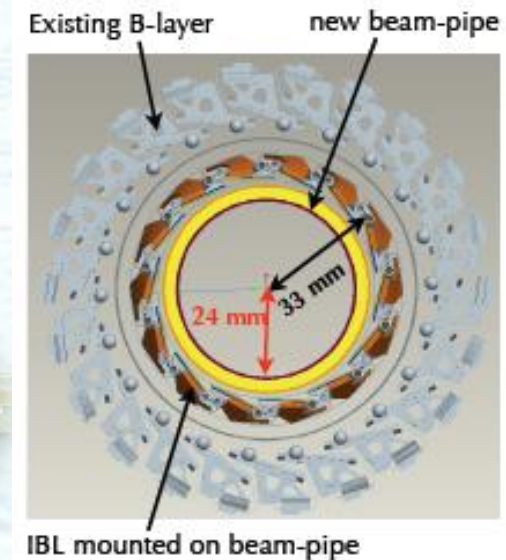
Insertable B-Layer

FE-I4 Pixel Chip (26880 channels)

19 x 20 mm^2 130 nm CMOS process, based on an array of 80 by 336 pixels (each 50 x 250 µm^2)

FE chip
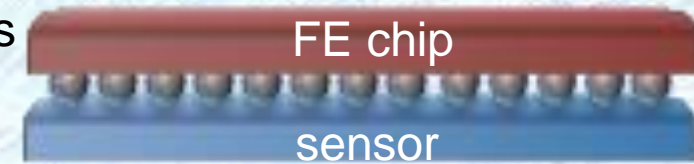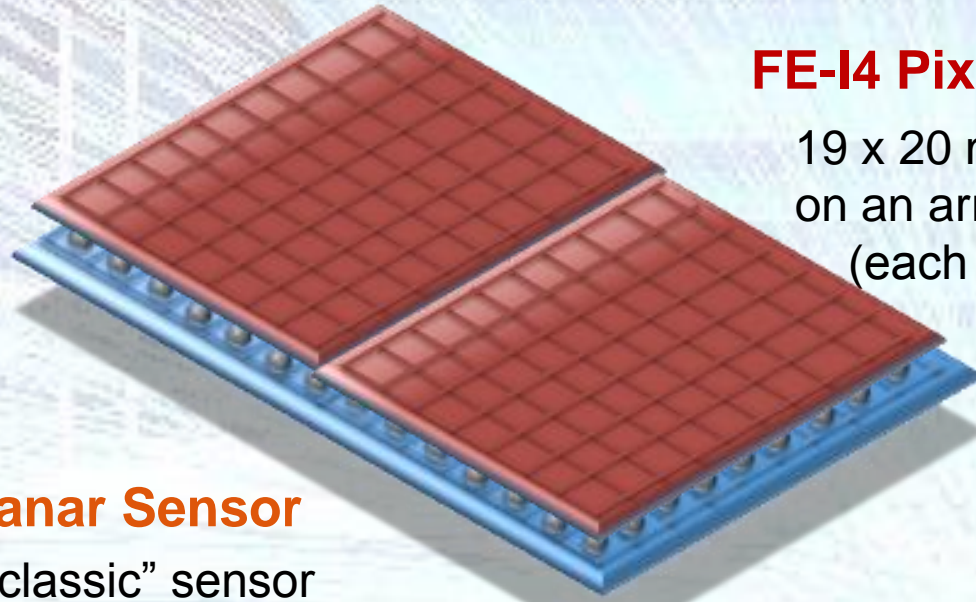
sensor

3D Sensor

- Both electrode types are processed inside the detector bulk

- Max. drift and depletion distance set by electrode spacing

- Reduced collection time and depletion voltage
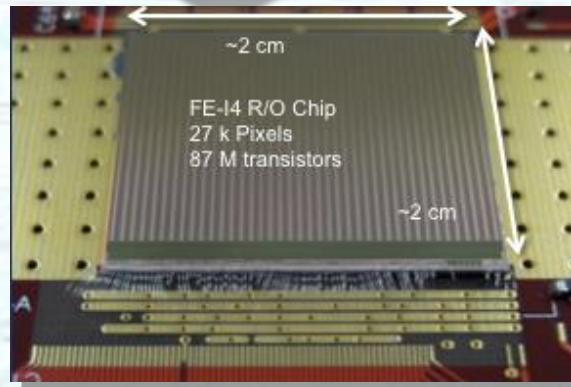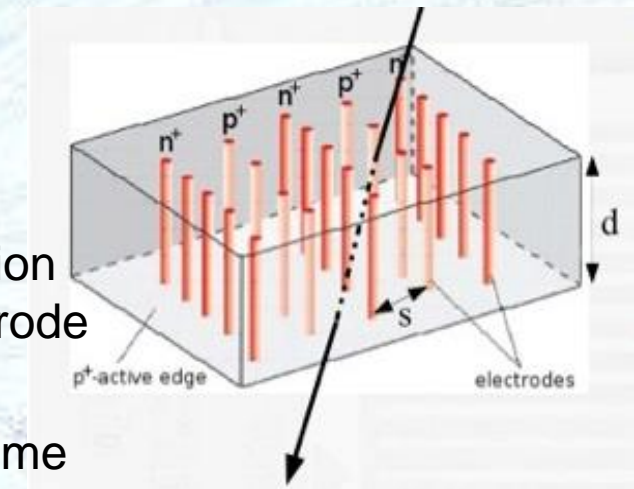
Planar Sensor

- "classic" sensor design
- oxygenated n-in-n
- 200µm thick
- Minimize inactive edge by shifting guard-ring under pixels (215 µm)
- Radiation hardness proven up to 2.4×10^{16} p/cm^2

~2 cm

FE-I4 R/O Chip
27 k Pixels
87 M transistors

~2 cm

3D

Planar

Module:
Sensor + 1x or 2x FEI4

3D

12 Double Chip (planar)

8 Single Chip (3D)

12M Pixel/stave

~ 1.9% X$_0$
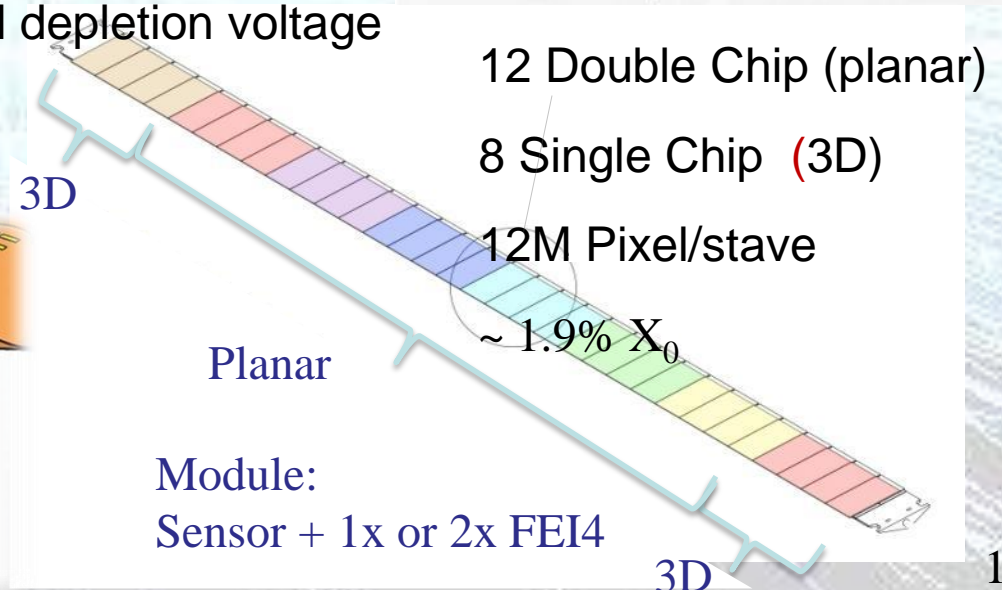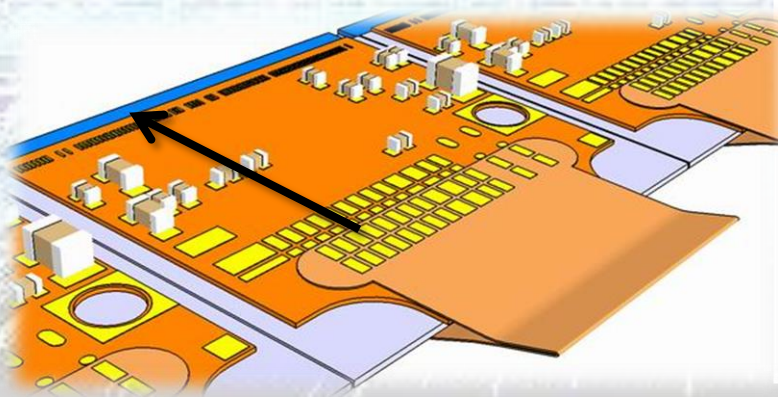
New Small Muon Wheels

The innermost station of the muon end-cap

Located between end-cap calorimeter and toroid

L1 trigger chambers

EI station small wheel
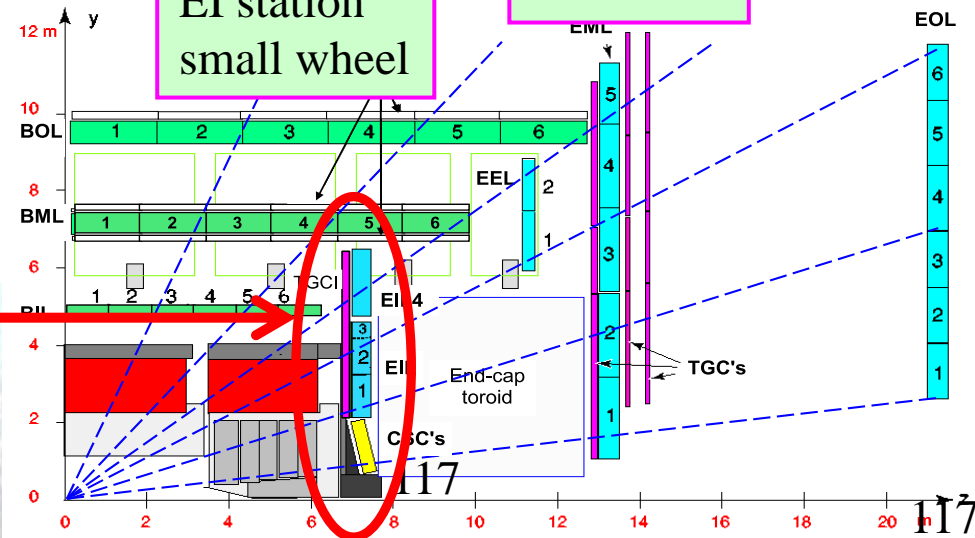
- **In furthest forward direction, chamber efficiencies fall with hit rate as luminosity goes well above the design values**
- **Rate of L1 muon triggers exceeds available bandwidth unless thresholds raised**
- → **Replace "small" muon wheels**
- **Kill fake muon triggers by requiring high quality (σ_θ~ 1mrad) pointing to interaction region**
- **Precision chambers combine sTGC and micromegas technologies for robustness to Phase-II luminosities**

117

LAr Electronics and TDAQ Upgrades

- Key target (as for New Small Wheel) is to maintain high efficeincy for Level-1 triggering on low P_T objects (here electrons and photons)

- In the LAr calorimeter this implies changes to the front-end electronics to allow greater granularity to be exploited at Level-1.

- Trigger upgrades include topological trigger, cluster and jet energy processor, feature extractors, muon sector logic and CTP

electron rate vs threshold

ATLAS simulation

$\langle\mu\rangle=81,\ L \approx 3 \times 10^{34}$

- $E_T>23$ GeV
- $E_T>23$ GeV and Isolation
- $E_T>23$ GeV Isolated, $R_\eta>0.94$
- $E_T>23$ GeV, Isolation, $R_\eta>0.94$ and $E_{core}^{had}<0.8$ GeV

L1 Rates [kHz] vs L1 EM E_T [GeV]
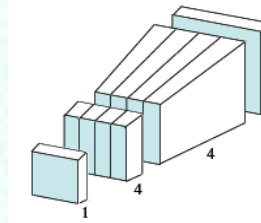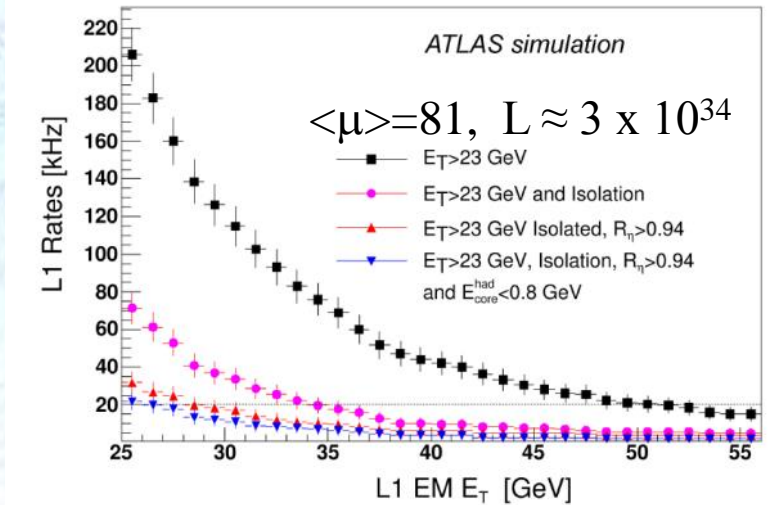
Selection criteria	Rate reduction	
	Fraction of (1)	Fraction of (2)
(1): Level-1 EM $E_T > 23$ GeV	100%	-
(2): (1) and Level-1 isolation	34.9%	100%
(3): (2) and R_η	14.25%	40.8%
(4): (3) and E_{core}^{had}	11.45%	32.8%

0.1×0.1 0.025×0.1
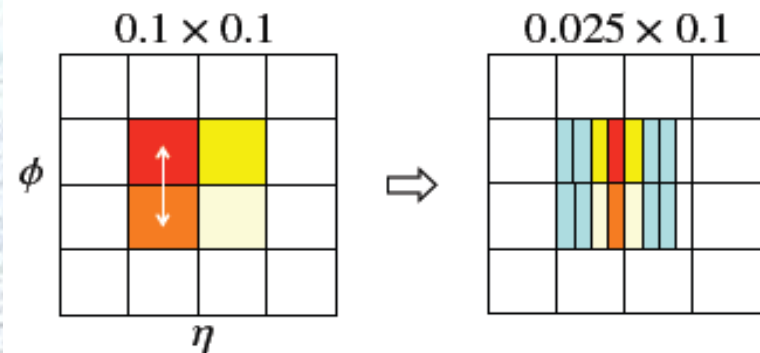
Distribution of the R_η parameter for electrons and jets, defined as the ratio of the energy in the 3x2 over the energy in the 7x2 clusters of the 2nd layer of the EM calorimeter.

ATLAS simulation
- Electrons
- Jets

dN/dR$_\eta$ vs R$_\eta$
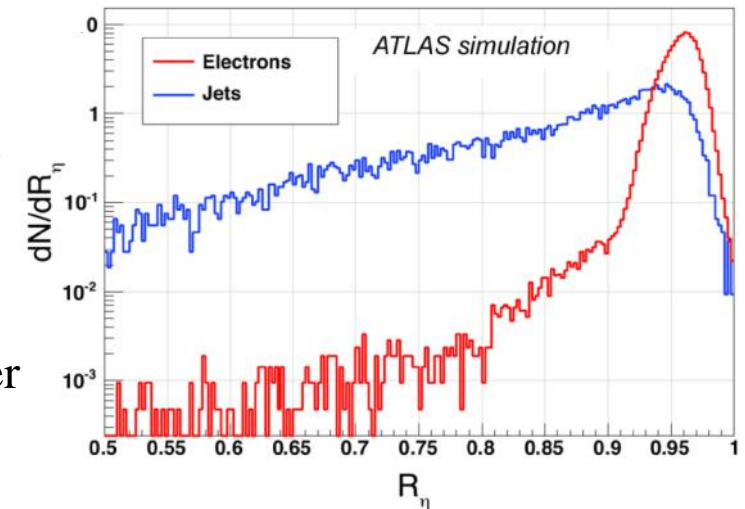
FTK and AFP

- **Fast TracK (FTK): Global hardware based tracking by start of L2**
  - Inputs from Pixel and SCT.
  - Data in parallel to normal read-out.
  - Provides inputs to L2 in ~ 25 µs with track parameters at ~offline precision for b tagging, tau ID and lepton isolation
  - Two phases:
    - Match hits to 10^9 stored patterns
    - Track fitting

Pattern recognition in coarse resolution (superstrip➔road)

Track fit in full resolution (hits in a road)
$F(x_1, x_2, x_3, ...) \sim a_0 + a_1\Delta x_1 + a_2\Delta x_2 + a_3\Delta x_3 + ... = 0$

→ New High Speed Optical link (HOLA) cards installed with dual outputs giving test of FTK functionality with real data
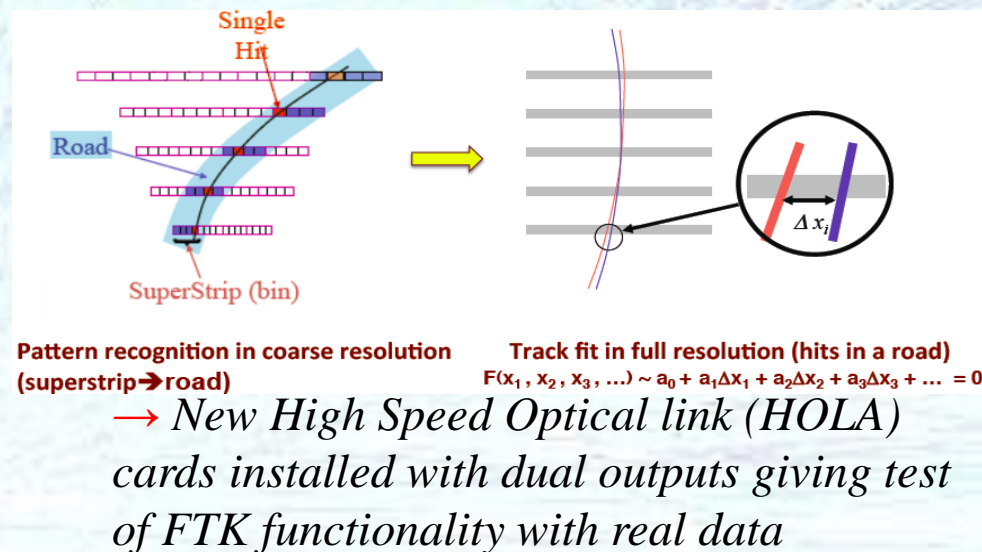
- **ATLAS Forward Physics (AFP)**
  - Tag and measure scattered protons at ± 210m
  - Link to system triggered in central ATLAS
  - **Radiation-hard edgeless 3D silicon** developed in IBL context
  - 10ps timing detector for association with high p_T primary vertex
  - Probe hard diffractive physics and central exclusive production of heavy systems/particles

→ <20 ps timing per bar demonstrated at 5MHz and minimum gain loss up to ~3C/cm²
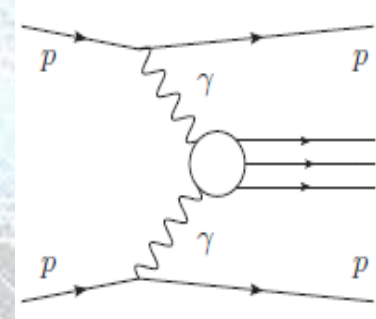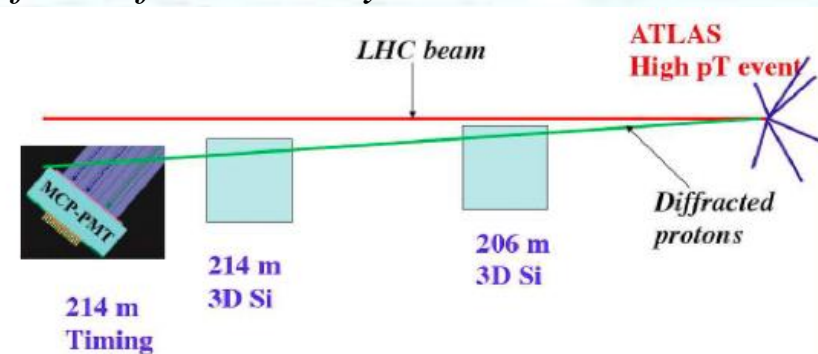
ATLAS: Draft Target Specifications

LHC up to 2021

		safer value
Peak Luminosity expected	$2 * 10^{34}$	$3 * 10^{34}$
Integrated Luminosity expected	300 fb^{-1}	400 fb^{-1}
μ = mean number of interactions per crossing (25nsec)	55 *	80
Safety factor to be used in the dose rate and integrated dose calculations	2?	2?

HL-LHC after 2022

		safer value
Peak Luminosity expected	$5 * 10^{34}$	$7 * 10^{34}$
Integrated Luminosity expected	2500 fb^{-1}	3000 fb^{-1}
Int. Luminosity per year expected	250 fb^{-1}	300 fb^{-1}
μ = mean number of interactions per crossing (25 nsec)	140 *	200
Safety factor to be used in the dose rate and integrated dose calculations	2?	2?

Plan for occupancy numbers based on this (see µ values below)

Plan integrated dose figures based on this

µ values going with the peak luminosity figure if achieved with 25ns beam crossing

When we calculate the dose figures which are used to specify the radiation hardness of components which can be reliably tested for post-irradiation performance (eg ASICs, silicon sensors, diamond, ...) apply this safety factor to the dose calculations in setting the radiation survival specification
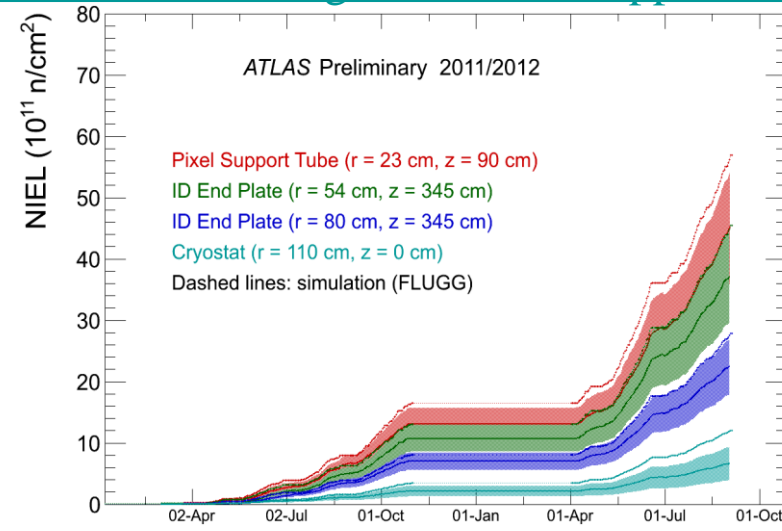
Current Detector Radiation Simulation

https://twiki.cern.ch/twiki/bin/view/AtlasPublic/SCTPublicResults#Figures
https://twiki.cern.ch/twiki/bin/view/AtlasPublic/ApprovedPlotsPixel#Radiation_damage_plots
https://twiki.cern.ch/twiki/bin/view/AtlasPublic/InDetTrackingPerformanceApprovedPlots#Alignment
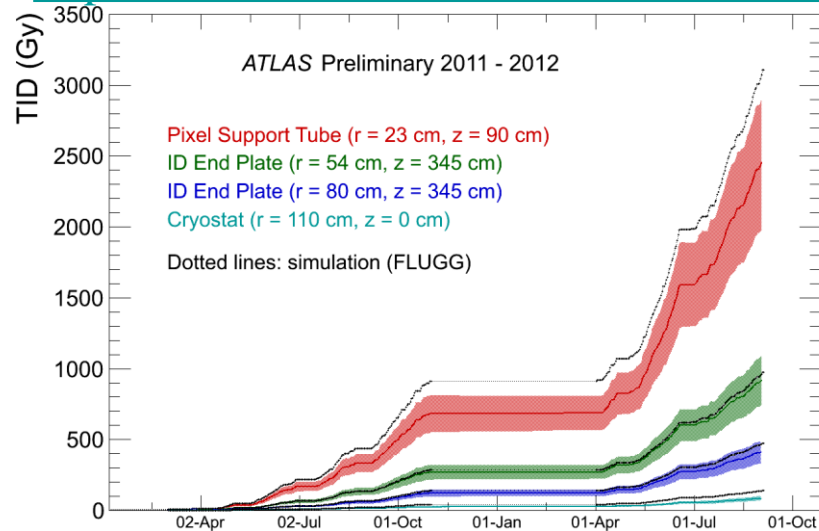
Simulation results fit with data to much better than a factor of 2 (and safety factor of 2 was assumed in dose specifications)

(Temperature history key to fitting I_{leak})

https://cds.cern.ch/record/1516824?ln=en

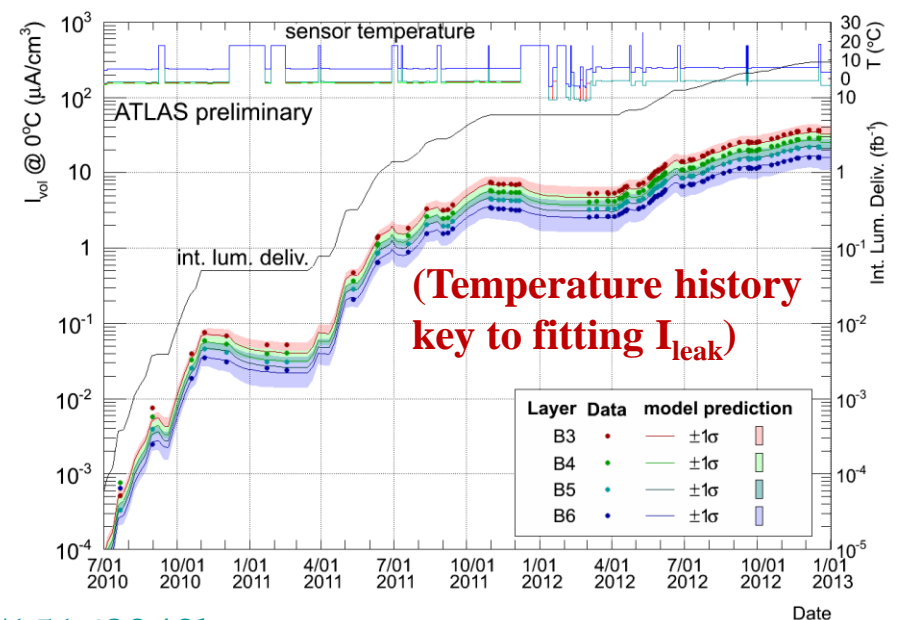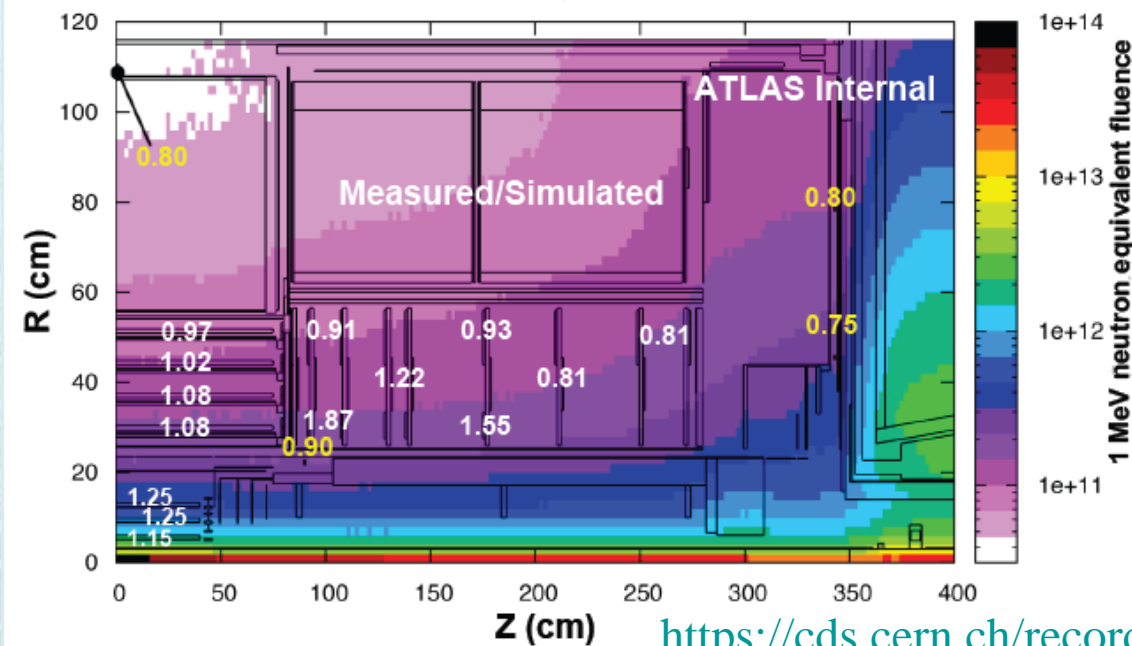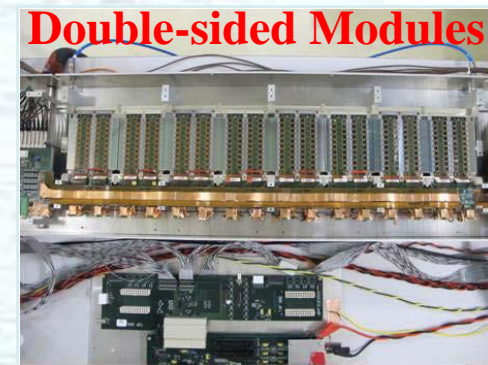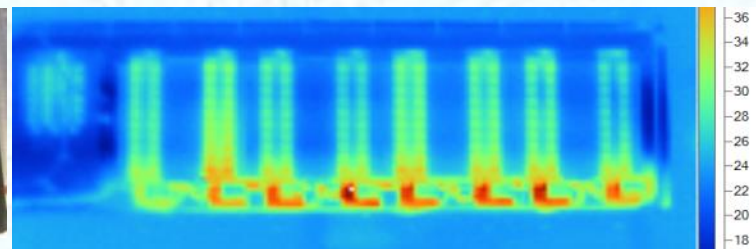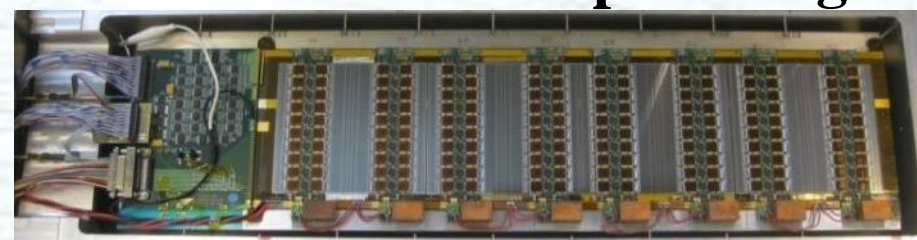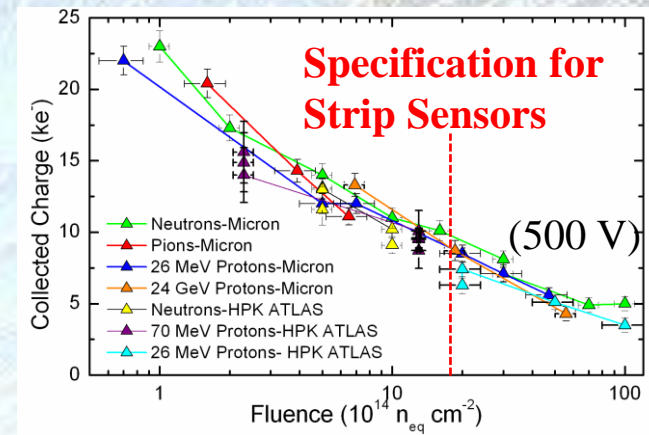# New All-silicon Inner Tracker

Strip Detector

- **Next iteration sensors being ordered**
- **Next (256 channel) ASIC: FDR completed**
- **Many strip modules prototyped with ABCN250 ASICs**
- **First forward module prototypes produced**
- **Serial and DC-DC powering studied in detail on short versions of the stave**

Specification for Strip Sensors

Collected Charge (ke) vs Fluence (10^{14} n_{eq} cm^{-2})

(500 V)

- Neutrons-Micron
- Pions-Micron
- 26 MeV Protons-Micron
- 24 GeV Protons-Micron
- Neutrons-HPK ATLAS
- 70 MeV Protons-HPK ATLAS
- 26 MeV Protons- HPK ATLAS

Double-sided Modules
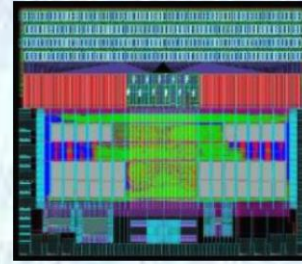
- **All components in place for full-length 1.2m electrical stave**
- **Several other new chips (HCC, HV multiplex, SP, DC-DC,..)**
- **Hybrid/module designs to use these are well advanced**
- **Local supports extensively prototyped and further material reduction achieved**

HV power

HV connection via screw (missing here)
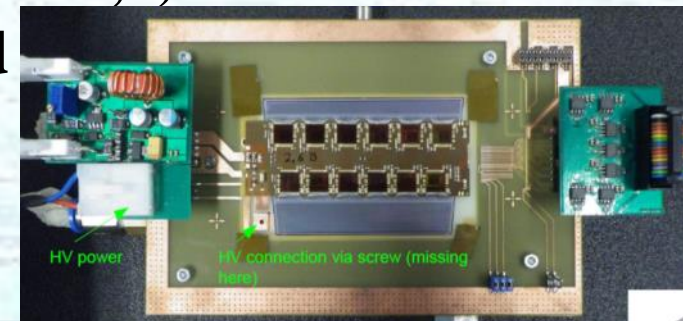
- **Progress in Petal and Stave support designs**
- **End-of-stave card for 130nm being developed**

Lamb and Flag
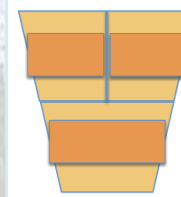
The Bear

Petalet: use 4" wafers to produce sensors and build a small petal

Allows to test petal specific issues, like how to configure the bus tapes.
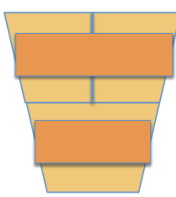
Current Silicon Microstrip (SCT) Material

Current Silicon Tracker
(4 barrel strip layers)

Module Material   **Support Material**
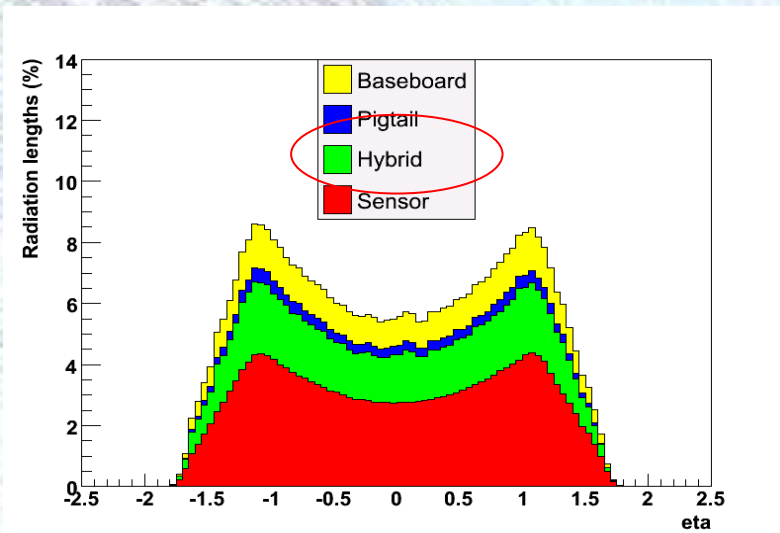
Old ATLAS Barrel Module
12 ASIC of 300µm thickness for double-sided module read-out
(*ie* just 6 read-out chips per side)
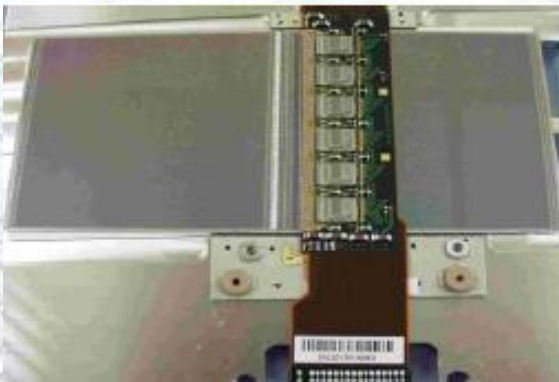
New ATLAS sLHC-Tracker Module will have 80 ASICs in two hybrid fingers for just one-sided read-out
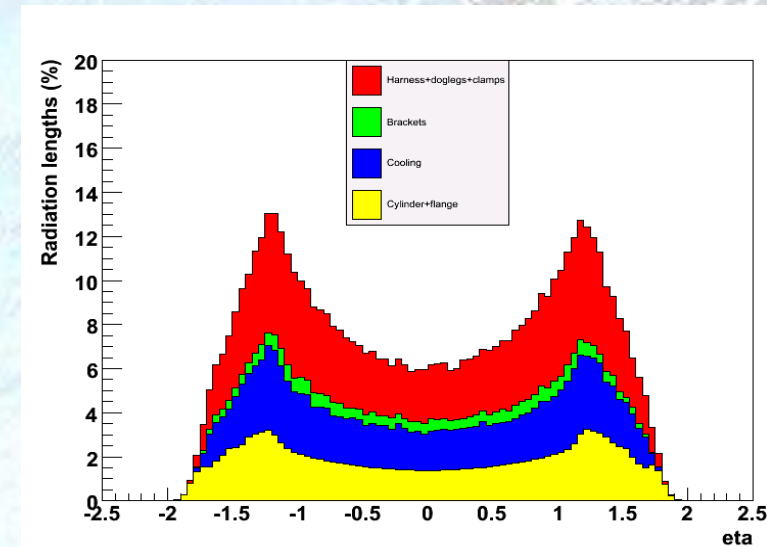
"The barrel modules of the ATLAS semiconductor tracker".
Nucl.Instrum.Meth.A568:642-671,2006.

Table 1
Radiation lengths and weights estimated for the SCT barrel module

Component	Radiation length [%Xo]	Weight [gr]	Fraction [%]
Silicon sensors and adhesives	0.612	10.9	44
Baseboard and BeO facings	0.194	6.7	27
ASIC's and adhesives	0.063	1.0	4
Cu/Polyimide/CC hybrid	0.221	4.7	19
Surface mount components	0.076	1.6	6
Total	1.17	24.9	100

Hybrid area per module roughly ×2 at HL-LHC: much higher R/O granularity

123

Stave: Hybrids **glued to** Sensors **glued to** Bus Tape **glued to** Cooling Substrate

Glue

Glue

cable
cable

1   2   3   12

1.2m
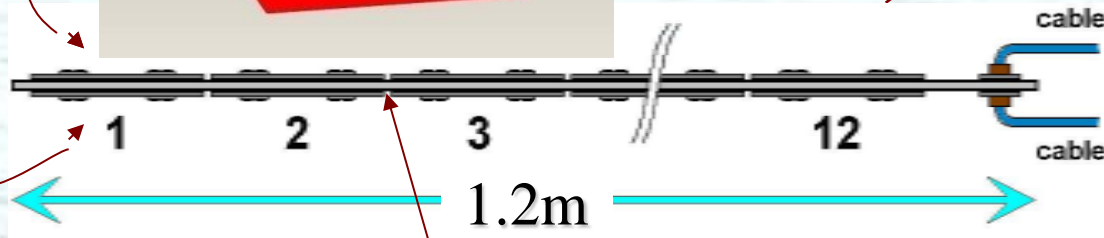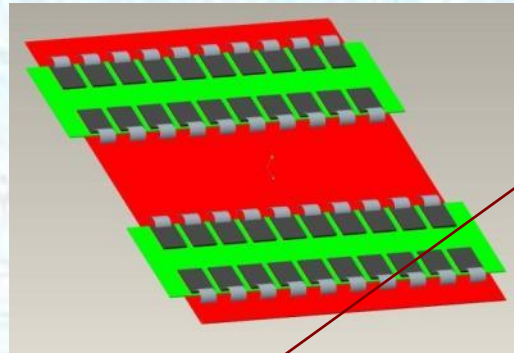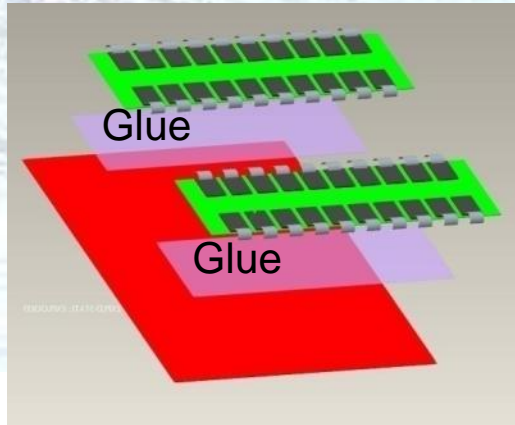
Current Prototypes
250nm ASIC Designs
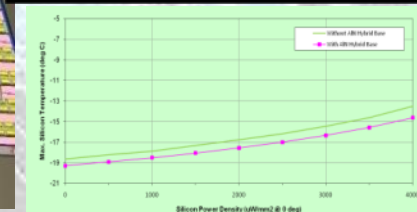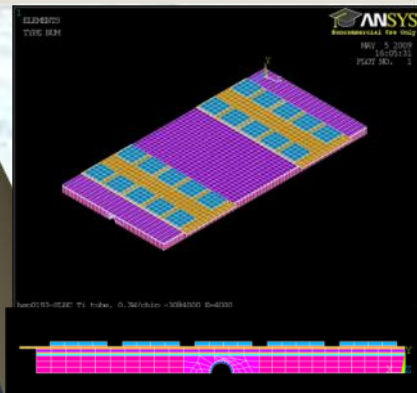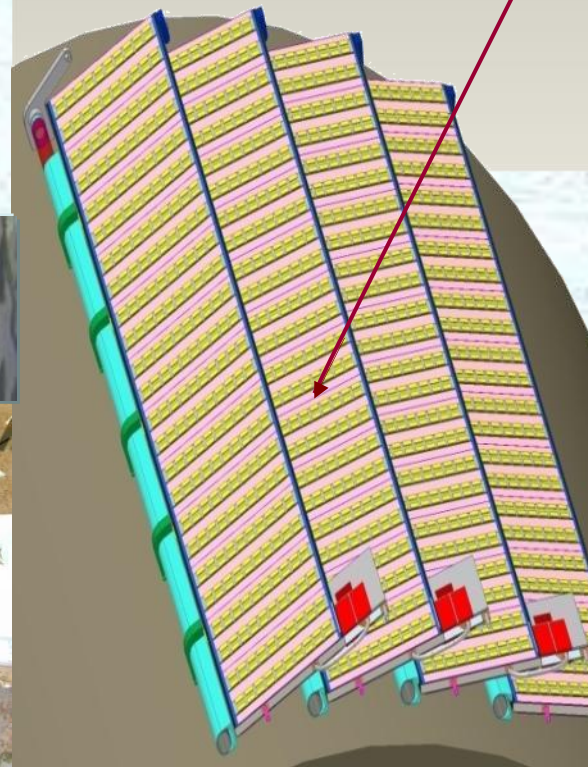
Stave: Hybrids glued to Sensors glued to Bus Tape glued to Cooling Substrate
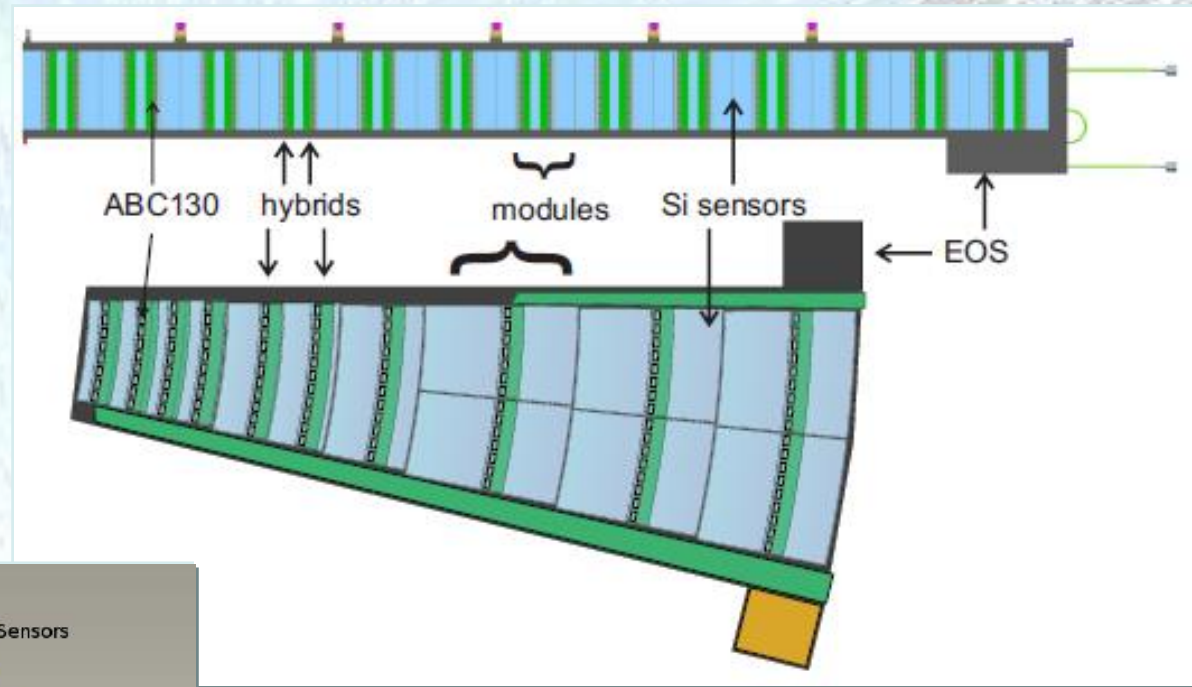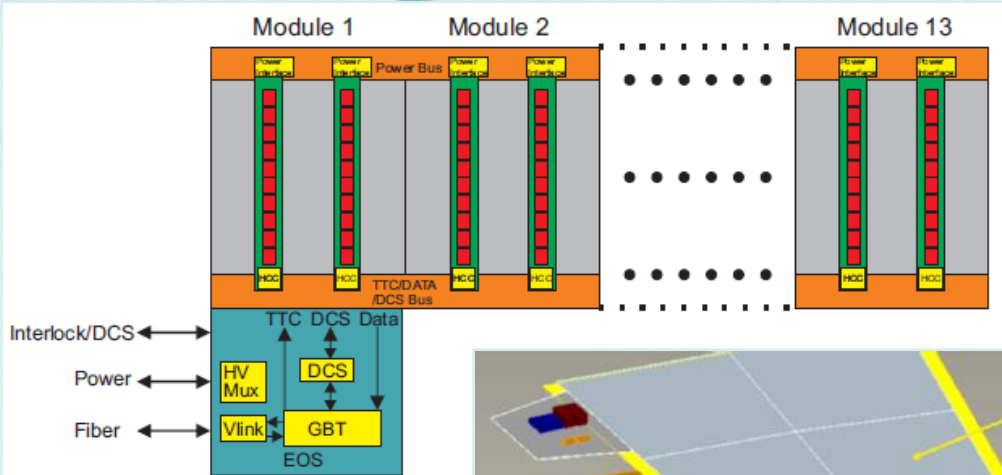
Module, Stave and Petal concepts with **130nm ASIC**: 256 channels so each row of ASICs address two rows of strips
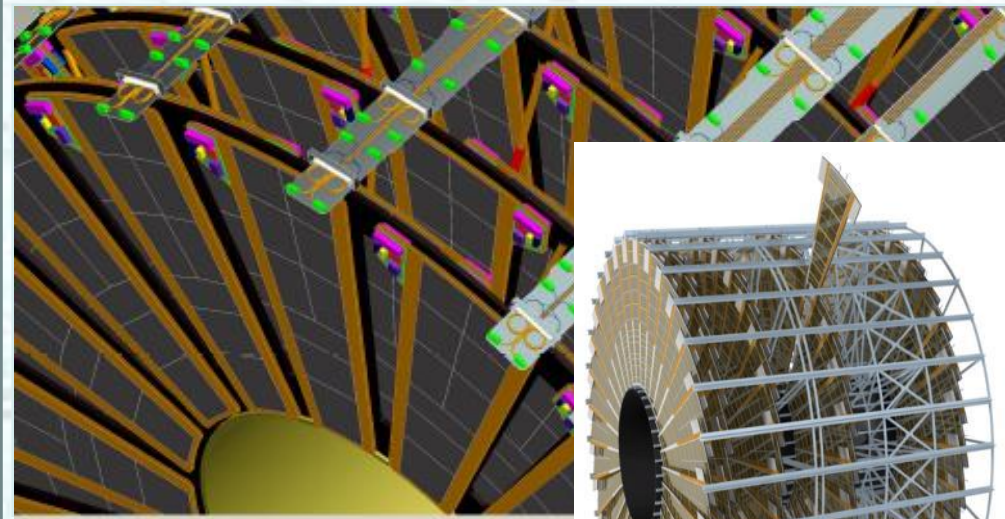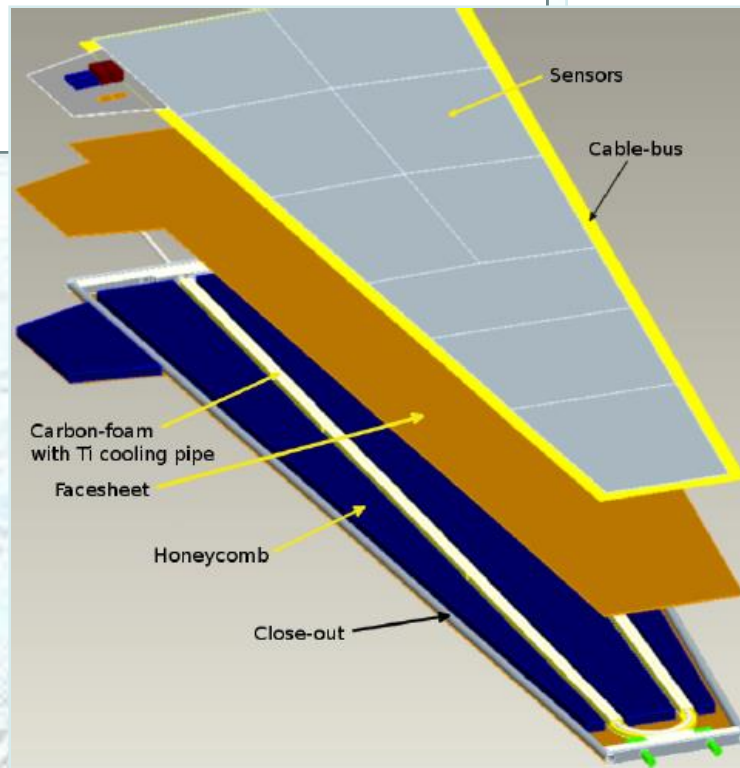
CMS: p_T Modules Types: "2S Module"

- 2x Strip sensors
- Light and "simple"
- No z information
- Suitable for outer part

Second version of FE ASIC (flip-chip version) back from foundry, about to be tested
CBC (CMS Binary Chip)
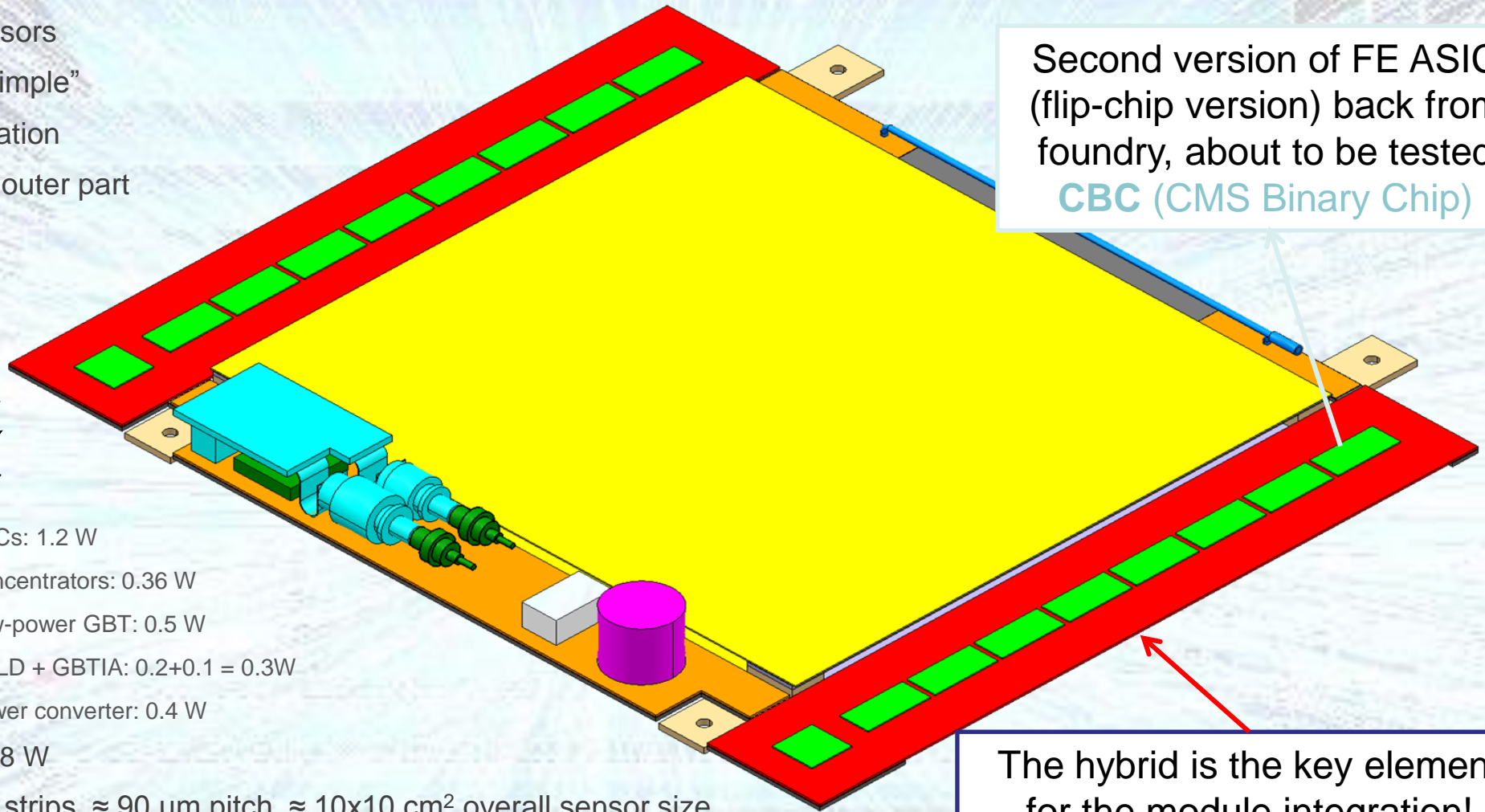
- Power
  - ★ CBCs: 1.2 W
  - ★ Concentrators: 0.36 W
  - ★ Low-power GBT: 0.5 W
  - ★ GBLD + GBTIA: 0.2+0.1 = 0.3W
  - ★ Power converter: 0.4 W
  - ⊙ Total 2.8 W
- ≈ 5 cm long strips, ≈ 90 μm pitch, ≈ 10x10 cm^2 overall sensor size
- Wirebonds from the sensors to the hybrid **on the two sides**
  - ⊙ 2048 channels on each hybrid
- Chips bump-bonded onto the hybrid
- **Prototyping started**

The hybrid is the key element for the module integration!

2S Module

Strip sensor (1)

FE hybrid with strip ASICs

Bias kapton

Service hybrid

Thermal management

Support frame

Cooling contacts

Sensors supports

Strip sensor (2)

Bias kapton
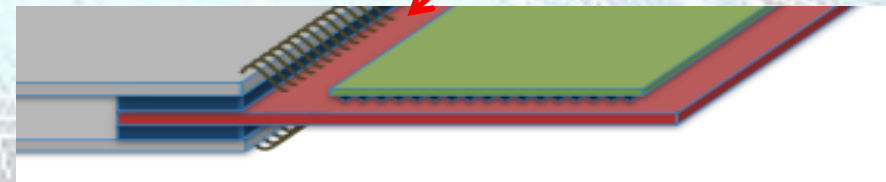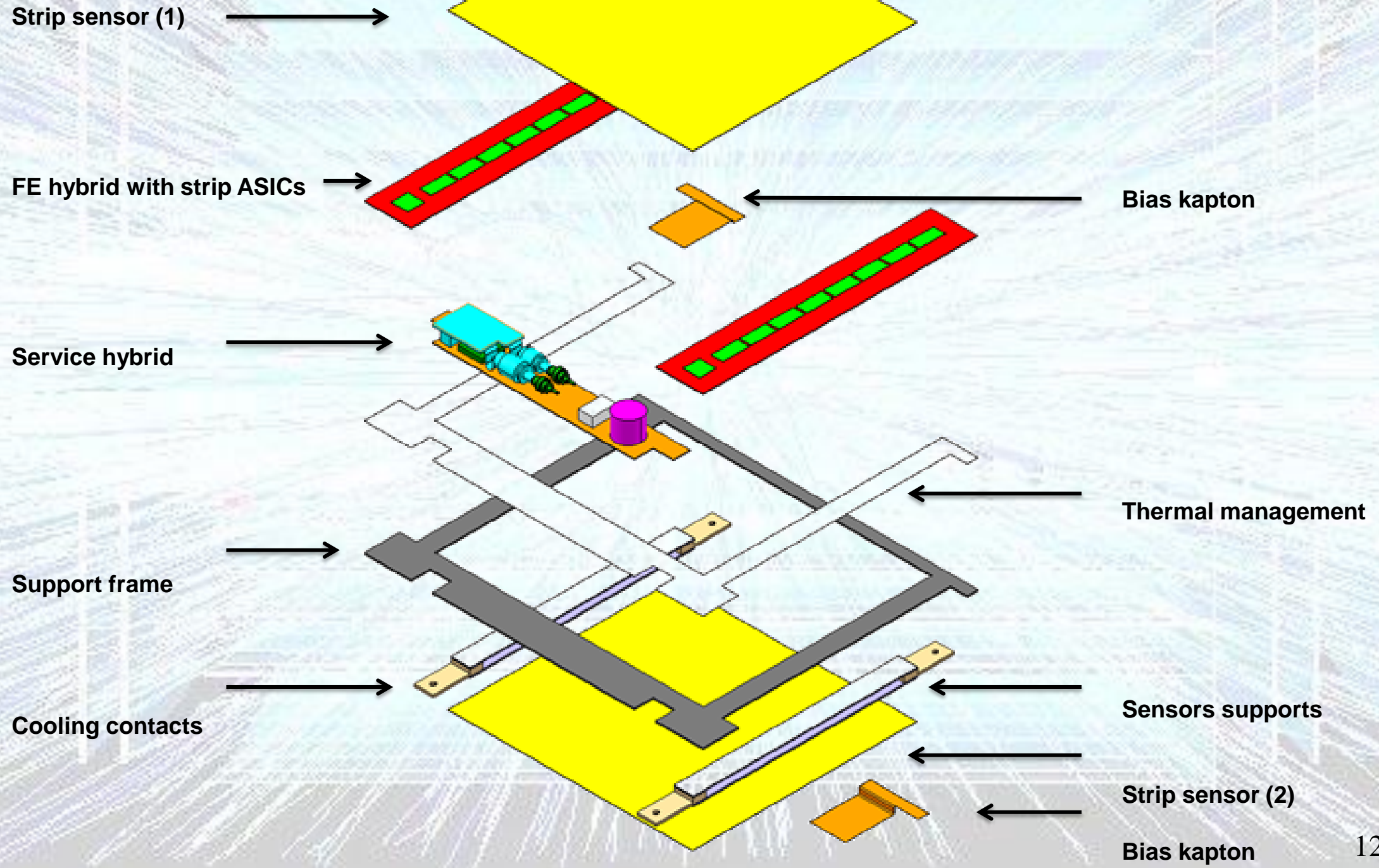
CMS: p_T Modules Types: "PS Module"

➢ Sensors:

  ⊙ Top sensor: strips

    ★ 2×25 mm, 100 μm pitch

  ⊙ Bottom sensor: long pixels

    ★ 100 μm × 1500 μm

  ⊙ ≈ 5x10 cm² overall sensor size

➢ Readout:

  ⊙ Top: wirebonds to "hybrid"

  ⊙ Bottom: pixel chips wirebonded to hybrid

  ⊙ Correlation logic in the pixel chips

➢ Sensors spacing tunable

➢ Power estimates

    ★ Pixels + Strips + Logic ~ 2.62 + 0.51 + 0.38 W = 3.51 W

    ★ Low-power GBT + GBLD + GBTIA ~ 0.5 + 0.2 + 0.1 = 0.8 W

    ★ Power converter ~0.75 W

  ⊙ Total ~ 5.1 W, pixel chip is the driver
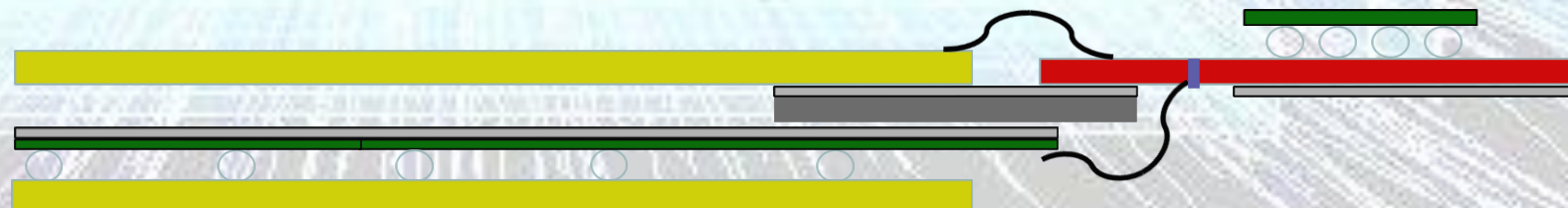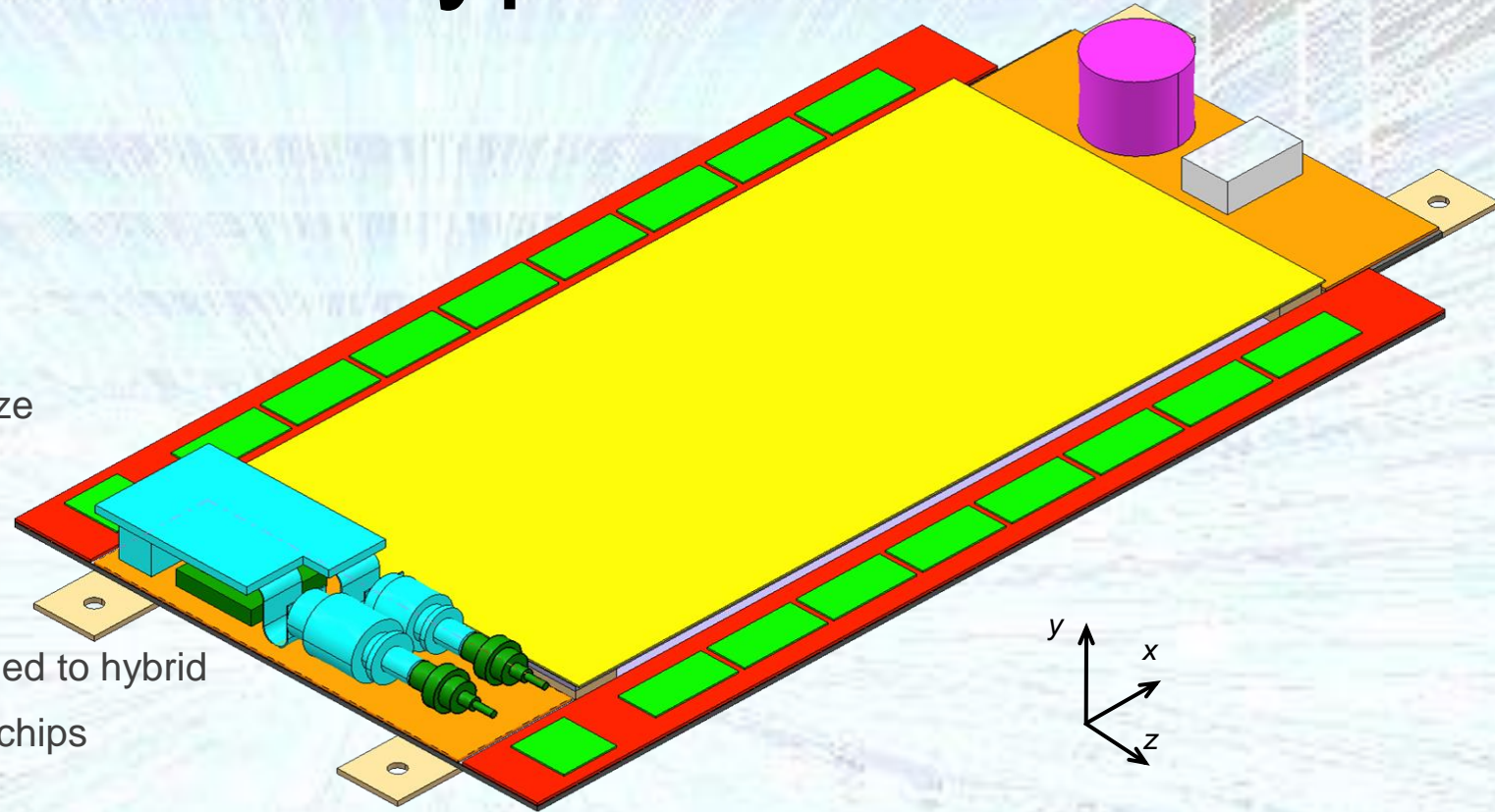
PS Module

Strip sensor

Bias kapton

Service hybrid (power)

FE hybrid with strip ASICs

Thermal management

Service hybrid (readout)

Support frame

Sensors supports

Thermal management

Pixel ASICs

Cooling contacts

Pixel sensor

Bias kapton

CMS: Phase-II Pixel

➢ The Phase-I pixel detector is not the CMS ultimate pixel

➢ Construction time is shorter, ~ 2 more years to converge on a design compared to the outer tracker

➢ Discussions started; convergence on some basic concepts
  ⊙ Aiming at a significantly smaller pixel size. Possibly as small as 30×100 µm^2?
  ⊙ 65 nm seems to be a good technology choice
    ★ Strong technology node, likely to be available for very long
    ★ Can squeeze 4× digital logic in same area wrt 130 nm
  ⊙ Thin planar sensors with small pixels could be a robust baseline
  ⊙ 3d silicon very appealing option with potentially excellent performance
  ⊙ Diamonds the ultimate radiation hardness? Production and cost still an issue
    ★ In any case low signal requires a chip with low threshold
  ⊙ Several important system issues need to be addressed
    ★ Synergies with Outer Tracker are necessary, but differences are relevant

➢ Simulation effort started to support ASIC development

CMS: Summary and outlook

- ➢ Designing an Outer Tracker with:
  - ⊙ Higher granularity
  - ⊙ Enhanced radiation hardness
  - ⊙ Improved tracking performance (… lighter!)
  - ⊙ L1 Track finding capability
    - ★ Reconstruct tracks above ~ 2÷2.5 GeV
    - ★ With ~ 1mm z_0 resolution

- ➢ All the necessary R&D activities are ongoing
  - ⊙ Not yet proven that goals can be met, but results are encouraging…

- ➢ Draft schedule developed for delivery in LS3

- ➢ Phase-II pixel project on the starting blocks
  - ⊙ Possible extension of the tracking acceptance towards high rapidity

Phase-II: Split TDAQ L1 Scheme
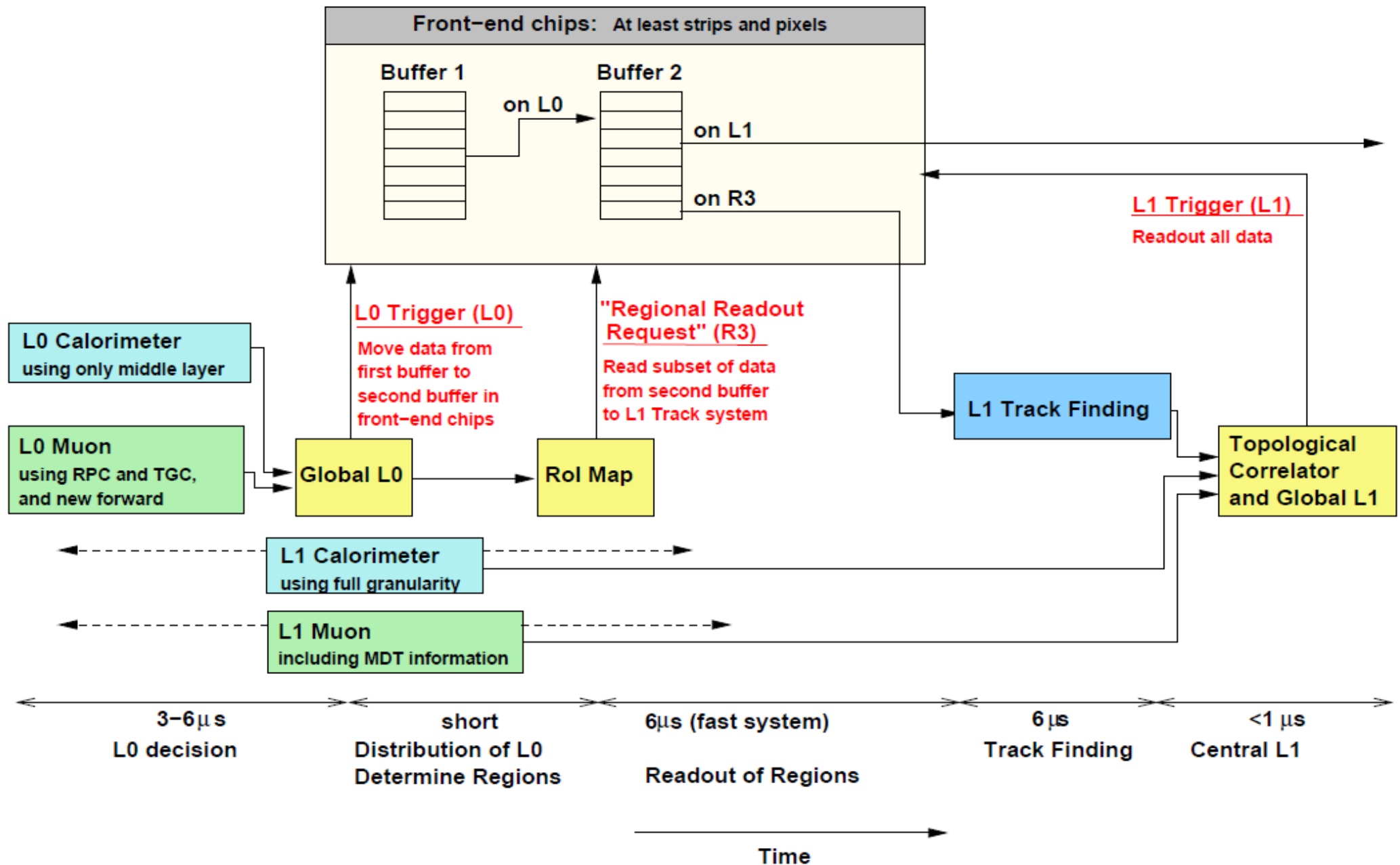
TDAQ and Detector Readout

- New TDAQ architecture requires upgrade to readout of detector systems
- General comments on need for upgrades of detector readout
  - In addition to the changes in TDAQ architecture. Upgraded readout electronics is required due to ageing and radiation damage.
  - More functionality moved to the counting room, taking advantage of large bandwidth optical links to move data off-detector; allows use of FPGAs rather than dedicated ASICs
    - GBTx group studies give 4.8Gbps rad-hard can already be reasonably assumed achievable in low mass custom package
    - Faster ($\geq$10 Gbps) can be expected for COTS systems with hardware only needed by the end of the decade
  - Detectors are evaluating a common readout architecture based on GBTs and possibly a common ROD.
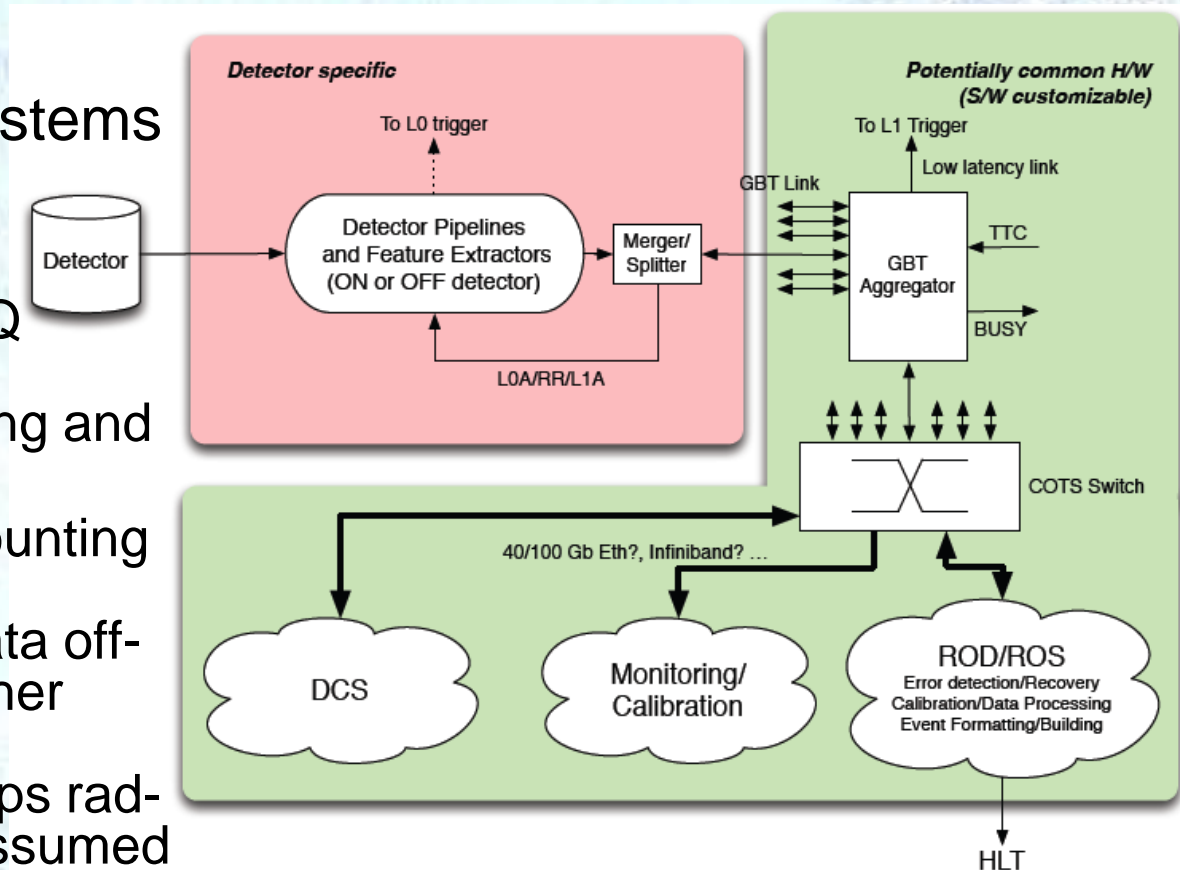
Phase-II Proposed Readout Architecture

Phase-II Upgrades to LAr Electronics

- Replace all FE boards (warm)
  - ➢ Gives flexible, free-running architecture sending data off-detector for all bunch-crossings
  - ➢ Natural evolution of Phase-I new digital trigger boards
  - ➢ Replacement required due to aging and radiation limits
  - ➢ Allows implementation of L0/L1 scheme using Phase-I L1 upgrades for Phase-II L0

- Replace Forward calorimeter (FCal) **if required**
  - ➢ Install new sFCAL in cryostat or miniFCAL in front of cryostat if significant degradation in current FCAL

- Replace Hadronic calorimeter electronics **if required**
  - ➢ Replace HEC cold preamps if significant degradation in performance

Simulation results of FCAL study in HiLum experiment. Preliminary results are similar to simulation
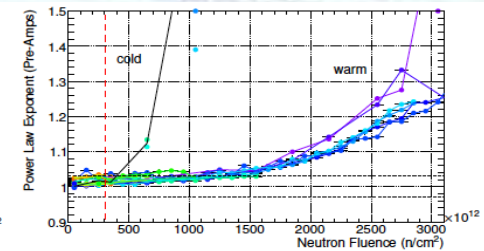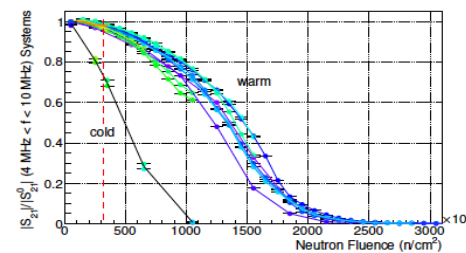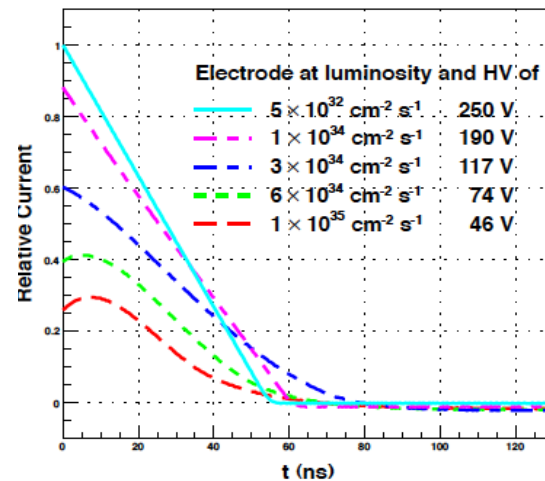
Performance of cold HEC electronics under irradiation

134

HEC and FCAL Phase-II Options

- **Option 0**
  - detector unchanged
- or **Option 1**: HEC cold electronics will not survive the 3000/fb
  - *Open cryostat*
  - Exchange cold electronics
  - Replace FCal by sFCal
- or **Option 2**: HEC cold electronics will survive the 3000/fb
  - Exchange FCal by sFCal
  - Opening the warm cover and "only" the inner bore of the cold vessel
- or **Option 3**: HEC cold electronics will survive the 3000/fb
  - Install miniFCal in front of EC cryostat
- Timeline not fully defined, many studies ongoing

- *Critically dependent on understanding safety factors on fluence estimates and projected performance degradation*
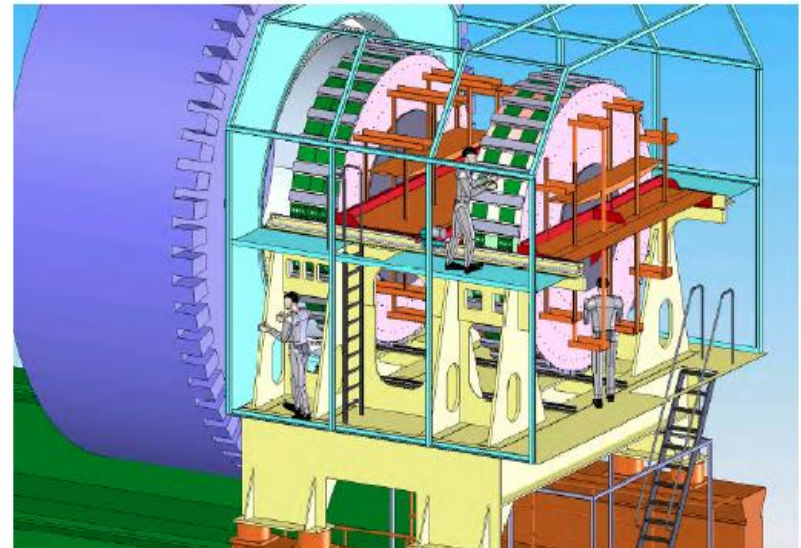
The two HEC wheels extracted from the cryostat and supported by the Super-T6 tooling.
The protective tent's frame is also shown.

TileCal Phase-II Upgrade

- No major changes foreseen in the readout or trigger during Phase-I
- In Phase-II complete FE&BE electronics replacement.
  New read-out architecture.
  - **Full digitization** of data at 40MHz and transmission to off-detector system
  - **Digital** information to L1/L0 **trigger**

Move FE functionalities to BE:
- Increase x100 the **input** of the ROD
- Output to DAQ after L1 unchanged
- New output to L1/L0 Calo

Present
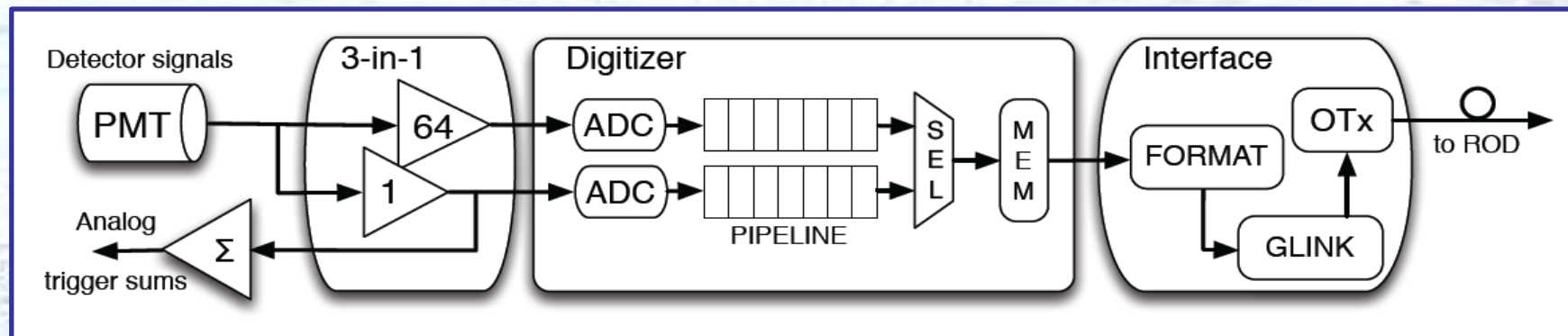
Phase-II Upgrade
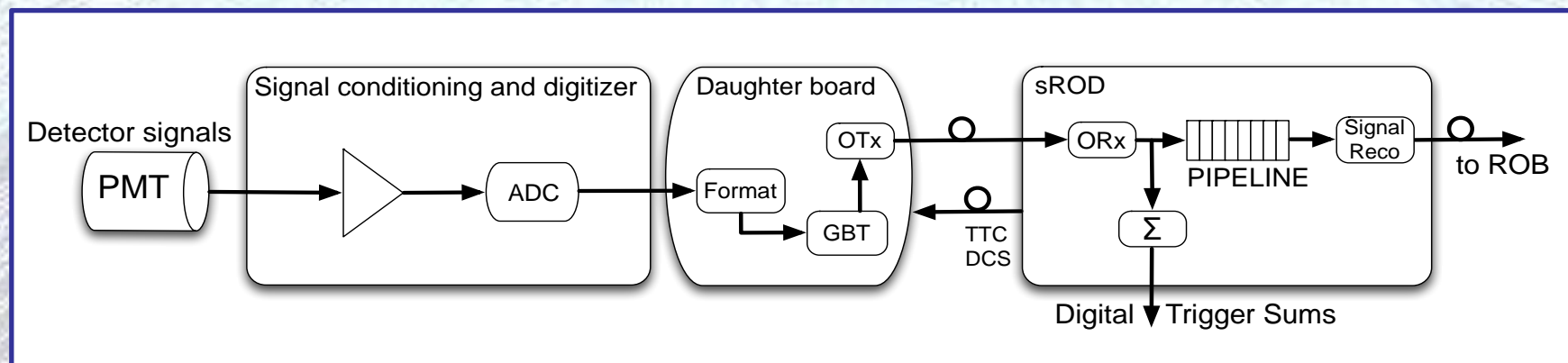
TileCal Phase-II Upgrade

- Replace and upgrade readout system to provide full digital readout
- Front-End boards – three alternative designs under development
  - ➢ Modified 3-in-1 (modification of existing FE)
  - ➢ FE-ASIC (including ADCs)
  - ➢ QIE (multirange charge converter)
  - ➢ Improved robustness: cells are read out independently by 2 PMTs
- Power supplies
  - ➢ Voltage dividers capable of compensating for non-linear response due to high current flow
  - ➢ Upgrade LV supplies using low noise DC-DC convertors with radiation hard point-of-load regulation being developed by CERN
- Drawer mechanics (Standard or mini drawers)
  - ➢ To improve access

Muon Electronics Upgrade

- Upgrade front-end electronics (accommodate L0/L1 scheme)
- Improve L1 p_T resolution
  - Implement new system to improve p_T-resolution using MDT information and/or improving spatial resolution of the RPC
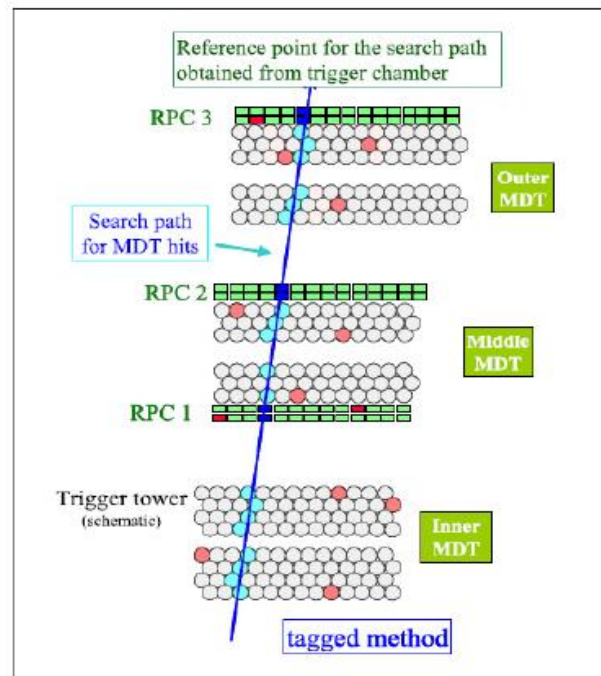
Use precision MDT information to improve p_T resolution of RPC ROI objects (seeded option)

  unseeded option requires×3 more fibres

Improved spatial resolution using charge sharing in RPC strips is also being investigated

The "RoI seeded" method. The RoI information for a high-p_T track from an adjacent trigger chamber (here the outer chamber RPC3) is used as a search road for MDT hits of the candidate track. Track segments of several MDT chambers can be combined to give a precise pT estimate for the candidate track.

138

Upgrade Computing & Software

- Project covers:
  - Frameworks (job, IO, Event Data Model)
  - Databases
  - Simulation
  - Reconstruction
  - Distributed Computing
  - Analysis
  - Software infrastructure
  - Data preservation and access
- Trigger integration & common developments a recurring theme
- Factor of 10 in data rate should be accommodated by 2020s through hardware improvements and software speed-up
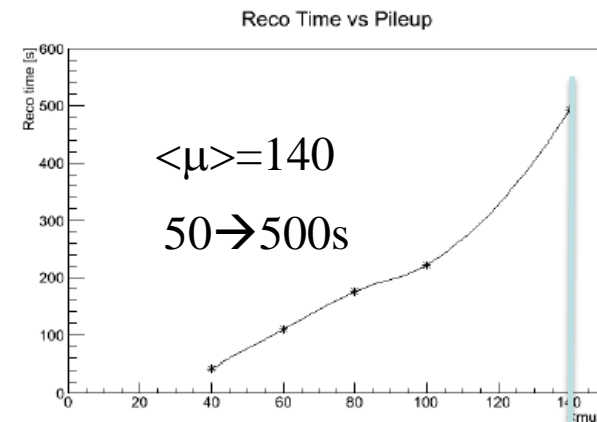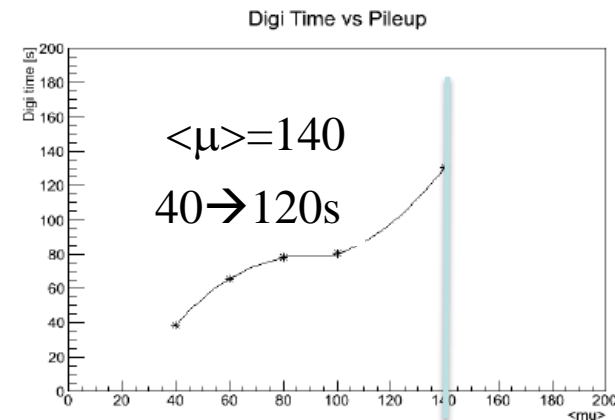
The impact of increasing pile-up on the existing simulation digitisation step (upper plot) and for the reconstruction step (lower plot).

$\langle\mu\rangle = 140$

$40 \rightarrow 120s$

$\langle\mu\rangle = 140$

$50 \rightarrow 500s$

Projected Cost

- **Total CORE cost: 230.334MCHF**
  - **+45.013MCHF of possible additions**
- **Common fund is currently: 16.28MCHF**
  - **this is expected to increase as a fraction of the total cost as common items across the project are identified**

Item	CORE cost (MCHF)	Possible additions	2015	2016	2017	2018	2019	2020	2021	2022
New Inner detector	131.500	26.000	2.400	5.600	35.660	32.460	29.160	15.360	10.860	0.000
LAr Calorimeter upgrades	32.124	15.096	0.547	3.170	1.015	2.003	4.517	14.379	6.494	0.000
Tile Calorimeter upgrades	7.483	2.517	0.000	0.000	0.000	1.122	1.629	4.070	0.602	0.060
Muon spectrometer upgrades	19.632	0.500	0.100	0.275	0.675	3.791	5.041	6.750	2.800	0.200
Trigger and DAQ upgrades	23.315	0.900	0.000	0.075	0.315	1.565	2.085	9.805	4.350	5.120
Common Fund	16.280	0.000	0.000	0.100	0.400	0.600	2.850	4.100	4.880	3.350
Total (MCHF)	230.334	45.013	3.047	9.220	38.065	41.541	45.282	54.464	29.986	8.730

Table 10.18: CORE Cost table

Details at: https://edms.cern.ch/document/1258343/1

Single-sided Strip Modules

- Module building community working towards completion of the 250 nm ASIC programme

- More than 170 hybrids and 65 barrel modules produced for stave-lets and stave-250

- First forward module recently assembled

- Studying performance, and scrutinizing properties

	Produced Hybrids	Produced Modules
Cambridge	23	6
DESY	5	Soon
Freiburg	26B , 8EC	12B, 1EC
Glasgow	4	1
LBL		7
Liverpool	77	33
Santa Cruz	39	6
Birmingham	Soon	
Total	174 B, 8 EC	65B,1EC

Barrel Module
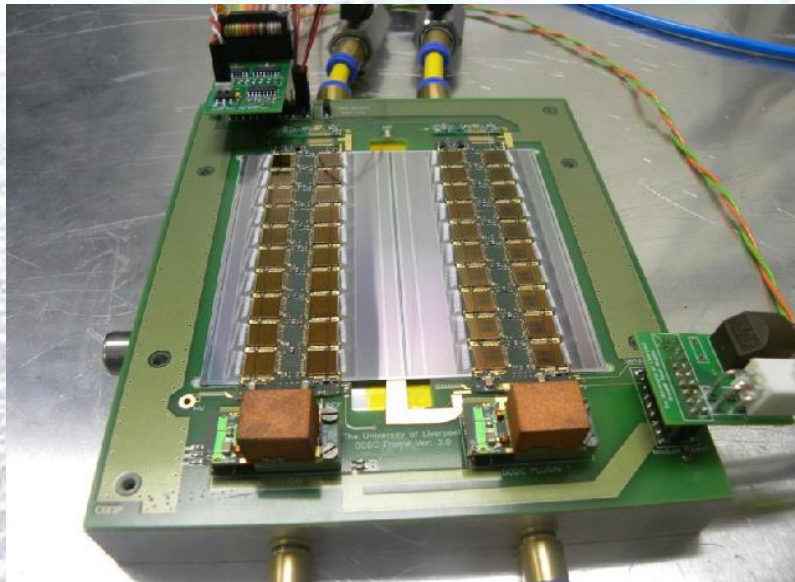
Petal Module
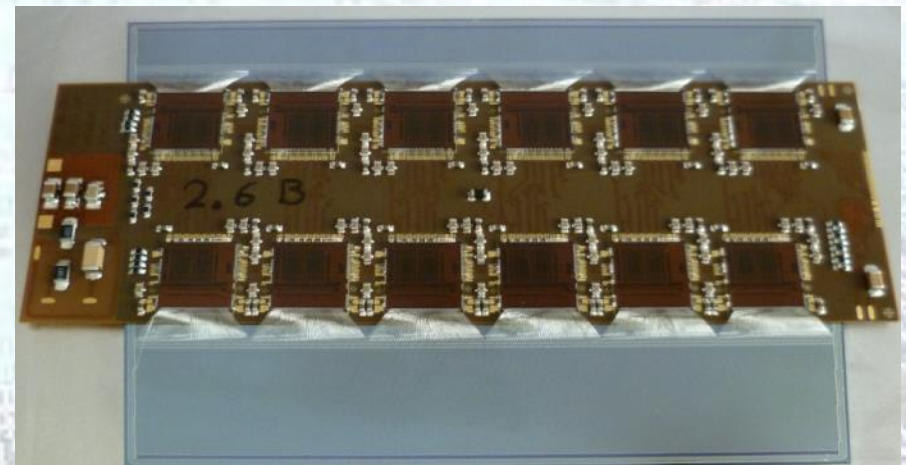
Barrel Single-sided Modules

- **250nm ASIC barrel module assembly in a rather mature state**

  - **Well known electrical properties, mass-production assembly methods, …**

  - **Common jigs and bonding programs**

  - **Hybrids by Stevenage Circuits Ltd and surface mount by Hawk Electronics Ltd**

- **Recent new developments/studies:**

  - **Test of first module with 4-layer build hybrids**
    No integrated shield, lower mass and thinner build (~20% overall reduction)

    - **Similar noise performances as shielded hybrids (baseline hybrids from now on)**

  - **Transport boxes for safe transport of assemble modules sites to stave assembly sites**
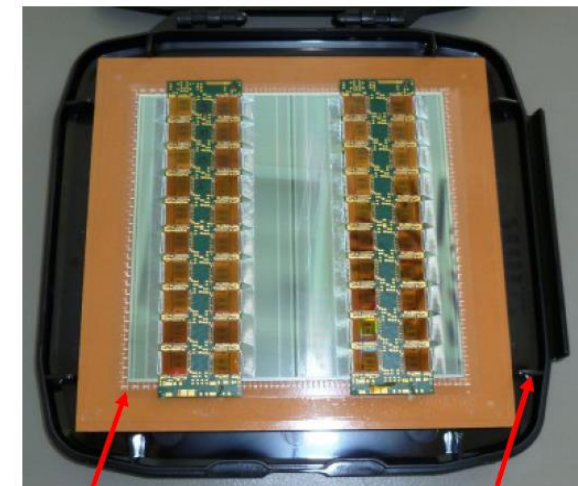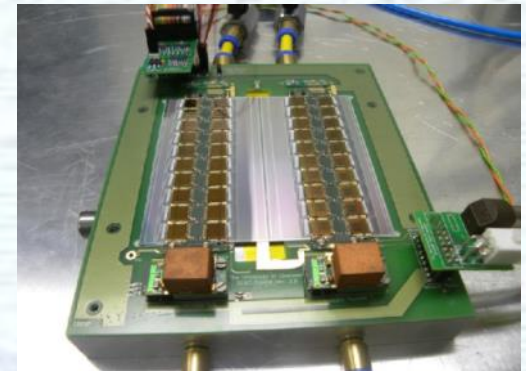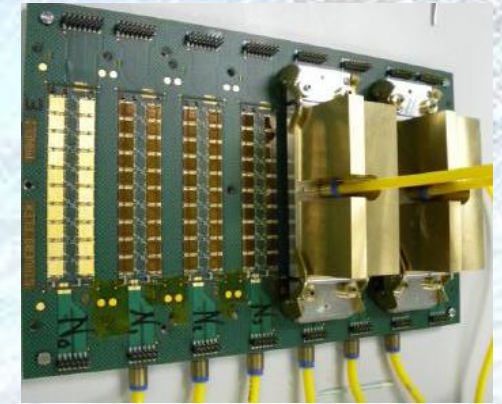
vacuum release gel-tray   plastic box

New 130nm Hybrids/Modules

- **130nm (256 channel) ASIC barrel hybrids: design well advanced**
  - **10 ABCN130 and HCC on each hybrid**
  - **3 layers build**
  - **Power protection/control and HV filtering moved off hybrid (attached to bus cable)**
  - **Material budget significantly reduced wrt 250 nm**
- **Tooling for hybrid/module build ready**

Legend: Copper, ASICs, Solder, Kapton, Discretes, ASIC Glue, Flash metal, Solder Resist, Wire Bonds

130 nm / 250 nm material budget chart (0 to 0.25)

Layer 1 — Layer 2 (VDD) — Layer 3 (GND)

97.54mm × 16.5mm

Preliminary
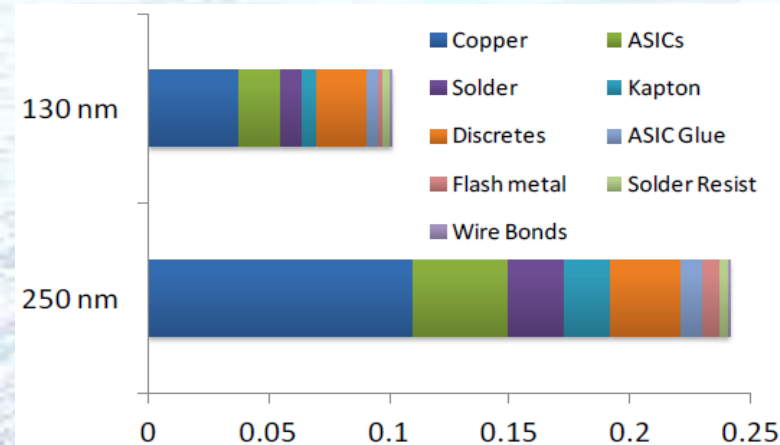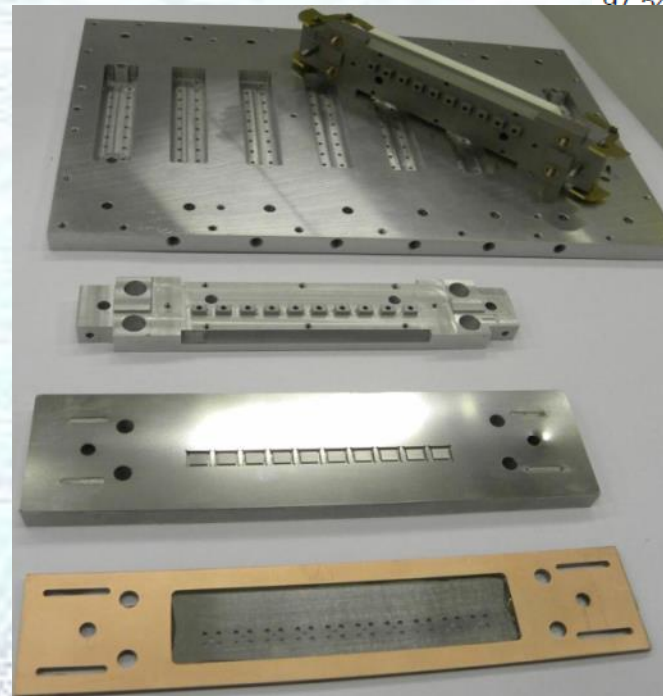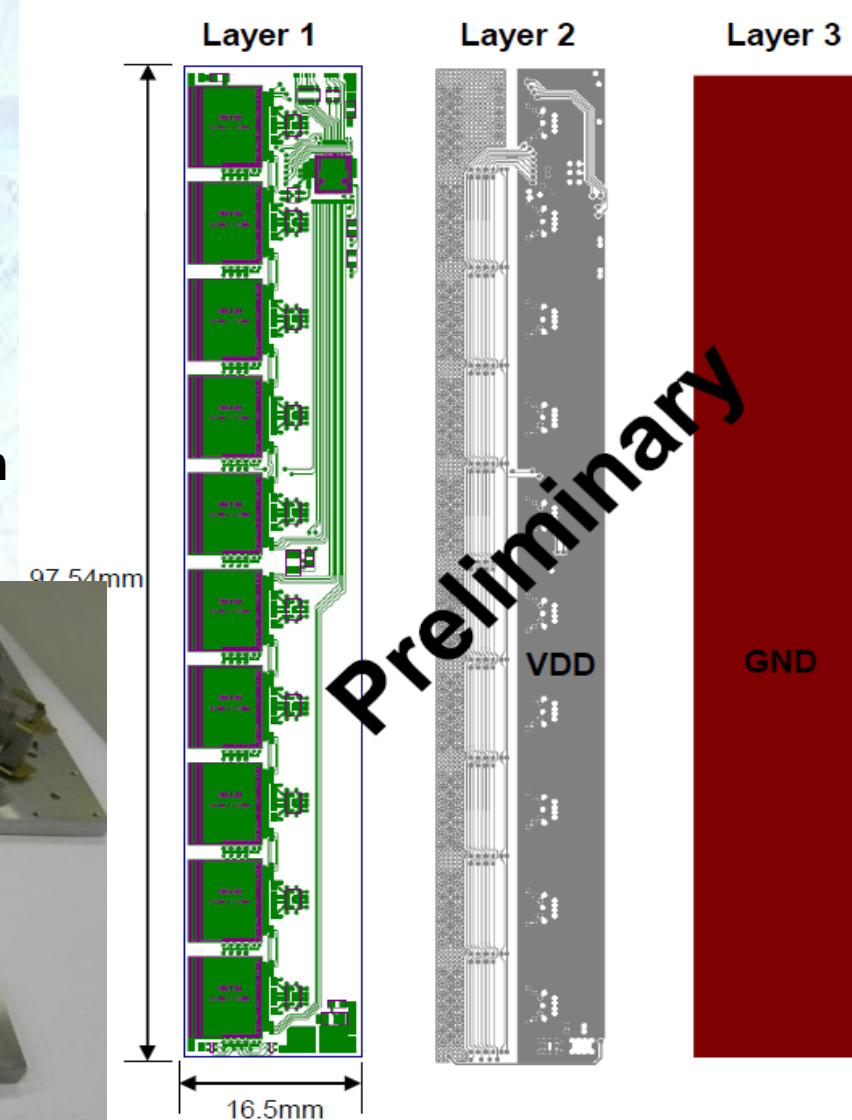
Barrel		End-Cap	
Element	% Radiation Length	Element	% Radiation Length
Stave Core	0.55	Petal Core	0.47
Bus Cable	0.30	Bus cables	0.03
Short-Strip Modules	1.07	Modules	1.04
Module Adhesive	0.06	module adhesive	0.06
Total	1.98	Total	1.60

ESWG Performance Assumptions

Offline trigger thresholds with estimated efficiencies and η coverage. The effective efficiencies are the product of the efficiency of the present system and a predicted efficiency for the track requirements.

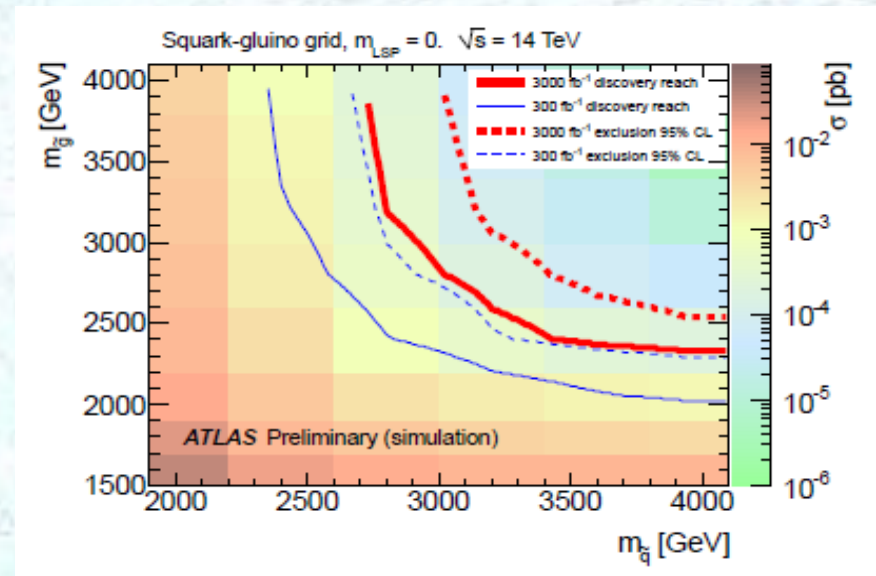| Object	L1 threshold	Offline	Eta Cov.	Efficiency $\approx \epsilon_{cur} \times \epsilon_{trk}$
Single object				
Electrons	EM18VH + ID track	25 GeV	$\lvert\eta\rvert < 2.5$	$93\% \times 95\% = 88\%$
Muons	MU20 + ID track	25 GeV	$\lvert\eta\rvert < 2.4$	$67\% \times 95\% = 64\%\ \lvert\eta\rvert < 1.0$
				$91\% \times 95\% = 86\%\ \lvert\eta\rvert > 1.0$
Tau	TAU40 + track-iso	60 GeV	$\lvert\eta\rvert < 2.5$	80%
Photon	L0_EM30 + L1calo	60 GeV	$\lvert\eta\rvert < 2.5$	$\approx 100\%$
MET	XE150	180 GeV	-	$\approx 100\%$
Multi-object				
$ee, e\mu, \mu\mu$	-	15 GeV	η from above	product of ϵ_e and ϵ_μ
				$e : 93\% \times 95\% = 88\%$
				$\mu, \lvert\eta\rvert < 1.0 : 77\% \times 95\% = 73\%$
				$\mu, \lvert\eta\rvert > 1.0 : 95\% \times 95\% = 90\%$
$e\tau, \mu\tau$		e/μ :15, τ :25 GeV	η as above	product of single obj ϵ_e, ϵ_μ, and ϵ_τ
$\tau\tau$	2TAU15I + ID tracks	40 GeV	$\lvert\eta\rvert < 2.5$	64%
Diphotons	2EM10VH	15 GeV	$\lvert\eta\rvert < 2.5$	$\approx 100\%$
4 70 GeV Jets		70 GeV	$\lvert\eta\rvert < 3.2$	$\approx 100\%$

ATLAS: Searches for SuperSymmetry

- Very stringent constraints from LHC on strongly produced sparticles (1st, 2nd generation mass degenerate squarks, gluinos) → can be quite heavy **(multi-TeV)**

- Direct production of 3rd generation squarks and weak gauginos is becoming accessible as the amount of integrated luminosity increases **(low cross sections)**

- **If No deviations from the SM observed in 300/fb**
  - Extension of sensitivity (mass & cross section reach) with 3000/fb

- **Deviations from the SM observed in 300/fb**
  - Signal characterization with **3000/fb**

Squark-gluino grid, $m_{LSP} = 0$. $\sqrt{s} = 14$ TeV

- 3000 fb^{-1} discovery reach
- 300 fb^{-1} discovery reach
- 3000 fb^{-1} exclusion 95% CL
- 300 fb^{-1} exclusion 95% CL

ATLAS Preliminary (simulation)

$m_{\tilde{g}}$ [GeV], $m_{\tilde{q}}$ [GeV], σ [pb]

- Determination of masses by measuring endpoints of visible mass distributions
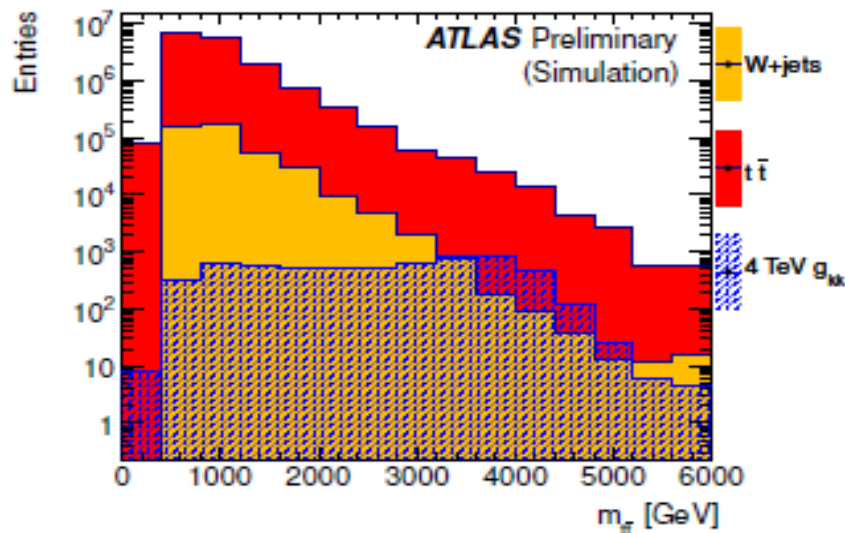
- Measurement of couplings and spin (via angular analysis)

Weak Gauginos and 3rd Generation

- Low cross sections (≈ fb) expected for stop and chargino/neutralino pair production
- Possibly the only sparticles with mass below 1-2 TeV because of naturalness
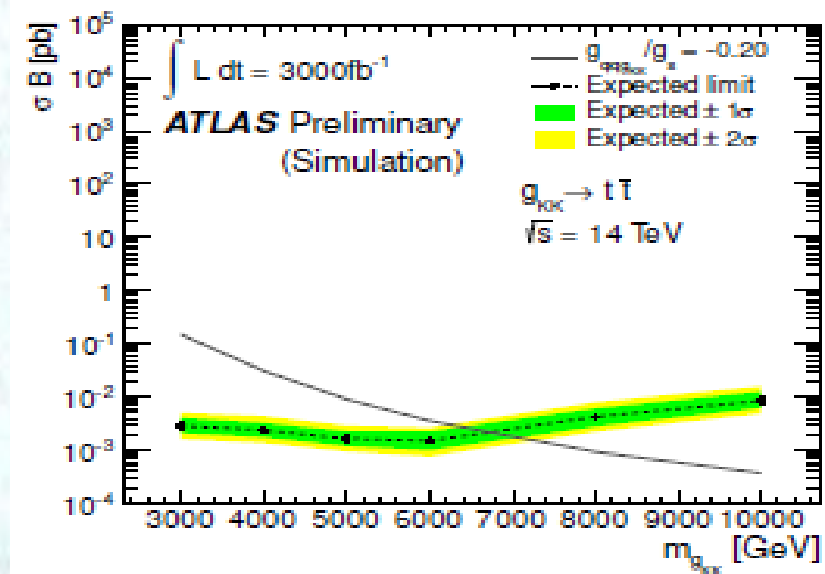- Factor of 10 in integrated luminosity will extend the reach considerably
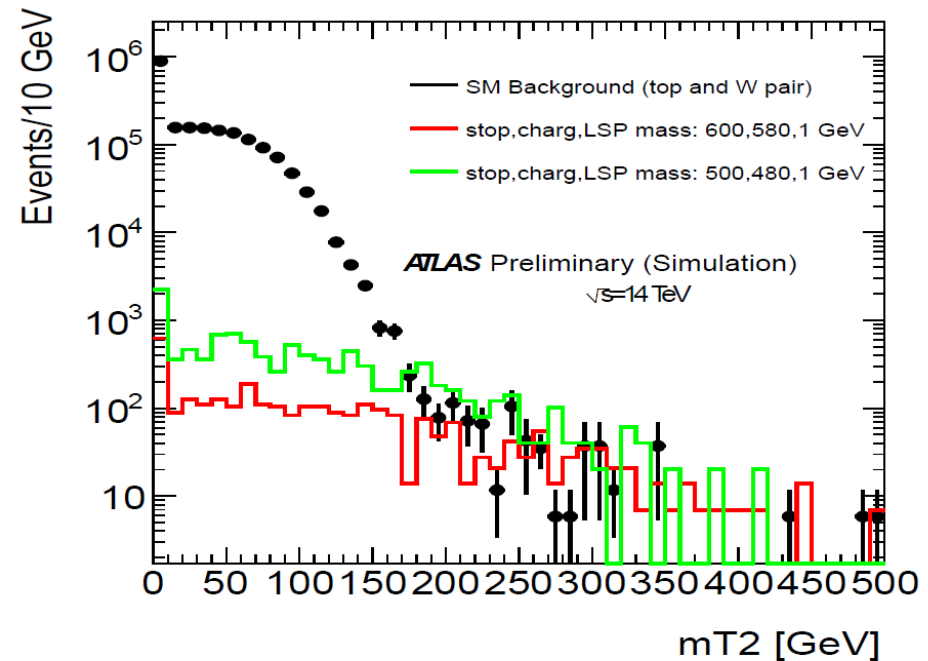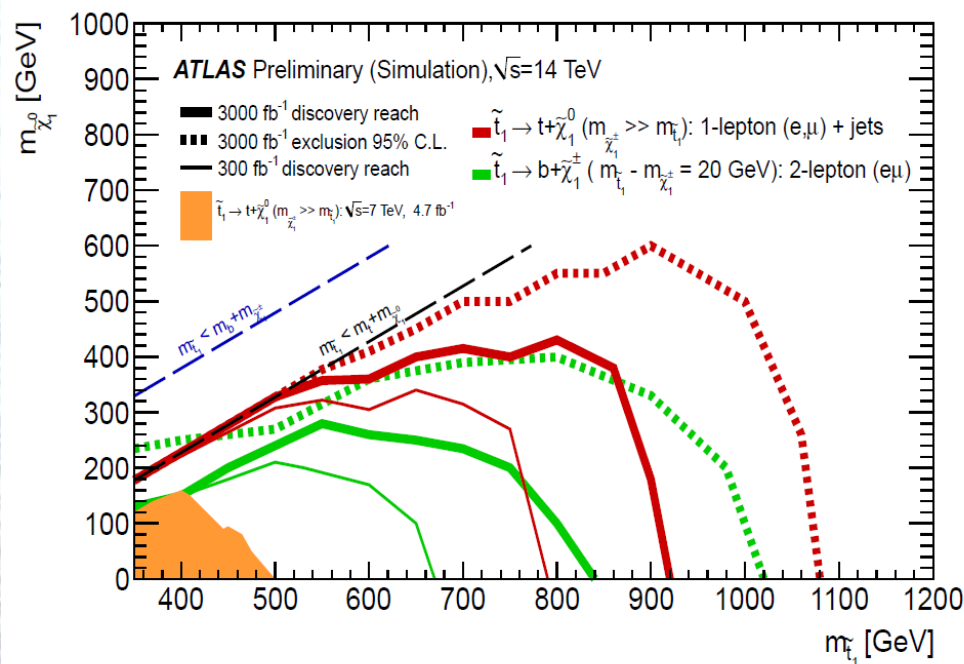
New Resonances

- Several BSM predicts i.e. new gauge bosons (Z')
  - Explore ditop resonances, as well as dileptons.

Di-top

Di-lepton

model	300 fb^{-1}	1000 fb^{-1}	3000 fb^{-1}
g_{KK}	4.3 (4.0)	5.6 (4.9)	6.7 (5.6)
$Z'_{Topcolour}$	3.3 (1.8)	4.5 (2.6)	5.5 (3.2)
$Z'_{SSM} \rightarrow ee$	6.5	7.2	7.8
$Z'_{SSM} \rightarrow \mu\mu$	6.4	7.1	7.6

→ Sensitivity up to about 8 TeV